The behavioural role of glutamate co-release from 5-HT neurons

L. Sophie Gullino

A thesis submitted in partial fulfilment of the requirements for the degree of

Doctor of Philosophy

Departments of Pharmacology and Experimental Psychology

Balliol College

University of Oxford

Trinity Term 2024

Abstract

L. Sophie Gullino, Balliol College Oxford, DPhil, Trinity Term 2024

The behavioural role of glutamate co-release from 5-HT neurons

5-hydroxytryptamine (5-HT) is a key neurotransmitter involved in a variety of critical functions including emotional modulation and reward processing. Recent evidence suggests that many 5-HT neurons express the vesicular glutamate transporter 3 (VGLUT3) and release both 5-HT and glutamate. Yet, the role of this co-released glutamate is unknown. This thesis aimed to further our understanding of the role of 5-HT-glutamate co-release in behaviour using a novel mouse model with conditional VGLUT3 knockout from 5-HT neurons (VGLUT3 cKO$^{5\text{-HT}}$).

A combination of immunohistochemistry and qPCR confirmed the depletion of VGLUT3 expression in 5-HT neurons in VGLUT3 cKO$^{5\text{-HT}}$ mice. Initial behavioural analysis showed no alteration in natural behaviour, nor evidence of anxiety-like behaviour in a variety of tests. However, VGLUT3 cKO$^{5\text{-HT}}$ mice displayed decreased sucrose preference, which might indicate anhedonia.

C-Fos immunohistochemistry experiments using wildtype mice revealed that VGLUT3-expressing 5-HT neurons in the ventral DRN were activated by exposure to an uncontrollable stressor, acute swim stress. This effect was reversed by the selective serotonin reuptake inhibitor fluoxetine. Additionally, VGLUT3 cKO$^{5\text{-HT}}$ mice spent more time climbing during swim stress, suggesting increased active coping.

Reward function was then assessed in VGLUT3 cKO$^{5\text{-HT}}$ mice using two operant paradigms. In both paradigms transgenic mice were able to learn over time but showed reduced performance, compared to controls. Conversely, VGLUT3 cKO$^{5\text{-HT}}$ mice did not differ from controls in tests probing learning and memory in other domains, suggesting that impairments might be specific to reward-based learning.

Finally, *in vivo* fibre photometry with a DA biosensor was used to probe DA release in the nucleus accumbens during reward-based tasks. Interestingly, VGLUT3 cKO$^{5\text{-HT}}$ mice demonstrated increased DA release in response to a reward-predictive auditory cue but a reduced DA response to the reward as learning progressed. This finding suggested faster transfer of DA neuronal activation from the reward to the reward-predictive cue. This apparent shift toward Pavlovian learning is consistent with a propensity for sign-tracking behaviour which may contribute to the observed deficits in reward-based learning.

Altogether, through the use of a novel transgenic mouse model the current thesis provides new insights into the role of 5-HT-glutamate co-release in stress coping and reward processing.

Acknowledgements

Firstly, I would like to thank my supervisors: Prof Trevor Sharp and Prof David Bannerman. Thank you for the opportunity to pursue this project and for your scientific vision, it has been a privilege to work with you both. But also, thank you for your constant support and encouragement.

I am also very grateful to the Medical Research Council, Balliol College and Department of Pharmacology for their financial input that enabled this work.

I'd like to thank Helen Collins for teaching me everything that I know about behaviour, for her patience in answering my endless questions, and for being such a great friend. Thank you also to all the other members of the Sharp Lab. In particular, Aurelija for the fun lab chats, and my students Cara, Poppy and Ellen. You all made mouse work much more enjoyable.

Thanks to everyone who has helped or guided me during experiments, including Richard (OQF), Debbie (BMS), Katie Hewitt (BNU), and Chris Barkus. Thank you to Mark Walton, Lauren Burgeno and Rebecca Smausz for your support during the photometry experiment. Thanks also to the Anthony lab for the use of their equipment for the PCR experiments and behavioural analysis.

Thank you to all my friends for their endless support, and for making me feel at home here in Oxford. A special thank goes to Isaac, for always being there to listen and for making me feel seen.

Thanks to my parents, for their love and support, and for never getting tired of hearing me talk about mice.

And lastly, thanks to Tom for being my rock. Thank you for your patience, for all your help, and for always making my days brighter.

Table of contents

Abbreviations

5-CSRTT	5-Choice serial reaction time task
5-HIAA	5-Hydroxyindoleacetic acid
5-HT	5-Hydroxytryptamine
5-HTP	5-Hydroxytryptophan
5-HTT (SERT)	5-HT transporter
ANOVA	Analysis of variance
ARRIVE	Animal Research: Reporting of In Vivo Experiments
AUC	Area under the curve
cDNA	Complementary deoxyribonucleic acid
CNS	Central nervous system
CS	Conditioned stimulus
Ct	Threshold cycle
DA	Dopamine
DNA	Deoxyribonucleic acid
DOPAC	3,4-Dihydroxyphenylacetic acid
DRN	Dorsal raphe nucleus
EPM	Elevated plus maze
FLX	Fluoxetine
GAD	Glutamate decarboxylase
GAPDH	Glyceraldehyde 3-phosphate dehydrogenase
HPA	hypothalamic-pituitary-adrenal
HPLC-ED	High performance liquid chromatography with electrochemical detection
I.p.	Intraperitoneal
ITI	Inter trial interval
KO	Knockout
MAO	Monoamine oxidase
MAOI	MAO inhibitor
mGLUR	Metabotropic glutamate receptors

MRN	Median raphe nucleus
mRNA	Messenger ribonucleic acid
NAc	Nucleus accumbens
PAG	Periaqueductal grey
PBS	Phosphate buffered saline
qPCR	Quantitative real-time polymerase chain reaction
RNA	Ribonucleic acid
S.c.	Subcutaneous
SSRI	Selective serotonin reuptake inhibitor
TPH2	Tryptophan hydroxylase 2
US	Unconditioned stimulus
VGLUT	Vesicular glutamate transporter
VMAT2	Vesicular monoamine transporter 2
VTA	Ventral tegmental area

Publications

Parts of the work included in this thesis have been presented in the following publications and conference abstracts:

Gullino, L. S., Fuller, C., Dunn, P., Collins, H. M., El Mestikawy, S., & Sharp, T. (2023). Evidence for a role of 5-HT-glutamate co-releasing neurons in acute stress mechanisms. ACS Chemical Neuroscience. https://doi.org/10.1021/acschemneuro.3c00758;

Oral presentation at the FENS Hertie Winter School 2023 (Obergurgl);

Poster presentation and abstract at the 36th ECNP Congress 2023 (Barcelona);

Poster presentation at the International Mouse Phenotyping Consortium meeting 2023 (Oxford);

Featured oral presentation at the Oxford MRC-DTP student symposium 2023;

Featured oral communication at the CINP World Congress in Neuropharmacology 2023 (Montreal);

Poster presentation at the International Society for Serotonin Research meeting 2023 (Cancún);

Oral communication at the CINP World Congress in Neuropharmacology 2022 (Online);

Oral presentation and abstract at British Neuroscience Association Members Meeting 2022 (Online).

Contributions

Prof Salah El Mestikawy kindly gifted us theVGLUT3 cKO$^{5\text{-}HT}$ mice that allowed us to start our own colony, making this work possible. Raquel Pinacho and Helen Collins were responsible the VGLUT3 cKO$^{5\text{-}HT}$ colony prior to my DPhil.

In *Chapter 2*, Helen Collins assisted me in the novelty induced hyponeophagia and Spatika Jayaram helped with the marble burying test and scored the videos.

In *Chapter 3*, Helen Collins assisted me with acute swim stress pilot on wildtype mice, while Cara Fuller performed the histology, imaging and cell counting, under my supervision. Cara Fuller also helped me carry out the swim stress experiment on the VGLUT3 cKO$^{5\text{-}HT}$ mice., under my supervision. Poppy Dunn contributed to the acute social defeat experiment and performed the histology, imaging and cell counting, under my supervision.

In Chapter 4, Spatika Jayaram helped me with running the operant paradigm with milkshake reward.

In Chapter 5, Lauren Burgeno taught me and assisted me with the surgeries. The Python script used for running the water-based operant paradigms was adapted from Rebecca Smausz. The Python script used for the photometry pre-processing and analysis was adapted from Thomas Akam.

Chapter 1
Introduction

1.1 Scope of this thesis

A recent development is the discovery that many neuron types are capable of co-releasing more than one neurotransmitter (Svensson et al., 2019). Evidence indicates that the majority of 5-hydroxytryptamine (5-HT) neurons in the dorsal raphe nucleus (DRN) release not only 5-HT, but also glutamate (Johnson, 1994; Schäfer et al., 2002; Sengupta et al., 2017). This capacity to co-release glutamate is mediated by the vesicular glutamate transporter 3 (VGLUT3), which accumulates glutamate in pre-synaptic vesicles prior to release (Fremeau et al., 2002; Gras et al., 2002). Separate lines of recent evidence employing transgenic mouse models and optogenetics have suggested a role for co-released glutamate in anxiety (Amilhon et al., 2010), stress coping (Ren et al., 2018), and reward processing (Liu et al., 2014; Wang et al., 2019). However, most of these studies target all populations of VGLUT3-expressing neurons and not glutamate co-released specifically from 5-HT neurons. This thesis aimed to investigate the behavioural role of glutamate co-released from 5-HT neurons using a novel transgenic mouse model with conditional VGLUT3 knockout in 5-HT neurons (Gullino et al., 2024; Mansouri-Guilani et al., 2019). The following chapter introduces the central 5-HT system, the concept of co-release, and the current understanding of 5-HT-glutamate co-release.

1.2 The 5-HT system

1.2.1 Chemical aspects of 5-HT neurotransmission

1.2.1.1 5-HT synthesis, release, and metabolism

5-HT (also known as serotonin) is a monoamine neurotransmitter present in the central (CNS) and peripheral nervous system (Dahlström & Fuxe, 1964; Erspamer & Asero, 1952; Twarog & Page, 1953). Within the CNS, 5-HT is synthesised in the midbrain raphe nuclei from the essential amino acid L-tryptophan which is converted to 5-hydroxytryptophan (5-HTP) by tryptophan hydroxylase (TPH), the rate-limiting enzyme in 5-HT synthesis (Fitzpatrick, 1999). In turn, 5-HTP is converted into 5-HT by L-amino acid decarboxylase (Nakamura & Hasegawa, 2009). In the CNS, TPH2 is the predominant TPH isoform (Walther et al., 2003), but TPH1 is also expressed during the late developmental stage (Nakamura et al., 2006). TPH2 is synthesised in the soma of 5-HT neurons from where it can be transported to axonal terminals for local 5-HT synthesis (Deguchi & Barchas, 1972; Koubi et al., 2001), thus constituting a useful marker for 5-HT neurons.

Once synthesised, 5-HT is packaged and stored into vesicles in neuronal terminals by the vesicular monoamine transporter 2 (VMAT2; Nickell et al., 2014). 5-HT is then released by depolarisation, which opens voltage-gated calcium channels and triggers exocytosis (Südhof, 2012). In the extracellular space, neurotransmission is terminated either by degradation of 5-HT by monoamine oxidase (MAO), or by removal of 5-HT by the 5-HT transporter (5-HTT, also known as serotonin

transporter, SERT; Blakely et al., 1994). 5-HTT is a transmembrane protein and a sodium-dependent transporter expressed in soma, axons, dendrites, and presynaptic terminals of 5-HT neurons (Bengel et al., 1997; Blakely et al., 1998; Fujita et al., 1993; Lesch, 1998). 5-HTT controls the extent and duration of activation of 5-HT receptors, and it is the target of selective serotonin reuptake inhibitors (SSRI; Hyttel, 1994), which are currently the first line of treatment for anxiety and depression.

After reuptake by the 5-HTT, 5-HT is either reloaded into vesicles or degraded by MAO on mitochondrial membranes (Bortolato et al., 2010). MAO oxidises 5-HT into hydroxyindole acetaldehyde, and in turn aldehyde dehydrogenase converts hydroxyindole acetaldehyde into 5-hydroxyindole acetic acid (5-HIAA), the main metabolite of 5-HT (Bortolato et al., 2010; Nestler et al., 2015).

1.2.1.2 5-HT receptors

5-HT exerts its effects by binding to 14 known receptors, grouped into 7 families (Barnes & Sharp, 1999; Hoyer et al., 2002; Sharp & Barnes, 2020; ***Table 1.1***). All 5-HT receptors are heteroreceptors, thus they are expressed post-synaptically on non-5-HT neurons. However, they can also act as autoreceptors when located pre-synaptically on the soma (5-HT_{1A}) or axon terminals (5-HT_{1B}, 5-HT_{1D}) of 5-HT neurons, controlling 5-HT release. 5-HT receptors are predominantly metabotropic, and signal via G-protein coupled receptors. Different families of 5-HT receptors are $G_{i/o}$-coupled inhibitory receptors (5-HT_1 and 5-HT_5 families), G_s-coupled excitatory receptors (5-HT_4, 5-HT_6 and 5-HT_7) or $G_{q/11}$-coupled excitatory receptors (5-HT_2).

The 5-HT_3 receptor is the only ligand-gated ionotropic 5-HT receptor. Within each family, 5-HT receptor subtypes differ for their affinities for 5-HT, distributions, functions, and downstream signalling cascades (summarised in ***Table 1.1***), thus adding to the complexity of 5-HT transmission (for reviews see Barnes & Sharp, 1999; Sharp & Barnes, 2020).

Table 1.1 | 5-HT receptors. Details from Barnes and Sharp (1999), Hoyer et al. (2002), Sharp and Barnes (2020).

Receptor	Distribution	Localisation	Mechanism	Effect
5-HT_{1A}	Raphe nuclei (autoreceptor), cortex, hippocampus, limbic areas (heteroreceptor)	Somatodendritic, presynaptic, postsynaptic, extrasynaptic	$G_{i/o}$-coupled	Hyperpolarisation
5-HT_{1B}	Raphe nuclei, cortex, basal ganglia, substantia nigra	Presynaptic, postsynaptic	$G_{i/o}$-coupled	Hyperpolarisation
5-HT_{1D}	Raphe nuclei (5-HT neurons), trigeminal nucleus, substantia nigra, nucleus accumbens, hippocampus, cortex	Presynaptic	$G_{i/o}$-coupled	Hyperpolarisation
5-HT_{1E}	Trigeminal nucleus, cortex, caudate, putamen, claustrum, hippocampus, amygdala, striatum	Postsynaptic	$G_{i/o}$-coupled	Hyperpolarisation
5-HT_{1F}	Raphe nuclei (5-HT neurons) trigeminal nucleus, hippocampus, cortex, claustrum, caudate, putamen	Presynaptic	$G_{i/o}$-coupled	Hyperpolarisation
5-HT_{2A}	Cortex, nucleus accumbens, olfactory tubercle, hippocampus, basal ganglia, caudate, claustrum	Postsynaptic	$G_{q/11}$-coupled	Depolarisation
5-HT_{2B}	Hypothalamus, cortex, amygdala, cerebellum, lateral septum, hypothalamus	Postsynaptic	$G_{q/11}$-coupled	Depolarisation

5-HT$_{2C}$	Raphe nuclei (GABA interneurons), cortex, hippocampus, limbic areas, nucleus accumbens, basal ganglia, hypothalamus, substantia nigra	Postsynaptic	$G_{q/11}$-coupled	Depolarisation
5-HT$_3$	Cortex, limbic areas, vagus nerve, area postrema, hippocampus, brainstem nuclei, amygdala	Postsynaptic	Ligand-gated ion channel	Depolarisation
5-HT$_4$	Cortex, limbic areas, basal ganglia, hippocampus, striatum, substantia nigra, nucleus accumbens	Postsynaptic	G_s-coupled	Depolarisation
5-HT$_{5A}$	Frontal cortex, raphe nuclei (5-HT neurons), hippocampus, cerebellum, olfactory bulb	Unknown	$G_{i/o}$-coupled	Hyperpolarisation
5-HT$_{5B}$ (rodents)	Raphe nuclei, hippocampus, habenula	Unknown	$G_{i/o}$-coupled	Unknown
5-HT$_6$	Cortex, limbic areas, basal ganglia, striatum, nucleus accumbens, hippocampus	Postsynaptic	G_s-coupled	Depolarisation
5-HT$_7$	Suprachiasmatic nucleus, hypothalamus, cortex, hippocampus	Postsynaptic	G_s-coupled	Depolarisation

1.2.1.3 5-HT transmission

5-HT neurons are characterised by tonic slow, regular "clock-like" firing patterns, predominantly firing at low frequencies (1-5 Hz), with broad action potentials and large after-hyperpolarisations (Allers & Sharp, 2003; Vandermaelen & Aghajanian, 1983). Nonetheless, 5-HT can also be released by burst firing, consisting of short bursts of high-frequency groups of spikes followed by periods of quiescence (Hajós & Sharp, 1996). Signalling is likely to involve a combination of volume transmission, involving diffusion in extracellular fluids without defined physical constraints (Descarries et al., 2006; Descarries & Riad, 2012), and direct transmission at synapses (Gianni & Pasqualetti, 2023).

1.2.2 Neuroanatomical organisation of the 5-HT system

1.2.2.1 The raphe nuclei

Cell bodies of 5-HT neurons are located in the brainstem raphe nuclei, including a rostral group residing in the midbrain and rostral pons (caudal linear, dorsal and median raphe nuclei) and a caudal group situated in the pons and the medulla (raphe magnus, obscurus and pallidus nuclei, lateral medullary reticular formation; Hornung, 2010). The DRN and median raphe nucleus (MRN) are the most well-characterised, and in rodents they are located ventral to the cerebral aqueduct and periaqueductal grey (PAG; Baker et al., 1991; Jacobs & Azmitia, 1981; Jacobs & Fornal, 1991; Steinbusch et al., 1981). The DRN alone contains a third of all 5-HT neurons in the brain and, based on its anatomical and functional properties, it can be further divided into ventral DRN, dorsal DRN, and lateral wings (Hornung, 2010; Lowry, 2002). The raphe nuclei are highly heterogeneous structures containing several other neuronal types including neurons releasing glutamate, γ-aminobutyric acid (GABA), dopamine (DA), and neuropeptides (Huang et al., 2019).

5-HT neurons are characterised by their ability to synthesise 5-HT, thus sharing the expression of several essential markers described in *Section 1.2.1* (such as TPH2 and 5-HTT). Nonetheless, they also demonstrate heterogeneity with subpopulations of 5-HT neurons presenting different transcriptional profiles (Gaspar & Lillesaar, 2012; Huang et al., 2019; Okaty et al., 2019, 2020). For example, recent single-cell transcriptomic analysis revealed non-overlapping subpopulations of 5-HT neurons expressing markers of glutamatergic transmission (VGLUT3) or GABA-ergic

transmission (glutamate decarboxylase; GAD65 and GAD67; Huang et al., 2019), indicating the usage of a second neurotransmitter. Specifically, 5-HT neurons expressing VGLUT3 are abundant in the ventromedial, medial, and caudal DRN, whereas 5-HT neurons expressing GAD are found more rostrally, in the dorsal DRN and lateral wings (Okaty et al., 2020; Ren et al., 2018; Shikanai et al., 2012; Spaethling et al., 2014).

1.2.2.2 5-HT projections

From the raphe nuclei 5-HT neurons project extensively throughout the brain (Muzerelle et al., 2016). Rostral 5-HT neurons from the DRN and MRN innervate forebrain regions including the prefrontal cortex, thalamus, hippocampus, and amygdala (Hornung, 2003). DRN and MRN projections are predominantly complementary, with the DRN preferentially innervating the cortex, amygdala, striatum, and dorsal hippocampus, while the MRN primarily projects to limbic regions and ventral hippocampus (Muzerelle et al., 2016). Recent retrograde tracing studies revealed that the DRN comprises two anatomically defined and functionally distinct 5-HT subsystems, with neurons located in ventral DRN projecting preferentially to the frontal cortex, and dorsal DRN neurons innervating the amygdala (Ren et al., 2018). In turn, midbrain 5-HT neurons also receive dense inputs from the forebrain, such as from the prefrontal cortex, amygdala, nucleus accumbens (NAc), and hypothalamus (Peyron et al., 1997). Conversely, caudal 5-HT neurons project to the cerebellum, brainstem, and spinal cord (Steinbusch et al., 1981; Jacobs & Azmitia, 1992; Nestler et al., 2015).

1.2.2.3 5-HT and behaviour

As a result of its plethora of projections and diverse transmission modalities, 5-HT can act as a neuromodulator, influencing a wide variety of physiological processes and behaviours. Firstly, 5-HT plays a central role in emotional modulation and mood, regulating stress coping, anxiety, and depressive behaviour, but it has also been implicated in cognition, attention, appetite, reward, arousal, aggression, sleep, thermoregulation, and sensory processing (Abela et al., 2020; Cohen et al., 2015; He et al., 2020; Jacobs & Fornal, 1991; Paulus & Mintz, 2016; Pourhamzeh et al., 2022).

Dysregulation of the 5-HT system is implicated in several neuropsychiatric disorders in particular mood and anxiety disorders, but also schizophrenia and autism (Nemeroff & Owens, 2002; Sharp & Cowen, 2011). Moreover, the 5-HT system is the target of many pharmacological therapies, with SSRIs currently being the first-line treatment for depression and anxiety (Geddes et al., 1996; Song et al., 1993). Nonetheless, a full explanation for the mechanisms of action of antidepressants and the specific role of 5-HT in pathological conditions has remained elusive (Cowen & Browning, 2015; Harmer et al., 2017; Nemeroff & Owens, 2002).

1.3 5-HT-glutamate co-release

1.3.1 Historic perspective on co-transmission

Chemical neurotransmission, postulating neuronal communication via neurotransmitters as opposed to direct electrical connections, was first accepted in the 1950s. In the midst of the debate over chemical versus electrical transmission, the "Dale's Principle" was coined referring to the idea that the same chemical transmitter is released from all synaptic terminals of a neuron (Eccles et al., 1954). Nonetheless, in the following years several lines of evidence have indicated colocalisation or co-release of different neurotransmitters from the same neuronal terminal (for early reviews see Burnstock, 1980; Cuello, 1982; Potter et al., 1981). Colocalisation refers to the presence of two substances in the same neuronal terminal or varicosity, which can be released to act as chemical messengers in a process commonly known as co-transmission. Conversely, co-release refers to the simultaneous release of two substances stored in the same vesicle (Jonas et al., 1998; Merighi et al., 2011; Vaaga et al., 2014; Vilim et al., 2000). Nonetheless, the difficulty in establishing the precise mechanisms of release (see *Section 1.3.2* for further details) has often resulted in the terms co-release and co-transmission being used interchangeably.

In 1976, Eccles proposed that the "Dale's Principle" should be revised stating that "*at all the axonal branches of a neuron, there was liberation of the same transmitter substance or substances*", thus allowing for the release of more than one neurotransmitter type (Eccles et al., 1997). This general principle was also

questioned in the 1990s when evidence emerged that separate compartments of a single neuron could contain and release different neurotransmitters (Blitz & Nusbaum, 1999; Sossin et al., 1990; Sulzer & Rayport, 2000). The development of immunohistochemistry finally allowed the detection of substances colocalised in the same soma, neuronal terminal, axonal bouton, or varicosity, and thus co-transmission became widely accepted (for reviews see Burnstock, 1980; Cuello, 1982; Hökfelt et al., 2000; Kupfermann, 1991; Osborne, 2013; Potter et al., 1981; Svensson et al., 2019). Recent examples of colocalisation, co-transmission and co-release are summarised in ***Table 1.2***.

Table 1.2 | Examples of CNS neurons that co-release a second neurotransmitter. In most cases evidence indicated colocalisation, but there are also a few cases where functional co-release has been reported**.** The below classification between primary and secondary neurotransmitter is often arbitrary. For reviews on co-transmission and co-release see Nusbaum et al., 2001; Svensson et al., 2019; Vaaga et al., 2014.

Primary neuro-transmitter	**Secondary neuro-transmitter**	**Soma location**	**References**
5-HT	Glutamate	DRN, MRN	(Gras et al., 2002; Sengupta et al., 2017)
5-HT	GABA	Raphe nuclei (e.g. DRN, raphe magnus)	(Belin et al., 1983; Okaty et al., 2015, 2020)
5-HT	Neuropeptides	DRN, MRN	(reviewed in Okaty et al., 2020)
DA	Glutamate	VTA, substantia nigra	(Adrover et al., 2014; Hnasko et al., 2010; Sulzer et al., 1998)
DA	GABA	Olfactory bulb, VTA, substantia nigra	(Borisovska et al., 2013; Liu et al., 2013; Tritsch et al., 2012)
GABA	Glutamate	VTA, basal ganglia	(Root et al., 2014; Shabel et al., 2014)
Acetylcholine	Glutamate	Striatum	(Gras et al., 2002, 2008)
Acetylcholine	GABA	Forebrain, basal ganglia	(Granger et al., 2016; Lee et al., 2010; Saunders, Granger, et al., 2015; Saunders, Oldenburg, et al., 2015)
Glycine	GABA	Striatum, hippocampus	(Wojcik et al., 2006; reviewed in Vaaga et al., 2014)

Noradrenaline	DA	Locus coeruleus	(Devoto et al., 2001, 2005)
Histamine	GABA	Tuberomammillary nucleus	(Haas et al., 2008; Tritsch et al., 2014; Yu et al., 2015)

1.3.2 Mechanisms and function of co-transmission

Across systems, neurotransmitters of low molecular weight, including amino acids such as glutamate, glycine, GABA, and acetylcholine, are typically contained in small clear synaptic vesicles located in proximity to the active zone (i.e. the site of neurotransmitter release). Conversely, neuropeptides are found in large dense-core vesicles, located away from active zones (Hökfelt et al., 2003; Pelletier et al., 1981). Immunoelectromicroscopic evidence suggests that monoamines, such as 5-HT, can be contained both in small clear vesicles (Johansson et al., 1980; Pelletier et al., 1977; Van Bockstaele & Chan, 1997) and in dense-core vesicles (Pelletier et al., 1981). Furthermore, there is evidence that larger neurotransmitters including monoamines and neuropeptides are often co-packaged together with other substances (Hökfelt et al., 2000; Pelletier et al., 1981; Salio et al., 2006). Compared to smaller vesicles, dense-core vesicles are usually slower to release due to their location away from active zones and the lack of synapsins, proteins that regulate synaptic neurotransmitter release (Xia et al., 2009). As a result, lower firing frequencies generally cause rapid mobilisation of small synaptic vesicles, while dense-core vesicles are mobilised by higher frequencies or burst firing, thus allowing for frequency-dependent release of different neurotransmitter types (Svensson et al., 2019).

Generally, neurotransmitters are released by exocytosis, a process in which the complete fusion of the vesicle with the plasma membrane results in the release of all the substances stored in the vesicle (Winkler et al., 1986). However, exocytosis can also occur by "kiss-and-run" mechanisms involving partial release through a smaller fusion pore that allows selective expulsion of smaller neurotransmitters (Stevens & Williams, 2000; Xia et al., 2009; Zhang et al., 2011).

The main purpose of co-transmission could be to increase synaptic flexibility, allowing the same anatomical connection to generate a wide variety of outputs, through multiple neurotransmitters and a variety of release modes. In fact, co-transmission likely involves a combination of divergent or convergent signalling mechanisms and a range of interactions between co-transmitters with additive, subtractive or non-linear effects in different systems (Brezina, 2010; Harris-Warrick & Johnson, 2010; Nusbaum et al., 2001). Furthermore, increasing evidence suggests that levels of colocalisation are not fixed during the lifetime of an individual. Rather, colocalisation may vary during development as well as in response to injury, disease (for a review see Vaaga et al., 2014) and environmental triggers (Li et al., 2024; Prakash et al., 2020), a phenomenon known as "phenotype switching" (Dulcis et al., 2013; Li et al., 2020; Spitzer, 2015). For instance, a decrease in VGLUT3 expression in 5-HT neurons has been reported in rats exposed to chronic stress (Prakash et al., 2020), and during acquisition of generalised fear following acute stress (Li et al., 2024), suggesting alterations in 5-HT-glutamate co-release (see *Chapter 6, Section 6.3*, for further discussion). Altogether, this highlights the complexity of

understanding how colocalisation, co-transmission and co-release can impact behaviour.

1.3.3 Evidence of 5-HT-glutamate co-release

1.3.3.1 Vesicular glutamate transporter 3 (VGLUT3)

Alongside a plethora of studies documenting the presence of co-transmission across different neuronal populations, it has recently been shown that 5-HT neurons are capable of not only releasing 5-HT but also glutamate (see *Section 1.3.3.2* for further details; Fremeau et al., 2002; Johnson, 1994). In this case, glutamate co-release is facilitated by VGLUT3, one of three vesicular glutamate transporters (VGLUT1, VGLUT2 and VGLUT3) responsible for storing cytosolic glutamate in pre-synaptic vesicles prior to release (El Mestikawy et al., 2011; Gras et al., 2002; Liguz-Lecznar & Skangiel-Kramska, 2007; Takamori et al., 2002). While all VGLUTs share a similar function, they are expressed in a predominantly complementary manner, with VGLUT1 being prevalent in glutamatergic neurons in cortical areas and VGLUT2 in glutamatergic neurons in subcortical regions (Vigneault et al., 2015). Conversely, VGLUT3 is primarily expressed in cortical and hippocampal GABAergic interneurons, striatal cholinergic interneurons, and 5-HT neurons in the raphe nuclei. Some specific populations of glutamatergic neurons, including glutamatergic DRN neurons, also express VGLUT3 (Favier et al., 2021; Schäfer et al., 2002; Takamori et al., 2002; Vigneault et al., 2015)

1.3.3.2 Colocalisation and co-release of 5-HT and glutamate

The first evidence of 5-HT-glutamate co-release was identified by electrophysiological studies in cultured rat 5-HT neurons, where 60% of 5-HT neurons evoked excitatory glutamatergic potentials (Johnson, 1994). This was followed by in situ hybridisation studies reporting VGLUT3 expression in approximately two-thirds of midbrain 5-HT neurons (Hioki et al., 2010). VGLUT3 was found to be prevalent in the soma of 5-HT neurons of the ventral DRN and MRN, with only sparse colocalisation in the dorsal DRN and lateral wings (Fremeau et al., 2002; Gras et al., 2002; Hioki et al., 2010; Schäfer et al., 2002). VGLUT3 also colocalised with VMAT2 in several brain regions, including 50% of 5-HT varicosities of the prelimbic cortex and in specific hippocampal subregions (e.g. ~30% in CA1, ~50% in CA3 and dentate gyrus, and ~79% in the hippocampal fissure; Amilhon et al., 2010). Conversely, it was reported that VGLUT3 rarely colocalises with 5-HTT, and raphe 5-HT neurons express 5-HTT and VGLUT3 mainly in segregated axon terminals (Amilhon et al., 2010; Voisin et al., 2016). These terminals colocalising VMAT2 and VGLUT3 but lacking 5-HTT might display enhanced extracellular 5-HT levels after release due to low reuptake.

More recently, it was demonstrated that optogenetic activation of 5-HT neurons released both 5-HT and glutamate, eliciting fast post-synaptic excitation via ionotropic glutamate receptors in the hippocampus, amygdala, and striatum (Kapoor et al., 2016; Liu et al., 2014; Sengupta et al., 2017; Varga et al., 2009), thus confirming a functional role of VGLUT3 in 5-HT neurons.

1.3.3.3 Mechanisms of 5-HT-glutamate co-release

The mechanisms of 5-HT-glutamate co-release remain to be clarified. It has been suggested that VGLUT3 promotes vesicular loading of 5-HT by enhancing the activity of VMAT2 (Amilhon et al., 2010; El Mestikawy et al., 2011). Thus, amino acid uptake assays indicate that hippocampal and cortical vesicles accumulate more [^{3}H]5-HT in the presence of glutamate (Amilhon et al., 2010). This idea is in line with evidence that VGLUT3 also facilitates vesicular filling of acetylcholine in striatal cholinergic neurons (Gras et al., 2008). This phenomenon, known as "vesicular synergy", involves 5-HT and glutamate being released from the same vesicle (El Mestikawy et al., 2011), thus warranting the use of the term "co-release".

Nonetheless, optogenetic evidence has demonstrated that low frequency (≤1 Hz) stimulation of 5-HT terminals in the amygdala preferentially elicits glutamate release, whilst 5-HT release was observed in response to higher frequencies (10–20 Hz; Sengupta et al., 2017). As 5-HT neurons predominantly fire at low frequencies (Allers & Sharp, 2003), it is possible that under these circumstances 5-HT neurons might preferentially release glutamate (Sengupta et al., 2017; Trudeau & El Mestikawy, 2018). Similarly, in a separate study (Zou et al., 2020) optogenetic activation of 5-HT neurons by a single-pulse light stimulation elicited glutamate-mediated excitation in the ventral tegmental area (VTA), while prolonged stimulation of the same neurons (20 Hz for 30 s) produced 5-HT mediated currents (Zou et al., 2020). Furthermore, the above evidence is consistent with glutamate being packaged in small clear vesicles located in proximity to the active zone, while 5-HT might be accumulated into dense-core vesicles which are typically mobilised

by higher frequencies (as discussed in *Section 1.3.2*). Thus, this frequency-dependent release might indicate that 5-HT and glutamate are released from separate vesicles (Trudeau & El Mestikawy, 2018), albeit alternative mechanisms of partial release such as "kiss-and-run" could also occur. Due to the lack of consensus on the mechanisms of release, here we use the term "5-HT-glutamate co-release" in a broad manner encompassing the possibility of both co-release from the same vesicle and of co-transmission from separate vesicular pools.

1.3.4 Behavioural role of 5-HT-glutamate co-release

1.3.4.1 5-HT-glutamate co-release in anxiety and fear learning

Transgenic mice have been used to shed light on the role of VGLUT3-mediated co-release, with several studies employing mice with global VGLUT3 KO (KO; Amilhon et al., 2010; Balázsfi et al., 2018; De Almeida et al., 2023; Fazekas et al., 2019). Adult VGLUT3 KO mice demonstrated increased anxiety-like behaviour on the elevated plus maze (EPM), novelty suppressed feeding test and marble burying, while VGLUT3 KO pups displayed increased ultrasonic vocalisation (Amilhon et al., 2010). Due to the well-established links between 5-HT and anxiety (Graeff et al., 1996; Ohmura et al., 2020), this high anxiety phenotype of VGLUT3 KO mice was hypothesised to be driven by the lack of glutamate co-released specifically from 5-HT neurons (Amilhon et al., 2010). Interestingly, VGLUT3 KO mice also showed decreased sensitivity of 5-HT_{1A} autoreceptors as indicated by hyposensitivity to hypothermia induced by the 5-HT_{1A} receptor agonist 8-OH-DPAT. This finding, together with increased 5-HT turnover (5-HIAA/5-HT ratio) in the hippocampus of

VGLUT3 KO mice, suggested a role for VGLUT3 in the control of 5-HT function (Amilhon et al., 2010). Nonetheless, mice with VGLUT3 KO targeted to Pet1 neurons (including the majority of 5-HT neurons) displayed hypolocomotion in the open field and EPM, but no difference in time spent in the centre zone or open arms (Cunha et al., 2020), thus calling into question the proposed role of 5-HT-glutamate co-release in anxiety.

Mice with global VGLUT3 KO also displayed increased contextual fear and fear generalisation, as evidenced by exaggerated freezing during fear conditioning, which was attributed to a pattern separation deficit (Balázsfi et al., 2018; De Almeida et al., 2023). VGLUT3 KO mice also displayed mild learning deficits, including reduced performance in avoidance-based learning tasks (e.g. the "shuttle-box") and reduced reversal learning in a reward-based operant paradigm (Fazekas et al., 2019). These changes were accompanied by alteration of the hypothalamic-pituitary-adrenal (HPA) axis involving enhanced resting HPA activity, but lowered HPA axis stress-reactivity as indicated by reduced stressor-induced corticosterone elevations (Balázsfi et al., 2018). Nonetheless, the role of glutamate co-release from 5-HT neurons in fear remains unclear.

1.3.4.2 5-HT-glutamate co-release and stress coping

5-HT neurons are highly responsive to stress, threats, and noxious stimuli and are likely to mediate stress coping, the behavioural and physiological responses exhibited in reaction to perceived threats (Deakin & Graeff, 1991; Grahn et al., 1999). In particular, DRN 5-HT neurons are reported to be robustly activated by

uncontrollable stressors such as swim stress, restraint, and foot shock, as demonstrated by increased expression of the activity-dependent immediate early gene *c-fos* under these conditions (Bonapersona et al., 2022; Hale et al., 2008; Kelly et al., 2011; Roche et al., 2003; Senba et al., 1993). Furthermore, *in vivo* microdialysis studies found that exposure to acute stress, such as to predator stress or inescapable foot shock, increased extracellular levels of 5-HT or 5-HT turnover in terminal regions, including the hippocampus, cortex, and amygdala (Amat et al., 1998; Beekman et al., 2005; Rueter & Jacobs, 1996; for a review see Linthorst & Reul, 2010).

Interestingly, in a recent study chemogenetic activation of 5-HT neurons projecting to the prefrontal cortex from the ventral DRN, comprising predominantly 5-HT-glutamate co-releasing neurons, increased active stress coping measured as decreased immobility during swim stress (Ren et al., 2018). The latter finding suggests that glutamate co-releasing 5-HT neurons may be involved in stress coping behaviour.

1.3.4.3 5-HT-glutamate co-release and SSRI treatment

It has also been suggested that co-released glutamate might play an important role in the clinical actions of SSRIs (Fischer et al., 2015; Gras et al., 2002), although this hypothesis remains to be tested. Current thinking is that acute SSRI administration causes an increase in extracellular 5-HT, leading to activation of 5-HT_{1A} autoreceptors and a decrease in 5-HT neuronal firing, which is expected to reduce the release of both 5-HT and glutamate. However, with continued SSRI

administration 5-HT_{1A} autoreceptors are thought to desensitise resulting in a return of 5-HT neuronal activity, albeit in the presence of continued 5-HTT blockade (Beyer & Cremers, 2008; Blier & de Montigny, 1994; Fischer et al., 2015). The latter is predicted to shift the 5-HT/glutamate balance at their receptors towards 5-HT. Interestingly, the timing of this shift could be consistent with the delayed onset of the antidepressant effect of SSRIs (Fischer et al., 2015).

1.3.4.4 5-HT-glutamate co-release and reward

The DRN has dense reciprocal connections with several brain regions involved in the reward system (Vertes, 1991; Vertes & Linley, 2008). Moreover, a plethora of evidence from pharmacological, optogenetic, and imaging studies links the DRN to reward processing (for a review see Luo et al., 2015). Nonetheless, there is no consensus on the role of 5-HT in reward, as evident in recent conflicting theories (for a review see Liu et al., 2020). For example, it has been suggested that 5-HT neurons might encode punishment and frustration by opposing the DA system (Boureau & Dayan, 2011; Daw et al., 2002; Deakin & Graeff, 1991). Alternatively, 5-HT neurons might promote waiting for rewards by increasing tonic activity in the reward anticipatory phase (Miyazaki et al., 2012). More recent photometry and electrophysiological studies have shown that 5-HT can differentially encode reward expectation and reward value (with tonic and phasic activities respectively) enabling the tracking of beneficial or aversive value of the current environment to guide behaviour (Cohen et al., 2015; Li et al., 2016; Zhong et al., 2017).

Recently, it has been suggested that the release of 5-HT might act in synergy with co-released glutamate in signalling reward (Liu et al., 2020). Thus, *in vitro* electrophysiological studies found that VGLUT3-expressing 5-HT neurons excite DA neurons in the VTA which project to the NAc, a key pathway for reward processing (Cunha et al., 2020; Wang et al., 2019). Furthermore, optogenetic activation of either VGLUT3-positive or 5-HTT-positive DRN projections to the VTA elicited conditioned place preference (Wang et al., 2019). These rewarding effects of 5-HT neuron activation were reduced by knocking out VGLUT3 from Pet1 neurons (including the majority of 5-HT neurons), and any residual effects were blocked by 5-HT depletion (Liu et al., 2014).

Nonetheless, it is reported that only 14% of DRN projections to the VTA co-release 5-HT and glutamate, 13% released only 5-HT, whereas the majority are non-5-HT-containing neurons and include many (46%) VGLUT3-expressing glutamatergic projections (Qi et al., 2014). Recent optogenetic studies indicate that activation of DRN neurons is strongly rewarding in a VGLUT3-dependent manner (McDevitt et al., 2014), therefore these rewarding effects could be driven exclusively by glutamatergic signalling (McDevitt et al., 2014; Qi et al., 2014). Altogether, this lack of consensus suggests that the role of glutamate co-released from 5-HT neurons in reward warrants further investigation.

1.3.5 Aim of this thesis

The majority of 5-HT neurons in the DRN express VGLUT3 and co-release 5-HT and glutamate, yet the role of this co-released glutamate is poorly understood. The behavioural effects of global VGLUT3 deletion have been characterised in several studies, but there is a sparsity of research specifically investigating the role of VGLUT3 in 5-HT neurons. In this thesis, a novel transgenic mouse model with conditional VGLUT3 KO in 5-HT neurons (VGLUT3 cKO$^{5\text{-HT}}$) was validated (*Chapter 2*) and then used to investigate the behavioural role of 5-HT-glutamate co-release. Specifically, *Chapter 2* explored the performance of VGLUT3 cKO$^{5\text{-HT}}$ mice in tests of anxiety, and also assessed whether these mice have altered 5-HT neurochemistry and expression of 5-HT-related genes. *Chapter 3* used c-Fos immunohistochemistry to investigate whether 5-HT-glutamate co-releasing neurons are activated by acute stress, and assessed stress coping behaviour in VGLUT3 cKO$^{5\text{-HT}}$ mice. *Chapter 4* examined reward-based learning in VGLUT3 cKO$^{5\text{-HT}}$ mice employing several different behavioural paradigms. *Chapter 5* used fibre photometry with a DA biosensor to measure DA release in the NAc of behaving VGLUT3 cKO$^{5\text{-HT}}$ mice in a reward-based operant task. Altogether this thesis aims to further our understanding of the behavioural role 5-HT-glutamate co-release, with a focus on anxiety, stress coping, reward processing, and its interactions with the DA system.

Chapter 2
Phenotyping of a novel transgenic mouse with conditional VGLUT3 knockout in 5-HT neurons

2.1 Introduction

Evidence suggests that the majority of 5-HT neurons expresses VGLUT3 and therefore co-releases 5-HT and glutamate, yet the role of this co-released glutamate is unknown. This chapter investigated a novel transgenic mouse model with conditional VGLUT3 knockout in 5-HT neurons (VGLUT3 cKO$^{5\text{-HT}}$), and thus with a presumed deficit in glutamate co-release. Upon validation, VGLUT3 cKO$^{5\text{-HT}}$ mice will be used for characterisation of the behavioural role of glutamate co-released from 5-HT neurons.

2.1.1 Development of a novel transgenic mouse with conditional VGLUT3 KO in 5-HT neurons

VGLUT3 cKO$^{5\text{-HT}}$ mice were first developed by our collaborators from the Sorbonne University (Mansouri-Guilani et al., 2019). They used the CreLox system to insert in the mouse genome a site-specific Cre recombinase which recognises two directly repeated loxP sites and excises the loxP flanked DNA (Kim et al., 2018). Specifically, a floxed VGLUT3 mouse (VGLUT3$^{\text{LoxP/LoxP}}$, *Slc17a8* mutant; Fasano et al., 2017) was crossed with a SERT-Cre line, where Cre recombinase is inserted upstream of the SERT gene (*Slc6a4*), to achieve a conditional VGLUT3 knockout from SERT-expressing neurons (SERT-Cre::VGLUT3$^{\text{LoxP/LoxP}}$; ***Fig. 2.1***). Control littermates also had floxed VGLUT3 but did not

express Cre under the SERT promoter (SERT$^{+/+}$::VGLUT3$^{LoxP/LoxP}$; see *Section 2.2.1* for further details). Prior to the experiments described here, the behaviour of these VGLUT3 cKO$^{5\text{-}HT}$ mice had not been fully characterised. Specifically, this mouse model had only previously used in one published study (Mansouri-Guilani et al., 2019) which investigated the potential involvement of glutamate co-transmission in modulating psychostimulant-induced maladaptive behaviours. Evidence showed that VGLUT3 cKO$^{5\text{-}HT}$ mice had no alteration in amphetamine sensitivity, specifically in terms of locomotor and stereotypy responses (Mansouri-Guilani et al., 2019). In comparison, two previous studies (Cunha et al., 2020; Liu et al., 2014; see below for further discussion) have reported the generation of mice with conditional VGLUT3 KO from neurons expressing Pet1, a transcription factor regulating the expression of genes required for 5-HT function (Hendricks et al., 2003; Liu et al., 2010). Pet1 is expressed by 95% of 5-HT neurons in the DRN, but also in a subpopulation of glutamatergic neurons which amounts to 10% of total Pet1 neurons (Luo et al., 2015; Scott et al., 2005). Due to the higher 5-HT neuron selectivity of the SERT gene the VGLUT3 cKO$^{5\text{-}HT}$ mouse has advantages over the conditional Pet1 KO mouse for investigating the role of glutamate co-release from 5-HT neurons.

2.1.2 Evidence for a role co-released glutamate in anxiety

Previous evidence indicates that mice with global VGLUT3 KO exhibit a high anxiety phenotype, as demonstrated by their behaviour in the EPM, novelty-suppressed feeding and marble burying tests (Amilhon et al., 2010). Due to the well-established links between 5-HT and anxiety (Graeff et al., 1996; Ohmura et al., 2020), this phenotype has been hypothesised to be driven by the lack of glutamate co-release specifically from 5-HT

neurons. Additionally, VGLUT3 KO mice also showed decreased 5-HT_{1A} autoreceptor function in the DRN and increased 5-HT turnover in the hippocampus (Amilhon et al., 2010), suggesting a role for VGLUT3 in the control of 5-HT neuronal activity.

Furthermore, mice with conditional VGLUT3 KO from Pet1 neurons were reported to spend more time in the dark compartment of the light/dark box, and demonstrated hypolocomotion in the open field and on the EPM (Cunha et al., 2020), potentially consistent with an increase in anxiety. However, these mice did not show altered number of open arm entries or time spent in the open arms of the EPM (Cunha et al., 2020), which would normally be indicative of anxiety-like behaviour. Thus, on the basis of experiments to date a role for glutamate co-released from 5-HT neurons in anxiety is unclear.

2.1.3 Evidence for a role of VGLUT3 in reward and learning

Mice with global VGLUT3 KO also displayed mild learning deficits, including impairments in avoidance-based learning tasks and appetitively-motivated reversal learning (Fazekas et al., 2019). Furthermore, a recent study reported conditional VGLUT3 KO from Pet1 neurons significantly reduced the behavioural reinforcing effects of optogenetic activation of Pet1 neurons (Liu et al., 2014). The latter study adds to a body of evidence suggesting that DRN glutamatergic inputs to the VTA are reinforcing during behaviour, but a role for the glutamate co-released from 5-HT neurons remains to be clarified (for a more detailed discussion on glutamate co-release and reward, see *Chapter 4*).

2.1.4 Hypothesis and aim

Firstly, experiments described in this chapter aimed to validate the conditional VGLUT3 KO from 5-HT neurons in VGLUT3 cKO$^{5\text{-HT}}$ mice by immunohistochemistry and gene expression. Additionally, 5-HT and DA function in VGLUT3 cKO$^{5\text{-HT}}$ mice was also assessed via gene expression analysis of a panel of 5-HT and DA-related genes, and neurochemical analysis of 5-HT, DA and their main metabolites. The second aim of this chapter involved investigating the role of glutamate co-released from 5-HT neurons in anxiety and reward mechanisms. To this end VGLUT3 cKO$^{5\text{-HT}}$ mice were examined in a battery of tests probing naturalistic, anxiety-like, and appetitively-motivated behaviours. These paradigms were selected to shed light on the role of glutamate co-release in both anxiety and reward, as well as to probe the general wellbeing of the mice.

2.2 Methods

2.2.1 Animals

Experiments used transgenic mice with conditional VGLUT3 knockout in 5-HT neurons (VGLUT3 cKO$^{5\text{-HT}}$ or SERT-Cre::VGLUT3$^{\text{LoxP/LoxP}}$, C57BL/*6J* background, aged 8-30 weeks) and their control littermates (SERT$^{+/+}$::VGLUT3$^{\text{LoxP/LoxP}}$). VGLUT3 cKO$^{5\text{-HT}}$ mice were originally generated by crossing VGLUT3$^{\text{loxP/loxP}}$ mice (a *Slc17a8* mutant mouse line with specific knockout of a DNA fragment encompassing exon 2; Fasano et al., 2017) with a SERT-Cre line (Mansouri-Guilani et al., 2019). For the experiments described in this thesis, mice were bred by crossing SERT-Cre::VGLUT3$^{\text{LoxP/LoxP}}$ mice with SERT$^{+/+}$::VGLUT3$^{\text{LoxP/LoxP}}$ mice, hence both VGLUT3 cKO$^{5\text{-HT}}$ mice and control littermates have floxed VGLUT3, but VGLUT3 cKO$^{5\text{-HT}}$ mice also express Cre under the control of the

SERT promoter (unlike their control littermates which are wildtype for SERT). As Cre expression has been reported to inadvertently affect behavioural phenotypes (Chohan et al., 2020; Costa et al., 2021), a phenotyping pilot was also carried out on SERT-Cre mice compared to wildtype ($SERT^{+/+}$) controls to ensure that Cre expression itself was not responsible for behavioural changes.

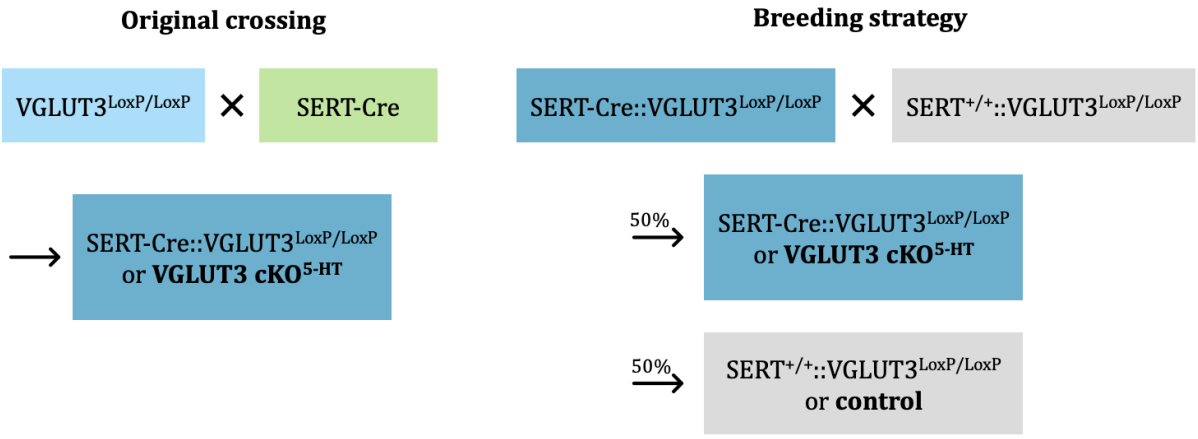

Figure 2.1 | Breeding diagrams detailing the development of VGLUT3 $cKO^{5\text{-}HT}$ mice and current breeding strategy. VGLUT3 $cKO^{5\text{-}HT}$ mice ($SERT\text{-}Cre::VGLUT3^{LoxP/LoxP}$) were originally obtained by crossing a $VGLUT3^{LoxP/LoxP}$ mouse with a SERT-Cre line. Mice used in this thesis were bred by crossing $SERT\text{-}Cre::VGLUT3^{LoxP/LoxP}$ (heterozygous for SERT-Cre) and $SERT^{+/+}::VGLUT3^{LoxP/LoxP}$ (wildtype for SERT-Cre). Thus, all mice had a floxed VGLUT3, but VGLUT3 $cKO^{5\text{-}HT}$ mice also expressed Cre under the SERT promoter, while controls did not express Cre.

Male and female mice were group-housed (2-6 per cage) with littermates in individually ventilated cages, in a temperature-controlled room (21°C) with a 12 h light/dark cycle (light on 07:00, lights off 19:00). Mice had *ad libitum* access to food and water (unless otherwise specified), and cages were lined with sawdust bedding and contained cage enrichment consisting of sizzle nest and a cardboard tube. To minimise stress, mice were habituated to handling on three occasions before any experiment, and handling was

always carried out using a cardboard tunnel (Gouveia & Hurst, 2019; Hurst & West, 2010).

Experiments followed the principles of the Animal Research: Reporting of In Vivo Experiments (ARRIVE) guidelines and were conducted according to the United Kingdom Animals (Scientific Procedures) Act of 1986, with appropriate personal and project licence coverage. All measurements were obtained and analysed by a researcher blind to genotype.

2.2.2 Behavioural tests

VGLUT3 cKO$^{5\text{-HT}}$ mice and control littermates underwent one of the following batteries of tests, with at least two days of rest in between each test.

a. *Tests of anxiety-like behaviour*: novelty-induced hyponeophagia, non-anxiogenic open field, EPM, and light/dark box (***Fig. 2.2A***).
b. *Marble burying:* this test was performed separately in a cohort of naïve mice.
c. *Exploratory cohort (comprising naturalistic behaviours and appetitively-motivated tests of anxiety, anhedonia and reward)*: measurement of food/water consumption, body weight and nest building; novelty-induced hyponeophagia, sucrose preference test, and appetitively-motivated spatial reference memory test (***Fig. 2.2B***).

Additionally, the behaviour of SERT-Cre mice, compared to wildtype controls (SERT$^{+/+}$), was assessed in the non-anxiogenic open field, EPM, and sucrose preference test.

All experiments were conducted during the light phase (10:00-17:00) unless otherwise specified. Mice were always allowed to habituate to the testing room for at least 30 min prior to experimentation. In all experiments involving an apparatus without bedding, the apparatus was wiped between animals with 0.5% Anistel (Tristel) to remove odours.

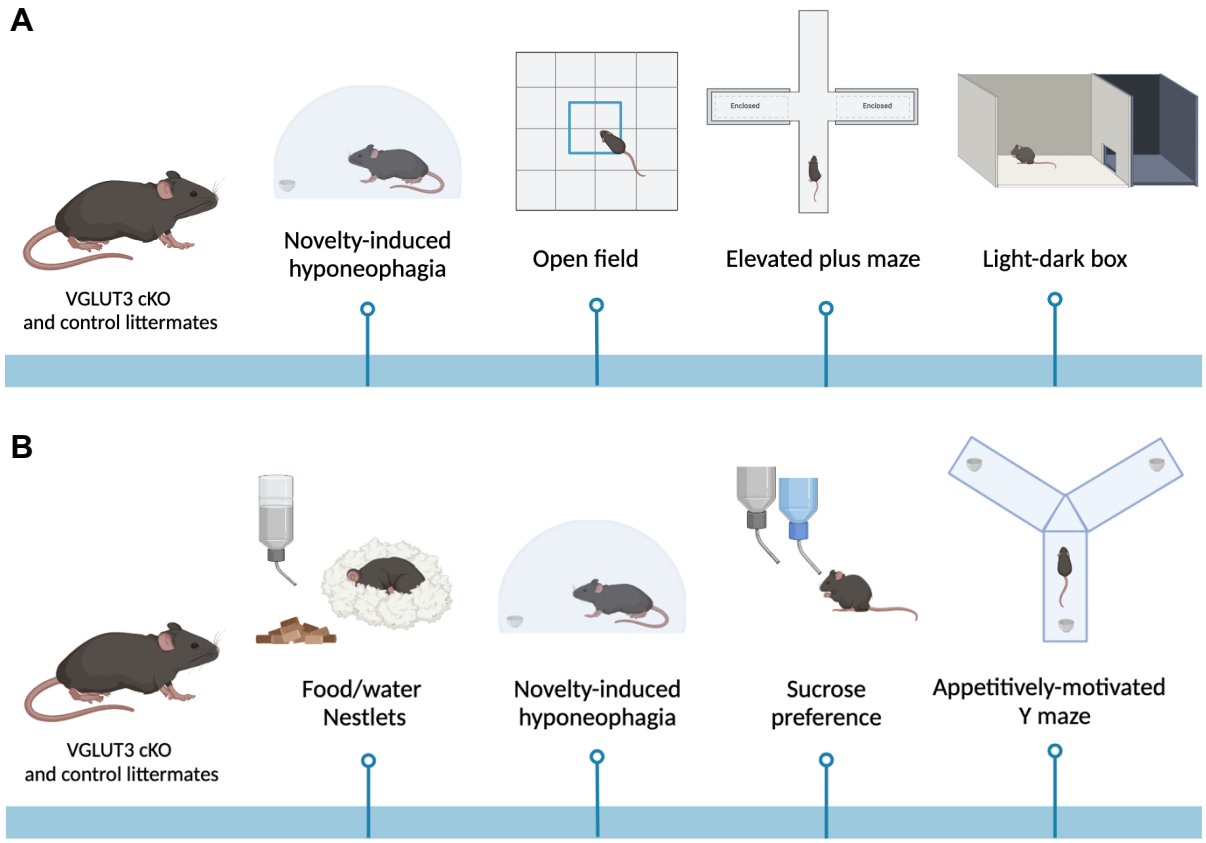

Figure 2.2 | Experimental timeline of behavioural experiments. **(A)** Experimental timeline of *cohort a*, including tests of anxiety-like behaviour. **(B)** Experimental timeline of *cohort c*, comprising tests of naturalistic behaviours and appetitively-motivated tests of anxiety, anhedonia, and reward. Figure made with Biorender©.

2.2.2.1 Food/water consumption, body weight and nesting abilities

Mice were single-housed overnight (5pm-9am) in individually ventilated cages (14 × 32 × 13 cm), with *ad libitum* water and 7 g of regular chow (which was familiar to them). Cages were lined with sawdust bedding and contained a 3 g square of compressed cotton

("Nestlet", Datesand). Each morning (9am) food and water consumption were measured and nesting abilities were assessed using a 5-point scoring scale, as previously described (Deacon, 2006): 1 = minimum shredding (<10%) of the cotton, 2 = 10-50% of the cotton was shredded, 3 = most of the cotton was shredded (50-90%) but a nest configuration was lacking, 4 = identifiable nest site, but with flat walls, 5 = good circular nests with tall walls. If a nest had features associated with more than one score (e.g. circular configuration, but <50% of the cotton was shredded), the two relevant scores were averaged (Deacon, 2006). Nest building was assessed once, while food and water consumption were recorded over two nights, and measurements were averaged.

2.2.2.2 Non-anxiogenic open field

The non-anxiogenic open field was carried out to control for possible differences in locomotion and exploratory activity which will be relevant for interpreting the data from anxiety tests. Mice were exposed to a non-anxiogenic open field consisting of an empty square arena, with white plastic floor and grey wooden wall (50 × 50 cm) located in a dimly lit room. Mice were placed in the outer zone (close to the walls) and were then free to explore the arena for 10 min, as previously described (Seibenhener & Wooten, 2015). Locomotor activity was recorded with an overhead camera and ANY-maze software (Stoelting Europe) was used for offline analysis of total distance travelled and distance travelled in the outer and centre zones (15 cm radius).

2.2.2.3 Elevated plus maze (EPM)

The EPM is one of the most commonly used tests of unconditioned anxiety. It is based on the approach-avoid conflict, as mice prefer dark and enclosed spaces due to lower chance

of predation, but have an innate drive to explore in search of food, shelter, or mates. Specifically, in the EPM the open arms are brighter and more exposed than the closed arms and thus are aversive to mice (Komada et al., 2008; Lister, 1987; Pellow et al., 1985). Here, the EPM comprised a cross-shaped elevated maze (50 cm height) with two open arms (35 × 6 cm) perpendicular to two closed arms (35 × 6 cm, 20 cm walls) located in a dimly-lit room (Lister, 1987). Mice were placed in the closed arm (counterbalanced between the two closed arms), and left free to explore for 5 min. Movement on the EPM was monitored using an overhead camera. ANY-maze (Stoelting Europe) tracking software was used for offline analysis of time spent, distance travelled, latency to enter and number of entries into the open arms as measures of anxious behaviour. Total distance travelled was also measured.

2.2.2.4 Light/dark box

The light/dark box is also based on the approach-avoid conflict and takes advantage of the aversion of mice for bright and open spaces (Bourin & Hascoët, 2003; Crawley & Goodwin, 1980). Here, the light/dark box was made of wood, and comprised of a black covered compartment (21 × 16 cm, 16 cm walls) with a small doorway leading to a white and brightly lit open compartment (21 x 16 cm, 16 cm walls). The light source consisted of a lamp which illuminated the open compartment from above. Mice were placed into the dark compartment and were then free to explore both areas for 10 min, during which their movements were monitored via an overhead camera. Total entries and time spent in the light compartment were manually scored later off-line.

2.2.2.5 Marble burying

VGLUT3 cKO$^{5\text{-HT}}$ mice were exposed to the marble burying test as it has been reported that mice global VGLUT3 KO were faster to bury marbles compared to controls, which was interpreted as neophobia (Amilhon et al., 2010). The marble burying test is based on the tendency of rodents to bury novel objects. Specifically, sawdust digging and burying behaviour has been previously used to model stereotypes typical of obsessive-compulsive disorders (De Brouwer et al., 2019). Here, the marble burying test was carried out using a clean cage (14 × 32 × 13 cm) containing a 5 cm layer of sawdust bedding and 12 colourful glass marbles (20 mm diameter), which were positioned on surface of the sawdust, evenly spaced in four rows of three. All mice were injected with saline *i.p.* (as the data reported here were part of a larger pharmacological study) and were individually placed in the cage for 30 min. In between animals the bedding was flattened and marbles were wiped with 0.5% Anistel (Tristel) to remove odours. Burying activity was recorded by an overhead camera. Latency to start digging anywhere in the cage, and number of marbles buried (in 3 min time bins) were obtained from the video recordings. A marble was considered buried when over two-thirds of its surface was covered in sawdust, as previously described (Amilhon et al., 2010; Deacon, 2009).

2.2.2.6 Novelty-induced hyponeophagia

Mice were food deprived overnight and novelty-induced hyponeophagia was conducted the following day (~18 hr later), as previously described (Barkus et al., 2012; Santarelli et al., 2003). Specifically, at 6:00 pm mice were weighed, and the chow was removed from their home cage. The test was conducted the following day from 11:30 am onwards, and mice were weighed prior to testing to ensure that their body weight had not fallen below

90%. The testing apparatus consisted of a white plastic arena covered with an upturned transparent jug (15 cm diameter) with a spout protruding 2cm to a food well. The well was filled with 50% sweetened condensed milk in water, which was novel to the mice. Mice were tested across a maximum of three 120 s trials, during which latency to approach the novel food (e.g. by sniffing it or moving in close proximity) and latency to continuously drink were both manually recorded. In between each trial mice were placed in a clean cage. When drinking commenced, the trial would end, the mice would be removed from the apparatus, and no further trials would take place. If a mouse did not drink during the three trials, the latency was recorded as 360 s.

2.2.2.7 Sucrose preference test

The sucrose preference test was conducted in the dark phase, over four consecutive evenings, as previously described (Strekalova & Steinbusch, 2010). For the first two evenings (3 h each) mice were single-housed and habituated to the testing setup. This consisted of an open top cage (42 × 22 cm, 20 cm walls) lined with bedding, two water bottles and food available *ad libitum*. On the third evening (2 h) mice were offered 2.5% sucrose in a single bottle to reduce neophagia for the sucrose solution during the testing day. The testing took place on the fourth evening (7 h) when the mice were presented with one bottle containing water and another one containing 1 % sucrose. Previous evidence suggests that pre-exposure to sucrose (e.g. to reduce hyponeophagia) might increase sucrose preference, leading to potential ceiling effects. To avoid this, it is recommended to use a reduced sucrose concentration in the test phase, compared to the pre-exposure (Serchov et al., 2016; Strekalova et al., 2006). On the third and fourth evenings the positions of the bottles were swapped half-way through the session to

reduce the influence of any side preference. Following testing on day 4, sucrose preference was measured as 1% sucrose consumption minus water consumption.

2.2.2.8. Appetitively-motivated spatial reference memory test

To investigate reward function in VGLUT3 cKO$^{5\text{-HT}}$ mice, an appetitively-motivated, spatial reference memory test was carried out over 11 days (Barkus et al., 2012). From the day before testing and till the end of the experiment mice underwent food restriction to 90% of initial body weight. Mice were weighed daily after the task and chow was administered to group-housed mice. The specific amount of chow was dependent on weight loss. If a given mouse showed significantly less weight loss compared to cage-mates, it was housed individually. The apparatus consisted of a wooden elevated Y maze painted black (arms 50 × 9 cm, 0.5 cm high walls) placed in a room containing a variety of extra-maze cues (e.g. colourful posters and large objects). At the end of each arm, furthest from the centre, a food well was located. Prior to testing, each mouse was assigned a "target" arm which was always rewarded with 50% sweetened condensed milk in water throughout the testing. The "target" arm referred to a specific position of the arm within the testing room, requiring the mice to use allocentric extra-maze cues as opposed to intra-maze cues. Mice underwent one habituation day (during which they were allowed to freely explore the maze) and then 10 training days with 10 trials per day. In each trial mice were placed on the start arm, furthest from the centre of the maze. Mice were then allowed to reach the centre area and enter one arm of their choice. If their chosen arm was their "target" arm, they were allowed to drink the reward and this was recorded as a correct response. Conversely, if their chosen arm was unrewarded, the mice were removed from the apparatus after reaching the empty food well, and this was recorded as an incorrect response. In between trials mice were single-housed in clean

cages. On the final day of testing, to ensure that the reward was not providing a direct olfactory cue itself, the rewarded arm was baited only after the mice had made a choice and reached the target arm (i.e. post-choice baiting). The starting arm (i.e. either of the two arms that weren't baited) was assigned pseudo-randomly for each trial but was counterbalanced between groups, with equal number of left and right rewarded trails within a 10 trial block, and no more than 3 consecutive left or right trials. The target arms were also counterbalanced across groups and the maze was rotated 120° every few trials to avoid the use of intra-maze cues. Daily % of correct arm entries were recorded for each mouse.

2.2.3 Immunohistochemistry and microscopy

2.2.3.1 Perfusion fixation

Mice were deeply anesthetised by intraperitoneal (*i.p.*) injection of pentobarbitone 5 mg/kg, and intracardially perfused with phosphate buffered saline (PBS, Sigma Aldrich) followed by a fixative solution of 4% paraformaldehyde (PFA, Sigma Aldrich) in PBS. Brains were dissected, post-fixed by immersion in the same fixative for 48 h at 4°C, then stored long-term in cryoprotective 30% sucrose (Sigma Aldrich) in PBS at 4°C.

2.2.3.2 Brain sectioning

Prior to sectioning, fixed brains were coated in Cryo-M-Bed embedding compound (Bright) and stored at -80°C for 45 min. Coronal sections (30 µm) were cut using a Bright LOFT cryostat, and free-floating sections were stored in antifreeze solution (40% PBS, 30% ethylene glycol, 30% bi-distilled glycerol, all Sigma Aldrich) at -20 °C until use. Midbrain sections were selected based on their distance from Bregma (AP= -4.7 to 4.8 mm) to contain the DRN (Franklin & Paxinos, 1997).

2.2.3.3 Immunohistochemistry

Immunohistochemistry was performed as previously described (Sengupta & Holmes, 2019). Briefly, sections were washed 3 x 10 min in 500 µl PBS, 10 min in 500 µl ammonium chloride and 3 x 10 min in 500 µl PBS with 0.3% Tween (Sigma Aldrich; PBS-T). Next sections were blocked in PBS-T with 10% donkey serum (Sigma Aldrich) for 1 h at room temperature. Sections were then incubated in primary antibodies (***Table 2.1***) made up in PBS-T with 2% donkey serum for 1 h at room temperature then overnight at 4^{o}C.

Table 2.1 | Antibodies used for immunohistochemistry.

Target	Host	Conjugate	Concentration	Company	Ref. number
Primary antibodies					
TPH2	Goat	N/A	1:1000	Abcam	Ab121013
VGLUT3	Guinea Pig	N/A	1:500	Synaptic Systems	135-204
Secondary antibodies					
Goat IgG (H+L)	Donkey	Alexa Fluor 647	1:1000	Invitrogen	A21206
Guinea Pig Cy3	Donkey	Cy3	1:1000	Jackson Immuno Research	706-165-148

The next day, sections were washed 2 x 10 min in 500 µl PBS-T before incubating with secondary antibodies (***Table 2.1***) made up in 500 µl PBS-T with 2% donkey serum for 2 h at room temperature. Then, sections were washed 2 x 10 min in 500 µl PBS-T, and cell nuclei were stained using DAPI (1:1000, 5 min), prior to a 10 min wash in PBS. Sections were mounted onto glass slides with Vectashield Antifade Mounting Medium (Vector Laboratories) and covered with a glass coverslip, prior to being stored in the dark at 4^{o}C.

2.2.3.4 Imaging and analysis

Images were acquired using an Olympus Epifluorescence Microscope BX40 with ImageJ Micromanager v1.4 with 500 ms exposure. Specifically, the ventral DRN was imaged at 20x magnification, including an area of 0.14 mm^2 (Paxinos & Franklin, 2001). Cell

counting and quantification of colocalisation was performed employing the ImageJ Software package, by an experimenter blind to treatment. A graticule (Graticules Optics Ltd) was used to ascertain the area of the region of interest.

For each mouse, the mean cell count of three sections was used for statistical analysis. TPH2-immunoreactive neurons were defined as neurons where TPH2 immunoreactivity colocalised with DAPI immunoreactivity. Colocalisation between DAPI, TPH2 and VGLUT3 identified TPH2/VGLUT3 double-labelled neurons.

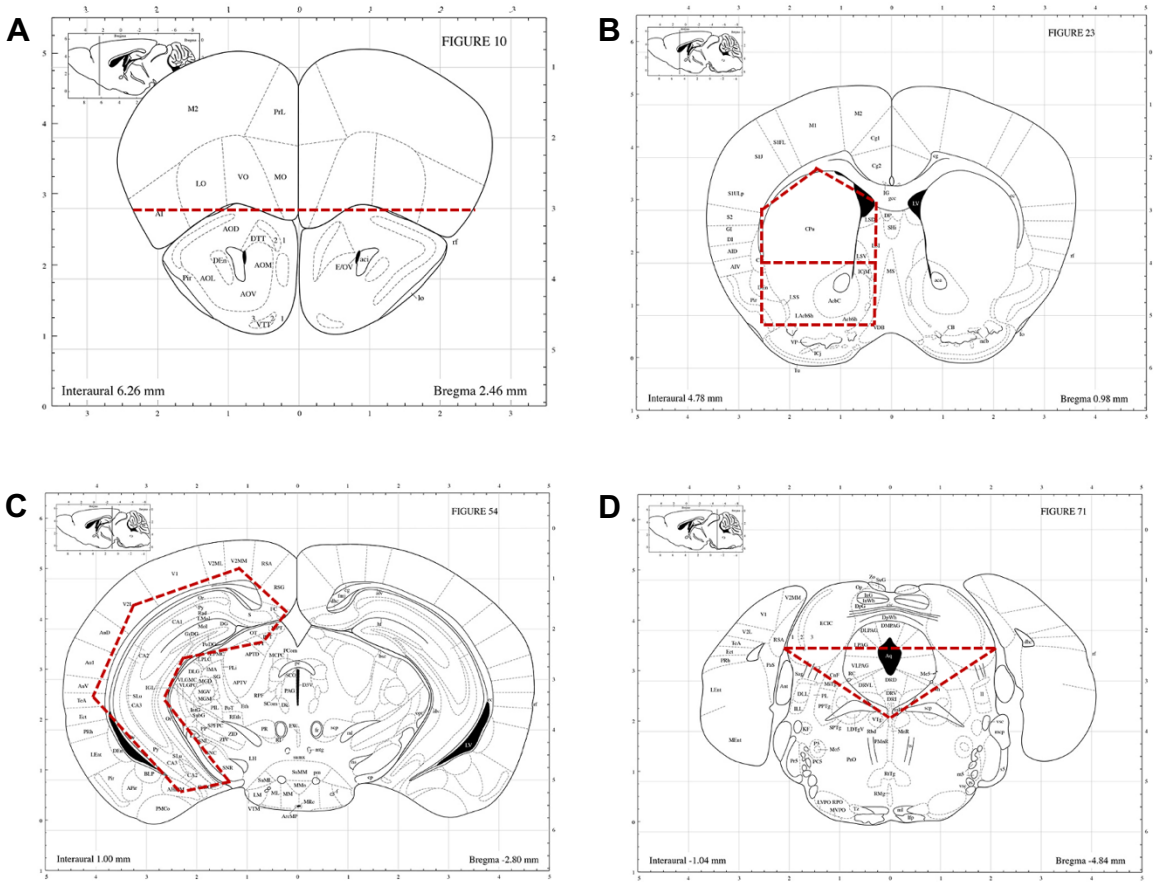

Figure 2.3 | Dissected regions of interest based on stereotaxic atlas. Dissection were based on Franklin & Paxinos, 1997. Regions were **(A)** prefrontal cortex, **(B)** dorsal striatum and NAc, **(C)** hippocampus, **(D)** dorsal raphe region (including ventrolateral periaqueductal gray). Red dashes indicate the approximate location of the scalpel cuts.

2.2.4 Frozen tissue collection and dissections

For qPCR and HPLC-ED experiments mice were culled by cervical dislocation followed by decapitation. Mice used in these experiments had previously undergone behavioural testing, but were culled at least one week after any testing took place to avoid any potential effect of behavioural testing or handling on gene expression and neurochemistry. After decapitation brains were quickly removed and frozen in dry ice-cold isopentane (Sigma-Aldrich) prior to long-term storage at -80°C. Prior to dissection, frozen brains were left to acclimatise to -20°C for 15 mins and then 1 mm thick coronal frozen slices were cut using a stainless-steel brain slicer (Zivic Instruments) with fine edge blades. Fine forceps and a scalpel were then used to isolate the prefrontal cortex, NAc, dorsal striatum, hippocampus, and dorsal raphe region (including both the DRN and ventrolateral periaqueductal gray; as shown in ***Fig. 2.3***), based on their anatomical locations (Franklin & Paxinos, 1997).

2.2.5 Quantitative real-time polymerase chain reaction (qPCR)

2.2.5.1 RNA extraction

Following dissection (as described in *Section 2.2.4*), samples containing the prefrontal correct, hippocampus, DRN, and NAc were placed into empty RNase-free Eppendorf tubes on dry ice and stored at -80°C until RNA extraction. RNA was extracted using the TRIzol method (Rio et al., 2010) as previously described. Briefly, samples were immersed in 500 µl of TRIzol (Invitrogen) prior to being homogenised with an RNAse free pestle. Next, 250 µl of chloroform (Sigma-Aldrich) was added to the samples followed by centrifugation for 15 min at 10,000 rpm. RNA was then isolated using the Qiagen RNeasy Mini Kit, according to manufacturer's instructions. This involved washing the lysate with 70% ethanol to

provide appropriate conditions for binding the RNA to the RNeasy silica membrane, thereby allowing contaminants to be washed away with appropriate buffers. Finally, RNA was eluted into 20 µl RNase-free water and both total RNA and RNA purity were immediately measured using a NanoDrop (ThermoFisher). If the 260/280 nm ratio (indicating RNA purity) was between 1.8 and 2.2, the sample was deemed sufficiently pure for cDNA conversion. RNA was stored at -80°C until cDNA conversion.

2.2.5.2 cDNA conversion

DNA conversion and qPCR were conducted as described previously (Radford-Smith et al., 2022). For each reaction, 800 ng of RNA was converted to cDNA using a high-capacity cDNA Reverse Transcription Kit (Life Technologies), relying on the random primers method for initiating cDNA synthesis as per the manufacturer's instructions. The obtained reaction solution was processed using a T100 Thermocycler (Bio-Rad) for 10 min at 25°C, 120 min at 37°C and 5 min at 85°C. Following reverse transcription, cDNA was stored at -20°C until qPCR analysis.

2.2.5.3 Primers

Wherever possible previously published primers were used (as detailed in ***Table 2.2***), otherwise primers were designed using the National Center of Biotechnology Information (NCBI) Primer-BLAST tool (Ye et al., 2012). Optimal primer pairs aimed to meet the following specifications whenever possible (ThermoFisher Scientific, 2019): crossing one exon-exon boundary, comprising of 18-24 bases, having no self-dimers, no secondary structures, and no off-target binding, producing a product of 70-200 bases with 40-60% GC content, having annealing temperatures between 65-75°C and within

5°C of each other. Primer details were confirmed using the NCBI Primer-BLAST tool (Ye et al., 2012), Oligo Analysis Tool (Eurofins Genomics, 2024) and the OligoEvaluator Tool (Sigma-Aldrich, 2014). VGLUT3 primers (*Slc17a8* gene) were designed specifically to target exon 2, as this is where the VGLUT3 knockout is located (Fasano et al., 2017). After determining suitable primers, these were custom-made by ThermoFisher, except for glyceraldehyde 3-phosphate dehydrogenase (GAPDH) which was pre-designed (Santa Cruz Biotechnology).

Table 2.2 | Details of the primer sequences for qPCR analysis

Gene	Forward Sequence (5' to 3')	Reverse sequence (5' to 3')	Sequence source
VGLUT3 (Slc17a8)	CGATGGGACCAATGAAGAGGA	CAGTCACAGACAGGGCGATG	Designed
VGLUT1 (Slc17a7)	TCGTACCCATTGGAGGCCAG	AGTGCGAGTATCCGACCACC	Designed
VGLUT2 (Slc17a6)	CTGTCCGTGGTCCTGAAATGC	CCGGGGGAGACCTTCCATAAA	Designed
VMAT2 (Slc18a20)	CATCACGCAGACTTGAAAGAC	CGCCTCGCCTTGCTTATCC	(Hwang et al., 2009).
Tph2	CAGGGTCGAGTACACA GAAG	CTTTCAGAAACATGGA GACG	(Vogelgesang et al., 2017)
5-HTT (Slc6A4)	TGCCTTTTATATCGCCT CCTAC	CAGTTGCCAGTGTTCCA AGA	(Couch et al., 2015)
5-HT$_{1A}$	GACAGGCGGCAACGA TACT	CCAAGGAGCCGATGAGA TAGTT	(Gorlova et al., 2020)
5-HT$_{1B}$	CCCATCAGCACCATGT ACAC	GACTTGGTTCACGTACAC AG	(Guilloux et al., 2011)
5-HT$_{2A}$	CAGGCAAGTCACAGGA TAGC	TTAAGCAGAAAGAAAA TCCCACAG	(Couch et al., 2015)
5-HT$_{2C}$	CTAATTGGCCTATTGGTTTGGCA	CGGGAATTGAAACAAGCGTCC	(Veniaminova et al., 2020)
5-HT$_{4}$	CCTCACAGCAACTTCTC CTT	TCCCCTGACTTCCTCAA ATA	(Vogelgesang et al., 2017)
β-actin	CATTGCTGACAGGATG CAGAAGG	TGCTGGAAGGTGGACA GTGAGG	(Yu et al., 2019)
DA1	CTCCCAGATCGGGCATTTG	CTTCTGGGTTCAGTGCTCCA	Designed
DA2	ATCTCTTGCCCACTGCTCTTTGGA	ATAGACCAGCAGGGTGACGAT GAA	(Kramer et al., 2011)

2.2.5.4 qPCR

QPCR was performed using a LightCycler® 480 instrument (Roche Diagnostics). Primers were used at 300 nM, with a total of 10 µl reaction volume used per well in a 384 well plate, which contained 5 µl Precision®PLUS qPCR Master Mix with SYBRgreen (Primer Design). For each reaction 25 ng cDNA was made up in RNase-free water. The following PCR reaction cycle was used: enzyme activation for 2 min at 95°C, then 40 cycles of 10 s at 95°C and 1 min at 60°C, then held at 4°C. Generation of a melt curve was included in each experiment to confirm that only one PCR product was generated. All samples were run in triplicates. Since normalising to the housekeeping gene GAPDH or β-actin did not affect the results, data were normalised to GAPDH only.

2.2.5.5 qPCR analysis

The ΔCt method was employed to analyse qPCR data using Microsoft Excel. Triplicates were averaged to give a Ct (threshold cycle) value for each target gene per animal (values from failed cycles or large outliers were not included in the Ct values). For each target gene, the Ct of the housekeeping gene was subtracted from the Ct of the target gene ($\Delta CT = CT_{\text{target gene}} - CT_{\text{houekeeping gene}}$). The mean ΔCt for the control group was then subtracted from each gene ΔCt value (ΔΔCt). Fold changes in gene expression relative to control were calculated per animal and gene as $2^{-\Delta\Delta Ct}$. Outliers were identified in the $2^{-\Delta\Delta Ct}$ values using ROUT analysis (GraphPad Prism), and these mice excluded from the raw data for that particular gene. The ΔCt method was then reapplied on the cleaned dataset to recalculate fold changes.

2.2.6 High performance liquid chromatography (HPLC) with electrochemical detection (ED)

HPLC-ED was used to measure concentrations of 5-HT, 5-HIAA, DA and 3,4-dihydroxyphenylacetic acid (DOPAC). The HPLC-ED system consisted of an amperometric detector (Bioanalytical SystemsLC-4/C and CC-4 analyser), 4.6×150 mm column (Waters Spherisorb, ODS2, 3 μm), and a dual 3mm glassy carbon electrode (Basi) set at +0.7 V. The mobile phase comprised of 12.5% (v/v) methanol, 0.85 mM EDTA disodium salt (VWR Int. ltd), 0.13 M sodium phosphate monobasic (Sigma-Aldrich), 0.025 mM 1-octane sulfonic acid sodium salt (Fisher Scientific) dissolved in distilled water. The mobile phase was filtered using Merck Millipore 0.22 μm MCE membranes and a vacuum pump, and adjusted to pH 3.3 using phosphoric acid (Acros Organics). Samples were run at 1.0 mL/min flow rate. Peak times and heights were plotted on an integrator (ChromJet CH1, Thermo Separation Products).

An external standard method was used for quantification. Standard concentrations of each neurotransmitter were made up in 0.09 M perchloric acid (PCA, Fisher Scientific). A representative chromatogram of a standard solution comprising of 5 pmol of 5-HT creatinine sulphate monohydrate, 5-HIAA, DA hydrochloride and DOPAC is presented in ***Fig. 2.4B***. Prior to analysis, a standard curve for each neurotransmitter was made to verify the system could quantify the analytes linearly at the required concentration range (0.5-10 pmol/50μl sample). Appropriate attenuation, inhibit integrate and autozero functions were used as exemplified in ***Fig. 2.4A*** to allow for accurate quantification of each neurotransmitter.

Figure 2.4 | Representative chromatograms and time functions used. (A) Representative time functions (TT) used, **(B)** representative chromatograms for a standard solution, **(C)** representative chromatograms of a dorsal raphe sample**.** Peak height in AU, concentration in nM. Numbers next to peaks indicate retention time (min).

A

TT(1)=	0.1	TF(1)="AZ"	TV(1)= 1.
TT(2)=	0.15	TF(2)="II"	TV(2)= 1.
TT(3)=	0.2	TF(3)="AT"	TV(3)= 64.
TT(4)=	2.1	TF(4)="II"	TV(4)= 0.
TT(5)=	2.2	TF(5)="AT"	TV(5)= 64.
TT(6)=	4.	TF(6)="II"	TV(6)= 1.
TT(7)=	4.2	TF(7)="II"	TV(7)= 0.
TT(8)=	5.	TF(8)="AT"	TV(8)= 64.
TT(9)=	14.	TF(9)="ER"	TV(9)= 1.
TT(10)=	16.	TF(10)="ER"	TV(10)= 1.

TT: time within a run

TF: time functions
AZ: autozero
II: inhibit integrate
AT: attenuation
ER: end run

TV: 1= on, 0=off,
64=attenuation setting

B

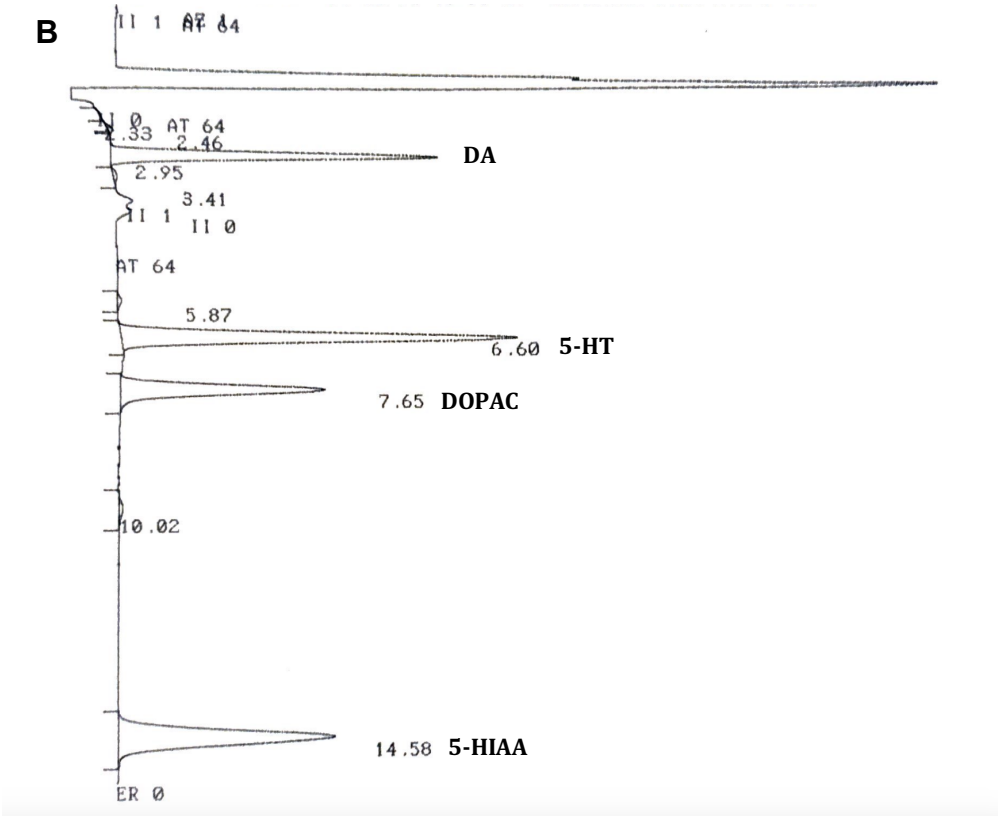

Name	Concentration	Retention time	Peak height
1	0.	2.33	395 02
2	0.	2.46	509 03
DA	5.	2.95	28359 02
4	0.	3.41	281 03
5	0.	5.87	299 01
5HT	5.	6.6	34683 01
DOPACC	5.	7.65	17784 01
8	0.	10.02	378 01
5HIAA	5.	14.58	18739 01
TOTALS	20.		101427

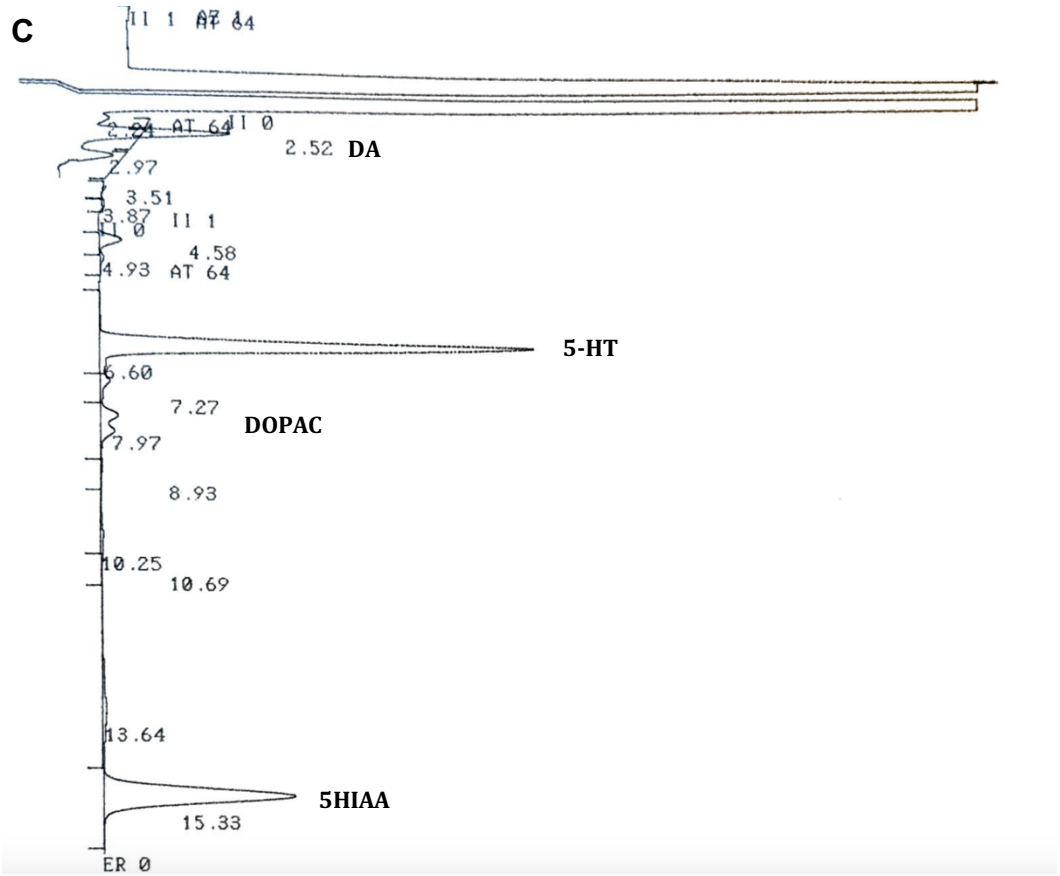

2.2.6.1 Sample preparation

Frozen tissue samples (dissected as described in *Section 2.2.4*) were placed into Eppendorf tubes containing 500µl of 0.09 M PCA and weighed. Next, samples were sonicated and centrifuged at 13,000 rpm for 15 min at 4°C. The supernatants were analysed with HPLC-ED to calculate the concentration of 5-HT, 5-HIAA, DA and DOPAC, expressed as nmol/mg of wet tissue. 5-HT turnover was calculated as the ratio of 5-HIAA to 5-HT concentration (5-HIAA/5-HT ratio), while DA turnover was calculated as the ratio of DOPAC to DA concentration (DOPAC/DA ratio). An example chromatogram is presented in ***Fig. 2.4C***.

2.2.7 Statistical Analysis

The Shapiro-Wilk test for normality was applied to all data sets. If data were normally distributed, then either a t test alone, or a one/two-way ANOVA was carried out as appropriate. For two-way analysis with repeated measures, a two-way ANOVA was used on dataset with no missing values, while a mixed effect model was employed in presence of missing values or unbalanced dataset (e.g. due to technical issues or outlier removal). If data were non-parametric then a Mann-Whitney test was employed where appropriate. Tukey's post hoc was used for balanced data (e.g. behavioural data), while Šídák's post hoc was selected for unbalanced data and repeated measures analyses (e.g. neurochemistry analysis). ROUT analysis was used to remove significantly outlying datapoints from qPCR and HPLC experiments. Parametric data are presented as mean ± standard error of the mean (SEM), whilst non-parametric data are presented as median ± interquartile range values; $p<0.05$ was considered statistically significant. GraphPad Prism (v10) was used for analysis and plotting of graphs.

2.3 Results

2.3.1 Validation of the novel VGLUT3 cKO$^{5\text{-HT}}$ mouse model

Firstly, deletion of VGLUT3 was confirmed in the DRN of VGLUT3 cKO$^{5\text{-HT}}$ mice. Initial qPCR analysis demonstrated a 33.9 ± 5.7 % reduction of VGLUT3 mRNA in the DRN of VGLUT3 cKO$^{5\text{-HT}}$ mice compared to controls ($t_{(14)}=3.734$, $p=0.002$; ***Fig 2.5B***). Conversely, no changes in VMAT2 ($t_{(14)}=0.366$, $p=0.720$, ***Fig 2.5B***), VGLUT1 or VGLUT2 expression (***Table 2.3***) were found in the DRN of VGLUT3 cKO$^{5\text{-HT}}$ mice.

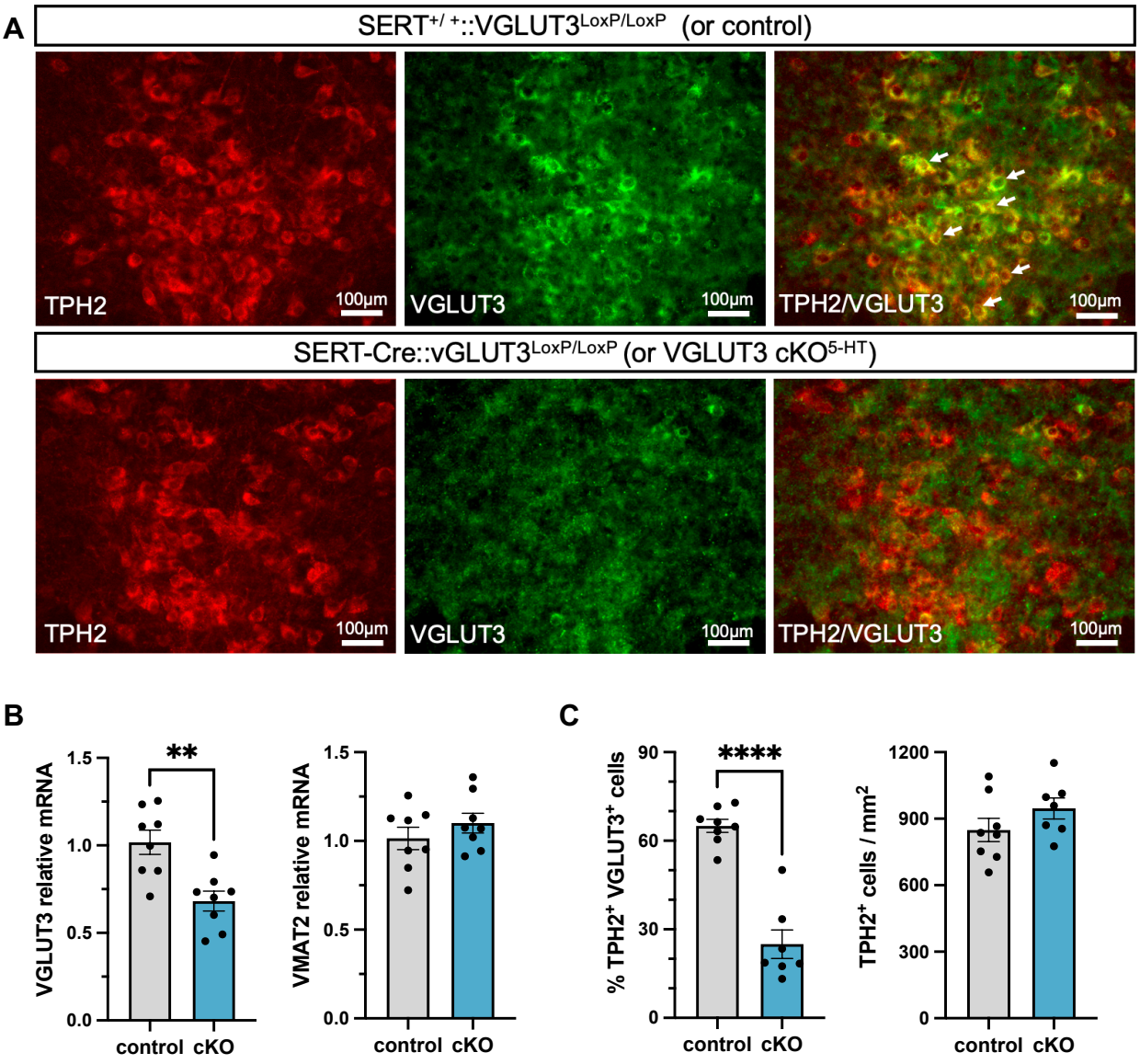

Figure 2.5 | Molecular characterisation of VGLUT3 cKO$^{5\text{-HT}}$ mice. (A) Representative image of TPH2/VGLUT3 double-labelled neurons (white arrows) in the ventral DRN of control mice (top) and VGLUT3 cKO$^{5\text{-HT}}$ (bottom). **(B)** VGLUT3 and VMAT2 mRNA in the midbrain raphe region of VGLUT3 cKO$^{5\text{-HT}}$ mice (n=8) and littermate controls (n=8). **(C)** Percentage of TPH2 neurons co-labelled with VGLUT3, and number of TPH2 neurons in the ventral DRN of VGLUT3 cKO$^{5\text{-HT}}$ mice (n=7) and littermate controls (n=8). Columns are mean ± SEM values. Individual values are indicated by closed circles. Analysed by unpaired t test. **** $p<0.0001$ ** $p<0.01$

However, qPCR analysis measures VGLUT3 expression both in dual 5-HT-glutamate neurons and in purely glutamatergic neurons. Therefore, VGLUT3 expression was then assessed specifically in 5-HT neurons, as identified by the 5-HT-specific marker TPH2 using immunohistochemistry (***Fig. 2.5A***). The number of TPH2/VGLUT3 co-labelled neurons in the ventral DRN of VGLUT3 cKO$^{5\text{-HT}}$ mice was reduced by 62.6 ± 4.8 % compared to controls ($t_{(13)}$=7.879, p<0.0001, ***Fig. 2.5C***). The number of TPH2-immunoreactive neurons in the ventral DRN was not different between VGLUT3 cKO$^{5\text{-HT}}$ mice and controls ($t_{(13)}$=1.365, p=0.195, ***Fig. 2.5C***). Altogether, this confirms a reduction in VGLUT3 expression specific to ventral 5-HT neurons.

2.3.2 Assessment of 5-HT and DA function in VGLUT3 cKO$^{5\text{-HT}}$ mice

Gene expression analysis of a wide panel of 5-HT-related genes was carried out to further investigate 5-HT function in VGLUT3 cKO$^{5\text{-HT}}$ mice. Specifically, gene expression of Tph2 and 5-HTT, $5HT_{1A}$, $5HT_{1B}$, $5HT_{2C}$, 5-HT_4 receptors was assessed in the DRN, expression of 5-HT_{1A}, 5-HT_{1B}, 5-HT_{2A}, 5-HT_{2C}, and 5-HT_4 receptors was measured in the hippocampus and prefrontal cortex. Additionally, expression of DA receptors D_1, D_2 and expression of $5HT_{1A}$, $5HT_{1B}$, $5HT_{2A}$, 5-HT_{2C} receptors was measured in the NAc, due to links between 5-HT-glutamate co-release and DA reward function. Interestingly, $5HT_{1A}$ expression was increased in the prefrontal cortex of VGLUT3 cKO$^{5\text{-HT}}$ mice, compared to control (***Table 2.3***). Additionally, D_1 and 5-HT_{1B} receptors expression were also increased in the NAc of VGLUT3 cKO$^{5\text{-HT}}$ mice compared control (***Table 2.3***). No other statistically significant changes in gene expression were observed in the DRN, hippocampus, prefrontal cortex, and NAc of VGLUT3 cKO$^{5\text{-HT}}$ mice compared to controls (***Table 2.3***).

Table 2.3 | Gene expression in the DRN, hippocampus, prefrontal cortex, and NAc of VGLUT3 cKO$^{5\text{-HT}}$ mice, compared to controls. Genes of interest were VGLUT1, VGLUT2, a panel of 5-HT-related genes, DA D_1 and D_2 receptors. Groups were VGLUT3 cKO$^{5\text{-HT}}$ mice (n=8) and (n=8 for DRN, hippocampus, NAc; n=11 for prefrontal cortex). Variability in group size was due to outlier removals by ROUT analysis, or missing values due to technical issues**.** Analysed by unpaired t test. * $p<0.05$.

	Relative mRNA (mean ± SEM)		
Gene of interest	**Control**	**VGLUT3 cKO$^{5\text{-HT}}$**	**t test**
Dorsal raphe region			
VGLUT1 (Slc17a7)	1.0 ± 0.0	1.0 ± 0.0	$t_{(14)}$=0.156, p=0.878
VGLUT2 (Slc17a6)	1.0 ± 0.3	1.3 ± 0.3	$t_{(12)}$=0.639, p=0.535
Tph2	1.0 ± 0.1	1.1 ± 0.1	$t_{(14)}$=0.532, p=0.603
5-HTT	1.0 ± 0.1	1.2 ± 0.1	$t_{(14)}$=1.396, p=0.184
5-HT_{1A}	1.0 ± 0.1	1.1 ± 0.1	$t_{(14)}$=0.649, p=0.527
5-HT_{1B}	1.0 ± 0.1	1.0 ± 0.1	$t_{(14)}$=0.554, p=0.588
5-HT_{2c}	1.0 ± 0.1	1.0 ± 0.0	$t_{(14)}$=0.169, p=0.868
5-HT_4	1.0 ± 0.1	1.2 ± 0.1	$t_{(14)}$=1.388, p=0.187
Hippocampus			
5-HT_{1A}	1.0 ± 0.1	1.1 ± 0.1	$t_{(14)}$=0.987, p=0.341
5-HT_{1B}	0.9 ± 0.1	0.9 ± 0.1	$t_{(13)}$=0.386, p=0.706
5-HT_{2A}	0.9 ± 0.1	1.1 ± 0.1	$t_{(13)}$=1.344, p=0.202
5-HT_{2C}	1.2 ± 0.1	1.3 ± 0.1	$t_{(14)}$=0.318, p=0.755
5-HT_4	1.0 ± 0.1	1.1 ± 0.1	$t_{(14)}$=0.903, p=0.382
Prefrontal cortex			
5-HT_{1A}	1.1 ± 0.2	2.0 ± 0.2	$t_{(15)}$=2.486, p=0.025 *
5-HT_{1B}	1.0 ± 0.1	1.0 ± 0.2	$t_{(17)}$=0.150, p=0.883
5-HT_{2A}	1.0 ± 0.1	1.1 ± 0.2	$t_{(17)}$=0.358, p=0.725
5-HT_{2C}	1.1 ± 0.2	1.6 ± 0.3	$t_{(17)}$=1.325, p=0.203
5-HT_4	1.3 ± 0.4	0.8 ± 0.1	$t_{(17)}$=1.441, p=0.168
Nucleus accumbens			
DA D_1	1.1 ± 0.2	1.9 ± 0.2	$t_{(14)}$=2.537, p=0.024 *
DA D_2	1.1 ± 0.2	1.0 ± 0.1	$t_{(14)}$=0.822, p=0.425
5-HT_{1A}	1.1 ± 0.1	0.9 ± 0.1	$t_{(14)}$=1.180, p=0.258
5-HT_{1B}	1.1 ± 0.2	1.7 ± 0.2	$t_{(14)}$=2.512, p=0.025 *
5-HT_{2A}	1.0 ± 0.1	0.9 ± 0.1	$t_{(14)}$=0.848, p=0.411
5-HT_{2C}	1.1 ± 0.1	1.2 ± 0.1	$t_{(14)}$=0.670, p=0.514

Ex vivo neurochemistry revealed no statistically significant difference in 5-HT levels in the prefrontal cortex, hippocampus, DRN, dorsal striatum or NAc of VGLUT3 cKO$^{5\text{-HT}}$ mice compared to controls (***Fig. 2.6A***). A repeated measure mixed effect model found an effect of region ($F_{(4, 92)}$=34.66, p<0.0001) but no effect of genotype ($F_{(1, 22)}$=0.1876, p=0.666), or genotype x region interaction ($F_{(4, 84)}$=0.353, p=0.842). Interestingly, analysis of 5-HIAA levels showed both an effect of region ($F_{(4, 84)}$=51.36, p<0.0001) and a strong trend effect of genotype x region interaction ($F_{(4, 80)}$=2.405, p=0.056), but no effect of genotype alone ($F_{(1, 23)}$=0.467, p=0.501). Šídák's multiple comparisons test revealed a reduction (p=0.035; ***Fig. 2.6B***) in 5-HIAA in the DRN of VGLUT3 cKO$^{5\text{-HT}}$ mice compared to controls, and no statistically significant effects in any other region. Similarly, analysis of the 5-HIAA/5-HT ratio found an effect of region ($F_{(4, 72)}$=73.96, p<0.0001) but no effect of genotype ($F_{(1, 22)}$=1.412, p=0.135), but a trend effect of region x genotype interaction was identified ($F_{(4, 72)}$=2.317, p=0.065). Whilst strictly not appropriate due to the lack of a statistically significant interaction, Šídák's post hoc analysis revealed a significant reduction (p=0.009; ***Fig. 2.6C***) in the 5-HIAA/5-HT ratio in the DRN of VGLUT3 cKO$^{5\text{-HT}}$ mice compared to controls, while the 5-HIAA/5-HT ratio was not different in the remaining regions. Altogether this suggests a reduction in 5-HT turnover in the DRN of VGLUT3 cKO$^{5\text{-HT}}$ mice.

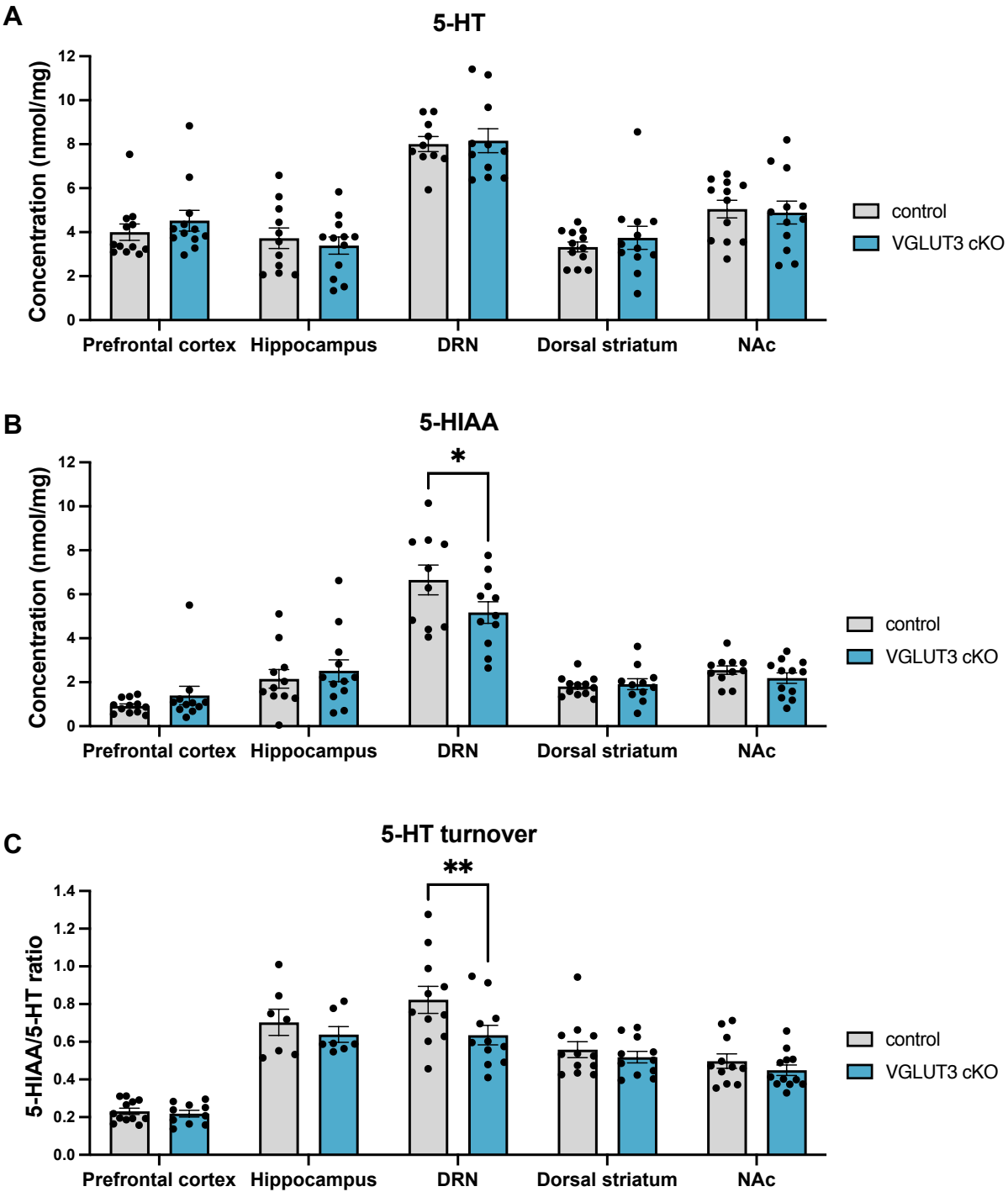

Figure 2.6 | *Ex vivo* 5-HT neurochemistry in VGLUT3 cKO$^{5\text{-HT}}$ mice and controls. Bars represent the mean ± SEM values for concentration of 5-HT **(A)**, 5-HIAA **(B)**, and the 5-HIAA/5-HT ratio **(C)**. Groups sizes were is n=7-12 per group. Variability in group size was due to outlier removals by ROUT analysis, and missing values due to technical issues**.** Individual values are indicated by closed circles. Analysed by repeated measures mix effect model, with post hoc Šídák's multiple comparisons test. *p<0.05.

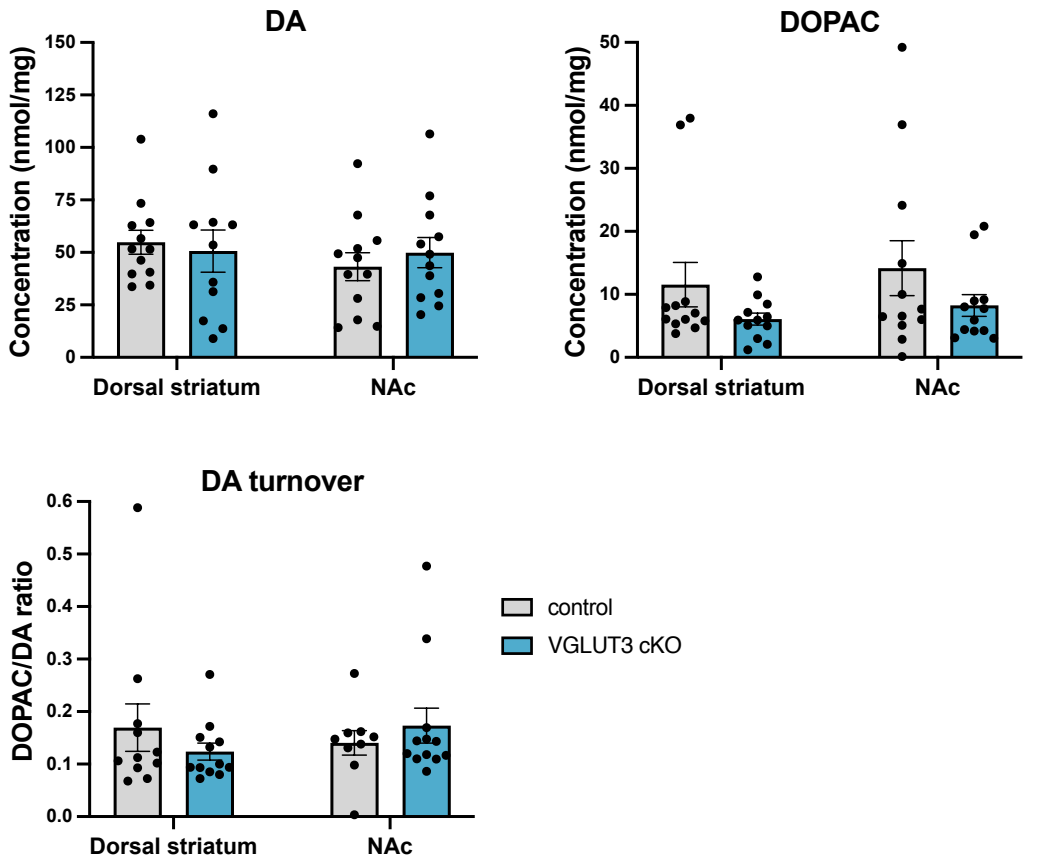

Figure 2.7 | *Ex vivo* DA neurochemistry in the dorsal striatum and NAc of VGLUT3 cKO$^{5\text{-HT}}$ mice and controls. Bars represent the mean ± SEM values for concentration of DA, DOPAC, and the DOPAC/DA ratio in VGLUT3 cKO$^{5\text{-HT}}$ mice (n=10-12) and controls (n=11-12). Variability in group size was due to outlier removals by ROUT analysis, and missing values due to technical issues**.** Individual values are indicated by closed circles. Analysed by repeated measures mix effect model, with post hoc Šídák's multiple comparisons test.

Ex vivo neurochemistry revealed no statistically significant difference in DA levels, in the dorsal striatum and NAc of VGLUT3 cKO$^{5\text{-HT}}$ mice compared to controls (effect of genotype: $F_{(1,\ 22)}$=0.012, p=0.915; region: $F_{(1,\ 22)}$=0.887, p=0.357; region x genotype interaction: $F_{(1,\ 22)}$=0.821, p=0.375; ***Fig. 2.7***). Analysis of DOPAC levels showed an effect of region ($F_{(1,\ 22)}$=0.735, p=0.401) but no effect of genotype ($F_{(1,\ 22)}$=3.315, p=0.082), or region x genotype interaction ($F_{(1,\ 22)}$=0.006, p=0.937; ***Fig. 2.7***). Analysis of the DOPAC/DA ratio also indicated no difference between groups (effect of genotype:

$F_{(1, 22)}$=0.039, p=0.845; region: $F_{(1, 22)}$=0.103, p=0.750; region x genotype interaction: $F_{(1, 22)}$=1.503, p=0.227; ***Fig. 2.7***).

2.3.3 Home cage food/water consumption, body weight, and nest building

Body weight, home cage food/water consumption and nest building were assessed to test whether appetite and general wellbeing of VGLUT3 cKO$^{5\text{-HT}}$ mice were altered, and therefore likely to disrupt other behavioural measurements. VGLUT3 cKO$^{5\text{-HT}}$ mice did not show any difference in body weight ($F_{(1, 68)}$=1.720, p=0.194) compared to controls, and there was no interaction between genotype and sex ($F_{(1, 68)}$=1.396, p=0.242). Home cage consumption of food ($t_{(70)}$=0.966, p=0.337, ***Fig. 2.8***) or water ($t_{(70)}$=0.551, p=0.584, ***Fig. 2.8***) was similarly unaffected. VGLUT3 cKO$^{5\text{-HT}}$ mice also showed unimpaired nesting abilities compared to control littermates (Mann-Whitney U=549, p=0.260, ***Fig. 2.8***).

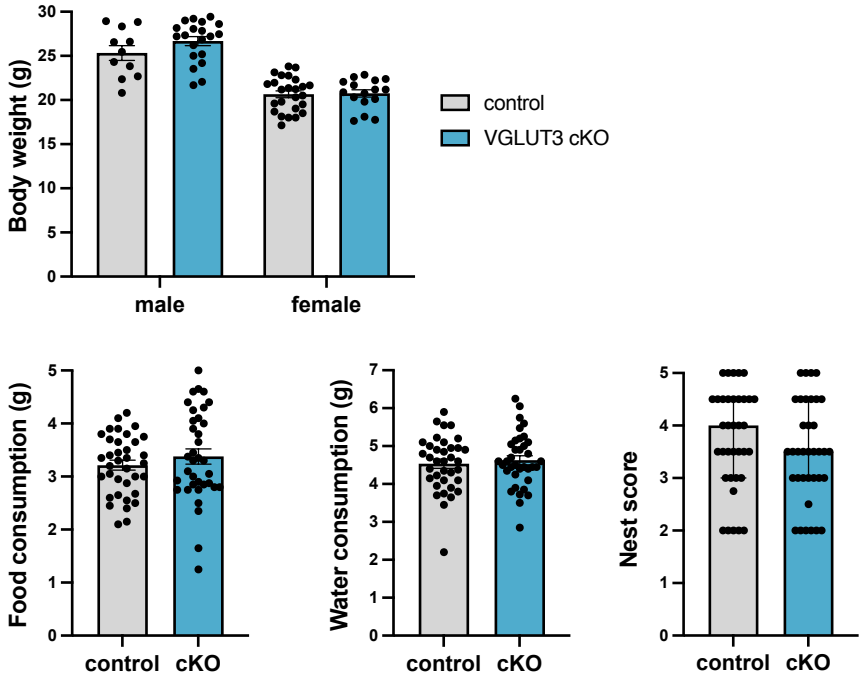

Figure 2.8 | Body weight, home cage food/water consumption, and nest building in VGLUT3 cKO$^{5\text{-HT}}$ mice and control littermates. Bars represent the mean ± SEM values, with the exception of the nest score where they indicate median ± interquartile range. Individual values are indicated

by closed circles. Groups were VGLUT3 cKO$^{5\text{-HT}}$ mice (n=36) and control littermates (n=36). Data were analysed with two-way ANOVA (body weight), unpaired t test (food and water consumption), and Mann-Whitney U (nest score).

2.3.4 Tests of anxiety-like behaviour and locomotion

To assess locomotor activity and exploration in a novel environment, VGLUT3 cKO$^{5\text{-HT}}$ mice and control littermates were exposed to a non-anxiogenic open field. Total distance travelled ($F_{(1,\ 21)}$=0.053, p=0.821; ***Fig. 2.9A***) and time spent in the centre zone ($F_{(1,\ 21)}$=0.018, p=0.894, ***Fig. 2.9A***) were not different between groups. Time spent in the centre zone was 13.8 ± 1.8 % of total time in the open field for VGLUT3 cKO$^{5\text{-HT}}$ mice and 14.5 ± 1.5 % for control littermates. Average speed was 5.9 ± 0.3 cm/s and 6 ± 0.3 cm/s for VGLUT3 cKO$^{5\text{-HT}}$ mice and controls, respectively. There was also no effect of sex or genotype x sex interaction on either distance travelled (sex: $F_{(1,\ 21)}$=1.874, p=0.186; genotype x sex interaction: $F_{(1,\ 21)}$=1.494, p=0.235) or time spent in the centre zone (sex: $F_{(1,\ 21)}$=0.116, p=0.736; genotype x sex interaction: $F_{(1,\ 21)}$=3.782, p=0.065).

The EPM also did not reveal differences between VGLUT3 cKO$^{5\text{-HT}}$ mice and control littermates. On the EPM there was no effect of genotype on the number of open arm entries ($F_{(1,\ 21)}$=0.004, p=0.952, ***Fig. 2.9C***), time spent in the open arms ($F_{(1,\ 21)}$= ***Fig. 2.9C***), latency to first enter the open arms ($F_{(1,\ 21)}$=0.015, p=0.904; ***Fig. 2.9C***), or total distance travelled ($F_{(1,\ 21)}$=0.001, p=0.973 ***Fig. 2.9C***). Time spent in open arms was 18.9 ± 2 % of total time on the apparatus for VGLUT3 cKO$^{5\text{-HT}}$ mice and the 16.9 ± 2.2 % for control littermates. There was also no effect of sex or genotype x sex interaction on the number of open arm entries (sex: $F_{(1,\ 21)}$=1.193, p=0.287; genotype x sex interaction: $F_{(1,\ 21)}$=0.847, p=0.368), time spent in the open arms (sex: $F_{(1,\ 21)}$=1.335, p=0.261; genotype x sex

interaction: $F_{(1, 21)}$=1.801, p=0.194), or total distance travelled (sex: $F_{(1, 21)}$=1.077, p=0.311; genotype x sex interaction: $F_{(1, 21)}$=0.464, p=0.503)

In the light/dark box there was no difference in the time spent in the light zone ($F_{(1, 21)}$=0.621, p=0.440, ***Fig. 2.9B***) or total entries ($F_{(1, 21)}$=0.241, p=0.629, ***Fig. 2.9B***) into the light compartment. Time spent in the light zone was 34 ± 4.5 % of total time in the apparatus for VGLUT3 cKO$^{5\text{-HT}}$ mice and the 30.7 ± 3.9 % for control littermates. There was also no effect of sex or genotype x sex interaction on the time spent in the light zone (sex: $F_{(1, 21)}$=3.286, p=0.084; genotype x sex interaction: $F_{(1, 21)}$=0.1478, p=0.705), or the number of light zone entries (sex: $F_{(1, 21)}$=0.069, p=0.795; genotype x sex interaction: $F_{(1, 21)}$=0.157, p=0.696).

In a separate cohort of mice, the marble burying test also revealed no statistically significant difference in the number of marbles buried over time by VGLUT3 cKO$^{5\text{-HT}}$ mice and control littermates ($F_{(1, 24)}$=2.42, p=0.133, ***Fig. 2.9D***). All mice progressively buried the marbles during the test (effect of time: $F_{(9, 216)}$=127, p<0.0001, ***Fig. 2.9D***), and there was no interaction between the effect of time and that of genotype ($F_{(9, 216)}$=0.596, p=0.800, ***Fig. 2.9D***). The latency to start burying was also not different between groups ($t_{(22)}$=1.080, p=0.292, ***Fig. 2.9D***). Sex effects were not investigated here, as this cohort was predominantly male, with only a few female mice.

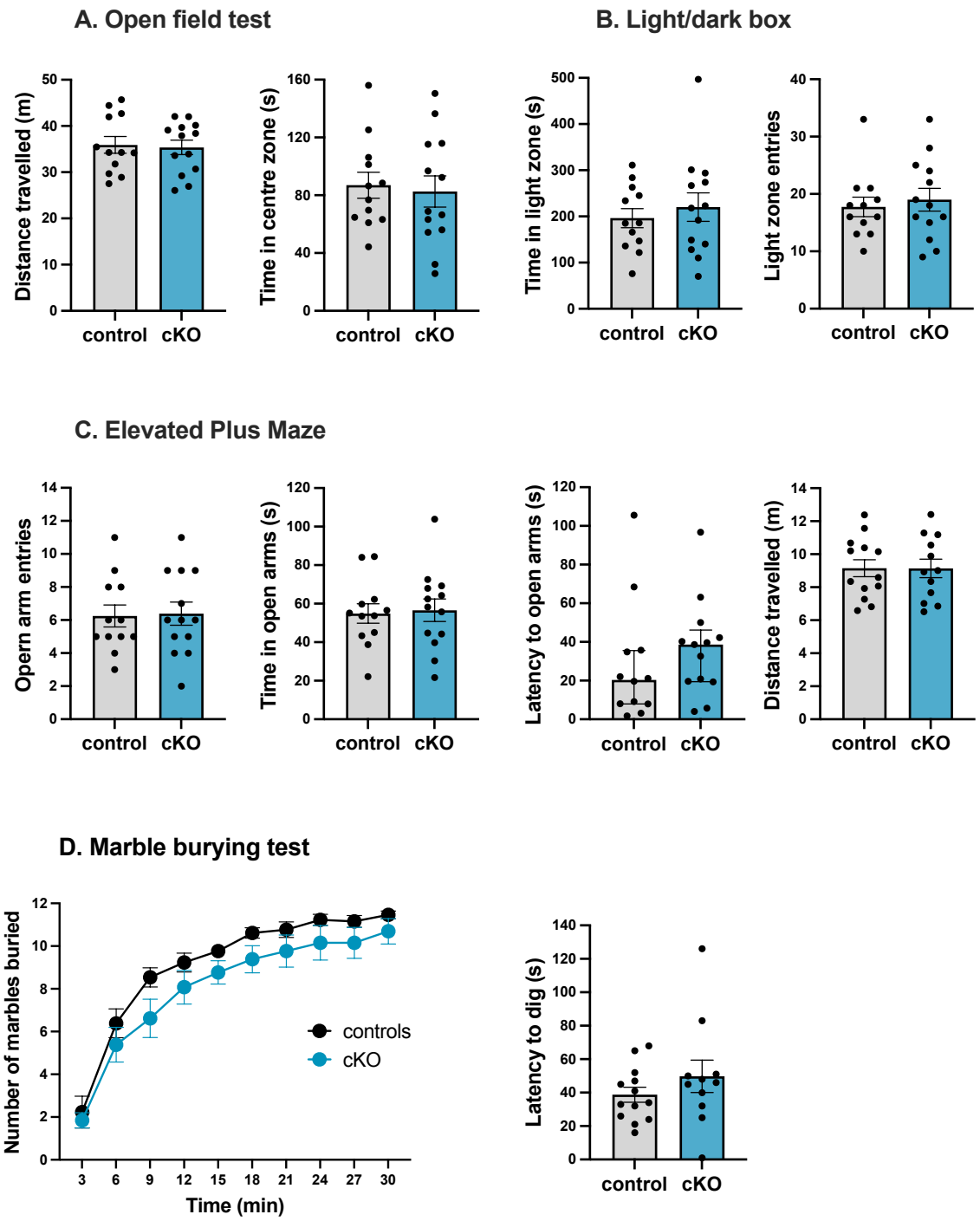

Figure 2.9 | Performance of VGLUT3 cKO$^{5\text{-HT}}$ mice in tests of anxiety-like behaviour and locomotion, compared to controls. In **(A)**, **(B)** and **(C)** bars represent the mean ± SEM values, with the exception of latencies which are median ± interquartile range. In **(D)** closed circles and bars represent mean ± SEM values. Individual values are indicated by smaller closed circles. Groups were VGLUT3 cKO$^{5\text{-HT}}$ mice (n=13) and controls (n=12 in anxiety test, and n=13 in the marble burying test). Analysed with two-way repeated measure ANOVA and unpaired t test.

SERT-Cre mice were also tested on the EPM and their behaviour did not differ from that of littermate controls. Specifically, on the EPM the number of open arm entries ($t_{(17)}$=0.335, p=0.742, ***Table 2.4***), time spent in the open arms ($t_{(17)}$=0.819, p=0.424, ***Table 2.4***) and total distance travelled ($t_{(17)}$=0.575, p=0.573, ***Table 2.4***) were unaffected by genotype.

Altogether the data presented in this section indicates no evidence of anxiety-like behaviour in either VGLUT3 cKO$^{5\text{-HT}}$ mice nor SERT-Cre mice, compared to control littermates.

Table 2.4 | Behaviour of SERT-Cre mice compared to control littermates. Analysed by t test. Values are mean ± SEM or median [25th, 75th].

Test and parameter	Control	SERT-Cre
EPM	n=10	n=9
Entries to open arms	9.7 ± 2.2	8.9 ± 0.8
Time in open arms (s)	78.2 ± 13.0	65.6 ± 7.3
Total distance travelled (m)	12.9 ± 1.3	13.6 ± 0.4
Novelty-induced hyponeophagia	n=10	n=13
Latency to contact (s)	3.5, [2, 6.8]	5, [3, 7]
Latency to eat (s)	54.3 ± 21.7	49.6 ± 9.8
Sucrose preference test	n=9	n=6
Sucrose preference	1.7 ± 0.2	1.3 ± 0.3

2.3.5 Novelty-induced hyponeophagia

The novelty-induced hyponeophagia test revealed that VGLUT3 cKO$^{5\text{-HT}}$ mice had increased latency to first contact with the novel food compared to control littermates (Mann-Whitney U=216, p=0.033, ***Fig. 2.10A***). However, latency to first drink was not different between groups (Mann-Whitney U=275, p=0.351, ***Fig. 2.10A***). A two-way ANOVA on the same dataset, revealed no effect of sex or interaction between sex and

genotype on latency to first contact (effect of sex: $F_{(1, 47)}$=0.044, p=0.856; interaction: $F_{(1, 47)}$=0.318, p=0.576) or latency to eat (effect of sex: $F_{(1, 47)}$=0.795, p=0.377; interaction: $F_{(1, 47)}$=0.790, p=0.379).

SERT-Cre mice were also tested in the novelty-induced hyponeophagia and their performance was not different from controls in either latency to first contact (Mann-Whitney U=50, p=0.364) or latency to eat ($t_{(21)}$=0.214, p=0.833, ***Table 2.4***).

2.3.6 Sucrose preference test

In the sucrose preference test, both VGLUT3 cKO$^{5\text{-HT}}$ mice and controls consumed significantly more 1% sucrose than water ($F_{(1, 72)}$=239.5, p<0.0001), amounting to 83.5 ± 2.3 % of the total fluid consumption in controls, and 77.2 ± 2.3 % in VGLUT3 cKO$^{5\text{-HT}}$ mice. A two-way ANOVA revealed an interaction between the effect of genotype and the kind of solution ($F_{(1, 72)}$=5.357, p=0.024), with Tukey's post hoc indicating that VGLUT3 cKO$^{5\text{-HT}}$ mice drank less sucrose then controls (p=0.019, ***Fig. 2.10B***), while water consumption was unchanged (p=0.804). Accordingly, VGLUT3 cKO$^{5\text{-HT}}$ mice showed decreased preference for sucrose over water compared to their control littermates. A two-way ANOVA on the same dataset showed that this effect was unaffected by sex (effect of sex: $F_{(1, 34)}$=0.918, p=0.345; effect sex x genotype interaction: $F_{(1, 34)}$=0.129, p=0.722).

However, when VGLUT3 cKO$^{5\text{-HT}}$ mice were exposed to a single bottle of 2.5% sucrose solution during the pre-test to avoid hyponeophagia, there was no difference in consumption between groups ($t_{(36)}$=0.599, p=0.530; mean ± SEM of control: 1.852 ± 0.204 g ; mean ± SEM of VGLUT3 cKO$^{5\text{-HT}}$: 1.695 ± 0.213 g).

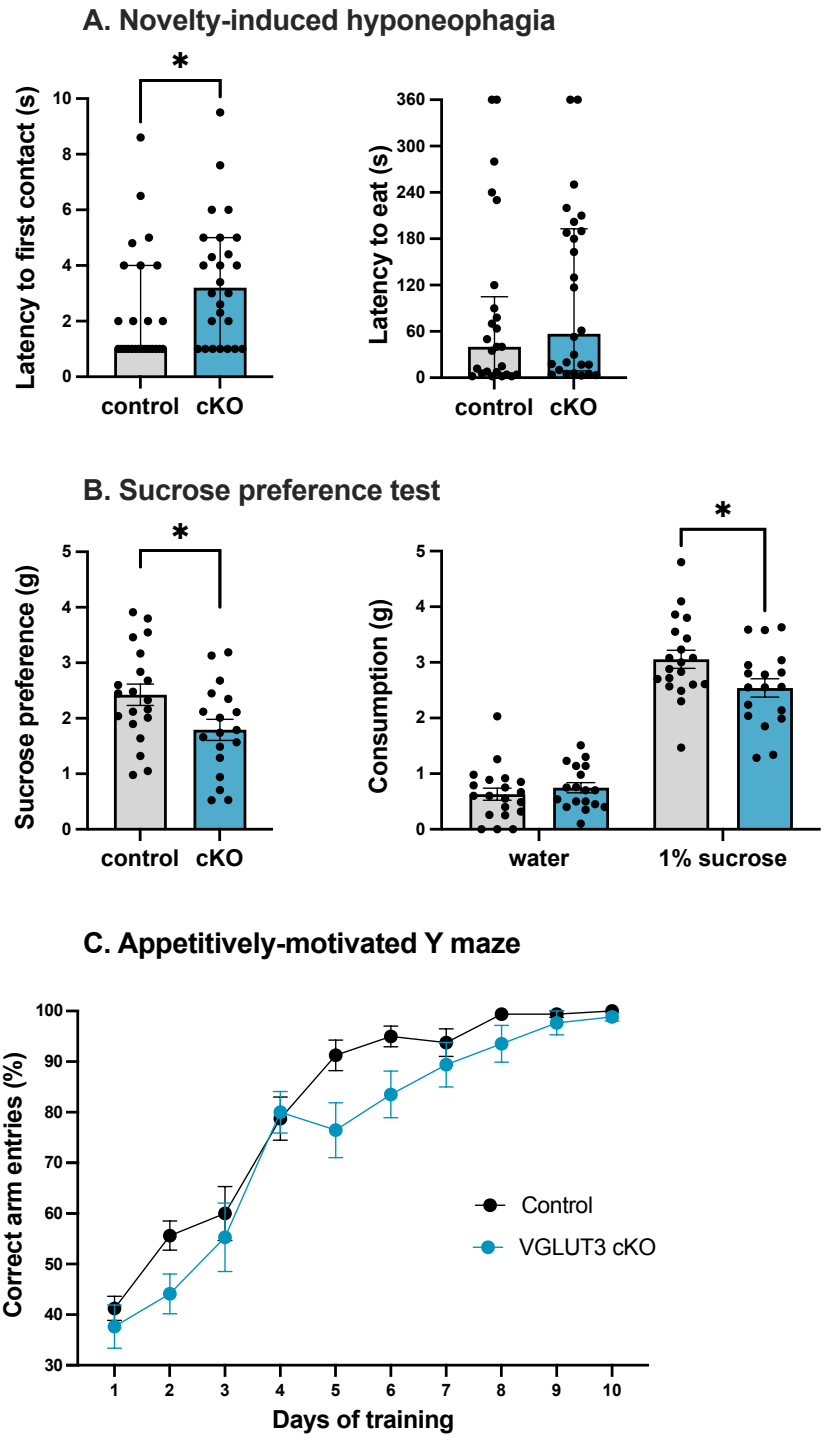

Figure 2.10 | Performance of VGLUT3 cKO$^{5\text{-HT}}$ in the novelty-induced hyponeophagia, sucrose preference test, and appetitively-motivated spatial reference Y maze, compared to controls. (A) Mice were exposed to a novel food in a novel environment**.** Groups were VGLUT3 cKO$^{5\text{-HT}}$ mice (n=26) and controls (n=25). Bars represent the mean median ± interquartile range of latencies. Analysed by Mann-Whitney U. **(B)** Sucrose preference expressed as sucrose solution minus water consumption (left) and raw values for water and sucrose consumption (right) in VGLUT3 cKO$^{5\text{-HT}}$ mice (n=18) and controls (n=20). Bars represent mean ± SEM values. Analysed

by two-way ANOVA followed by Tukey's post hoc **(C)** The appetitively-motivated spatial reference memory test (Y maze) was carried out as described in *Section 2.2.2.8*. Percentage of correct trials (chance = 33%) in VGLUT3 cKO$^{5\text{-HT}}$ mice (n=17) and controls (n=16). Full circles represent mean ± SEM values. Some error bars are too small to be depicted. Analysed by two-way repeated measure ANOVA.

SERT-Cre mice showed no difference in sucrose preference compared to controls ($t_{(13)}$=1.062, p=0.308, ***Table 2.4***).

2.3.7 Appetitively-motivated spatial reference memory test

In the appetitively motivated Y maze task, all mice were able to learn effectively over time (effect of training day: $F_{(9, 279)}$=87.020, p<0.0001) but VGLUT3 cKO$^{5\text{-HT}}$ mice showed a small reduction in overall performance compared to control littermates (effect of genotype: $F_{(1, 31)}$=4.246, p=0.048; ***Fig. 2.10C***). In the last training session (day 10), post-choice baiting confirmed that mice were not relying on olfactory cues. The interaction between genotype and days of training was not statistically significant ($F_{(9, 279)}$=1.233, p=0.275).

2.4 Discussion

This chapter investigated a novel transgenic mouse with conditional VGLUT3 KO in 5-HT neurons using a combination of gene expression, immunohistochemistry, *ex vivo* neurochemistry, and behaviour. Conditional VGLUT3 KO in 5-HT neurons caused a reduction in 5-HT turnover in the DRN, increased expression of $5HT_{1A}$ receptor in the prefrontal cortex, and increased expression of 5-HT_{1B} and DA D_1 receptors in the NAc. Further, VGLUT3 cKO$^{5\text{-HT}}$ mice were healthy and did not present any gross alterations in

naturalistic behaviour, nor any evidence of increased anxiety-like behaviour. However, VGLUT3 cKO$^{5\text{-HT}}$ mice displayed reduced sucrose preference and mild deficits in an appetitively-motivated spatial reference task.

2.4.1 VGLUT3 cKO$^{5\text{-HT}}$ mice present reduced VGLUT3

Firstly, the VGLUT3 cKO$^{5\text{-HT}}$ mouse model was validated by showing a significant reduction in VGLUT3 mRNA in the dorsal raphe region. Furthermore, immunohistochemical experiments demonstrated a selective loss of VGLUT3 in DRN 5-HT neurons, as indicated by a 60% reduction in neurons double-labelled with VGLUT3 and the 5-HT-specific marker TPH2. The incomplete depletion of VGLUT3 in 5-HT neurons may reflect cross-reactivity of our antibody with non-functional VGLUT3 protein fragments that may be transcribed following the conditional KO. Also, even though the distribution of immunolabelling with this antibody closely matched that of VGLUT3 mRNA reported in previous in situ hybridisation studies (Hioki et al., 2010), the possibility of a low level of non-specific labelling cannot be excluded.

Importantly, the KO of VGLUT3 in 5-HT neurons did not impact on the total number of 5-HT neurons, as the number of TPH2-labelled cells and quantity of VMAT2 mRNA were unaffected in VGLUT3 cKO$^{5\text{-HT}}$ mice. Similarly, VGLUT3 cKO$^{5\text{-HT}}$ mice did not display compensatory changes in DRN expression of VGLUT1 and VGLUT2, two other vesicular glutamate transporters expressed respectively in non-5-HT DRN neurons projecting to cortical and subcortical regions (Soiza-Reilly & Commons, 2011).

2.4.2 VGLUT3 cKO$^{5\text{-HT}}$ mice display decreased 5-HT turnover in the DRN

Analysis of *ex vivo* tissue levels of 5-HT and 5-HIAA revealed decreased 5-HIAA and 5-HT turnover in the DRN of VGLUT3 cKO$^{5\text{-HT}}$ mice compared to controls. This result could be consistent with previous reports of VGLUT3 contributing to the regulation of 5-HT function (Amilhon et al., 2010). Specifically, it has been hypothesised that VGLUT3 synergises with VMAT2 in facilitating vesicular accumulation of 5-HT (Amilhon et al., 2010; El Mestikawy et al., 2011). According to the latter hypothesis, lack of VGLUT3 in 5-HT neurons would decrease vesicular loading of 5-HT, thus reducing 5-HT release and 5-HT turnover. However, 5-HT, 5-HIAA and 5-HT turnover were not different in 5-HT terminal areas including the hippocampus, prefrontal cortex and NAc of VGLUT3 cKO$^{5\text{-HT}}$ mice compared to controls. This might suggest that the increase in 5-HT turnover observed in the hippocampus of mice with global VGLUT3 KO (Amilhon et al., 2010) is not caused by the lack of VGLUT3 in 5-HT neurons, but rather the lack of VGLUT3 in other neuronal populations. Nonetheless, it is also possible that either our sample size or the sensitivity of our *ex vivo* measurements of 5-HT and 5-HIAA might not accurately reflect changes in 5-HT release. Further experiments could quantify 5-HT release in VGLUT3 cKO$^{5\text{-HT}}$ mice using *in vivo* microdialysis (e.g. in the hippocampus or other terminal areas) to rule out this possibility.

Interestingly, VGLUT3 cKO$^{5\text{-HT}}$ mice displayed increased 5-HT$_{1A}$ gene expression in the prefrontal cortex and increased 5-HT$_{1B}$ gene expression in the NAc, compared to controls. This adaptation to loss of glutamate release, might indicate that glutamate restrains the expression of cortical 5-HT$_{1A}$ receptors and NAc 5-HT$_{1B}$ receptors in wildtype mice. However, upregulation of these 5-HT receptors might also result from the decrease in 5-HT release, due to the potential lack of synergism between VGLUT3 and VMAT2. Additionally, previous studies reported altered 5-HT$_{1A}$ autoreceptor sensitivity in the

DRN of mice with global VGLUT3 KO (Amilhon et al., 2010), but the impact of VGLUT3 on cortical 5-HT_{1A} receptors had not been previously investigated. Future studies could investigate 5-HT_{1A} autoreceptor sensitivity in VGLUT3 cKO$^{5\text{-HT}}$ mice using 8-OH-DPAT-induced hypothermia, a commonly used measure of 5-HT_{1A} autoreceptor function in mice (Hedlund et al., 2004).

No other differences were detected in the expression of other 5-HT-related genes in the DRN, hippocampus, prefrontal cortex, and NAc of VGLUT3 cKO$^{5\text{-HT}}$ mice compared to control littermates.

2.4.3 VGLUT3 cKO$^{5\text{-HT}}$ mice displayed increased expression of DA D_1 receptor in the NAc

Ex vivo tissue levels of DA, DOPAC and DA turnover in the NAc and dorsal striatum of VGLUT3 cKO$^{5\text{-HT}}$ mice were not different from control littermates. However, gene expression analysis revealed increased expression of DA D_1 receptor in the NAc of VGLUT3 cKO$^{5\text{-HT}}$ mice, compared to controls. Interestingly, mice with global VGLUT3 KO also showed increased DA D_1 receptor density in the NAc (Sakae et al., 2015), and this was associated with increased potassium-evoked DA release in the NAc during voltammetry experiments. 5-HT-glutamate co-releasing neurons have been reported to establish excitatory synapses on VTA DA neurons projecting to the NAc (Wang et al., 2019), thus it is possible that in VGLUT3 cKO$^{5\text{-HT}}$ mice the predicted lack of glutamate co-release could affect NAc DA release.

2.4.4 VGLUT3 cKO$^{5\text{-}HT}$ mice do not display an anxious phenotype

After validating the VGLUT3 cKO$^{5\text{-}HT}$ mice, their naturalistic behaviour was assessed. Specifically, food and water consumption, body weight and nest building, did not differ from controls. Distance travelled in a non-anxiogenic open field was also unchanged, suggesting unimpaired locomotion and exploration. Altogether these mice appeared normal and displayed no gross alteration in naturalistic behaviour, which is important as changes in these parameters would likely affect performance in subsequent tests of anxiety and reward.

Behaviour of VGLUT3 cKO$^{5\text{-}HT}$ mice was then examined in the EPM and light/dark box, two well established tests of anxiety (Himanshu et al., 2020), which revealed no effect of genotype compared to controls. Additionally, VGLUT3 cKO$^{5\text{-}HT}$ mice did not differ from controls in the time spent in the centre zone of the non-anxiogenic open field. In these tests mice spent a typical amount of time in the more anxiogenic area of the apparatus, thus the lack of differences between groups is not likely caused by floor or ceilings effects. VGLUT3 cKO$^{5\text{-}HT}$ mice also performed similarly to controls in the marble burying test, which assesses naturalistic digging behaviour, as well as anxiety-like and repetitive behaviour (De Brouwer et al., 2019; Deacon, 2009). Taken together these data suggest that VGLUT3 cKO$^{5\text{-}HT}$ mice do not have an anxious phenotype.

Nonetheless, in the novelty-induced hyponeophagia test VGLUT3 cKO$^{5\text{-}HT}$ mice were slower to approach a novel food in a novel environment, which is often considered a readout of anxiety-like behaviour (Dulawa & Hen, 2005). However, this difference was rather small (e.g. average latency of ~3.5 s compared to ~2 s) and there was no difference

in the latency to consume the novel food, which is the main readout of the novelty-induced hyponeophagia test.

Thus, VGLUT3 cKO$^{5\text{-HT}}$ mice differed from mice with conditional VGLUT3 KO in Pet1 neurons, which showed hypolocomotion in the open field and on the EPM, as well as increased time spent in, and latency to exit the dark compartment of the light/dark box (Cunha et al., 2020). Similarly, VGLUT3 cKO$^{5\text{-HT}}$ mice also differed from mice with global VGLUT3 KO, which displayed decreased time spent in open arms on the EPM, as well as increased ultrasonic vocalisation in pups. Thus, the current data suggest that the anxious phenotype observed in mice with global VGLUT3 KO is not directly caused by lack of VGLUT3 from 5-HT neurons (Amilhon et al., 2010). Conversely, it could therefore be caused by VGLUT3 KO in other neuronal populations.

2.4.5 VGLUT3 cKO$^{5\text{-HT}}$ mice show reduced sucrose preference and reduced performance in a spatial reward task

Interestingly, VGLUT3 cKO$^{5\text{-HT}}$ mice showed reduced sucrose preference in a test which probes anhedonia, a common feature of a depressive-like phenotype. However, VGLUT3 cKO$^{5\text{-HT}}$ mice did not differ from controls in nest building, an indication of wellbeing and a marker of goal-directed behaviour which often deteriorates in mouse models of apathy and depression (Jirkof, 2014; Nollet et al., 2019; Planchez et al., 2019).

Importantly, SERT-Cre mice did not differ from controls in the sucrose preference test, in the novelty-induced hyponeophagia test, or in other tests of anxiety, indicating that Cre

expression under the SERT promoter does not contribute to the behavioural phenotype of VGLUT3 cKO$^{5\text{-HT}}$ mice in these studies.

In the light of previous evidence linking 5-HT-glutamate co-release to reward processing (Liu et al., 2020; Wang et al., 2019; see *Chapter 1, Section 1.3.4.4*) it was hypothesised that the reduced preference for sucrose might reflect an underlying reward deficit in the VGLUT3 cKO$^{5\text{-HT}}$ mice. To test this hypothesis VGLUT3 cKO$^{5\text{-HT}}$ mice were exposed to an appetitively-motivated Y maze, where mice had to use extra-maze spatial cues to learn the position of a reward. This task revealed a small but statistically significant impairment in the performance of VGLUT3 cKO$^{5\text{-HT}}$ mice. The idea that VGLUT3 cKO$^{5\text{-HT}}$ mice might have a reward deficit is potentially consistent with the finding that 5-HT-glutamate co-releasing neurons project to the VTA and evoke DA release in the nucleus accumbens (Cunha et al., 2020; Liu et al., 2014; Wang et al., 2019). However, the appetitively-motivated Y maze task, had several limitations, such as requiring unimpaired spatial learning and allowing only a limited number of trials per day, due to the labour-intensive nature of the paradigm. Therefore, experiments reported in the next chapters (*Chapter 4* and *5*) carried out a more in-depth investigation of reward function in these animals. Specifically, experiments assessed the behaviour of VGLUT3 cKO$^{5\text{-HT}}$ mice in operant reward paradigms involving numerous daily trials, allowing to address more specific research questions. Other tests probing spatial learning and short-term memory will also be carried to out to control for potential learning deficits in these domains. Additionally, *Chapter 3* investigated whether the observed evidence of anhedonia discussed in this chapter could be linked to altered stress sensitivity of VGLUT3 cKO$^{5\text{-HT}}$ mice.

Chapter 3
Investigation into the role of 5-HT-glutamate co-releasing neurons in acute stress mechanisms

3.1 Introduction

The previous chapter, discussed a role for glutamate co-released from 5-HT neurons in anhedonia and reward-based learning. Anhedonic behaviour and motivation to work for rewards can be affected by stress exposure, and it has been suggested that susceptibility to stress can lead to anhedonia (for a review see Pizzagalli, 2014; Stanton et al., 2019). Thus, here we investigated whether glutamate co-released from 5-HT neurons is involved in coping with acute stress.

3.1.1 5-HT and acute stress

5-HT is a key neurotransmitter for emotional modulation, stress sensitivity and stress coping behaviour (Chaouloff et al., 1999; Cools et al., 2008). As discussed in *Chapter 1* (*Section 1.3.4.2*) 5-HT neurons are highly responsive to stress, threats, and noxious stimuli and are likely to mediate stress coping (Deakin & Graeff, 1991; Grahn et al., 1999). In particular, 5-HT neurons in the DRN are robustly activated by acute uncontrollable stressors, such as swim stress, restraint, and foot shock, as demonstrated by increased expression of the activity-dependent immediate early gene *c-fos* (Bonapersona et al., 2022; Hale et al., 2008; Kelly et al., 2011; Roche et al., 2003; Senba et al., 1993). Thus, the degree to which the animal can exert behavioural control over the stressor has been suggested to impact of this stress-induced activation of 5-HT neurons (Amat et al., 1998,

2005), with c-Fos studies showing greater activation of DRN 5-HT neurons in presence of uncontrollable stressors, compared to controllable stressors of the same magnitude (Grahn et al., 1999).

3.1.2 C-Fos as a measure of stress-induced activation

C-Fos is a transiently inducible transcription factor, which is triggered by neuronal activation. It is encoded by the c-*fos* gene, which like other immediate early genes, translates extracellular signals into activity-dependent changes in gene expression (Herdegen & Leah, 1998; Morgan et al., 1987; Morgan & Curran, 1986; Sheng & Greenberg, 1990). However, c-Fos is unique as its mRNA can be detected as early as 20 min after stimulation, with protein expression peaking after 90 min, thus being a useful experimental tool to measure neural activity (Dragunow & Faull, 1989; Hu et al., 1994; Kovács, 1998). Under unstimulated conditions c-Fos expression is low, but can it be easily triggered by a variety of aversive experimental manipulations. Thus, c-Fos has been extensively used to measure stress-induced neuronal activation, with a large body of literature focusing specifically on the swim stress circuitry (Hale et al., 2012; Kelly et al., 2011).

3.1.3 Behavioural paradigms to assess stress coping

Several paradigms have been developed to study the mechanisms of acute stress in rodents, nonetheless swim stress stands out as a method to assess coping behaviour in response to inescapable stress in a controllable manner (Commons et al., 2017; De Kloet & Molendijk, 2016; Molendijk & de Kloet, 2019). For example, when initially exposed to swim stress rodents display escape-driven behaviours such as swimming or climbing, but

over time these are replaced by passive coping strategies such as floating (Commons et al., 2017). Furthermore, acute administration of antidepressants, such as SSRIs, increases active coping during swim stress (David et al., 2003; Lucki, 1997; Petit-Demouliere et al., 2005), which has caused floating during swim stress to often be interpreted as depressive-like behaviour. This has raised a debate on whether floating represents a coping failure or an adaptive strategy to conserve energy (De Kloet & Molendijk, 2016). In this chapter we employed swim stress merely as a tool to probe neuronal activation and to assess coping strategies following genetic or pharmacological manipulations, but not as a measure of depressive-like behaviour or antidepressant action.

Another paradigm that can be used to probe stress coping is acute social defeat, a more controllable stressor with higher ecological validity, which involves a physical encounter between two conspecifics (Hollis & Kabbaj, 2014). In this test the intruder animal adopts a variety of active coping strategies to minimise interactions with the opponent, such as escaping, cornering, freezing, and upright submissive postures (Diaz & Lin, 2020). Whilst there is ample evidence that swim stress activates DRN 5-HT neurons in rodents, it is less well-established whether acute social defeat has similar effects (Lkhagvasuren et al., 2014; Matsuda et al., 1996; Numa et al., 2019).

3.1.4 5-HT-glutamate co-releasing neurons and stress coping

As previously discussed in *Chapter 1*, it has recently become clear that 5-HT neurons are capable of releasing not only 5-HT but also glutamate, as electrophysiological studies demonstrate that activation of 5-HT neurons elicits 5-HT and glutamate-mediated synaptic responses both *in vitro* and *in vivo*, in different forebrain regions (Liu et al., 2014;

Sengupta et al., 2017; Varga et al., 2009). Thus, approximately two-thirds of 5-HT neurons express VGLUT3 which stores glutamate in pre-synaptic vesicles prior to release (Gras et al., 2002; Schäfer et al., 2002). VGLUT3 expression is prevalent in 5-HT neurons located in the ventral part of the DRN and in the MRN, with only sparse VGLUT3 expression in the dorsal DRN and in the lateral wings (Hioki et al., 2010). Accordingly, in a recent study a subpopulation of ventral DRN 5-HT neurons projecting to the prefrontal cortex, was found to predominantly express VGLUT3 (Ren et al., 2018). Interestingly, chemogenetic activation of these 5-HT neurons projecting to the prefrontal cortex was shown to increase active coping, measured as decreased immobility, during swim stress (Ren et al., 2018). This evidence suggests a role for 5-HT-glutamate co-releasing neurons in stress coping.

3.1.5 Hypothesis and aims

On the basis of the above findings, we hypothesised that glutamate co-releasing 5-HT neurons in the DRN, especially in the ventral region, would be activated by uncontrollable stress and may be involved in stress coping behaviour. This prediction was tested by performing c-Fos immunohistochemistry in midbrain subregions of wildtype mice exposed to swim stress. To investigate whether these effects would generalise to a different stressor, effects were compared with acute social defeat. Lastly, behavioural experiments used VGLUT3 cKO$^{5\text{-HT}}$ mice to examine the causal link between changes in activity of 5-HT-glutamate co-releasing neurons and stress coping behaviour.

3.2 Methods

3.2.1 Animals

Mice were group-housed (2-6 per cage) with littermates in individually ventilated cages, in a temperature-controlled room (21^{o}C) with a 12 h light/dark cycle. Mice had *ad libitum* access to food and water, and cages were lined with sawdust bedding and contained cage enrichment, consisting of sizzle nest and cardboard tube. All experiments were conducted during the light phase (10:00–17:00). Both females and males were used, with the exception of the social defeat experiment, which necessarily involved only males. All mice were habituated to handling on three occasions before any experiment, and were handled using a cardboard tunnel to minimise background stress (Gouveia & Hurst, 2019; Hurst & West, 2010).

Depending on the experiment mice were either C57BL/6J (Charles River, age 8-10 weeks) or VGLUT3 cKO$^{5\text{-HT}}$ mice, with control littermates (see *Chapter 2, Section 2.2.1* for more details). Retired breeder CD1 mice (Charles River, age 22-30 weeks) were also employed in the acute social defeat experiment, and were single-housed to increase their territorial nature. C57BL/6J and CD1 mice were purchased from Charles River and habituated to the holding facility for one week before the start of experiments, while VGLUT3 cKO$^{5\text{-HT}}$ and control littermates were bred in-house.

Experiments followed the principles of the Animal Research: Reporting of In Vivo Experiments (ARRIVE) guidelines and were conducted according to the United Kingdom Animals (Scientific Procedures) Act of 1986, with appropriate personal and project licence coverage.

3.2.2 Acute swim stress paradigm

3.2.2.1 Experimental Design

Mice were randomly allocated to 1 of 3 experimental groups by stratified randomisation: i) saline + "new cage" (control); ii) saline + swim stress; iii) fluoxetine (10 mg/kg) + swim stress. All mice were removed from their home cages and single-housed in a clean cage for the entire duration of the experiment. Saline or fluoxetine were injected *i.p*. 30 min prior to a 6 min swim stress. Control mice remained in their "new cage" instead of being exposed to the stressor, as this controlled for the stress of handling, injections and being single-housed. Mice were deeply anesthetised with sodium pentobarbital (90 mg/kg, Euthatal), 90 min after swim stress (***Fig. 3.1***). This was followed by perfusion and collection of brain tissue for c-Fos immunohistochemistry. This timescale was chosen to allow for optimum c-Fos expression before tissue collection (Kovács, 1998).

3.2.2.2 Drugs

Fluoxetine (Stratech) was dissolved in saline (Aqupharm) in a volume of 2 mg/ml, and was administered *i.p.* at a dose of 10 mg/kg. Control animals received saline in a volume of 2 ml/kg. All solutions were prepared fresh daily. The dose and administration protocol were based on previous evidence showing that 10 mg/kg is the lowest effective dose at reducing immobility in C57BL6 mice exposed to an acute swim stressor (Jin et al., 2017; Tang et al., 2014).

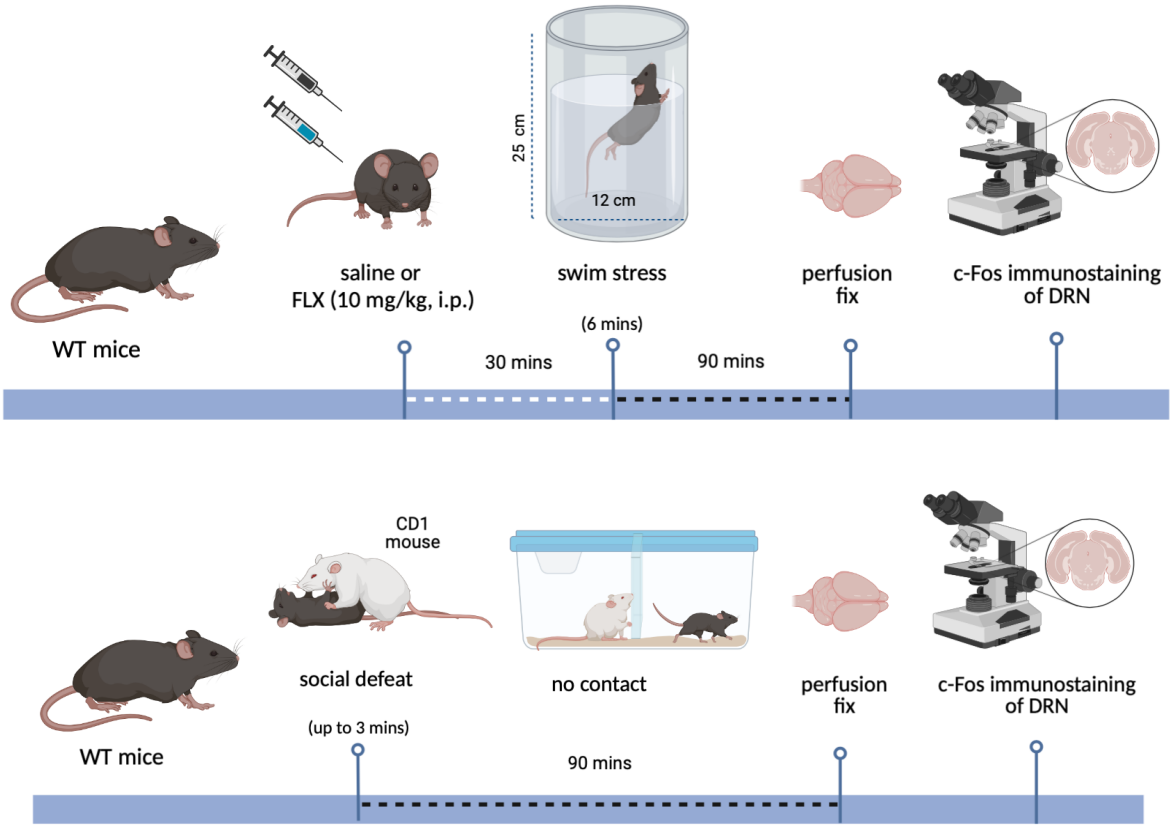

Figure 3.1 | Experimental timeline of the swim stress and social defeat experiments. WT, wildtype; FLX, fluoxetine; DRN, dorsal raphe nucleus. Figure made with Biorender ©.

3.2.2.3 Behaviour

During the last 5 min prior to swim stress, mice were placed in a clean but familiar cage, and their locomotor activity was recorded via an overhead camera for offline tracking of distance travelled using ANY-maze (Stoelting Europe) tracking software.

Next, mice were placed individually for 6 min in a Pyrex glass cylinder (25 cm height, 12 cm diameter) containing water (20 cm height) maintained at 20 °C (Bogdanova et al., 2013; Porsolt et al., 1977). Mice were video-recorded from a horizontal viewing plane, to allow for offline manual scoring of the videos. The last 4 min were manually scored for immobility, swimming and climbing, as described previously (Commons et al., 2017; Costa et al., 2013), by an experimenter blind to treatment. Climbing was defined as

placement of the front paws on the glass surface, while kicking with the hind legs in an attempt to escape. Immobility (or floating) consists of the absence of escape-oriented behaviours, but can involve small movements aimed solely at keeping afloat. Swimming was characterised by active movement across the cylinder, and was calculated as *total time – (immobility + immobility)*. After the test, the animals were towel-dried and placed in a heated cage until fully dry to avoid hypothermia.

3.2.3 Acute social defeat paradigm

3.2.3.1 Experimental Design

Male C57BL/6J mice were allocated to 1 of 2 experimental groups by stratified randomisation: i) "new cage" control group, ii) social defeat group. All mice were removed from their home cages and single-housed in a clean cage for the duration of the experiment. The "new cage" control mice remained in a clean cage throughout. The "social defeat" group experienced a single episode of social defeat by the CD1 resident mouse, via the protocol defined below, after which they were placed behind the partition for the remainder of the 90 min. After the 90 min had passed, all mice were perfused and brains collected for immunohistochemistry.

3.2.3.2 Aggressor mouse training and selection

One CD1 mouse was selected out of 3, based on its persistent level of aggression. Selection was carried out as previously described (Golden et al., 2011). Briefly, on three consecutive days one screener C57BL/6J mouse was placed in a CD1 mouse cage for a maximum of 3 min or until it was socially defeated. Social defeat was defined as a clear pin down, or supine posture by the C57BL/6J. Each CD1 mice interacted with a different C57BL/6J mice each day. All interactions were filmed, and video analysis of the latency to

attack and number of attacks allowed selection of a single CD1 mouse with appropriate and consistent levels of aggression, repeatedly attacking within the first 20 s.

3.2.3.3 Social defeat protocol

C57BL/6J mice were individually placed in the CD1 mouse cage until socially defeated, at which point they were immediately removed. Then, the socially defeated mouse was placed back in the CD1 home cage, but was separated from the aggressor by a transparent acrylic partition (12 cm height, 17.5 cm length) for 90 min prior to perfusion and collection of brain tissue for immunohistochemistry. The partition was perforated with 10 holes to allow for auditory, visual, and olfactory interaction with the attacker (Golden et al., 2011). The social defeat interaction was recorded from an aerial perspective, and offline behavioural analysis using the ANY-maze software (Stoelting Europe) allowed for measurements of the latency to attack, number of attacks and time spent moving.

3.2.4 Immunohistochemistry and microscopy

Perfusion fixation and brain sectioning were carried out as previously described in *Chapter 2*, *Section 2.2.3.1* and *2.2.3.2*. Midbrain sections were selected based on their distance from Bregma (AP= -4.7 to 4.8 mm) to contain DRN, MRN and PAG regions (Franklin & Paxinos, 1997).

3.2.4.1 Immunohistochemistry

Immunohistochemistry was performed as previously described in *Chapter 2*, *Section 2.2.3.3*. Briefly, sections were washed 3 x 10 min in 500 µl PBS, 10 min in 500 µl ammonium chloride and 3 x 10 min in 500 µl PBS with 0.3% Tween (Sigma Aldrich; PBS-T). Next, sections were blocked in PBS-T with 10% donkey serum (Sigma Aldrich) for 1 h

at room temperature. Sections were then incubated in primary antibodies (***Table 3.1***) made up in PBS-T with 2% donkey serum for 1 h at room temperature then overnight at 4°C.

Table 3.1 | Antibodies used for immunohistochemistry.

Target	Host	Conjugate	Concentration	Company	Ref. number
Primary antibodies					
c-Fos	Rabbit	N/A	1:1000	Abcam	Ab214672
TPH2	Goat	N/A	1:1000	Abcam	Ab121013
VGLUT3	Guinea Pig	N/A	1:500	Synaptic Systems	135-204
Secondary antibodies					
Rabbit IgG (H+L)	Donkey	Alexa Fluor 488	1:1000	Invitrogen	A21206
Goat IgG (H+L)	Donkey	Alexa Fluor 647	1:1000	Invitrogen	A21206
Guinea Pig Cy3	Donkey	Cy3	1:1000	Jackson Immuno Research	706-165-148

The next day, sections were washed 2 x 10 min in 500 µl PBS-T before incubating with secondary antibodies (***Table 3.1***) made up in 500 µl PBS-T with 2% donkey serum for 2 h at room temperature. Then, sections were washed 2 x 10 min in 500 µl PBS-T, and cell nuclei were stained using DAPI (1:1000, 5 min), prior to a 10 min wash in PBS. Sections were mounted onto glass slides with Vectashield Antifade Mounting Medium (Vector Laboratories) and covered with a glass coverslip, prior to being stored in the dark at 4°C.

3.2.4.2 Imaging and analysis

Images were acquired using an Olympus Epifluorescence Microscope BX40 with ImageJ Micromanager v1.4 with 500 ms exposure. Ventral DRN, dorsal DRN and MRN were imaged at 20x magnification, while 10x magnification was used for the entire DRN, lateral wings, ventrolateral and dorsal PAG (Paxinos & Franklin, 2001). Cell counting and quantification of colocalisation was performed employing the ImageJ Software package, by an experimenter blind to treatment. Cell counts were expressed as cells/mm^2 hence a graticule (Graticules Optics Ltd) was used to ascertain the area of the region of interest

in each case. Areas of the regions of interest were as follows: entire DRN 0.54 mm^2, ventral DRN 0.14 mm^2, lateral wings 0.17 mm^2, dorsal DRN 0.14 mm^2, MRN 0.15 mm^2, dorsal PAG 0.51 mm^2, and ventrolateral PAG 0.38 mm^2.

For each mouse, the mean cell count of three sections was used for statistical analysis. C-Fos-immunoreactive neurons were defined as neurons where c-Fos immunoreactivity colocalised with DAPI immunoreactivity. Colocalisation between DAPI and TPH2 immunoreactivity identified 5-HT neurons, as TPH2 is a rate-limiting enzyme required for 5-HT synthesis. Colocalisation between TPH2 and VGLUT3 was as used to identify 5-HT-glutamate neurons with the capacity to co-release glutamate.

3.2.5 Statistical Analysis

The Shapiro-Wilk test for normality was applied to all data sets. If data were normally distributed, then a t-test, one/two-way ANOVA was used followed by Tukey's post hoc tests as appropriate. Specifically, c-Fos data were analysed across multiple regions, with repeated-measures two-way ANOVA being employed for balanced data whereas a repeated-measure mixed-effect model was used for datasets with missing values. If the data were non-parametric then a single or multiple Mann-Whitney test was employed, with a Holm-Šídák correction for multiple comparison. GraphPad Prism (v10) was used for all analysis and plotting of graphs. Parametric data are presented as mean ± SEM values, whilst non parametric data are presented as median ± interquartile range; $p<0.05$ was considered statistically significant.

3.3 Results

3.3.1 Effect of swim stress on c-Fos expression in midbrains subregions

Immunohistochemistry demonstrated an abundance of c-Fos-immunoreactive neurons in the midbrain of mice exposed to acute, inescapable swim stress (***Fig. 3.2***). Specifically, swim stress increased the number of c-Fos-immunoreactive neurons in the DRN and MRN (effect of treatment: $F_{(2, 17)}$=5.503, p=0.014; effect of region: $F_{(1, 15)}$=17.160, p<0.001; region x treatment interaction: $F_{(2, 15)}$=0.272, p=0.766; ***Fig. 3.2B***, ***Fig. 3.2C***). Tukey's post hoc revealed that this effect was statistically significant in the DRN of stressed mice compared to non-stressed controls (p=0.017; ***Fig. 3.2C***).

The number of c-Fos-immunoreactive cells in the MRN of stressed mice was not significantly different to controls (p=0.142; ***Fig. 3.2C***), albeit this could be due to a type II statistical error (i.e. false negative). In both the DRN and MRN, c-Fos immunoreactivity in fluoxetine-treated stressed mice did not differ from mice treated with treated or exposed to swim stress (DRN: p=0.423, p=0.213; MRN: p=0.935, p=0.231; ***Fig. 3.2C***).

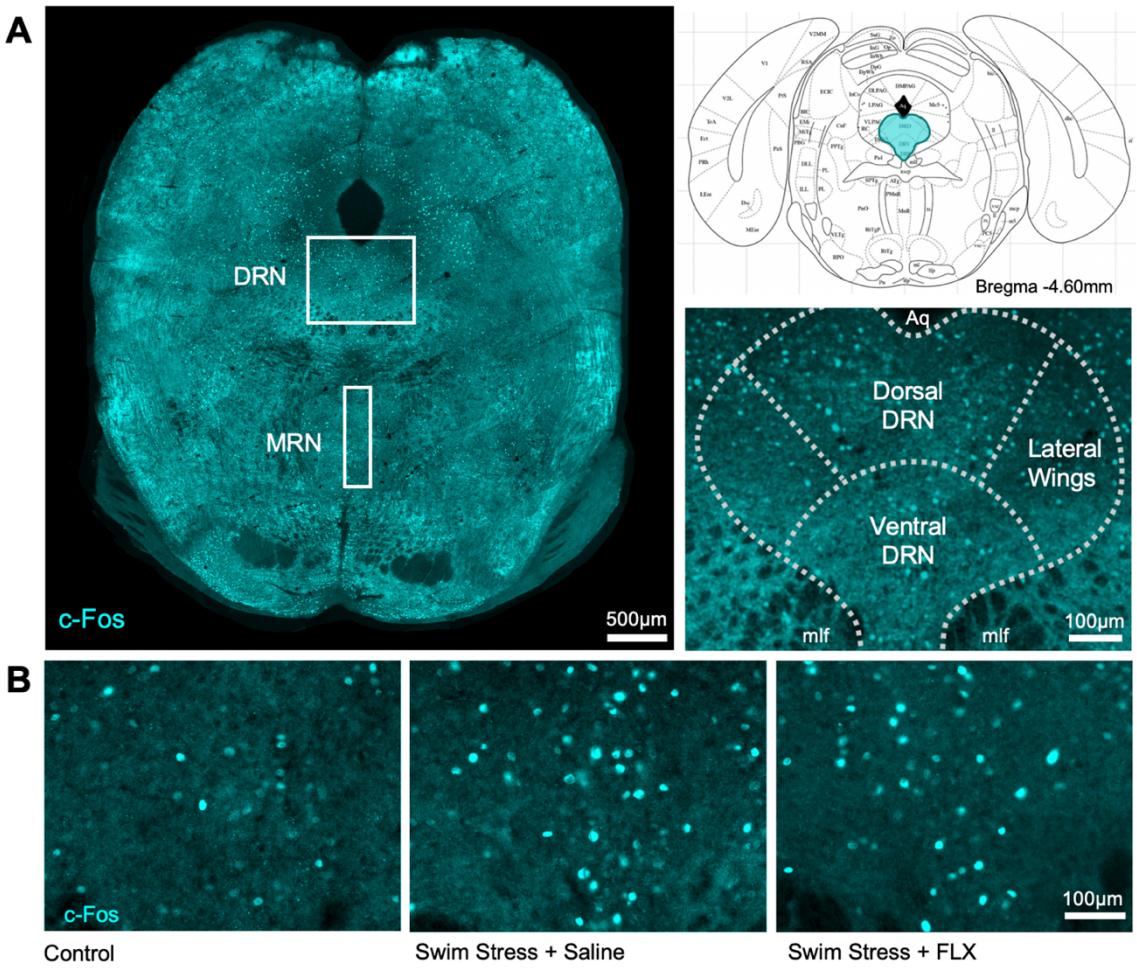
A
DRN
MRN
c-Fos
500µm
Bregma -4.60mm
Aq
Dorsal DRN
Lateral Wings
Ventral DRN
mlf
mlf
100µm
B
c-Fos
100µm
Control
Swim Stress + Saline
Swim Stress + FLX

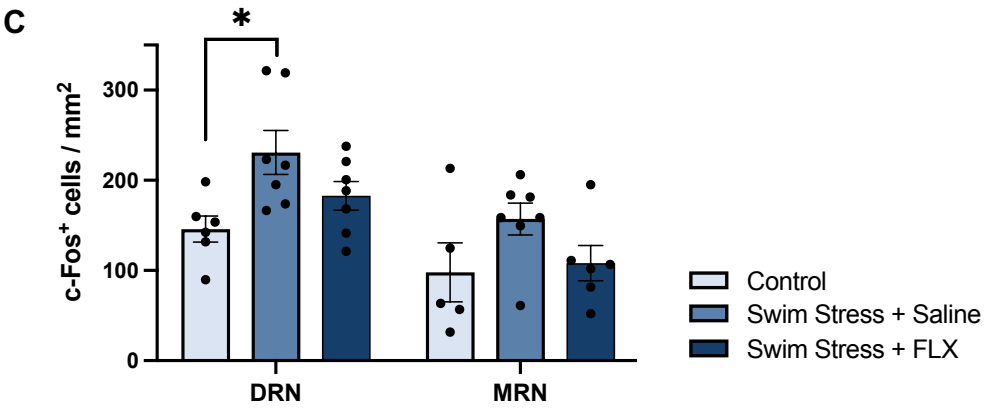
C
c-Fos+ cells / mm2
300
200
100
0
*
DRN
MRN
Control
Swim Stress + Saline
Swim Stress + FLX

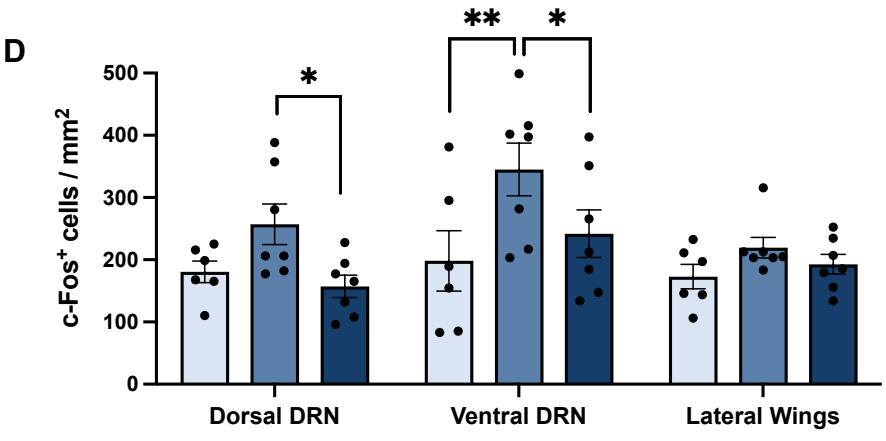
D
c-Fos+ cells / mm2
500
400
300
200
100
0
*
**
*
Dorsal DRN
Ventral DRN
Lateral Wings

Figure 3.2 | Effect of acute swim stress, with or without fluoxetine, on c-Fos expression in midbrain subregions. (A) C-Fos immunoreactivity in a midbrain section at the level of the DRN and MRN (top left) according to the stereotaxic atlas (Paxinos & Franklin, 2001; top right). Higher magnification images of DRN subregions (bottom right). **(B)** High magnification images of c-Fos immunoreactivity in the ventral DRN of control mice, and mice administered a single injection of either saline or fluoxetine (FLX) and exposed to swim stress. **(C)** C-Fos-immunoreactive neurons in the DRN and MRN. **(D)** C-Fos-immunoreactive neurons in DRN subregions. Columns are mean ± SEM values with individual values indicated by closed circles. **p<0.01 *p<0.05. Groups were control (n=6), saline + swim stress (n=7) and 10 mg/kg fluoxetine + swim stress (n=7). Abbreviations: aqueduct (Aq), medial longitudinal fasciculus (mlf).

Examination of DRN subregions (***Fig. 3.2D)*** revealed a statistically significant effect of both region ($F_{(2, 34)}$=5.884, p=0.006) and treatment ($F_{(2, 17)}$=5.721, p=0.013), while region x treatment interaction was not statistically significant ($F_{(4, 34)}$=1.512, p=0.221). Nonetheless, post hoc testing was deemed justified on the basis of our a priori hypothesis of a preferential involvement of ventral DRN neurons in stress coping. Tukey's post hoc analysis revealed a statistically significant increase in c-Fos-immunoreactive neurons in the ventral DRN of swim-stressed mice compared to non-stressed controls (p=0.002; ***Fig. 3.2B, Fig. 3.2D***), but non-significant effects in the dorsal DRN (p=0.181) and lateral wings (p=0.520).

Pre-treatment with fluoxetine prevented stress-induced c-Fos expression in the ventral DRN (post hoc p=0.028; ***Fig. 3.2D***), and reduced c-Fos expression in the dorsal DRN (FLX vs swim stress: p=0.047; ***Fig. 3.2D***), but had no effect in the lateral wings (FLX vs swim stress: p=0.790). See *Section 3.3.6* for the behavioural effects of fluoxetine administration in these animals.

3.3.2 Colocalisation of TPH2 and VGLUT3 in midbrain subregions

Next, experiments aimed to verify the spatial distribution of VGLUT3-expressing 5-HT neurons. In the midbrain, VGLUT3 is expressed in both glutamatergic neurons and 5-HT neurons, the latter of which co-release both 5-HT and glutamate (Fremeau et al., 2002; Hioki et al., 2010). Thus, colocalisation of VGLUT3 and the 5-HT-specific marker TPH2 was employed to identify 5-HT neuron with the capacity to co-release glutamate. VGLUT3 expression was particularly evident in TPH2-immunoreactive neurons located in the ventral DRN, with 67.9 ± 3.0 % of TPH2-immunoreactive neurons co-expressing VGLUT3 (***Fig. 3B***).

Conversely, only 31.3 ± 1.9 % of TPH2-immunoreactive neurons co-expressed VGLUT3 in the dorsal DRN (***Fig. 3.3B***), and there was only sparse colocalisation in the lateral wings (data not shown). Neurons with colocalised VGLUT3 and TPH2 were also evident in the MRN although these were less abundant than in the DRN, amounting to 34.9 ± 2.9 % of TPH2-immunoreactive neurons (***Fig. 3.3B***).

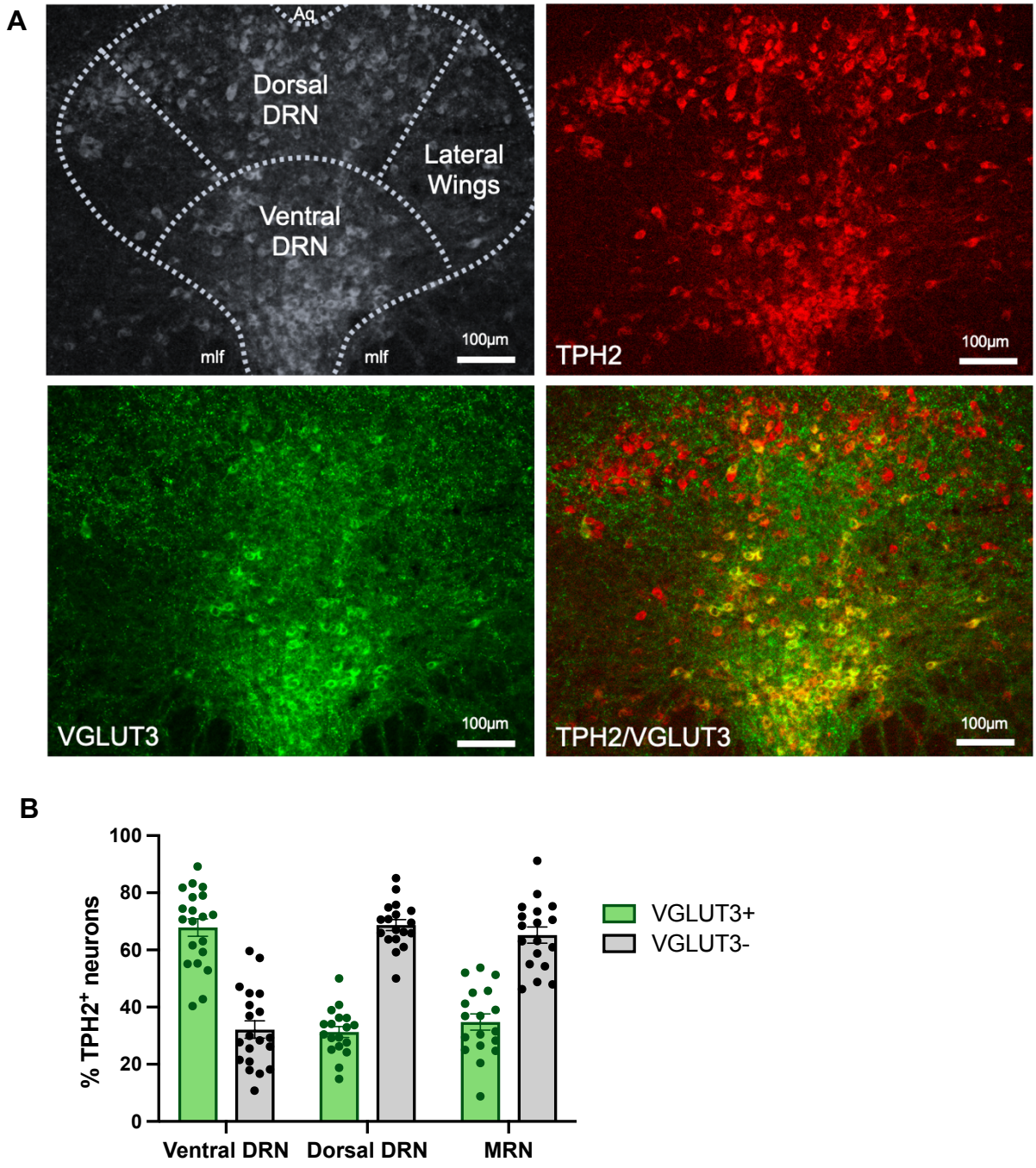

Figure 3.3 | Colocalisation of TPH2 and VGLUT3 in neurons of mouse raphe subregions. (A) Representative image of TPH2/VGLUT3 double-labelled neurons (AP= -4.6mm). **(B)** Percentage of TPH2 neurons that colocalised with VGLUT3, or were VGLUT3-immunonegative (n=17-20). Bars represent mean ± SEM values, with individual values are indicated by closed circles.

3.3.3 Effect of swim stress on c-Fos expression in ventral DRN neurons colocalising TPH2 and VGLUT3

Next, we investigated whether swim stress increased c-Fos immunoreactivity in 5-HT-glutamate co-releasing neurons using the same sections examined for c-Fos alone. Within the ventral DRN, swim stress significantly increased the number of c-Fos/TPH2/VGLUT3 triple-labelled neurons compared to non-stressed controls ($F_{(2, 17)}$=4.896, p=0.021; Tukey's post hoc p=0.036; ***Fig. 3.4B***). This effect of swim stress amounted to an increase in c-Fos in 32.3 ± 7.0 % of TPH2/VGLUT3-immunoreactive neurons in the ventral DRN. The stress-induced increase in c-Fos immunoreactivity in TPH2/VGLUT3 co-expressing neurons was prevented by pre-treatment with fluoxetine, compared to saline controls (Tukey's post hoc: p=0.042; ***Fig. 3.4B***).

Similarly, swim stress also increased the number of c-Fos/TPH2 double-labelled neurons in the ventral DRN ($F_{(2, 17)}$=5.535, p=0.014; post hoc p=0.034) compared to non-stressed controls, with c-Fos/TPH2 double-labelled neurons amounting to 26.1 ± 2.8 % of TPH2-immunoreactive neurons. This effect was also attenuated by fluoxetine administration ($F_{(2, 17)}$=5.535, p=0.014; post hoc p=0.023; ***Fig. 3.4B***).

Conversely, TPH2-immunoreactive neurons which did not colocalise with VGLUT3 did not show a significant increase in c-Fos expression in response to swim stress ($F_{(2, 17)}$=2.115, p=0.151; ***Fig. 3.4B***), compared to control. Further, the number of TPH2-immunoreactive neurons did not differ between groups (***Fig. 3.4B***).

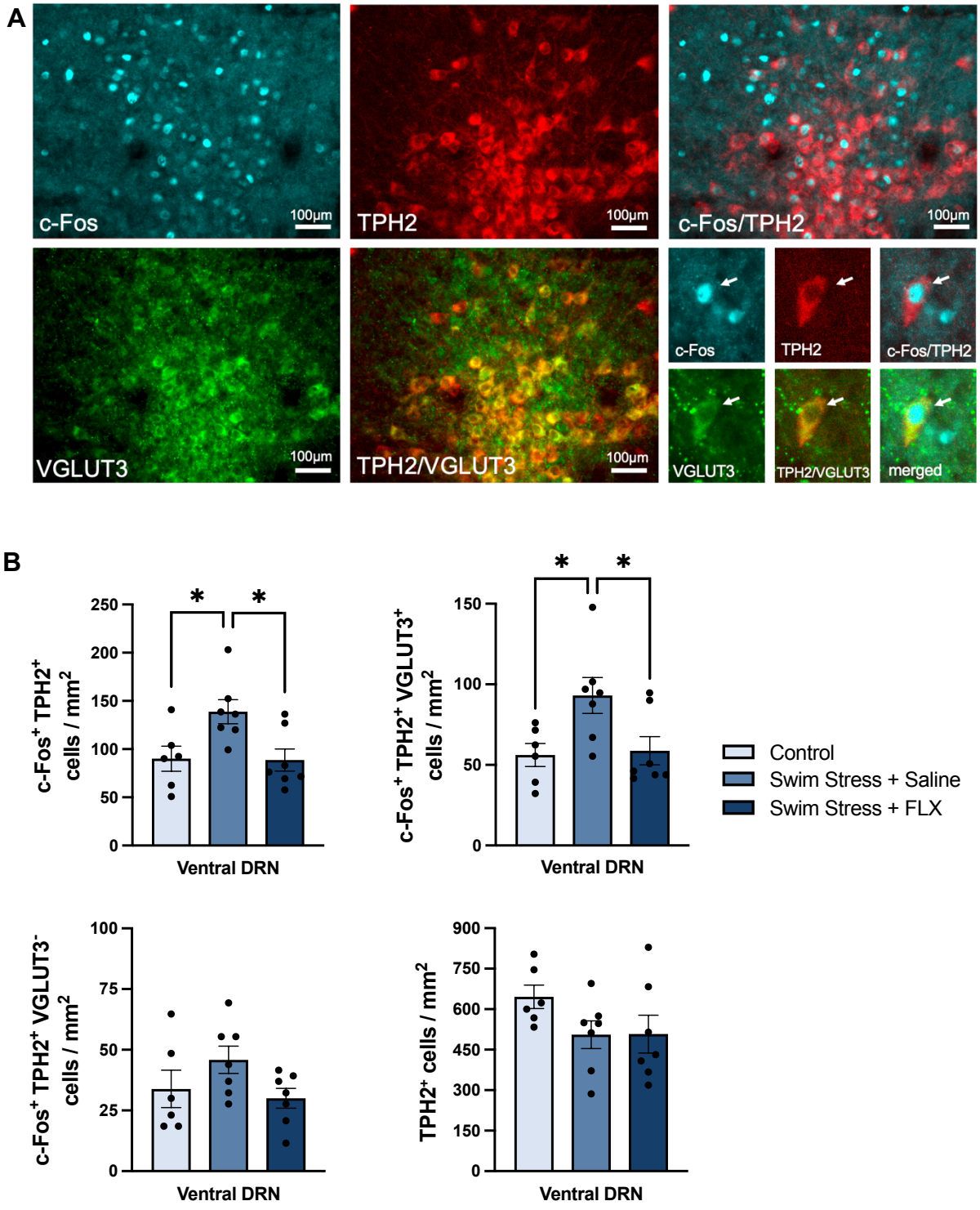

Figure 3.4 | Effect of swim stress, with or without fluoxetine, on c-Fos expression in neurons co-expressing TPH2 and VGLUT3 in the ventral DRN. (A) Representative image of c-Fos/TPH2/VGLUT3 triple-labelled neurons in the ventral DRN (AP= -4.6mm). **(B)** Effect of swim stress on number of c-Fos/TPH2 double-labelled neurons (top left), c-Fos/TPH2/VGLUT3

triple-labelled neurons (top right), c-Fos/TPH2 double-labelled neurons but VGLUT3-immunonegative (bottom left) and TPH2 immunolabelled neurons (bottom right). Columns represent the mean ± SEM values, with individual values indicated by closed circles. *p<0.05. Groups were control (n=6), saline + swim stress (n=7) and 10 mg/kg fluoxetine + swim stress (n=7).

3.3.4 Effect of swim stress on c-Fos expression in dorsal DRN and MRN neurons colocalising TPH2 and VGLUT3

In comparison to the ventral DRN, in the dorsal DRN swim stress did not significantly affect the number of c-Fos/TPH2/VGLUT3 triple-labelled neurons ($F_{(2, 15)}$=3.559, p=0.054, trend effect driven by saline vs fluoxetine; ***Fig. 3.5A)***. However, compared to controls, swim stress increased the number of c-Fos/TPH2 double-labelled neurons ($F_{(2, 15)}$=21.76, p<0.0001, post hoc p=0.0001; ***Fig. 3.5A***), and the number of or c-Fos/TPH2 neurons that were immunonegative for VGLUT3 ($F_{(2, 15)}$=34.62, p<0.0001, post hoc p<0.0001; ***Fig. 3.5A***) in the dorsal DRN.

Lastly, we examined the effect of swim stress on c-Fos expression in the MRN, and found no differences in the number of c-Fos/TPH2/VGLUT3 triple-labelled neurons ($F_{(2, 15)}$=2.845, p=0.09; ***Fig. 3.5B***), c-Fos/TPH2 neurons ($F_{(2, 15)}$=1.291, p=0.304; ***Fig. 3.5B***) or c-Fos/TPH2 neurons that were immunonegative for VGLUT3 ($F_{(2, 15)}$=0.686, p=0.519; ***Fig. 3.5B***), compared to non-stressed controls.

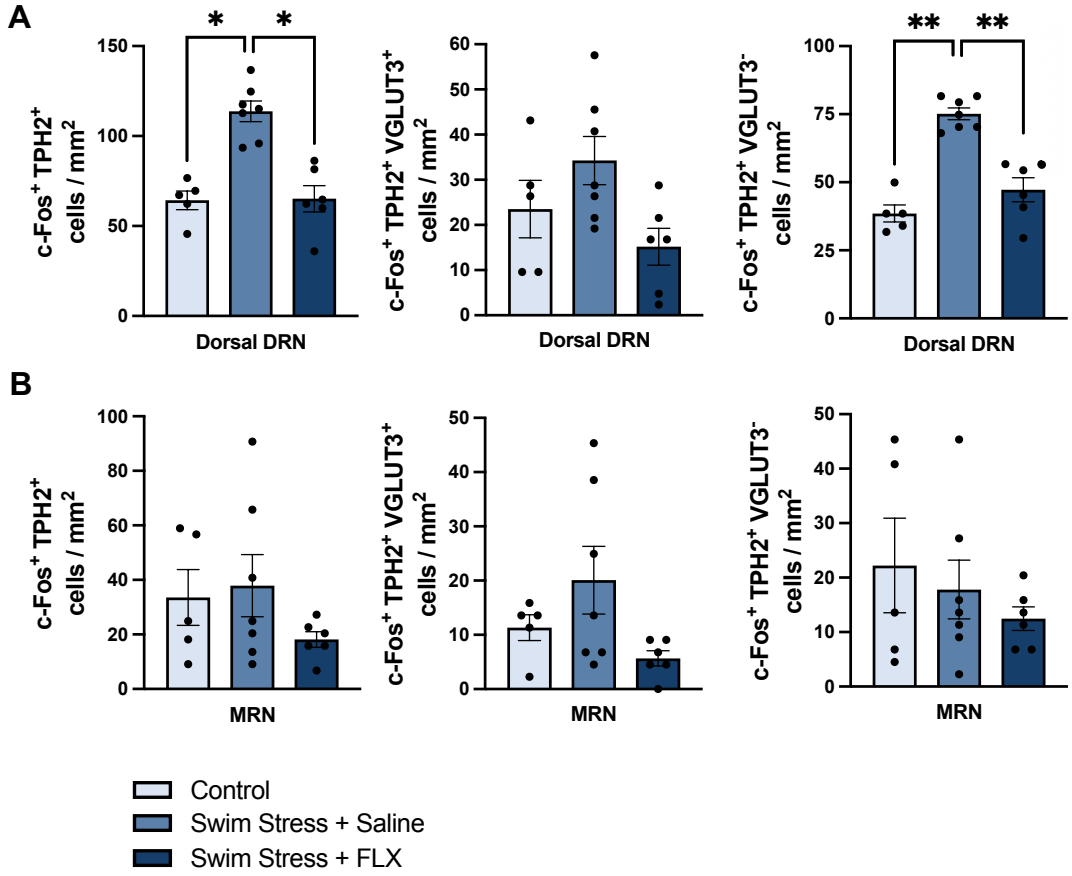

Figure 3.5 | Effect of swim stress on c-Fos expression in DRN neurons co-expressing TPH2 and VGLUT3 in the dorsal DRN and MRN. Effect of swim stress on number of c-Fos/TPH2 double-labelled neurons (left), c-Fos/TPH2/VGLUT3 triple-labelled neurons (middle), and c-Fos/TPH2 double-labelled neurons but VGLUT3-immunonegative (right). Columns represent the mean ± SEM values, with individual values indicated by closed circles. *p<0.005 **p<0.0001. Groups were control (n=6), saline + swim stress (n=7), and 10 mg/kg fluoxetine + swim stress (n=7).

3.3.5 Effect of single exposure to social defeat on c-Fos expression in DRN subregions

Next, we utilised the social defeat model to investigate the sensitivity of VGLUT3-expressing 5-HT neurons to a more controllable stressor. Naive intruder mice were exposed to a single episode of social defeat in the home cage of a larger territorially-dominant resident. Socially defeated mice were separated from the resident after a single

defeat episode, which typically occurred after a 1 min encounter, to prevent the stressor from becoming inescapable. The encounter involved a combination of biting, kicking, and wrestling, prior to a clear pin down (i.e. social defeat). The average latency for the resident to attack was 5.1 ± 1.7 s and the average number of attacks per encounter was 14.9 ± 2.8, (i.e. an attack every 3 s). During the encounter intruder mice spent most of the time moving (90 ± 3.1 %) and actively avoiding the resident (distance travelled 3.4 ± 0.8 m).

Region-specific analysis showed that acute social defeat had no effect on the number of c-Fos-immunoreactive neurons in the ventral DRN compared to non-stressed controls, and other DRN subregions were similarly unaffected (effect of region: $F_{(2, 27)}$=0.822, p=0.441, effect of treatment: $F_{(1, 14)}$=0.064, p=0.804, treatment x region interaction $F_{(2, 27)}$=1.123, p=0.340; ***Fig. 3.6A***). Moreover, the number of c-Fos/TPH2 double-labelled neurons in the ventral DRN was not different across groups ($t_{(13)}$=1.158, p=0.403; ***Fig. 3.6B***). In contrast to swim stress, acute social defeat did not alter the number of c-Fos/TPH2/VGLUT3 triple-labelled neurons in the ventral DRN compared to non-stressed controls ($t_{(13)}$=0.732, p=0.167; ***Fig. 3.6B***). Social defeat also had no effect on c-Fos expression in TPH2 neurons which were VGLUT3-immunonegative ($t_{(13)}$=1.167, p=0.264; ***Fig. 3.6B***), and the number of TPH2-immunoreactive neurons in the ventral DRN was also unchanged (***Fig. 3.6B***).

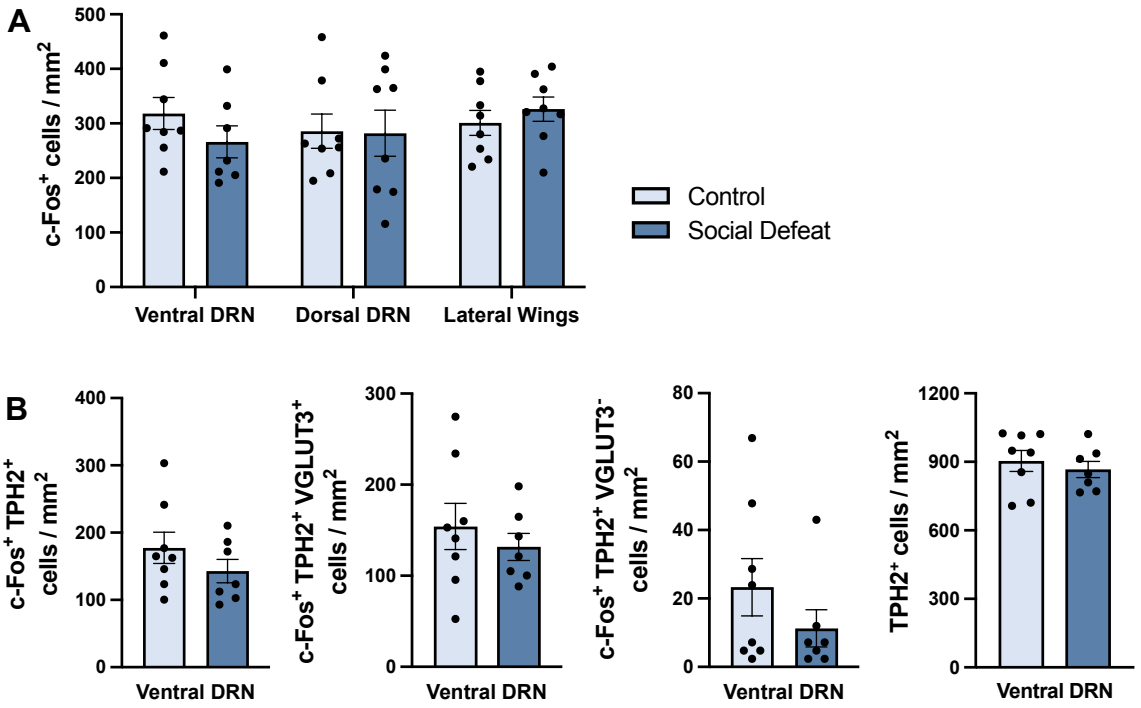

Figure 3.6 | Effect of acute social defeat on c-Fos expression in the DRN, including neurons co-labelled with TPH2 and VGLUT3. (A) C-Fos-immunoreactive neurons in DRN subregions. **(B)** C-Fos/TPH2 double-labelled neurons, c-Fos/TPH2/VGLUT3 triple-labelled neurons, c-Fos/TPH2 double-labelled neurons immunonegative for VGLUT3, and TPH2 neurons, in the ventral DRN. Columns represent mean ± SEM values, with individual values indicated by closed circles. Groups were non-stressed controls (n=8) and social defeat (n=7).

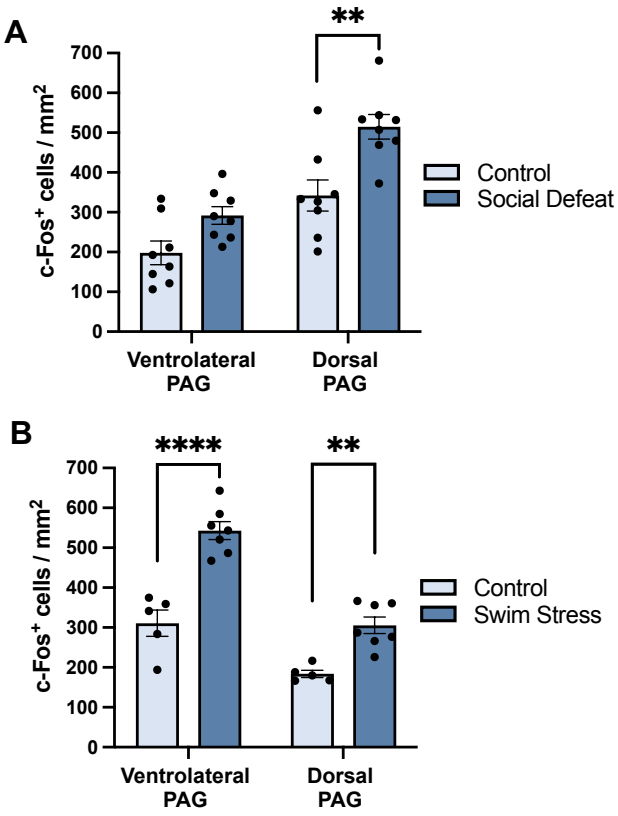

Figure 3.7 | Effect of acute social defeat and swim stress on c-Fos-immunoreactive neurons in the PAG. (A) C-Fos-immunoreactive cells in the PAG following social defeat (n=7) versus non-stressed controls (n=8). **(B)** C-Fos-immunoreactive cells in the PAG following swim stress (n=7), swim stress with fluoxetine (n=7) versus non-stressed controls (n=6). Columns represent mean ± SEM values, with individual values indicated by closed circles. **** p<0.0001 *** p<0.001 ** p<0.01 * p<0.05.

To confirm the efficacy of our social defeat paradigm, we examined c-Fos expression in other regions known to be activated by stress and involved in coping responses, specifically the dorsal PAG, which regulates fight or flight responses, and the ventrolateral PAG which mediates immobility, freezing and hypoactivity (Deakin & Graeff, 1991; Lino-de-Oliveira et al., 2006; Paul et al., 2014). Social defeat increased c-Fos expression in the dorsal PAG compared to non-stressed controls (effect of region: $F_{(1, 14)}$=181.4, p<0.0001, effect of treatment: $F_{(1, 14)}$=10.20, p=0.007, region x treatment

interaction: $F_{(1, 14)}$=8.358, p=0.012, post hoc p=0.001; ***Fig 3.7A***), while we observed a non-significant trend in the ventrolateral PAG (p=0.081).

In comparison, swim stress also increased c-Fos expression both in the dorsal and in ventrolateral PAG (effect of region: $F_{(1, 10)}$=60.77, p<0.0001, effect of treatment: $F_{(1, 10)}$=58.78, p<0.0001, region x treatment interaction: $F_{(1, 10)}$=5.597, p=0.04, post hoc p=0.001 and p<0.0001; ***Fig 3.7B***).

3.3.6 Behavioural response to swim stress in wildtype mice administered with fluoxetine

Lastly, we aimed to investigate the role of glutamate co-released from 5-HT neurons in coping behaviours in response to an acute stress. First, we analysed the performance of WT mice exposed to swim stress, to verify the efficacy of the paradigm. In WT mice treatment with fluoxetine prior to swim stress resulted in increased time spent climbing (Mann-Whitney U=6, p=0.016; ***Fig 3.8***), which is considered a measure of active coping behaviour (Commons et al., 2017). In comparison, fluoxetine did not alter time spent immobile ($t_{(12)}$=1.703, p=0.114; ***Fig 3.8***), or time spent swimming ($t_{(12)}$=0.294, p=0.884; calculated as, *total time – (time immobile + time climbing)*; ***Fig 3.8***). Latency to start floating was also similarly unaffected ($t_{(11)}$=1.149, p=0.275).

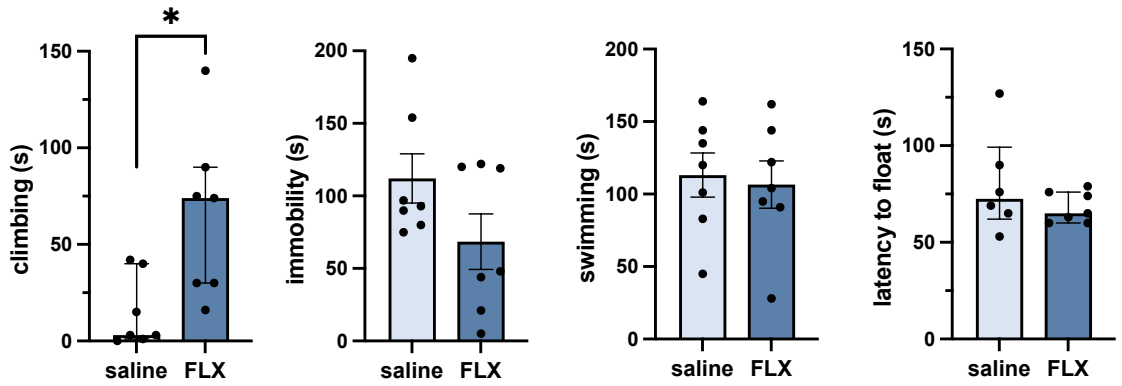

Figure 3.8 | Behaviour of wildtype mice exposed to swim stress with and without fluoxetine. Time spent climbing, immobile, swimming and latency to float during swim stress exposure. Columns represent mean ± SEM value, except for climbing where they indicate median ± interquartile range values. Individual values indicated by closed circles. * p<0.05. Groups were saline (n=7), and fluoxetine (FLX, n=7).

3.3.7 Behavioural response to swim stress in mice with VGLUT3-deficient 5-HT neurons

To further assess the role of glutamate co-release in stress coping behaviour, we also exposed genetically modified mice with conditional VGLUT3 deletion targeted to 5-HT neurons to the same swim stress paradigm. During swim stress, VGLUT3 cKO$^{5\text{-HT}}$ mice spent more time climbing versus littermate controls (Mann-Whitney U, p=0.043; ***Fig 3.9A***). Fluoxetine did not add further to this effect. Breakdown of the climbing data into smaller time bins (2 min) suggested that the VGLUT3 cKO$^{5\text{-HT}}$ mice showed persistent climbing over the duration of the experiment, while in controls climbing was reduced in the last 2 min (***Fig. 3.9A***). As seen with WT mice, fluoxetine did not affect time spent immobile in either genotypes (effect of fluoxetine: $F_{(1, 65)}$=3.93, p=0.052; effect of genotype: $F_{(1, 65)}$=0.019, p=0.892; fluoxetine x genotype interaction: $F_{(1, 65)}$=0.082, P=0.776; ***Fig 9B***), nor time spent swimming (effect of fluoxetine: $F_{(1, 65)}$=2.325, p=0.132;

effect of genotype: $F_{(1, 65)}$=0.031, p=0.861; fluoxetine x genotype interaction: $F_{(1, 65)}$=1.507, p=0.224).

Additionally, in a separate test, VGLUT3 cKO$^{5\text{-HT}}$ mice did not display any differences in locomotor activity after saline or fluoxetine administration, compared to littermate controls (effect of fluoxetine: $F_{(1, 34)}$=0.011, p=0.917; effect of genotype: $F_{(1, 34)}$=0.344, p=0.561; fluoxetine x genotype interaction: $F_{(1, 34)}$=0.9, p=0.378; ***Fig 9B***). Hence, the increase in climbing behaviour did not reflect an overall change in locomotion.

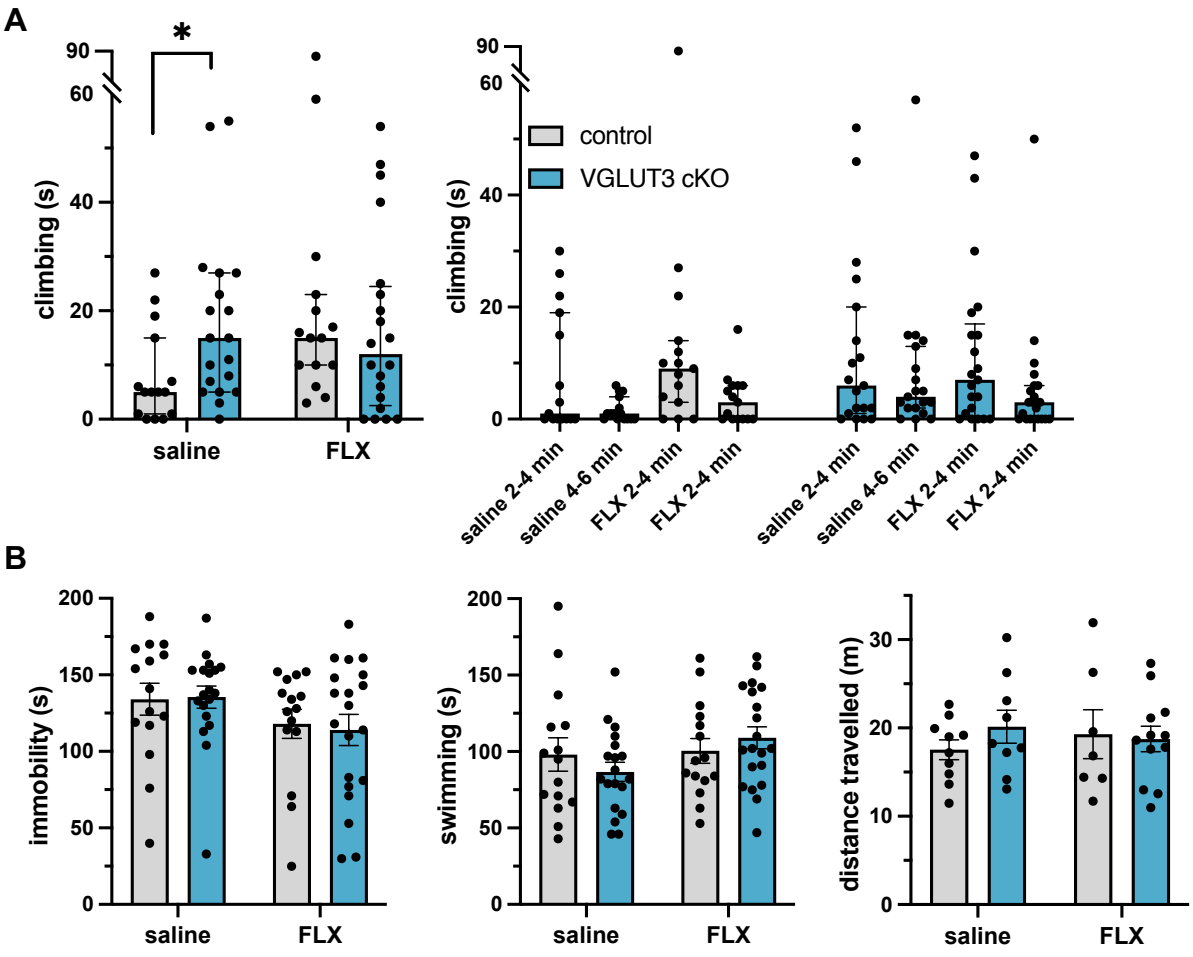

Figure 3.9 | Performance of VGLUT3 cKO$^{5\text{-HT}}$ mice and controls during acute swim stress with and without fluoxetine. **(A)** total time spent climbing during swim stress (left), and time spent climbing in 2 min time bins. **(B)** Time spent immobile during swim stress (left), time spent swimming during swim stress (middle) and total distance travelled in a clean cage 5 min prior to

swim stress. In (A) bars represent the median ± interquartile range value as data is non parametric, while in (B) bars depict mean ± SEM values. Individual values are indicated by closed circles. * $p<0.05$. VGLUT3 $cKO^{5\text{-}HT}$ mice (n=19-20), littermate controls (n=15).

3.4 Discussion

Here, immunohistochemistry was employed to investigate the colocalisation of TPH2 and VGLUT3 in the DRN, and to assess c-Fos expression in 5-HT neurons colocalising with VGLUT3 following acute stress. Thus, we report the first evidence that ventral DRN 5-HT-glutamate co-releasing neurons are activated by exposure to acute, uncontrollable swim stress. Additionally, VGLUT3 $cKO^{5\text{-}HT}$ mice showed increased climbing behaviour during swim stress, a measure of active coping. This behavioural response was similar to that of wildtype mice treated with fluoxetine, revealing an interesting parallel between the behavioural effects of genetic loss of VGLUT3 in 5-HT neurons and 5-HT reuptake inhibition.

3.4.1 TPH2 and VGLUT3 predominantly colocalised in the ventral DRN

Immunohistochemistry experiments using wildtype mice showed that TPH2 and VGLUT3 predominantly colocalise in the ventral DRN, thus this region was chosen to be the focus of further analyses. This finding replicated previous evidence from in situ hybridisation studies reporting VGLUT3 expression in TPH2 neurons (Hioki et al., 2010). More modest colocalisation of VGLUT3 and TPH2 was also observed in the dorsal DRN and MRN, as previously reported (Hioki et al., 2010). Conversely, in preliminary experiments we found only sparse colocalisation in the DRN lateral wings, thus this region was excluded from further analysis. Altogether, our results closely matched previous literature (Hioki et al., 2010), validating our methodology.

Here we focused on colocalisation between VGLUT3 and TPH2, but it has been reported that TPH2 also colocalises with GAD in the DRN (as discussed in *Chapter 1*, *Section 1.2.2.1*). Nonetheless, recent evidence from transcriptomics studies indicates that Pet1 neurons co-expressing GAD are located predominantly in the lateral wings and dorsal DRN, and that GAD does not colocalise with VGLUT3 (Okaty et al., 2020).

3.4.2 Swim stress evoked c-Fos expression in a region and cell-type specific manner

Following swim stress exposure we observed an increase in c-Fos expression in the DRN and MRN of wildtype mice, which is consistent with previous findings in rats (Hale et al., 2012; Kelly et al., 2011). However, region-specific analysis revealed that c-Fos expression was more prominent in the ventral DRN highlighting functional differences between DRN subregions. This result is consistent with the recent literature indicating a role of the ventral DRN in coping during swim stress (Ren et al., 2018).

Subsequent, cell-type specific analysis of the ventral DRN showed that this increase in c-Fos expression was greater in neurons colocalising TPH2 and VGLUT3, whist it did not reach statistical significance in TPH2 neurons that did not express VGLUT3. The stress-evoked c-Fos expression in ventral neurons colocalising TPH2 and VGLUT3 was inhibited by fluoxetine, which is in line with electrophysiological evidence that acute SSRI administration inhibits the firing of DRN 5-HT neurons through a 5-HT_{1A} autoreceptor mediated hyperpolarisation (El Mansari et al., 2005; Gartside et al., 1995; Rasmussen et al., 2004). To our knowledge this is the first report of evidence that in the ventral DRN

5-HT neurons with the capacity to co-release glutamate are activated by exposure to a stressor, specifically acute swim stress.

Conversely in the dorsal DRN, swim stress evoked c-Fos expression in neurons expressing TPH2, but not VGLUT3. Previous studies report that swim stress increases c-Fos in 5-HT neurons in the dorsal DRN (Kelly et al., 2011), but our data now suggest that these neurons lack the capacity to co-release glutamate. Further, in the dorsal DRN swim stress did not significantly affect the number of c-Fos/TPH2/VGLUT3 triple-labelled neurons, adding further evidence that the response of 5-HT-glutamate co-releasing neurons to stress in the ventral DRN were sub-region specific.

One caveat of using c-Fos as a marker of neuronal activation, is that it does not provide a direct measure of 5-HT-glutamate co-release in response to swim stress. Previous optogenetic studies on the basal amygdala indicate that glutamate is released by 5-HT neurons at low stimulation frequency (≤1 Hz), whereas 5-HT release occurs at higher frequencies (10–20 Hz; Sengupta et al., 2017). Electrophysiological studies also show that in response to stress or punishment 5-HT neurons typically present patterns of activation between 1-10 Hz (Cohen et al., 2015; Schweimer & Ungless, 2010). Thus, it seems plausible that during swim stress, both glutamate and 5-HT release would occur.

3.4.3 Single exposure to social defeat did not evoke c-Fos expression in DRN neurons colocalising TPH2 and VGLUT3

Next, it was investigated whether exposure to acute social defeat also elicited c-Fos expression in ventral DRN 5-HT neurons colocalising with VGLUT3, similar to swim stress. However, exposure to a single episode of social defeat did not increase c-Fos expression in DRN subregions, in DRN TPH2 neurons, nor in TPH2 neurons expressing VGLUT3. Previous evidence indicates that exposure to acute social defeat activates many brain areas involved in the general stress response (Martinez et al., 2002). Yet, reported effects on DRN 5-HT neurons are inconsistent, with different protocols yielding different results (Martinez et al., 2002; Matsuda et al., 1996). Indeed, an increase in c-Fos expression has been reported in the DRN of mice exposed to an aggressive conspecific for 10 min (Gardner et al., 2005; Numa et al., 2019), whilst others have reported no effect in this region following a stress exposure for 3 min (Matsuda et al., 1996), in line with the current results.

It is possible that longer social defeat protocols might act as an inescapable uncontrollable stressor, while in our paradigm a single brief defeat episode amount to the stressor being controllable. Here, while not being able to completely escape the aggressive resident animal, socially-defeated mice adopted a variety of active coping strategies and displayed little evidence of freezing or passive coping behaviour. As it has previously been shown that the 5-HT system is sensitive to the controllability of the stressor (Amat et al., 1998; Grahn et al., 1999), this could explain the differential c-Fos response to swim stress or acute social defeat.

Nonetheless, lack of differences between groups could also be due to a ceiling effect (as c-Fos expression in the control group was higher than expected), or it could be argued that the magnitude or length of the defeat encounter was insufficient to elicit a stress response. To confirm the efficacy of our paradigm, we examined c-Fos expression in regions known to process stress-induced fear and coping responses. Specifically, we quantified c-Fos expression both in the dorsal PAG, which mediates fight or flight responses, and the ventrolateral PAG, which is involved in freezing and immobility that characterises passive coping strategies (Deakin & Graeff, 1991; Paul et al., 2014). Interestingly, c-Fos expression increased in the dorsal PAG of socially defeated mice, hence corroborating the efficacy of our paradigm. Conversely, in mice exposed to swim stressed c-Fos expression increased in both the dorsal and ventrolateral PAG, with a greater response in the latter. This finding is line with previous studies (Lino-de-Oliveira et al., 2006), and might reflect the combination of active (i.e. climbing and swimming) and passive (i.e. immobility) coping strategies employed.

Thus, the current data suggest that 5-HT neurons with the capacity to co-release glutamate are preferentially activated by an uncontrollable versus controllable stressor. These data are consistent with previous c-Fos studies reporting that 5-HT neurons are more sensitive to uncontrollable versus controllable foot-shock (Amat et al., 1998; Grahn et al., 1999) but extend the findings to 5-HT-glutamate co-releasing neurons. Based on previous experiments involving localised injections of the GABA antagonist muscimol, it was concluded that controllable stressors have reduced impact on DRN 5-HT neurons due to the inhibitory influence of the medial prefrontal cortex (Amat et al., 2005). Thus, the greater effect of swim stress versus social defeat on VGLUT3-expressing 5-HT neurons could be explained by the same mechanism.

3.4.4 Wildtype mice administered with fluoxetine display increased climbing during swim stress

Acute swim stress has been widely used in the literature to assess responses to an inescapable stressor. It is well-known that acute treatment with an SSRI prior to swim stress increases active coping during swim stress, typically measured as time spent swimming as opposed to floating (Lucki, 1997; Petit-Demouliere et al., 2005). Here, we confirmed that in wildtype mice treatment with fluoxetine increased time spent climbing during swim stress, as previously reported (Carratalá-Ros et al., 2021; A. P. R. Costa et al., 2013). Whilst most swim stress studies in mice do not distinguish between swimming and climbing, it has been suggested that climbing is a more sensitive measure of active coping (Costa et al., 2013; Perona et al., 2008). Notably, in mice the climbing response to swim stress is 5-HT-sensitive, unlike in rats where the climbing response is also noradrenaline-dependent (Carratalá-Ros et al., 2021; Costa et al., 2013).

Perhaps surprisingly, fluoxetine had no effect on time spent immobile, but this has also been observed previously (Lucki et al., 2001; Perona et al., 2008). Here, C57BL/6 mice were employed due to comparability with the background strain of the VGLUT3 cKO$^{5\text{-HT}}$ mice, however this strain is known to be the least sensitive to SSRI-induced reduction in immobility during swim stress (Tang et al., 2014). Further, a water cylinder similar in dimensions to that used in the original Porsolt's experiment (Porsolt et al., 1977) was used, which is smaller than other water cylinder employed in the literature. As water cylinders of smaller size are also reported to increase immobility during swim stress (Rosas-Sánchez et al., 2022; Sunal et al., 1994), it was determined that climbing could be a more useful measure in this context.

3.4.5 VGLUT3 cKO$^{5\text{-HT}}$ mice displayed increased climbing during swim stress

Importantly, when exposed to swim stress VGLUT3 cKO$^{5\text{-HT}}$ mice spent more time climbing compared to control littermates, drawing an interesting parallel with the effect of fluoxetine in wildtype mice. Fluoxetine did not add further to the increase in climbing in the VGLUT3 cKO$^{5\text{-HT}}$ mice, potentially because of a ceiling effect. Further, the increase in climbing behaviour in the VGLUT3 cKO$^{5\text{-HT}}$ mice was not associated with increased locomotor activity in a separate test of locomotion.

As in wildtype mice no changes in time spent immobile were found across groups, likely due to the strain and water cylinder size, as discussed above. A previous study employing transgenic mice with complete VGLUT3 deletion also reported no differences in immobility during swim stress (using a similar strain and water cylinder size) compared to control mice, although interestingly these mice showed decreased swim stress-induced corticosterone levels (Balázsfi et al., 2018). Nonetheless, the latter study did not quantify climbing behaviour, thus limiting the comparability between the studies.

The increase in climbing behaviour exhibited by VGLUT3 cKO$^{5\text{-HT}}$ mice in the current study, is evidence of enhanced escape-driven active coping behaviour (Commons et al., 2017). Given our above immunohistochemical evidence that swim stress activates 5-HT-glutamate co-releasing neurons, it seems as if a deficiency in co-released glutamate in VGLUT3 cKO$^{5\text{-HT}}$ mice promotes active coping behaviour. This is surprising, as VGLUT3 cKO$^{5\text{-HT}}$ mice presented evidence of anhedonia and impairments in reward-based learning (*Chapter 2*), thus we might have expected VGLUT3 cKO$^{5\text{-HT}}$ mice to exhibit a reduction in coping behaviour as evidence of increased stress vulnerability.

It is possible that that the predicted lack of co-released glutamate in the VGLUT3 cKO$^{5\text{-HT}}$ mice would theoretically shift the 5-HT-glutamate balance at their receptors in favour of 5-HT. Interestingly fluoxetine, by selectively inhibiting 5-HT reuptake and causing an increase in extracellular 5-HT (Malagié et al., 1995; Stahl, 1998), would also shift the 5-HT-glutamate balance towards 5-HT (Fischer et al., 2015). Therefore, this shift in favour of 5-HT may promote active stress coping behaviour both in wildtype mice administered fluoxetine and in VGLUT3 cKO$^{5\text{-HT}}$ mice. This is also consistent with fluoxetine not affecting the behaviour of VGLUT3 cKO$^{5\text{-HT}}$ mice. The idea that a shift in the 5-HT/glutamate balance might be involved in SSRI action has been previously proposed, but it remains to be tested (Fischer et al., 2015).

The latter hypothesis that a shift towards 5-HT at its receptors might be linked to increased active coping could be consistent with the recent evidence indicating that chemogenetic activation of ventral DRN 5-HT neurons projecting to the prefrontal cortex increased active coping in mice exposed to swim stress (Ren et al., 2018). Since electrophysiological evidence (Sengupta et al., 2017) suggests that 5-HT-glutamate co-release is frequency-dependent, with 5-HT alone being preferentially released at higher frequencies (10-20 Hz), it is possible that chemogenetic activation may have preferentially released 5-HT, resulting in increased active coping. Conversely, conditional TPH2 KO from the same cortex-projecting ventral DRN 5-HT neurons was found to increase immobility (Ren et al., 2018), supporting the requirement for 5-HT in stress coping. Taken together, the above evidence suggests that altered balance of 5-HT-glutamate in favour of 5-HT, hence towards 5-HT signalling pathways, may increase active coping and play a role in the behavioural response to stress.

A caveat of this hypothesis is the current lack of consensus regarding the mechanisms of 5-HT-glutamate co-release (Trudeau & El Mestikawy, 2018). The evidence of the frequency-dependent nature of 5-HT-glutatamate co-release (Sengupta et al., 2017) suggests that 5-HT and glutamate are released from different vesicular pools. Conversely, co-release from the same vesicle has also been proposed (El Mestikawy et al., 2011) based on evidence that glutamate can promote vesicular accumulation of 5-HT in in presence of a VMAT2 inhibitor, an effect that was abolished in VGLUT3 KO mice (Amilhon et al., 2010; see *Chapter 1*, *Section 1.3.3.3* for more details). In presence of such vesicular synergy, a reduction of VGLUT3 expression may decrease the vesicular content of both glutamate and 5-HT, thus the loss of VGLUT3 in VGLUT3 cKO$^{5\text{-HT}}$ mice might disrupt the balance of glutamate-5-HT co-release less than expected. Nonetheless it is difficult to reconcile an increase in stress coping with an overall decrease in 5-HT release in these animals (e.g. Ren et al., 2018). A further caveat is that the VGLUT3 cKO$^{5\text{-HT}}$ mice may present changes in 5-HT neuronal function other than altered glutamate, that might contribute to altered stress coping.

Altogether, this suggests that the balance between 5-HT and glutamate released from 5-HT neurons might play a role in the behavioural response to stress, with the preferential release of 5-HT favouring active coping behaviour. This might be of relevance in situations where this balance is altered by environmental, genetic or pharmacological factors affecting expression of VGLUT3 (but also VMAT2 or SERT). Interestingly, there is evidence that VGLUT3 expression in 5-HT neurons is plastic, such that neurons can "switch phenotype" in response to an environmental trigger. For instance, a reduction in VGLUT3 expression in the ventral DRN has been observed in rats exposed to chronic stress (Prakash et al., 2020). Moreover, neurotransmitter switch from glutamate to GABA

has been reported in 5-HT neurons in lateral wings of the DRN during acquisition of generalised fear following acute stress (see *Chapter 6*, *Section 6.3* for further discussion; Li et al., 2024). Additionally, VGLUT3 expression transiently vary during neurodevelopment and early post-natal life (Boulland et al., 2004; Gras et al., 2005) and point mutations of the gene encoding VGLUT3 (Slc17a8) can lead to life-long alteration in levels of VGLUT3 (Ramet et al., 2017). Altogether, the above changes in VGLUT3 expression might affect the balance of 5-HT-glutamate at their receptors, and the present data suggest that they could impact on coping strategies and susceptibility to stress.

Chapter 4
Investigation of reward function in mice with conditional VGLUT3 knockout in 5-HT neurons

4.1 Introduction

In *Chapter 2*, it was reported that VGLUT3 cKO$^{5\text{-HT}}$ mice displayed decreased preference for sucrose, which could be indicative of anhedonia. *Chapter 3* investigated whether this putative anhedonia could be linked to increased sensitivity to stress, but instead VGLUT3 cKO$^{5\text{-HT}}$ mice showed evidence of increased active coping during swim stress. Therefore, it was hypothesised that in VGLUT3 cKO$^{5\text{-HT}}$ mice reduced sucrose preference could instead be linked to reduced sensitivity to reward. This hypothesis was based on evidence of reduced performance of VGLUT3 cKO$^{5\text{-HT}}$ mice in an appetitively-motivated spatial learning task (*Chapter 2*), as well as on previous evidence suggesting a role of 5-HT-glutamate co-release in reward processing (Liu et al., 2014; Wang et al., 2019). Therefore, this chapter will further investigate reward-based learning in VGLUT3 cKO$^{5\text{-HT}}$ mice, employing behavioural paradigms using operant chambers.

4.1.1 5-HT-glutamate co-release and reward

Much evidence from pharmacological, optogenetic and electrophysiological studies links the DRN to reward processing (see Luo et al., 2015 for a review). Importantly, experiments using slice electrophysiology showed that DRN VGLUT3-expressing 5-HT neurons excite VTA DA neurons which project to the NAc, a key reward area in the brain (Wang et al., 2019). However, retrograde labelling studies of DRN projections to the VTA

found that many of these neurons were non-5-HT glutamatergic neurons, and only 14% co-released 5-HT and glutamate (Qi et al., 2014).

Convergent evidence from behavioural studies using optogenetics and transgenic mice indicates that activation of DRN neurons is strongly rewarding in a glutamate-dependent manner (see *Chapter 1, Section 1.3.4.4*; McDevitt et al., 2014; Qi et al., 2014; Liu et al., 2014). Conversely, there is no consensus as to whether stimulation of DRN 5-HT neurons in reward-based behavioural tasks is reinforcing (Liu et al., 2014; Wang et al., 2019) or merely promotes patience in waiting for rewards (Fonseca et al., 2015; Miyazaki et al., 2012; Miyazaki et al., 2014). Nonetheless, a recent study found that optogenetic activation of either VGLUT3-positive or SERT-positive DRN projections to the VTA reinforced behaviour during conditioned place preference (Wang et al., 2019). Additionally, behavioural effects of optogenetic stimulation of 5-HT neurons during reward tasks were reduced, but not blocked completely by knocking out VGLUT3 from Pet1 neurons (consisting predominantly of 5-HT neurons but also 10% of glutamatergic neurons), whilst depletion of 5-HT blocked the residual effects (Liu et al., 2014). Altogether the evidence to date suggests that DRN neurons may play some role in reward processing via both 5-HT and glutamate, but the behavioural role of glutamate co-released from 5-HT neurons remains to be clarified.

4.1.2 5-HT-glutamate co-release and learning

Previous studies showed that mice with global VGLUT3 deletion displayed mild learning deficits as evidenced by reduced spontaneous alteration in a Y maze, slower avoidance-based learning in the Morris water maze and shuttle-box, and slower reversal

learning in a reward-based operant task (Fazekas et al., 2019). However, these experiments do not specifically inform on the role of glutamate co-released from 5-HT neurons. Moreover, since reward-based tasks often involve a learning component and the latter studies do not exclude the possibility that apparent deficits in reward behaviour actually involved changes in non-appetitive learning and memory.

4.1.3 Reward-based behavioural paradigms

Reward-based learning is a subset of conditioning involving an instrumental or Pavlovian response which is maintained by a reinforcer (Schindler & Goldberg, 2013). Reinforcers include appetitive rewards, or other biologically significant stimuli, such as water or warmth (Carlisle, 1970; Schindler & Goldberg, 2013). Available behavioural setups include a variety of mazes (e.g. straight-alley runway, T maze, Y maze, radial maze, conditioned place preference) and operant boxes (Ettenberg, 2009; Skinner, 1988; Staddon & Cerutti, 2003). In reward paradigms using mazes rodents typically learn to find rewards in a specific and reliable spatial location within the maze, while operant paradigms usually involve training the mouse to perform an instrumental response (e.g. lever press or nose-poke) to receive a reward. Reward-predictive cues, such as a sound or light cue can also be introduced, and the process through which rodents learn to associate a neutral stimulus to the reward is known as Pavlovian conditioning (Domjan, 2018; Mackintosh, 1974; Rescorla, 1988). Operant boxes typically allow for longer and more complex experiments, compared to mazes. Furthermore, different paradigms can be used to probe specific aspects of reward-based learning (e.g. attention, motivation, effort, reversal learning) (Lang et al., 2023). Lastly, behavioural tasks run in operant chambers can more easily be combined with techniques such as fibre photometry or

optogenetics, allowing time-locking biological signals of interest to specific events in the behavioural task (e.g. delivery of stimuli and rewards, responses made by the animal). (Akam et al., 2022; Kapanaiah et al., 2021).

4.1.4 Hypothesis and aim

This chapter aimed to investigate the role of glutamate co-released from 5-HT neurons in reward processing. To this end VGLUT3 cKO$^{5\text{-HT}}$ mice were tested in two operant-based reward paradigms as well as a battery of tests probing non-appetitive learning and memory. Specifically, it was hypothesised that compared to control littermates, VGLUT3 cKO$^{5\text{-HT}}$ mice would display reduced performance in reward-based tasks together with unimpaired learning and memory in non-appetitive tasks.

4.2 Methods

4.2.1 Animals

Experiments used male and female VGLUT3 cKO$^{5\text{-HT}}$ mice (SERT-Cre::VGLUT3$^{\text{LoxP/LoxP}}$, C57BL/*6J* background, aged 8-30 weeks) and their control littermates (SERT$^{+/+}$::VGLUT3$^{\text{LoxP/LoxP}}$). VGLUT3 cKO$^{5\text{-HT}}$ mice were generated and bred as described in *Chapter 2*. VGLUT3 cKO$^{5\text{-HT}}$ mice express Cre under the control of the SERT promoter (unlike their control littermates), thus reward-based learning was also assessed in SERT-Cre mice compared to wildtype (SERT$^{+/+}$) controls to ensure that Cre expression itself was not responsible for behavioural changes.

Mice were group-housed (2-6 per cage) with littermates in individually ventilated cages, in a temperature-controlled room (21^{o}C) on a 12 h light/dark cycle (light on 07:00, lights off 19:00). Unless specified otherwise, mice had access to food and water *ad libitum*, and cages were lined with sawdust bedding and contained cage enrichment consisting of sizzle nests and a cardboard tube. Mice were habituated to handling on three occasions before any experiment, and handling was always carried out using a cardboard tunnel (Gouveia & Hurst, 2019; Hurst & West, 2010)

Experiments followed the principles of the ARRIVE guidelines and were conducted according to the UK Animals Act of 1986, with appropriate personal and project licence coverage. All experiments were conducted and scored blind to genotype.

4.2.2 Behavioural tests

VGLUT3 cKO$^{5\text{-HT}}$ mice and control littermates underwent one of the following tests or batteries of tests, with at least two days interval between each test:

a. *Tests of reward function and learning*: food-restricted appetitively-motivated operant paradigm (with milkshake rewards), measurements of milkshake consumption (one-bottle test) and milkshake preference, spatial novelty preference test, and novel object recognition test (***Fig. 4.1***). Mice in this cohort were previously exposed to the marble burying test (*Chapter 2*).
b. *Social preference test*.
c. *Operant paradigm with water rewards.*

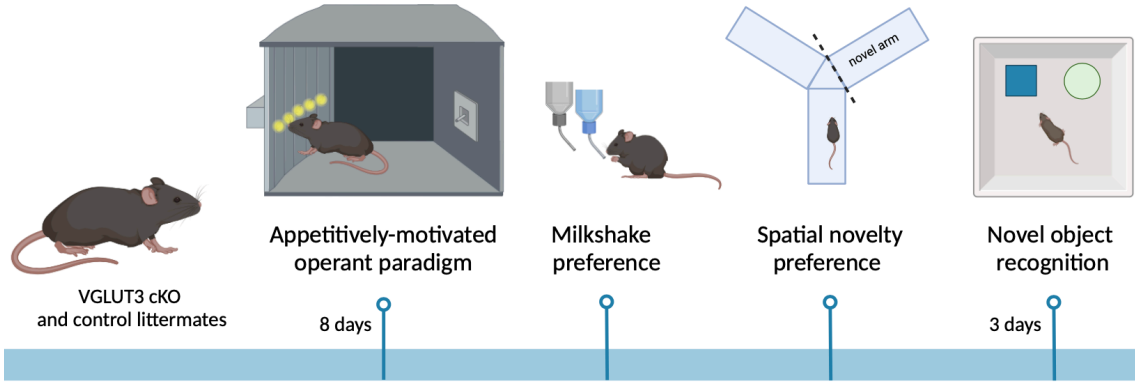

Figure 4.1| Experimental timeline of behavioural experiments investigating reward function and learning. Representation of experiments undergone by *cohort a*, with a minimum interval of 2 days between each test. Figure made with Biorender ©.

The behaviour of naïve SERT-Cre mice and littermate controls was assessed in the appetitively-motivated operant paradigm with milkshake rewards, as differences between VGLUT3 cKO$^{5\text{-HT}}$ mice and controls were particularly evident in this test.

All experiments were conducted during the light phase, unless otherwise specified. Mice were allowed to habituate to the testing room for at least 30 min prior to experimentation. In all experiments involving an apparatus without bedding, the apparatus was wiped with 0.5% Anistel (Tristel) to remove odours between animals.

4.2.3 Appetitively-motivated operant paradigm

Mice underwent food restriction from 5 days prior to the start of testing and then throughout the experiment, and were maintained at about 90% of initial body weight. Mice were weighed daily after the task and chow was administered to group-housed mice. The specific amount of chow was dependent on weight loss. If a given mouse showed significantly less weight loss compared to cage-mates, it was single-housed. Mice

were habituated to the reward which was strawberry milkshake (Yazoo kids) in their home cages to reduce subsequent hyponeophagia in the operant chambers. The operant apparatus was controlled using a Med-PC software package (Med Associates, SOF-735). Each operant box (20 × 20 cm, Med Associates, ***Fig. 4.2A***), contained a fan and was placed in a sound-attenuated dark chamber. Operant boxes were equipped with a panel of five nose-poke ports with recessed LED lights. On the wall opposite to these ports the milkshake "magazine" was installed (***Fig. 4.2A***), comprising of a drinking spout where milkshake (~12 μl) was dispensed by a syringe pump. The magazine was not equipped with a light to indicate reward availability, but it is possible that the smell of the milkshake and the noise of the syringe pump (which was, however, located outside of the sound-attenuated chamber) might have provided some cue of reward delivery.

Table 4.1 | Summary of the parameters employed in the operant paradigm with milkshake rewards

Day and session	Task	Description	Stimulus duration	ITI	Session duration
Day 1	**Habituation** to the setup	No ports are illuminated. Delivery of 5 milkshake rewards (12 μl each) from the magazine.	NA	5 min	30 min
Day 2-8	**Main task**	All 5 ports are illuminated, nose-poke of any illuminated port results in the port lights being switched off and triggers reward delivery (12 μl) from the magazine.	Until nose-poke	2 s	30 min or 40 correct responses

On the first day of training mice were habituated to the operant box for 30 min, during which 5 milkshake administrations were delivered (once every 5 min) from the magazine (***Table 4.1***). At this stage no ports were illuminated and no action was required to trigger milkshake delivery. The number of magazine head entries and nose-pokes into the ports were recorded.

In the following 7 days, mice were trained to perform an appetitively-motivated operant task in which a nose-poke into any of 5 illuminated ports triggered a milkshake reward from the magazine (***Table 4.1, Fig 4.2C***). This task has been previously used as a habituation stage to the 5-choice serial reaction time task (5-CSRTT; Bari et al., 2008) and involves all 5 ports always being illuminated simultaneously. Each training session started with a milkshake delivery (not contingent on any action) and its consumption triggered an inter trial interval (ITI) of 2 s, after which all 5 ports were illuminated until the mouse nose-poked any of the ports. This was recorded as a correct response and triggered the administration of a milkshake reward from the magazine (***Fig 4.2C***). Each day mice were tested for 30 min, or till 40 correct trials were reached. The number of magazine head entries, as well as latency to respond to the light stimulus with a nose-poke (timed from when the lights were turned on until nose-poke), and latency to consume the reward (timed from milkshake delivery until consumption) were also recorded. Any nose-poke occurring after a correct response but before reward consumption was considered a perseverative response (***Fig 4.2C***). In this task mice typically didn't perform any premature responses (i.e. responses during the ITI) due to the short ITI length (2 s) and the relatively large size of the box.

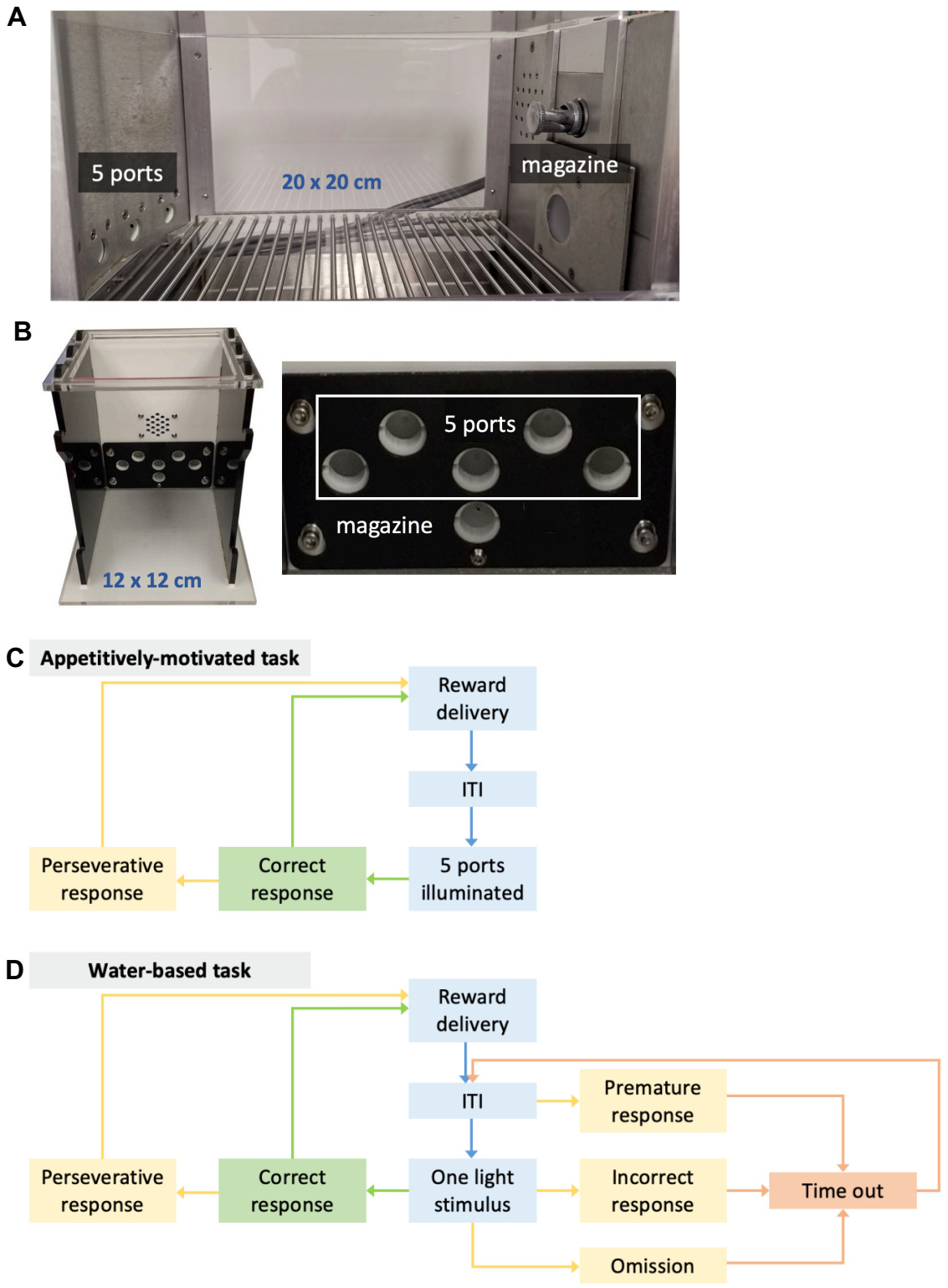

Figure 4.2 | Photographs of the operant chamber setups together with illustration of the main tasks used. (A) 5-poke operant chamber (Med Associates) used in the appetitively-motivated paradigm with milkshake rewards, and **(B)** custom-built operant chamber (Akam et al., 2022) used in the operant task with water rewards. **(C)** Tasks used in the appetitively-motivated paradigm with milkshake reward, and **(D)** in the operant paradigm with water reward.

4.2.4 Operant paradigm with water rewards

Animals were water-restricted throughout the experiment, commencing 48 h before the start of training. Mice were maintained at 90% of initial body weight and received most of their water intake from the task, but were individually topped up daily if necessary. The task was run using custom-built operant boxes (12 × 12 cm) controlled using PyControl software (Akam et al., 2022). Each box comprised 6 nose-poke ports located on the back wall (***Fig. 4.2***). Each port was equipped with a recessed LED light, and the lowest port placed in the centre of the wall also contained a solenoid to deliver water rewards, thus serving as a water magazine. The remaining 5 ports were 1.6 cm apart, located above the magazine port in an inverted W configuration (***Fig. 4.2B***). Mice were video-recorded using a FLIR Chameleon 3 camera positioned above each setup, and videos were analysed using a Bonsai based workflow (Akam et al., 2022)

Mice underwent two 30 min sessions per day, for 8 days. The parameters employed in each stage of training are summarised in ***Table 4.2***. Initially, the task was designed to mimic the training used for the food-restricted appetitively-motivated paradigm (described in *Section 4.2.3*). Therefore, it included a session of habituation to the setup (***Table 4.2***., day 1, session 1) as well as a stage in which mice had to poke any of 5 illuminated ports to receive a reward (***Fig 4.2C***, ***Table 4.2***., day 2). During the habituation to the setup (day 1, session 1) mice received 5 water administrations (at 5 min intervals) from the illuminated magazine port (***Table 4.2***), and magazine entries were recorded. On day 2, mice were allowed to perform a maximum of 40 correct responses (defined as a nose-poke of any of the 5 illuminated ports), and number of correct responses, time to reach 40 responses, response latency, number of magazine entries and reward latency

were measured. Nose-pokes during the ITI were recorded as premature responses, while nose-pokes after a correct response but prior to magazine entry/reward consumption were recorded as perseverative responses.

Table 4.2 | Summary of the parameters employed in operant paradigm with water rewards.

Day and session	Task	Description	Stimulus duration	ITI	Session duration
Day 1, session 1	**Habituation to the setup**	The 5 ports are never illuminated. At the start of the task the magazine light is on. Magazine entry causes the magazine light to switch off and delivers a water reward (10 µl). This is repeated 5 times.	NA	5 min	30 min
Day 1, session 2	**Magazine training**	The 5 ports are never illuminated. At the start of the task the magazine light is on. Magazine entry causes the magazine light to switch off and delivers a water reward (10 µl).	NA	30 s	30 min or 40 trials
Day 2, session 1-2	**Shaping for the main task**	All 5 ports are illuminated, nose-poke of any illuminated port turns off the 5 ports and turns on the magazine light. Entries into the illuminated magazine trigger reward delivery (10 µl).	till nose-poke	2 s	Maximum 40 correct responses
Day 3-8 (2 sessions per day)	**Main task**	At the start of the task, the magazine light is on. Magazine entry triggers a reward (10 µl) and initiates the task. During each trial one port illuminates randomly for 20 s. Nose-poke into the illuminated port (or in the following 2 seconds) switches off the port light, and turns on the magazine light. Mice can then collect the reward from the magazine. Premature, perseverative, and incorrect responses trigger a time-out of 5 s with house light off, prior to the ITI.	20 s	2 s	30 min

The setup for the water-based operant paradigm differed from that employed in the milkshake-based paradigm (***Fig. 4.2***), requiring the task to be adjusted accordingly. For example, in this setup mice had to nose-poke the illuminated magazine port in order to trigger water delivery, therefore an additional magazine training session was introduced (Day 1, session 2; see ***Table 4.2*** for details). During this session the number of magazine entries, number of rewards earned and latency to collect the reward (timed from when the port was illuminated to reward consumption) were recorded.

Furthermore, these custom-made operant boxes were much smaller than those used in the appetitively-motivated operant task, and involved the magazine being located on the same wall and in close proximity to the 5 ports (***Fig. 4.2***), which can facilitate the associative learning process. Thus, the difficulty of the task was increased from day 3 onwards, such that during each trial only one port was randomly illuminated for 20 s and the mouse was required to respond at this individual port in order to initiate the magazine light (as opposed to all 5 remaining lit until nose-poke, ***Table 4.2, Fig 4.2D***).

This task is similar to the first stage of the 5-CSRTT but with the caveat of the magazine being located on the same wall as the choice ports. Nose-poke of the illuminated port was recorded as a correct response while nose-poke of a non-illuminated port (when another port was illuminated) was recorded as an incorrect response (***Fig 4.2D)***. Failure to nose-poke during presentation of the light stimulus was recorded as an omission. Nose-pokes during the ITI were counted as premature responses while repeated pokes into the previously illuminated port (before reward consumption) were considered perseverative responses (***Fig 4.2D)***. Latency to nose-poke was measured from when the stimulus light was turned on until nose-poke, while latency to reward consumption was

measured from the correct response until magazine entry. Percentage accuracy was calculated as *correct responses/(correct responses + incorrect responses)*. Percentage correct, incorrect and omissions were calculated by dividing respective counts by the total number of trials. Results from the two daily sessions were averaged together to give one score per day.

4.2.5 Home cage milkshake consumption and preference

Milkshake consumption and preference were assessed to investigate whether altered preference for milkshake might impact performance in the operant task with milkshake rewards. Milkshake consumption and preference were measured over two non-consecutive evenings (18:00-24:00) during which mice were single-housed and exposed to strawberry milkshake *ad libitum* in a clean but familiar cage. Measurement of milkshake consumption was achieved in a one-bottle test in which mice were presented with a bottle containing milkshake (plus freely available food but no water bottle) for 4 h. The milkshake bottle was weighed prior to the test as well as after 1 h and at the end of the 4 h test period. On a separate evening mice underwent a milkshake preference test (7 h), involving simultaneous presentation of a milkshake bottle and a water bottle (as well as food). The positions of the bottles were swapped after 3.5 h to avoid place preference, and milkshake preference was measured as total milkshake consumption minus total water consumption.

4.2.6 Spatial novelty preference test

A spatial novelty preference test was carried out as previously described (Barkus et al., 2012; Sanderson et al., 2007), to investigate short-term spatial memory. The testing

apparatus consisted of a transparent Perspex Y maze (30 × 8 × 20 cm) lined with sawdust bedding which was placed in a dimly lit room containing a variety of extra-maze cues (e.g. colourful posters, large objects on nearby tables). Prior to testing each mouse was assigned one “familiar arm” and one “novel arm", counterbalanced between groups. The novel arm was closed off with a partition, and the mouse was placed in the “start arm” and allowed to explore the start arm and the familiar arm for 5 min, before being placed back in its cage. After 60 s, during which the partition was removed and the sawdust bedding was flattened, the mouse was placed back into the Y maze start arm and left free to explore all three arms for 2 min. The mice’s movements were recorded by an overhead camera, to allow for manual timing of time spent in each arm.

4.2.7 Novel object recognition test

The novel object recognition test was conducted over three consecutive days, as previously described (Leger et al., 2013) to investigate memory and response to novelty. On the first day the mice were habituated to the square arena (50 × 50 cm) for 10 min, in a dimly lit room. On the second day the mice were exposed for 10 min to two copies of the same object (the “familiar object”, counter-balanced between groups), secured on opposite sides of the arena. On the third day each mouse was presented for 10 min with a third copy of the familiar object, and a “novel object.” Both object identities and their positions within the arena were counter-balanced between groups. All sessions were recorded with an overhead camera and the amount of time spent exploring each object was timed manually. Exploration was defined as approaching, sniffing or touching the object. The objects used (a plastic unicorn toy and a wooden gnome) were of similar height (~7 cm) but varied in texture, shape, and colour.

4.2.8 Social preference test

The social preference test was carried out over two consecutive days (adapted from Rein et al., 2020), to assess preference for an unfamiliar conspecific compared to an inanimate object. The test setup consisted of a rectangular box (made of red see-through Plexiglas) comprising three connected consecutive chambers (19 × 45 cm; ***Fig. 4.3***). The two side chambers contained two barred cages (7 × 7 cm). On the first day of the test the barred cages were empty and mice were individually habituated to the three-chamber box for 10 min. On the testing day an unfamiliar mouse (of the same-sex and age-matched to the experimental mouse) was placed in a barred cage in one of the side chambers, whilst the cage located in the opposite side chamber contained a novel object (a roll of black tape). Positions of the unfamiliar mouse and the novel object were counterbalanced between groups. Mice were allowed to explore all 3 compartments for 10 min. Exploration of the compartment with the unfamiliar mouse was used as a measure for social preference.

Figure 4.3| Illustration the social preference test. Figure made with Biorender ©.

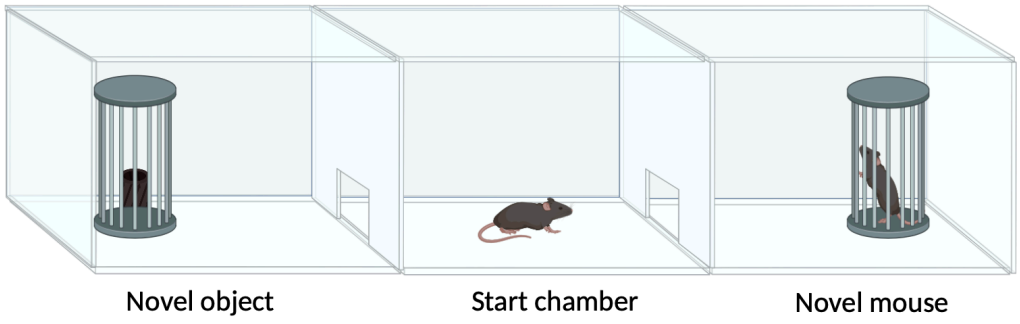

4.2.9 Statistical Analysis

The Shapiro-Wilk test for normality was applied to all data sets. All data were normally distributed, thus either a t-test or a one/two-way ANOVA was carried out as appropriate,

with the latter followed by Tukey's post hoc test. A two-way ANOVA with repeated measures was used on datasets with balanced groups, while a mixed effect model was employed in presence of unbalanced groups, or missing values due to technical issues. Data are presented as mean ± SEM values with $p<0.05$ being considered statistically significant. GraphPad Prism (v10) was used for analysis and plotting of graphs.

4.3 Results

4.3.1 Appetitively-motivated operant paradigm with milkshake rewards

During the first day of exposure to the operant boxes, in which mice received 5 milkshake deliveries (without needing to nose-poke), VGLUT3 cKO$^{5\text{-HT}}$ mice had a reduced number of magazine entries compared to littermate controls ($F_{(1, 29)}=4.254$, $p=0.048$; ***Fig. 4.4***). Analysis of magazine entries in 5 min time bins found no significant effect of time ($F_{(5, 145)}=0.932$, $p=0.462$; ***Fig. 4.4***) or interaction between time and genotype ($F_{(5, 145)}=0.962$, $p=0.443$; ***Fig. 4.4***), suggesting that the reduction in magazine entries was uniform across the whole session. The total number of nose-pokes in the 5 ports (which were never illuminated at this stage) was unchanged between groups ($t_{(29)}=0.875$, $p=0.389$, ***Fig. 4.4***), suggesting similar levels of exploration of the operant chamber.

In the subsequent appetitively-motivated operant paradigm all mice had an increased number of correct responses over the 7 days of training (effect of training day: $F_{(6, 180)}=50.65$, $p<0.0001$, ***Fig. 4.5A***). However, VGLUT3 cKO$^{5\text{-HT}}$ mice displayed a reduced number of correct responses compared to control littermates (effect of genotype: $F_{(1, 30)}=4.723$, $p=0.038$; genotype x training day interaction: $F_{(6, 180)}=4.752$, $p=0.0002$, ***Fig. 4.5A***). Tukey's post hoc revealed that this effect was significant on training days 6, 7, and

8 (p=0.008, 0.0001, 0.014). No sex-specific difference was detected in either genotype. VGLUT3 cKO$^{5\text{-HT}}$ mice also had a decreased number of entries in the magazine compared to controls (effect of genotype: $F_{(1,\ 30)}$=5.790, p=0.023; genotype x training day interaction: $F_{(1,\ 180)}$=2.98, p=0.009, ***Fig. 4.5B***), with a significant difference on days 6, 7, and 8 (p=0.024, 0.0002, 0.0009). Analysis of the number of perseverative responses revealed no effect of genotype or genotype x training day interaction ($F_{(1,\ 30)}$=1.390, p=0.248, $F_{(6,\ 180)}$=1.800, p=0.102, ***Fig. 4.5E***).

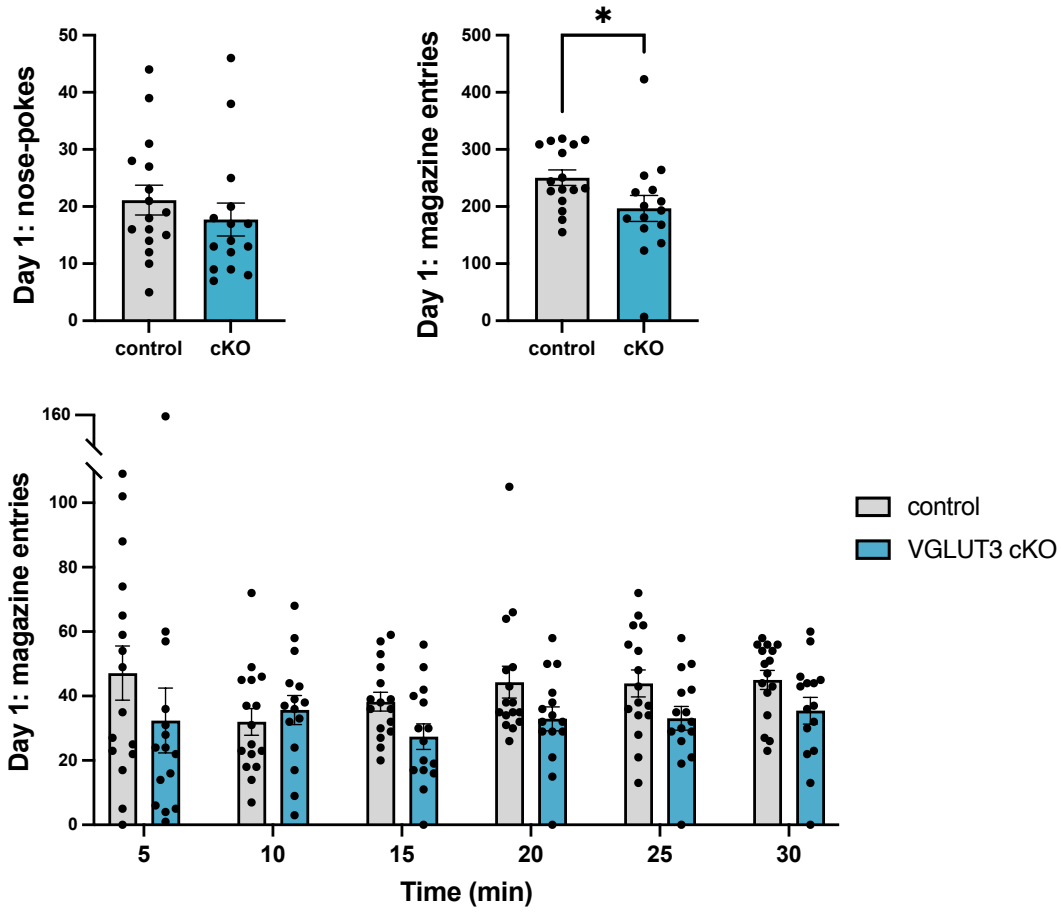

Figure 4.4 | Performance during habituation session (day 1) for the appetitively-motivated operant paradigm with milkshake rewards in VGLUT3 cKO$^{5\text{-HT}}$ mice and littermate controls. Columns represent mean number of nose-pokes in the 5 ports, which were not illuminated at this time (top left) and the mean number magazine entries, either during the whole session (top right) or in 5 min time bins (bottom). Data from VGLUT3 cKO$^{5\text{-HT}}$ mice (n=15) and control (n=17) were analysed by t-test or two-way repeated measures ANOVA. *p<0.05

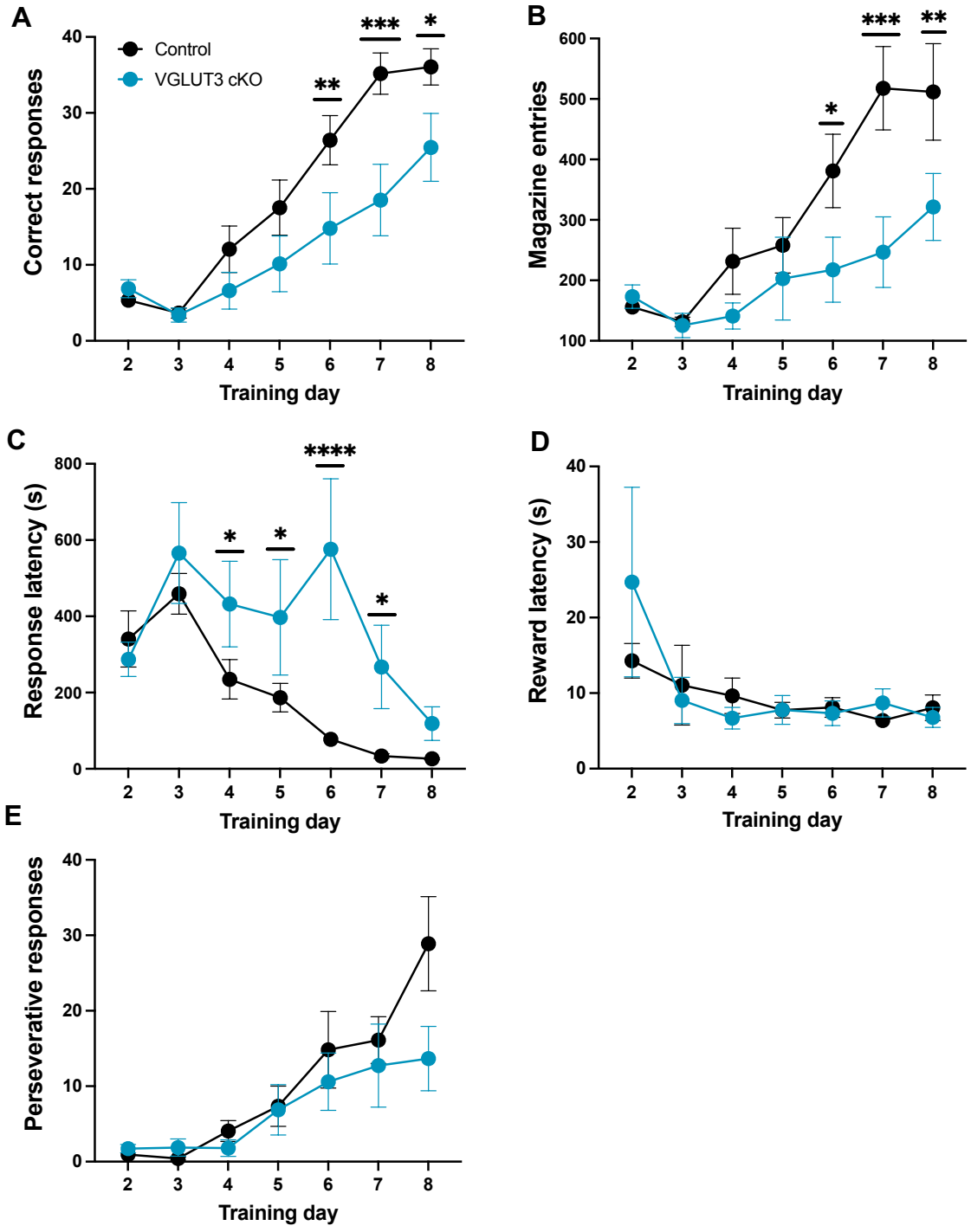

Figure 4.5 | Performance of VGLUT3 cKO$^{5\text{-HT}}$ mice and controls in the appetitively-motivated operant box paradigm. **(A)** Number of correct responses, **(B)** magazine entries, **(C)** response latency, **(D)** reward latency, **(E)** perseverative responses. Closed circle represent mean ± SEM values (some error bars are too small to be depicted) for VGLUT3 cKO$^{5\text{-HT}}$ mice (n=15) and controls (n=17). Data were analysed by repeated measures mixed-effect model, followed by Tukey's test. ****p<0.0001, ***p<0.001, **p<0.01, *p<0.05.

Additionally, VGLUT3 cKO$^{5\text{-HT}}$ mice were slower to nose-poke the light stimuli compared to control littermates (effect of genotype: $F_{(1,\ 30)}$=9.61, p=0.004; genotype x day interaction: $F_{(6,\ 158)}$=3.28, p=0.005 ***Fig. 4.5C***), with a significant difference on days 4, 5, 6 and 7 (p=0.049, 0.025, <0.0001, 0.047). Conversely, there was no difference between groups in the latency to consume the milkshake reward (effect of genotype: $F_{(1,\ 30)}$=0.201, p=0.657; genotype x day interaction: $F_{(6,\ 160)}$=0.690, p=0.658, ***Fig. 4.5D***).

VGLUT3 cKO$^{5\text{-HT}}$ mice express Cre under the SERT promoter to allow for the cKO of VGLUT3. Conversely, control littermates had floxed VGLUT3 but were wildtype for SERT (SERT$^{+/+}$). Therefore, to verify that Cre expression *per se* had no behavioural effects on reward based-learning we ran SERT-Cre mice through the same appetitively-motivated operant paradigm, compared to wildtype controls.

In the appetitively motivated operant task, SERT-Cre mice showed a trend increase in correct responses, compared to controls ($F_{(1,\ 14)}$=3.799, p=0.072, ***Fig. 4.6B***). VGLUT3 cKO$^{5\text{-HT}}$ mice also expressed Cre under the SERT promoter, but displayed a reduction in correct responses, thus it was concluded Cre expression was not responsible for this reduction in performance. Additionally, SERT-Cre mice did no differ from wildtype in their learning rate (effect of training day: $F_{(6,\ 84)}$=17.39, p<0.0001), with no interaction between time and genotype ($F_{(6,\ 84)}$=1.200, p=0.315).

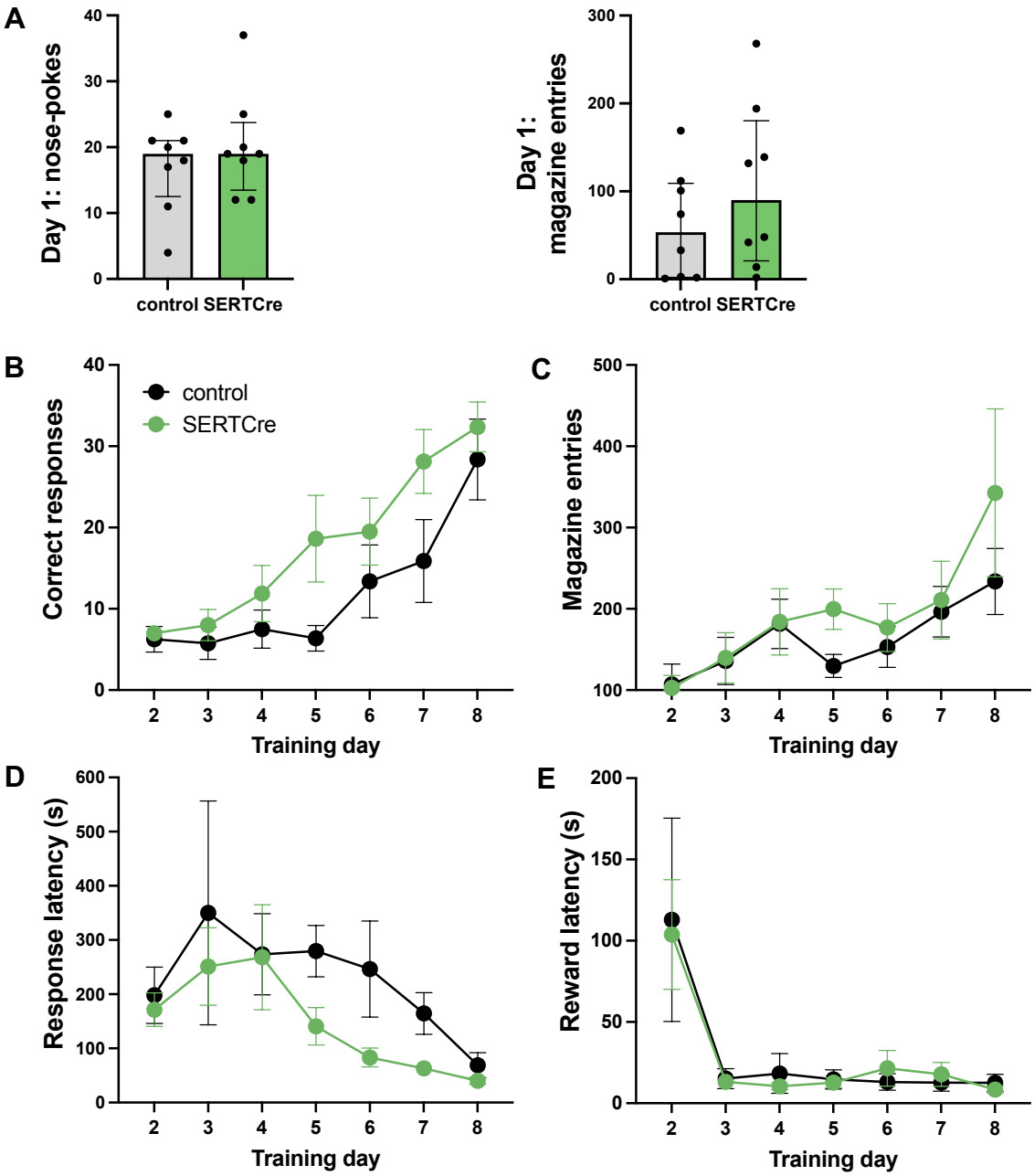

Figure 4.6 | Performance of SERT-Cre mice and controls in the appetitively-motivated operant box paradigm. **(A)** Data from day 1 (top row) and **(B-E)** days 2-7 for SERT-Cre mice (n=8) and littermate controls (n=8). **(B)** Number of correct responses, **(C)** magazine entries, **(D)** response latency, **(E)** reward latency. For the top row, columns represent mean ± SEM values with individual values indicated by closed circles. In the time plots, closed circles represent mean ± SEM values (some error bars are too small to be depicted). Data were analysed by t-test or repeated measures mixed-effect model.

The number of magazine head entries was also not different between SERT-Cre mice and controls (effect of genotype: $F_{(1, 14)}$=1.118, p=0.308; genotype x time interaction: $F_{(6, 82)}$=0.650, p=0.690, ***Fig. 4.6B***). Similarly, the latency to nose poke into the illuminated ports (effect of genotype: $F_{(1, 14)}$=1.855, p=0.195; genotype x time interaction: $F_{(6, 82)}$=0.372, p=0.895, ***Fig. 4.6D***), as well as latency to collect the milkshake reward (effect of genotype: $F_{(1, 96)}$=0.023, p=0.880; genotype x time interaction: $F_{(6, 96)}$=0.050, p=1.000, ***Fig. 4.6E***) were not different between groups. On the first day of exposure to the operant box, when the mice were habituating to the setup, the number of explorative nose-pokes ($t_{(14)}$=0.849, p=0.401***, Fig. 4.6A***) and magazine entries ($t_{(14)}$=1.074, p=0.301, ***Fig. 4.6A***) were also unaffected by genotype. Altogether this indicates that Cre expression in VGLUT3 cKO$^{5\text{-HT}}$ mice is not responsible for the observed impairments in reward-based learning.

4.3.2 Home cage milkshake consumption and preference

In a clean but familiar cage, VGLUT3 cKO$^{5\text{-HT}}$ mice showed no difference in milkshake consumption over 1 h ($t_{(30)}$=1.132, p=0.267) or 4 h ($t_{(30)}$=0.619, p=0.541, ***Fig. 4.7A***) in a one-bottle test. When presented with the choice of both milkshake and water, both genotypes consumed significantly more milkshake (main effect of solution: $F_{(1, 30)}$=321.200, p<0.0001), amounting to 90.5 ± 1.5 % of the total fluid consumption in controls and 91.5 ± 1.3 % in VGLUT3 cKO$^{5\text{-HT}}$ mice. There was no effect of genotype ($F_{(1, 30)}$=0.544, p=0.467) or interaction between genotype and the kind of solution ($F_{(1, 30)}$=0.652, p=0.423), thus milkshake preference (milkshake consumption minus water consumption; ***Fig. 4.7B***) was unchanged between groups.

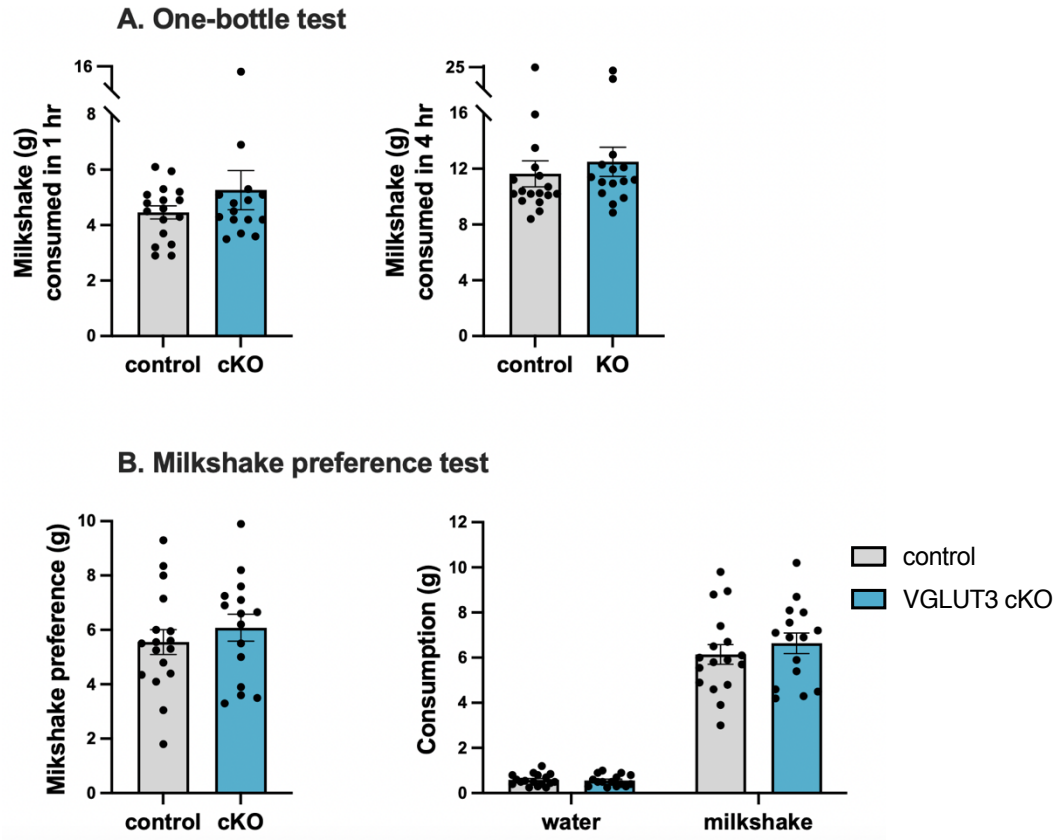

Figure 4.7 | Milkshake consumption and preference of VGLUT3 cKO$^{5\text{-HT}}$ mice versus littermate controls. (A) Total milkshake consumption in 1 h (left) or 4 h (right) by VGLUT3 cKO$^{5\text{-HT}}$ mice (n=15) and control littermates (n=17) **(B)** Milkshake preference (calculated as milkshake minus water) and raw values for water and milkshake consumption. Closed circles represent mean ± SEM values, individual values indicated by closed circles. Data were analysed by t-test or two-way ANOVA.

4.3.3 Spatial novelty preference test

The spatial novelty preference test was used to assess spatial short-term memory in VGLUT3 cKO$^{5\text{-HT}}$ mice and control littermates. Both groups showed preference for the novel arm, demonstrated by increased % time spent in the novel arm (performance of controls versus chance: $t_{(16)}$=3.923, p=0.001; performance of VGLUT3 cKO$^{5\text{-HT}}$ mice versus chance: $t_{(16)}$=2.789, p=0.014, ***Fig. 4.8A***) and there was no statistically significant difference in percentage time spent in the novel arm ($t_{(31)}$=1.430, p=0.163, ***Fig. 4.8A***) between VGLUT3 cKO$^{5\text{-HT}}$ mice and controls.

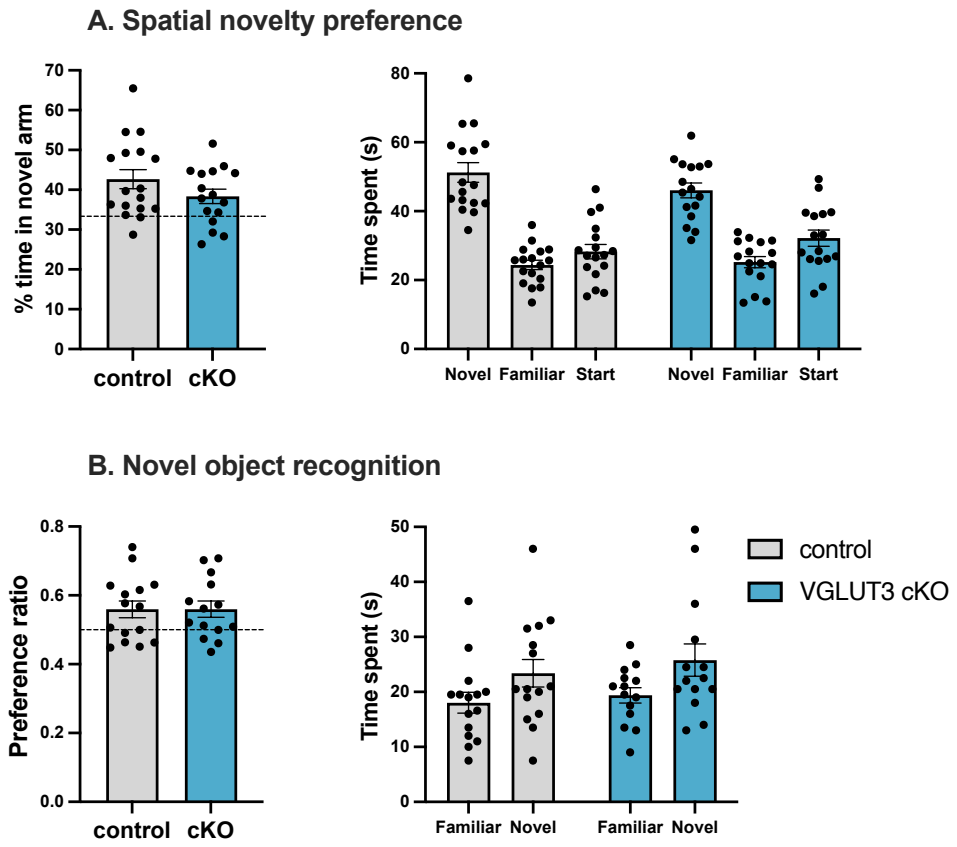

Figure 4.8 | Performance of VGLUT3 cKO$^{5\text{-HT}}$ mice and littermate controls in the spatial novelty preference and novel object recognition tests. (A) % time spent in the novel arm (left) and actual time spent in the novel familiar and start arms (right) by VGLUT3 cKO$^{5\text{-HT}}$ mice (n=16) and controls (n=17). **(B)** Preference ratio (time spent exploring novel object divided by total time spent exploring both objects; left), and actual time spent exploring the familiar and novel objects (right) in VGLUT3 cKO$^{5\text{-HT}}$ mice (n=14) and controls (n=15). Columns represent mean ± SEM values, with individual values indicated by closed circles. Data were analysed by t-test.

4.3.4 Novel object recognition test

The novel object recognition test was used for probing exploration as well as non-spatial short-term memory. Both VGLUT3 cKO$^{5\text{-HT}}$ mice and littermate controls showed a small but statistically significant preference for the novel object, with preference ratio measured as time spent exploring novel object divided by total time spent exploring both objects (performance of controls vs chance: $t_{(14)}$=2.455, p=0.028; performance of VGLUT3

cKO$^{5\text{-HT}}$ mice versus chance: $t_{(13)}$=2.531, p=0.025, ***Fig. 4.8B***) and there was no difference in terms of the novelty preference ratio between groups ($t_{(27)}$=0.011, p=0.992, ***Fig. 4.8B***).

4.3.5 Social preference test

The social preference test is reported to be useful as a non-appetitive measure of anhedonia (Scheggi et al., 2018), however it can also be used to probe anxiety-like behaviour (Bannerman et al., 2002). Both VGLUT3 cKO$^{5\text{-HT}}$ mice and control littermates spent more time in the chamber with the unfamiliar mouse, and this was statistically significant both compared to chance (control performance vs chance: $t_{(1)}$=7.715, p<0.0001; VGLUT3 cKO$^{5\text{-HT}}$ mice performance vs chance $t_{(1)}$=7.715, p<0.0001; chance was 33.33), or compared to time spent with the novel object (control: $t_{(22)}$=2.609; p=0.016; VGLUT3 cKO$^{5\text{-HT}}$ mice: $t_{(24)}$=2.995, p=0.006). Percentage time spent in the chamber with the unfamiliar mouse did not differ between groups ($F_{(1, 21)}$=0.164, p=0.690 ***Fig. 4.9***), but a two-way ANOVA found both an effect of sex ($F_{(1, 21)}$=10.69, p=0.004, ***Fig. 4.9***) and an interaction between sex and genotype ($F_{(1, 21)}$=11.25, p=0.003, ***Fig. 4.9***). Tukey's post hoc analysis showed that male VGLUT3 cKO$^{5\text{-HT}}$ mice spent more time in the chamber with the unfamiliar mouse (p=0.041) compared to male controls. Conversely, female VGLUT3 cKO$^{5\text{-HT}}$ mice spent less time in proximity of the unfamiliar mouse (p=0.0004) compared to male VGLUT3 cKO$^{5\text{-HT}}$ mice, but their performance was not different from female littermate controls (p=0.240). There was no effect of sex ($F_{(1, 21)}$=2.425, p=0.134), genotype ($F_{(1, 21)}$=1.879, p=0.185) or interaction between sex and genotype ($F_{(1, 21)}$=1.001, p=0.328) on distance travelled in the entire apparatus (***Fig. 4.9***).

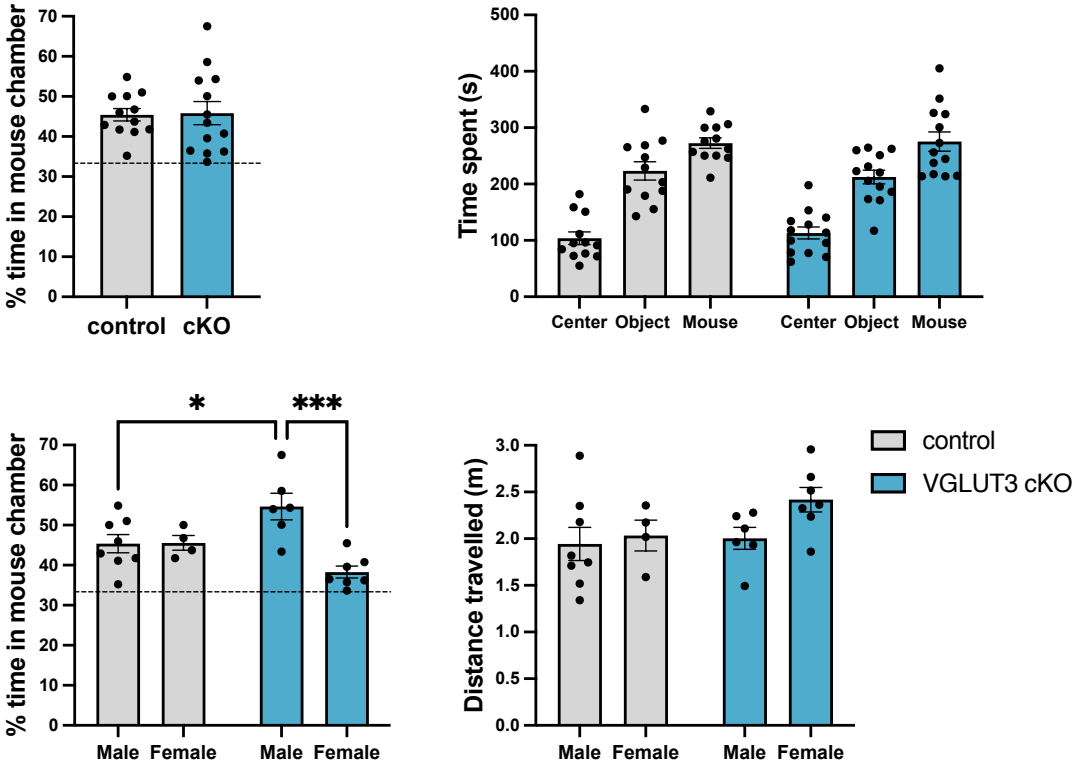

Figure 4.9 | Performance of VGLUT3 cKO$^{5\text{-HT}}$ mice and littermate controls in the social preference test. Percentage time spent in the chamber with the unfamiliar mouse (top left), and raw time spent in each of the 3 chambers (top right) for VGLUT3 cKO$^{5\text{-HT}}$ mice (n=12) and controls (n=13). Sex-specific analysis of % time spent in the chamber with the unfamiliar mouse (bottom left) and total distance travelled in the 3-chambers box (bottom right). Chance is represented by the dashed line (33%). Columns represent mean ± SEM values, with individual values indicated by closed circles. Data were analysed by t-test or two-way ANOVA followed by Tukey's test. ***p<0.001, *p<0.05

4.3.6 Operant box paradigm with water rewards

A different cohort of VGLUT3 cKO$^{5\text{-HT}}$ mice and control littermates were exposed to a reward-based operant task using water rewards to investigate whether the impairments displayed in the milkshake-based operant paradigm would generalise to water rewards as well. On the first day of training, when mice were habituated to the setup and received 5 water administrations, VGLUT3 cKO$^{5\text{-HT}}$ mice did not differ from controls in terms of number of magazine entries (see ***Table 4.3*** for statistical analysis) or nose-pokes in the 5

ports (which were not illuminated at this time). In the subsequent magazine training session there was also no difference in magazine entries (***Table 4.3***), with all mice successfully learning to receive water rewards upon nose-poke. On the second day, when mice learned to poke any of 5 illuminated ports to receive a water reward, VGLUT3 cKO$^{5\text{-HT}}$ mice did not differ from controls in the number of correct responses, time required to reach 40 responses, reward latency, or latency to nose-poke the illuminated port (***Table 4.3)***. Importantly, in this paradigm both genotypes performed 40 responses on the first day of training on this task. This highlights a difference between this setup and that used for the operant paradigm with milkshake rewards, where the majority of VGLUT3 cKO$^{5\text{-HT}}$ mice failed to reach 40 correct responses over 8 days of training.

Table 4.3 | Data for the first 3 days of training in the operant paradigm with water rewards. Groups were VGLUT3 cKO$^{5\text{-HT}}$ mice (n=8) and littermate controls (n=8). Data were analysed by t-test. Mean ± SEM values are shown.

Task and parameters	**Littermate controls**	**VGLUT3 cKO$^{5\text{-HT}}$**	**t test**
Day 1.1 Habituation to setup			
Magazine entries	107.5 ± 9.1	102.4 ± 13.9	$t_{(14)}$=0.306, p=0.764
Day 1.2 Magazine training			
Magazine entries	349.3 ± 28.1	346.1 ± 35.5	$t_{(14)}$=0.069, p=0.946
Number of rewards	36.0 ± 1.2	36.9 ± 1.3	$t_{(14)}$=0.484, p=0.636
Reward latency (s)	15.3 ± 1.4	15.2 ± 2.6	$t_{(14)}$=0.060, p=0.953
Day 2 Shaping for the main task			
Time to 40 rewards (s)	779.7 ± 112.8	704.8 ± 98.6	$t_{(14)}$=0.500, p=0.625
Magazine entries	341.6 ± 28.4	310.6 ± 17.4	$t_{(14)}$=0.930, p=0.368
Perseverative responses	52.3 ± 10.6	49.5 ± 6.2	$t_{(14)}$=0.224, p=0.826
Premature responses	16.2 ± 1.9	16.4 ± 2.5	$t_{(14)}$=0.080, p=0.937
Reward latency (s)	15.3 ± 1.4	15.2 ± 2.6	$t_{(14)}$=0.060, p=0.953
Choice latency (s)	10.9 ± 2.6	8.3 ± 2.1	$t_{(14)}$=0.775, p=0.451

During the main phase of the water-based paradigm, when only one of 5 ports was illuminated, VGLUT3 cKO$^{5\text{-HT}}$ mice were able to learn the paradigm over time, but showed a reduced number of correct responses and an increase in incorrect responses compared to littermate controls, amounting to a decrease in accuracy. Specifically, analysis of % correct responses revealed an effect of training day ($F_{(5, 70)}$=46.230, p<0.0001), no effect of genotype ($F_{(1, 14)}$=2.933, p=0.109) and an interaction between training day and genotype ($F_{(5, 70)}$=3.390, p=0.008), with post hoc analysis showing differences between genotypes on days 6 and 7 (p=0.010, 0.023, ***Fig. 4.10B***). Similarly, analysis of % incorrect responses found an effect of day ($F_{(5, 70)}$=20.700, p<0.0001), a trend effect of genotype ($F_{(1, 14)}$=3.89, p=0.069) and an interaction between day and genotype ($F_{(5, 70)}$=4.210, p=0.002). Differences between genotypes were observed on days 6, 7 and 8 (p=0.010, 0.012, 0.010, ***Fig. 4.10C***). Analysis of % accuracy also indicated an effect of day ($F_{(5, 70)}$=39.95, p<0.0001), a trend effect of genotype ($F_{(1, 14)}$=4.035, p=0.064), and an interaction between day and genotype ($F_{(5, 70)}$=4.385, p=0.002). Post hoc analysis revealed a statistically significant difference between VGLUT3 cKO$^{5\text{-HT}}$ mice and littermate controls on days 6, 7, and 8 (p=0.006, 0.010, 0.016, ***Fig. 4.10A***).

Conversely, VGLUT3 cKO$^{5\text{-HT}}$ mice did not differ from controls in % omissions (effect of genotype: $F_{(1, 14)}$=0.320, p=0.581; genotype x day interaction: $F_{(5, 70)}$=0.638, p=0.671, ***Fig. 4.10D***), number of premature responses (effect of genotype: $F_{(1, 14)}$=0.123, p=0.731; genotype x day interaction $F_{(5, 70)}$=0.404, p=0.844, ***Fig. 4.10E***) or number of perseverative responses (effect of genotype: $F_{(1, 14)}$=0.040, p=0.844; genotype x day interaction $F_{(5, 70)}$=0.720, p=0.610, ***Fig. 4.10F***).

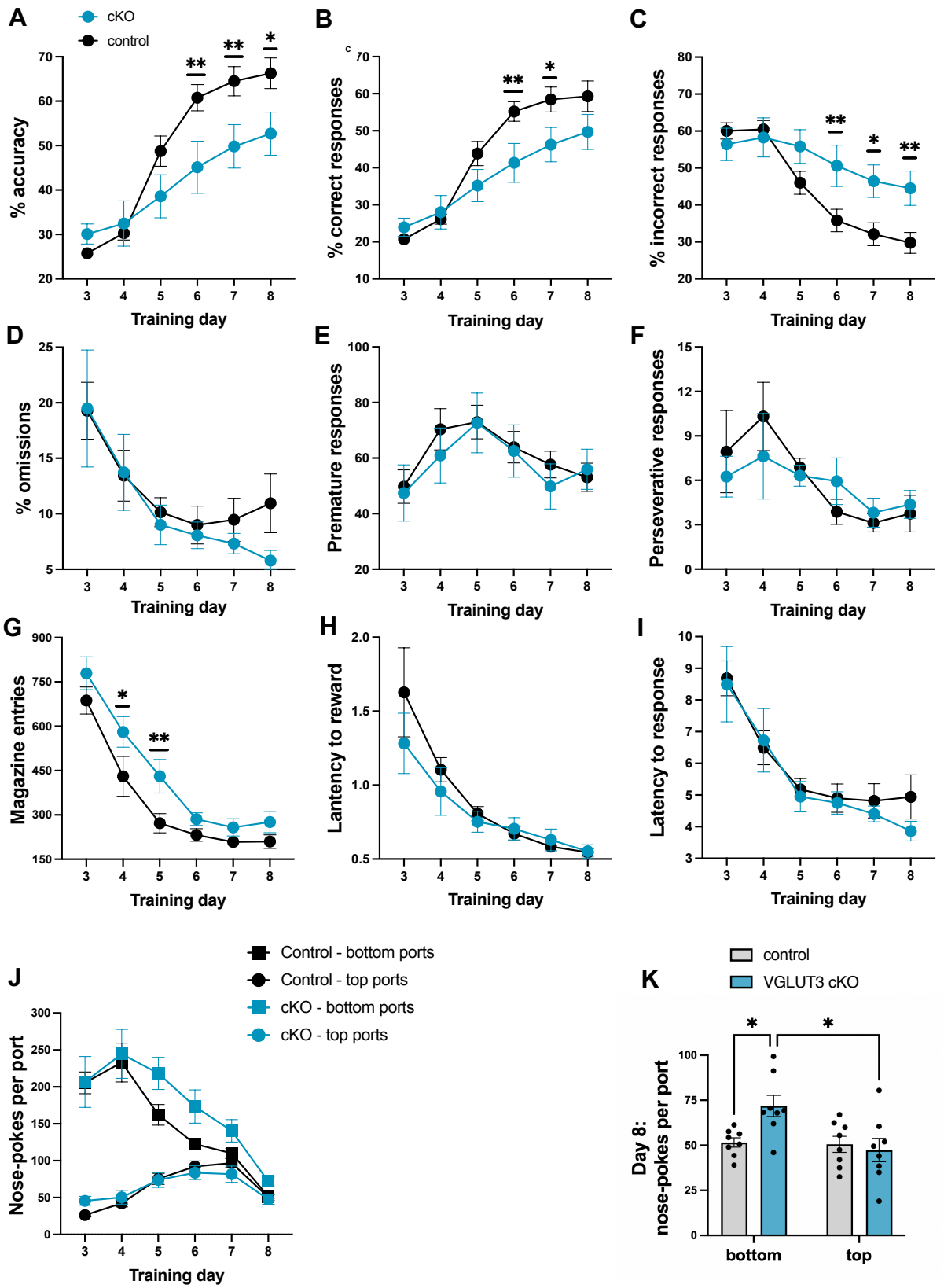

Figure 4.10 | Performance of VGLUT3 cKO$^{5\text{-HT}}$ mice and littermate controls in the water-based operant paradigm. (A-D) Percentage accuracy, correct and incorrect responses, and omission. **(E-G)** Number of premature and perseverative responses, and magazine entries. **(H-I)**

Latency to reward and choice. Closed circles represent mean ± SEM values. **(J)** Number of nose-poke entries per port. **(K)** Number of nose-poke entries in the lower or bottom ports, on day 8 of training. Groups were VGLUT3 cKO$^{5\text{-HT}}$ mice (n=8) and controls (n=8). Data were analysed by two-way ANOVA, followed by Tukey's test. ** p<0.01* p<0.05

Throughout the task VGLUT3 cKO$^{5\text{-HT}}$ mice performed a greater number of nose-pokes in the magazine port compared to littermate controls, with there being an effect of genotype ($F_{(1, 14)}$=7.973, p=0.014) and training day ($F_{(5, 70)}$=57.49, p<0.0001) but no genotype x day interaction ($F_{(5, 70)}$=0.871, p=0.506; ***Fig. 4.10G***). Conversely, there was no difference between genotypes in the latency to collect the water reward (effect of genotype: $F_{(1, 14)}$=0.716, p=0.412; genotype x day interaction: $F_{(5, 70)}$=0.798, p=0.555) or latency to respond to a light stimulus (effect of genotype: $F_{(1, 14)}$=0.206, p=0.657; genotype x day interaction: $F_{(5, 70)}$=0.499, p=0.776, ***Fig. 4.10H, Fig. 4.10I***).

In the first days of training all mice performed more nose-pokes in the bottom ports compared to the top ports (***Fig. 4.10J)***. This effect disappeared over time in control mice but not VGLUT3 cKO$^{5\text{-HT}}$ mice. For example, analysis of nose-poke locations on the last day of training (day 8) indicated a significant effect of port location ($F_{(1, 28)}$=49.23, p<0.0001), an effect of genotype ($F_{(1, 28)}$=4.802, p=0.037) and an interaction between port location and genotype ($F_{(1, 28)}$=7.311, p=0.012, ***Fig. 4.10K***). Post hoc analysis revealed that VGLUT3 cKO$^{5\text{-HT}}$ mice performed more nose-pokes in the bottom ports compared to the top ports (p=0.010), and had an increased number of nose-pokes in the bottom ports, compared to littermate controls (p=0.040, ***Fig. 4.10K***).

4.4 Discussion

In this chapter VGLUT3 cKO$^{5\text{-HT}}$ mice were used to investigate the role of glutamate co-released from 5-HT neurons in reward-based learning. Compared to littermate controls VGLUT3 cKO$^{5\text{-HT}}$ mice showed evidence of impairments in both a milkshake-motivated operant paradigm and a similar operant paradigm with water rewards. Furthermore, performance of VGLUT3 cKO$^{5\text{-HT}}$ mice was not different from controls in other tests probing learning and memory in other domains, suggesting that the role of glutamate co-released from 5-HT neurons is specific to reward-based learning.

4.4.1 VGLUT3 cKO$^{5\text{-HT}}$ mice show reduced performance in an appetitively-motivated operant task

Firstly, VGLUT3 cKO$^{5\text{-HT}}$ mice were tested in an appetitively-motivated operant task where nose-poke of any 5 illuminated port triggered delivery of a milkshake reward from a separate magazine. During training (days 2-8) VGLUT3 cKO$^{5\text{-HT}}$ mice demonstrated a reduced number of responses to the illuminated ports, fewer magazine entries, and were slower to respond to a light cue, compared to control littermates. On all these parameters, VGLUT3 cKO$^{5\text{-HT}}$ mice were able to improve over time but at a slower rate compared to controls. These findings could indicate impairments in reward processing, such as reduced interest in the reward or reduced motivation to work for rewards. Nonetheless, this task also involved learning and attention, thus deficits in these areas cannot be ruled out.

Importantly, in this task SERT-Cre mice did not differ from their control littermates, confirming that Cre expression under the SERT promoter is not the cause of the observed

behavioural phenotype and therefore the deficits reflect the predicted lack of glutamate co-release from 5-HT neurons.

Already on the first day of operant training (when mice received 5 rewards without having to nose-poke) VGLUT3 cKO$^{5\text{-HT}}$ mice approached the magazine less frequently, suggesting reduced interest in the milkshake reward. Nonetheless, when VGLUT3 cKO$^{5\text{-HT}}$ mice were presented with milkshake in their home cage neither their milkshake consumption nor milkshake preference over water were different from controls. This suggests that the behavioural differences in the operant paradigm were not caused by reduced preference for the reward.

In *Chapter 2*, it was reported that VGLUT3 cKO$^{5\text{-HT}}$ mice displayed reduced sucrose preference compared to littermate controls. This might seem in contrast with the current observation that milkshake preference was not different between groups. However, milkshake contains a greater amount of sucrose (specifically, 8.7%) compared to the 1% sucrose solution used in the sucrose preference test in *Chapter 2*. Moreover, previous evidence indicates that preference tests are most sensitive when using solution with low concentration of sugar, to avoid ceiling effects or high concentrations being aversive (Sclafani et al., 2010; Spector & Smith, 1984; Tordoff et al., 2008). As milkshake has a high sugar content the milkshake preference test might lack the sensitivity to identify subtle differences between groups.

4.4.2 VGLUT3 cKO$^{5\text{-}HT}$ mice display unimpaired social preference

As discussed in *Chapter 2*, the reduced preference for sucrose displayed by VGLUT3 cKO$^{5\text{-}HT}$ mice could be interpreted as anhedonia, which would likely affect other reward-related behaviours. In the present chapter VGLUT3 cKO$^{5\text{-}HT}$ mice were exposed to a social preference test aiming to assess anhedonia in a paradigm without an appetitive component. As mice naturally seek social interactions, reduced social preference may indicate anhedonia, depressive-like behaviour, or increased stress sensitivity, with mice models of depression often displaying reduced social preference (Scheggi et al., 2018; Yu et al., 2011). However, it is important to note that social preference has also been used as a measure of anxiety, with reduced social interactions being interpreted as evidence of anxiety-like behaviour (Bannerman et al., 2002). Both VGLUT3 cKO$^{5\text{-}HT}$ mice and control littermates spent more time interacting with an unfamiliar conspecific, compared to a novel object. Moreover, VGLUT3 cKO$^{5\text{-}HT}$ mice behaved similarly to controls and showed no evidence of reduced sociability or anhedonia.

Surprisingly, male VGLUT3 cKO$^{5\text{-}HT}$ mice showed increased social preference compared to male littermate controls, whereas female VGLUT3 cKO$^{5\text{-}HT}$ mice demonstrated reduced social preference compared to male VGLUT3 cKO$^{5\text{-}HT}$ mice. This is the first sex-specific difference of VGLUT3 cKO$^{5\text{-}HT}$ mice observed in this thesis, and no differences between sexes were observed in the sucrose preference test (*Chapter 2*) or the milkshake-motivated operant task.

4.4.3 VGLUT3 cKO$^{5\text{-HT}}$ mice show unimpaired short-term memory

VGLUT3 cKO$^{5\text{-HT}}$ mice were also exposed to a battery of tests probing learning and memory to clarify whether the observed reduction in performance in reward-based learning could be caused by a more generalised learning deficit. VGLUT3 cKO$^{5\text{-HT}}$ mice were not impaired in a spatial novelty preference test with recall after 1 min, or in the novel object recognition test with recall after 24 h. Thus, this evidence suggests that VGLUT3 cKO$^{5\text{-HT}}$ mice had unimpaired short-term memory in these tests.

Importantly, the tests discussed above were designed to probe non-associative learning, but they did not investigate non-appetitive associative learning. However, unpublished data from our collaborators from the Sorbonne University show that VGLUT3 cKO$^{5\text{-HT}}$ mice do not differ from control mice in terms of freezing behaviour during fear conditioning, in either contextual or cued tests. As fear conditioning relies on associative learning without an appetitive component, the latter result suggests that associative learning in the aversive domain is unimpaired in VGLUT3 cKO$^{5\text{-HT}}$ mice. Altogether, the evidence from the use of VGLUT3 cKO$^{5\text{-HT}}$ mice in various behavioural paradigms indicates that a lack of VGLUT3 in 5-HT neuron, and thus a predicted lack of co-released glutamate, causes deficits specific to reward-based learning and/or performance, with no concurrent learning impairments in other domains.

4.4.4 VGLUT3 cKO$^{5\text{-HT}}$ mice show reduced performance in a water-based operant task

Finally, to further investigate reward-based learning VGLUT3 cKO$^{5\text{-HT}}$ mice were assessed in an operant task using water rewards. This tested whether the deficits observed in the

milkshake-based operant task would generalise to another rewarding stimulus (i.e. water). Indeed, VGLUT3 cKO$^{5\text{-HT}}$ mice displayed a reduction in correct responses to receive water rewards. This finding suggests that the apparent deficit in reward-based learning generalises to both food and water rewards. However, the water-based task used here (in effect a low difficulty version of the 5-CSRTT) also included a greater attentional component, compared to the milkshake-based task, as mice were required to scan the 5 ports and select the illuminated one. Interestingly, VGLUT3 cKO$^{5\text{-HT}}$ mice displayed reduced accuracy and increased incorrect responses, which might suggest impairments in impulse control. However, the VGLUT3 cKO$^{5\text{-HT}}$ mice did not differ from controls in the number of premature and perseverative responses, which are often considered measures of impulsivity and compulsive behaviour respectively (Asinof & Paine, 2014).

The water-based operant paradigm differed from the milkshake-motivated operant task in that it involved operant boxes of a smaller size with the water magazine being located on the same wall and in close proximity to the 5 nose-poke ports, which facilitates associative learning. Additionally, unlike the milkshake-based task, in the paradigm with water reward the magazine was equipped with a LED light, and light cues were provided to indicate water availability, which might have facilitated associative learning. As a result of these differences in the operant setup, in the first stage of training of the water-based paradigm mice were able to learn the association between the light stimulus and reward delivery in only one day (compared to the 5-7 days required in the appetitively-motivated paradigm). At this point there was no difference in performance between groups. In the water-based paradigm there was also no difference between VGLUT3 cKO$^{5\text{-HT}}$ mice and their control littermates in the number of magazine entries in the habituation stage, nor in the magazine training, while differences in these training stages were already apparent

in the appetitively-motivated operant task. This result suggests that reward deficits of VGLUT3 cKO$^{5\text{-HT}}$ mice might be more apparent in more challenging or high-effort tasks, for example involving a choice between multiple ports, a larger chamber or an un-cued magazine located further away from the illuminated ports.

Furthermore, in the water-based operant task VGLUT3 cKO$^{5\text{-HT}}$ mice performed an increased number of magazine entries, which is surprising in the light of the reduction in magazine entries observed in the appetitively-motivated operant task. However, both these results could be explained by deficits in reward-based associative learning. As mentioned above, in the task with milkshake rewards the chamber was large and the light stimulus was located at a distance from the magazine, on the other side of the chamber. Thus, the VGLUT3 cKO$^{5\text{-HT}}$ mice were slower to learn to receive milkshake rewards from the magazine, resulting in reduced magazine entries. On the other hand, for the operant task with water rewards the source of the light stimulus was located on the same wall of the chamber as the water delivery. Thus, in this paradigm all mice were quick to learn the association between magazine entries and rewards, which encouraged nose-poking in the magazine. Nonetheless, learning the association between poking the correct light stimulus and receiving a reward from the magazine proved more challenging for VGLUT3 cKO$^{5\text{-HT}}$ mice, which kept entering the magazine instead of performing the task, leading to increased magazine entries. This might also be evidence of impairments in reversal learning, as having learnt to receive rewards from the magazine during the magazine training, VGLUT3 cKO$^{5\text{-HT}}$ mice might then struggle to switch to a different task, resulting in increased magazine entries. Further experiments could investigate the impact of reversal learning in VGLUT3 cKO$^{5\text{-HT}}$ mice, to clarify whether impairments in behavioural flexibility could contribute to the observed phenotype.

Altogether, the increase in both magazine entries and incorrect responses in the operant task with water rewards, might indicate that the VGLUT3 cKO$^{5\text{-HT}}$ mice were motivated to receive the reward but struggled to learn the task structure. In this task, on the whole the effort associated with nose-poking was relatively small due to the small chamber size. Analysis of nose-pokes locations revealed that at the end of training VGLUT3 cKO$^{5\text{-HT}}$ mice performed more nose-pokes in the bottom ports than top ports. This behaviour is also consistent with a lack of understanding of the task due to deficits in reward-based learning. However, as poking the top ports requires more effort, a contribution of reduced motivation or reduced ability to exert effort cannot be ruled out.

4.4.5 The role of co-released glutamate in reward

Altogether results reported here and in *Chapter 2* suggest that the VGLUT3 cKO$^{5\text{-HT}}$ mice have an impairment in reward-based learning, with no concurrent changes in appetite, short-term memory, exploration, anxiety, or aversive associative learning. Therefore, the data suggest that glutamate co-released from 5-HT neurons plays a role in processing of both food and water rewards. This is in line with previous evidence that glutamate co-released from 5-HT neurons leads to reinforcing effects during reward-based tasks (Liu et al., 2014; Wang et al., 2019). Future studies could investigate whether these impairments generalise to other types of non-appetitive rewards, such as finding a hidden platform in the water Y maze. This task relies on the innate drive of rodents to escape an aversive stimulus (i.e. water), nonetheless finding the platform also acts as a reward for the correct arm choice (Klapdop & Van Der Staay, 1996; Pistell & Ingram, 2010). Furthermore, sensitivity of VGLUT3 cKO$^{5\text{-HT}}$ mice to pharmacological rewards

could also be investigated in paradigms such as conditioned place preference or self-administration.

This chapter focussed on the behavioural effects of glutamate co-released from 5-HT neurons, while the molecular and anatomical pathways involved were not addressed. Previous optogenetic studies have shown that DRN 5-HT-glutamate co-releasing neurons establish synapses onto VTA DA neurons causing DA release into the NAc (Wang et al., 2019). Thus, it was hypothesised that the behavioural deficits displayed by VGLUT3 cKO$^{5\text{-HT}}$ mice might be caused by a reduction in function of this mesolimbic DA pathway. To probe *in vivo* DA function of VGLUT3 cKO$^{5\text{-HT}}$ mice, experiments in the next chapter used fibre photometry with a DA biosensor to record DA release in the NAc during reward task with water rewards.

Chapter 5
Investigation of dopamine signalling in mice with conditional VGLUT3 knockout in 5-HT neurons

5.1 Introduction

In *Chapter 4*, VGLUT3 cKO$^{5\text{-HT}}$ mice were tested in two reward-based operant paradigms in which they demonstrated impairments in reward-based learning compared to control littermates. As previous studies showed that 5-HT-glutamate co-releasing neurons excite VTA DA neurons projecting to the NAc (Wang et al., 2019), it was hypothesised that the observed deficits might be linked to a reduction in DA release in the NAc of VGLUT3 cKO$^{5\text{-HT}}$ mice. Therefore, in this chapter fibre photometry with a DA biosensor was used to assess *in vivo* DA release in the NAc during a reward-based operant task.

5.1.1 DA in reward processing

Much evidence indicates that the DA system plays an important role in reward processing (Arias-Carrión et al., 2010; Berridge & Robinson, 1998; Schultz, 2002, 2016a; Wise & Rompre, 1989). DA cell bodies are primarily located in the midbrain, in the VTA and substantia nigra, from where they give rise to several key pathways, including the mesolimbic pathway, mesocortical pathway, and nigrostriatal projections (Björklund & Dunnett, 2007; Hillarp et al., 1966; Ikemoto, 2010). The mesolimbic pathway arising from the VTA and projecting to the NAc, amygdala,

hippocampus, and prefrontal regions, is strongly activated by rewarding stimuli (Salamone et al., 2016). Thus in *in vivo* voltammetry studies, unsignalled or unexpected rewards are associated with a brief increase in the firing rate of DA neurons, leading to DA release in the NAc (Phillips et al., 2003; Roitman et al., 2004). This DA release is theorised to encode a reward prediction error signal, defined as the difference between expected and actual rewards, with unexpectedly greater rewards being associated with greater DA release (Matsumoto & Hikosaka, 2009; Schultz, 2016; Schultz et al., 1997).

In Pavlovian conditioning the reward prediction error facilitates learning of associative relationships between stimuli and rewards. In fact, when a conditioned stimulus (CS) is followed by an unexpected reward (unconditioned stimulus, US) it causes an increase in NAc DA release, which with repeated pairings leads to a stronger CS-US association (Day & Carelli, 2007). Specifically, early in learning DA neurons are robustly activated by reward occurrence but weakly to reward-predictive cues. However, after repeated presentations of the CS with the US, NAc DA release in response to the reward-predicting CS increases, while NAc DA release following the US diminishes. In other words, there is a gradual transfer of DA response from the US to the CS (Cohen et al., 2012; Pan et al., 2005; Pan & Hyland, 2005; Schultz et al., 1993). Additionally, when an expected reward does not occur a negative prediction error is generated, characterised by a pause in the firing of DA neurons and a drop in DA release below baseline levels (Diederen & Fletcher, 2020; Schultz, 2016, 2016; Schultz et al., 1990). This illustrates the role of DA as a "teaching signal" in associative learning, modulating expectations and adjusting future

behaviour based on past experiences (Bromberg-Martin et al., 2010). More generally, DA also plays a role in motivation, behavioural activation, movement, attention, and promoting effort to work for rewards (Nicola, 2010; Salamone et al., 2009; Salamone & Correa, 2012; Walton & Bouret, 2019).

5.1.2 Interactions between DA and 5-HT in reward processing

Viral tracing studies showed that the DA system interacts with the 5-HT system through reciprocal connections between DRN 5-HT neurons and DA neurons in the VTA, NAc, dorsal striatum, and substantia nigra (Beier et al., 2015; Ogawa et al., 2014; Ogawa & Watabe-Uchida, 2018). Moreover, in situ hybridisation evidence revealed that one-third of VTA DA neurons express the 5-HT_{3A} receptor (Wang et al., 2019). DA neurons can also be affected by several other 5-HT receptor subtypes, including 5-HT_{1A}, 5-HT_{1B}, 5-HT_{2A}, 5-HT_{2C} and 5-HT_{4} receptors (Di Giovanni et al., 2008). Additionally, 5-HT and DA neurons co-reside in the DRN (Matthews et al., 2016; Taylor et al., 2019) which could allow for direct cross-talk between these two neuronal subpopulations.

Historically, 5-HT was thought to oppose the DA system by encoding punishment, responding to aversive stimuli, and mediating behavioural inhibition (Amo et al., 2014; Boureau & Dayan, 2011; Cools et al., 2011; Daw et al., 2002; Deakin & Graeff, 1991; Takase et al., 2004). Based on more recent optogenetic evidence it has also been suggested that 5-HT neurons might also promote waiting for rewards by increasing tonic activity in the reward anticipatory phase (Miyazaki et al., 2011,

2012). Additionally, recent photometry and electrophysiological studies have shown that, similar to DA neurons, 5-HT neurons are activated by rewards and reward-predictive cues (Cohen et al., 2015; Liu et al., 2020; Miyazaki et al., 2011), and can differentially encode reward expectation and reward value (Li et al., 2016; Zhong et al., 2017). However, unlike DA, it is thought that 5-HT does not encode the direction of the prediction error, but rather it signals surprise (i.e. an unsigned prediction error) whenever contingencies are changed, such as in reversal learning tasks (Matias et al., 2017). Furthermore, DA and 5-HT responses appear to exhibit different kinetics whereby DA responses rise and decline rapidly, while 5-HT responses increase more slowly but take longer to decrease, suggesting that 5-HT is slower to adapt to changes in expectations compared to DA (Cools et al., 2011).

5.1.3 5-HT-glutamate co-releasing neurons and reward

As previously discussed (see *Chapter 1* and *Chapter 4*), it has recently been shown that 5-HT-glutamate co-releasing neurons in the DRN are both activated by reward and project to VTA DA neurons which innervate the NAc (Wang et al., 2019). Furthermore, optogenetic activation of DRN 5-HT-glutamate neurons promoted conditioned place preference, shifted sucrose preference, and drove optical self-stimulation (Liu et al., 2014). These rewarding effects were reversed by depletion of either glutamate or 5-HT (Liu et al., 2014) and shown to be mediated by both AMPA and 5-HT_3 receptors in the VTA (Wang et al., 2019). Interestingly, experiments using slice electrophysiology showed that DRN VGLUT3-expressing 5-HT neurons establish asymmetric synapses on VTA DA neurons, whereas 5-HT neurons which

do not express VGLUT3 establish symmetric synapses on VTA neurons (Wang et al., 2019). Asymmetric synapses, characterised by a thicker post-synaptic membrane compared to the pre-synaptic membrane, are typically excitatory, whereas symmetric synapses are thought to be inhibitory (Doherty & Pickel, 2000; Morales & Pickel, 2012). Therefore, it has been suggested that pure 5-HT neurons and dual 5-HT-glutamate neurons, might have differential effects by respectively inhibiting or exciting VTA DA projections (Wang et al., 2019).

5.1.4 Using fibre photometry for measuring DA *in vivo*

Several studies discussed in *Section 5.1.1* employed fibre photometry to measure DA signalling which allows real-time monitoring of DA dynamics. During fibre photometry recordings, an implanted optic fibre is used to deliver excitation light to trigger and collect fluctuations in fluorescence emitted by a genetically-encoded fluorescent indicator (Simpson et al., 2024). Initially, fibre photometry was primarily used to monitor calcium dynamics as a proxy for neural activity (Akerboom et al., 2012; Chen et al., 2013; Gunaydin et al., 2014) but, with the recent development of several fluorescent biosensors, it is now possible to monitor the dynamics of specific neurotransmitters. For example, DLight1 is a biosensor engineered to bind specifically to DA. Upon binding DA, DLight1 undergoes a conformational change which alters the fluorescence intensity of its green fluorescent protein, thereby causing light emission when exposed to a specific wavelength (Labouesse et al., 2020; Patriarchi et al., 2018; Salinas et al., 2023). Therefore, with fibre photometry and biosensors it is possible to probe DA release

with high specificity and high spatiotemporal precision *in vivo* in behaving animals, with repeated real-time recordings over extensive periods of time. Altogether, this allows for unprecedented insights into how DA dynamics relate to complex behaviour (Simpson et al., 2024).

5.1.5 Hypothesis and aims

This chapter investigates whether the behavioural deficits displayed by VGLUT3 cKO$^{5\text{-HT}}$ mice (*Chapter 4*) correlate with changes in mesolimbic DA function. In VGLUT3 cKO$^{5\text{-HT}}$ mice, glutamate release in the VTA is expected to be reduced as a consequence of the VGLUT3 KO in VTA-projecting 5-HT-glutamate neurons. As these projections have been shown to be excitatory (Wang et al., 2019), it was hypothesised that this reduced glutamate release would in turn lead to decreased excitation of DA VTA neurons, causing a reduction in NAc DA release. To test this hypothesis, measurements of *in vivo* DA release in the NAc were carried out in VGLUT3 cKO$^{5\text{-HT}}$ mice and control littermates during a reward-based task.

5.2 Methods

5.2.1 Animals

Experiments used male and female VGLUT3 cKO$^{5\text{-HT}}$ mice (SERT-Cre::VGLUT3$^{\text{LoxP/LoxP}}$, C57BL/*6J* background, aged 8-30 weeks) and their control littermates (SERT$^{+/+}$::VGLUT3$^{\text{LoxP/LoxP}}$). VGLUT3 cKO$^{5\text{-HT}}$ mice were generated and bred as described in *Chapter 2*.

Mice were group-housed (2-6 per cage) with littermates in individually ventilated cages. Temperature was kept at 21 ± 2 °C under 55% ± 10% humidity on a 12 hr light/dark cycle. Animals were tested during the light phase. Unless specified otherwise, mice had access to food and water *ad libitum*, and cages were lined with sawdust bedding and contained sizzle nest and nestlets. Mice were habituated to handling on three occasions before any experiment.

Experiments followed the principles of the ARRIVE guidelines. All procedures were performed in accordance with the Animals (Scientific Procedures) Act 1986 and University of Oxford guidelines. All experiments were covered by appropriate personal and project licences. Experiments were conducted and scored blind to genotype.

5.2.2 Behavioural testing

Animals were water-restricted throughout the experiment, commencing 48 h before the start of training. Mice were maintained at 90% of initial body weight and received most of their water intake from the task, but were topped up daily if necessary. The task was run using the same custom-built operant boxes described in *Chapter 4* (12 × 12 cm, ***Fig. 5.1***) controlled using PyControl software (Akam et al., 2022). Depending on the task, the back wall of the operant box had either a single port located closer to the floor ("port 1"), or two ports placed one on top of the other 3 cm apart ("port 1" and "port 2"). Each port was equipped with recessed LED lights

and a solenoid to deliver water rewards. Each box included a house light and speaker which were located above the ports. Mice were video-recorded using a FLIR Chameleon 3 camera positioned above each setup using a Bonsai based workflow (Akam et al., 2022). Mice were provided with standard chow during the task. The apparatus was wiped with 0.5% Anistel (Tristel) between each animal to remove odours.

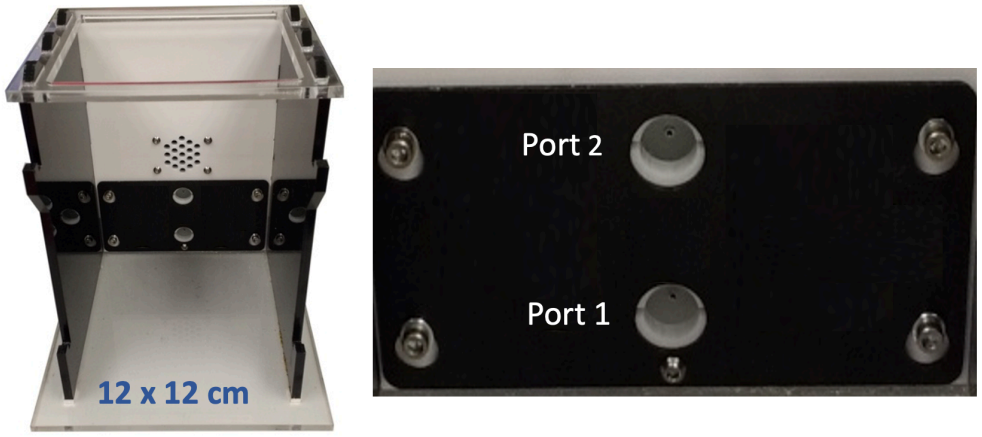

Figure 5.1 | Photographs of the operant chamber setups. Custom-built operant chamber (Akam et al., 2022) employed during operant training, including with two ports equipped with solenoids and LED lights.

Mice were tested once a day, and details of all testing parameters are listed in ***Table 5.1***. Briefly, during days 1-6 of training the operant chamber contained only port 1. Day 1 served as a magazine training session with port 1 being illuminated to indicate availability of a water reward (10 μl). Nose-poke of the illuminated port was associated with a sound cue (a sine wave, lasting 500 ms) which was followed by immediate water delivery in the first 15 trials, allowing the mice to learn to drink from the solenoid. After that, and for the remaining 15 days of training, water delivery was always delayed by 500 ms from the start of the sound cue (i.e.

coinciding with cue offset). This allowed the separation of DA responses to the sound cue and to reward consumption. On days 2 and 3, the task was identical to that on day 1 but rewards were varied randomly in size between 3 different volumes (5 μl, 10 μl, 15 μl) allow to investigation of the effect of reward size on DA release. On day 4 the reward size was set at 10 μl, but the ITI varied between long (duration randomly selected between 20 and 45 s) and short (duration randomly selected between 10 and 15 s) in alternating blocks of 10-20 trials. This allowed the probing of both behaviour and DA release in the presence of frequent or infrequent rewards. Next, days 5 and 6 aimed to investigate decreases in DA release in the context of a negative prediction error signal. Thus, mice received a reward in only 70% of entries in the illuminated port. These unrewarded trials were associated with a different sound cue (white noise).

Training days 7-15 were designed to investigate behaviour and DA dynamics during reversal learning, with various stages of incremental difficulty. Thus, on day 7 port 2 was introduced and served as the water magazine instead of port 1 (see ***Table 5.1*** for more details). Entries in the illuminated port 2 triggered the familiar 0.5 s reward-predictive cue prior to reward delivery. Port 1 was still available to poke but it did not trigger any reward nor any sound. On day 8 the task was similar to day 7 but when port 2 was illuminated port 1 entries triggered the white noise indicating lack of reward, and caused a timeout of 3 s prior to the ITI. Lastly, days 9-15 consisted of a 2-choice task where either port 1 or port 2 was illuminated in blocks of 10-12 trials. When one of the two ports was illuminated entries in the illuminated

port triggered the reward sound cue and reward delivery, while entries in the non-illuminated port triggered the white noise and a 3 s time out.

Table 5.1 | Summary of parameters employed in the water reward paradigm whilst measuring DA release. ITI were always variable, with length randomly selected between the values listed in the relevant column.

Day and session	Task	Description	Reward size	ITI	Length
Day 1	**Magazine training with fixed reward size**	Magazine port 1 (placed closer to the floor) is illuminated. Magazine entry triggers a sound cue (sine wave), switches off magazine light, and delivers a water reward (10 µl). Reward delivery occurs immediately after nose-poke for the first 15 rewards, while from the 16th reward onwards, rewards are delivered 500 ms after nose-poke.	10 µl	15-25 s	30 min
Days 2-3	**Magazine training with 3 reward sizes**	Magazine port 1 is illuminated. Magazine entry triggers a sound cue (sine wave, 500 ms), switches off magazine light, and after 500 ms delivers a water reward of variable size.	5, 10 or 15 µl	15-25 s	40 min
Day 4	**Magazine training with varying ITI in blocks**	Magazine port 1 is illuminated. Magazine entry triggers a sound cue (sine, 500 ms), switches off magazine light, and after 500 ms delivers a set water reward. ITIs vary in length in blocks of 10-20 trials.	10 µl	Short: 10-15 s Long: 20-45 s	60 min
Days 5-6	**Negative prediction error**	Port 1 is illuminated. Magazine entry switches off magazine light, and triggers reward delivery (with 500 ms delay) with 70% probability. Reward is preceded by the familiar sound cue (sine wave, 500 ms), while non- rewarded trials are preceded by a white noise (500 ms).	12 µl	10-20	40 min
Day 7	**Reversal without penalty**	Port 2 (located on top of port 1) is introduced and illuminated. Magazine 2 entry switches off magazine light,	12 µl	10-20	40 min

		triggers the reward sound cue (500 ms), and delivers a set water reward after 500 ms. Port 1 is available to nose-poke but does not trigger any rewards, nor any noise or penalty.			
Day 8	**Reversal with penalty**	Port 2 is illuminated. Port 2 entry triggers the reward sound cue (500 ms), switches off magazine light, and after 500 ms delivers a set water reward. Magazine port 1 entries, occurring when port 2 is illuminated, switch off port 2, triggers the white noise (500 ms), no reward is delivered and causes 3 s delay (time out) prior to ITI.	12 µl	10-20	40 min
Days 9-15	**Reversal 2-choice task, in blocks**	Either port 1 or 2 are illuminated, in blocks of 10-20 trials**.** Nose-poke of illuminated port triggers the reward sound cue (500 ms) and reward delivered after 500ms. Nose-poke of non-illuminated port triggers white noise (500ms) and a 3 s delay (time out) prior to ITI.	12 u µl (Except last 2 days, 10 µl)	10-20	55 min

Across training days numbers of entries in port 1 and 2 (whenever present) were counted, as well as the total number of rewards collected. Response latency was timed from when the port was illuminated until a nose-poke was made. On days 8-15 the number of correct entries were defined as entries in the illuminated port, while incorrect entries consisted of entries in the non-illuminated port whenever the opposite port was illuminated. Omissions were observed in less than 0.7% of trials, and therefore are not reported.

5.2.3 Surgery

Intracerebral viral injection and cannula implantation for dLight photometry were carried out under isoflurane anaesthesia (3% induction, 0.7–1% maintenance, in 2 L/min oxygen), as previously described (Blanco-Pozo et al., 2024). Anaesthetic depth was maintained through frequent monitoring of the animal's respiratory rate. Immediately before surgery, buprenorphine (Vetergesic, 0.08 mg/kg, *s.c*), meloxicam (Metacam, 5 mg/kg, *s.c.*) and 4% glucose-saline (~0.5ml, *s.c*) were administered for pain relief and hydration. The animal's head was shaved and bupivacaine (Marcain, 2 mg/kg, *s.c.*) was applied under the scalp for local anaesthesia. The scalp was then cleaned with anti-microbial disinfectant (Hibiscrub, 1:4 in water v/v), and the mouse was secured in a standard stereotaxic frame (David Kopf Instruments). Body temperature was maintained at ~37 °C using a heating blanket (Harvard Apparatus). Liquid gel (Viscotears) was applied as needed to keep the animal's eyes hydrated. All drugs used in this section were provided by Oxford University Veterinary Services.

Subsequent surgical steps were performed under sterile conditions. An incision was made to expose the skull, and bregma and lambda were located to ensure the skull was level in the dorsoventral plane. The skull was gently scratched to improve adhesion of dental cement, and a craniotomy (~1 mm diameter; AP: +1.4, ML: ±0.76 from bregma) was made using a manual drill equipped with a drill bit of 0.8 mm diameter. The skull was then cleaned with sterile saline (Aqupharm) and dried. Mice were intracranially injected in the NAc (AP: +1.4, ML: ±0.76, DV: −4.1 from bregma)

with 500 nl of saline containing a 1:5 dilution of pAAV5-CAG-dLight1.1 (titer of 1.4 × 1012 vg/ml; Addgene) and a 1:5 dilution of pssAAV-2/5-hSyn1-chI-tdTomato-WPRE-SV40p(A) (titer of 4.9 × 1011 vg/ml; ETH Zurich) (Blanco-Pozo et al., 2024; Patriarchi et al., 2018). The injection was achieved using a Nanoject (Drummond Nanoject III Auto-Nanolitre Injector) set at 2 nl/s equipped with a pulled glass capillary (Drummond, outer diameter of 1.14 mm prior to pulling). A total of 9 min elapsed between the start of injection and removal of the micropipette to allow for sufficient viral spread and diffusion away from the injection site. Next, a ceramic optical fibre (200 μm-diameter; RWD Life Scientific) was implanted chronically in the injection site (AP: +1.4, ML: ±0.76, DV: −4.2 from bregma). A dental bonding agent (Optibond) was applied to the skull to increase adhesion, and multiple layers of dental cement (3M, RelyX Unicem 2 Automix) were used to secure the cannula in place and cover the exposed skull. Each layer was appropriately cured with an LED dental curing light.

After the surgery mice were administered with 4% glucose-saline (~0.5ml, *s.c*) to aid rehydration and allowed to recover in heated recovery cages. Mice were given additional doses of meloxicam each day for 3 days after surgery, and were monitored carefully for 7 days after surgery. Monitoring involved daily scoring of body weight, behaviour, general appearance, and wound recovery. Animals were then given 3 to 4 weeks prior to behavioural testing to allow both wound healing and appropriate viral expression.

5.2.4 Perfusion fixation and histology

Following behavioural testing, mice from the dLight photometry experiment were culled by perfusion fixation to allow for histological assessment of the NAc. Mice were deeply anesthetised by injection of pentobarbitone (5 mg/kg, *i.p.*) and intracardially perfused with PBS (Sigma Aldrich) followed by a fixative solution of 4% PFA (Sigma Aldrich) in PBS. Brains were dissected, post-fixed by immersion in the same fixative for 48 hrs at 4^{o}C, then stored in cryoprotective 30% sucrose (Sigma Aldrich) in PBS at 4^{o}C.

Prior to sectioning, brains were coated in Cryo-M-Bed embedding compound (Bright) and stored at -80^{o}C for 45 min. Coronal sections (30 μm) were cut using a Bright LOFT cryostat, and free-floating slices were washed in PBS prior to mounting. Sections with the NAc were selected based on their distance from bregma (AP: +1.4 mm; Franklin & Paxinos, 1997). Sections were mounted onto glass slides with Vectashield antifade mounting medium (Vector Laboratories) and covered with a glass coverslip, prior to being stored in the dark at 4^{o}C. An Olympus Epifluorescence Microscope BX40 with ImageJ Micromanager v1.4 (10x magnification, 500 ms) was used to confirm viral expression and cannula location (see ***Fig. 5.2A*** for an example image).

5.2.5 Photometry recordings and pre-processing

DA release, based on the dLight fluorescence signal, was captured at a frequency of 130 Hz using pyPhotometry as previously described (Akam et al., 2022; Akam &

Walton, 2019; Blanco-Pozo et al., 2024). The optical setup included a 465-nm and a 560-nm LED, a five-port minicube, and two Newport 2151 photoreceivers. Optic fibres were bleached daily for 30-60 mins before the start of recordings. Time division illumination with background subtraction was used to minimise interference between fluorophores caused by overlapping emission spectra. Synchronisation pulses from pyControl to a digital input of the pyPhotometry board ensured alignment of the photometry signal with behaviour (Akam et al., 2022).

Pre-processing was run using a custom Python script and followed a recently described pipeline (Blanco-Pozo et al., 2024; Simpson et al., 2024). Firstly, a median filter (width of five samples), was applied to remove any electrical noise that might have been picked up by the photoreceptors. Next de-noising was achieved using a zero-phase filter with a 10 Hz cut-off frequency. Low pass filtering (between 2–10 Hz) is typically used for dLight1 to attenuate signals above the cut-off while the zero-phase filters avoid distorting the signal. As optic fibres and fluorophores tend to bleach over time, photobleaching correction was performed by subtracting a double exponential fit (see example in ***Fig 5.2***). This allows capturing of the two temporal dynamics of bleaching involving an initial rapid decay and then a second slower decrease (Simpson et al., 2024). To obtain motion correction of the signals, denoised signals were band-passed between 0.001 Hz and 5 Hz, and a linear regression was used to predict the dLight signal using the signal from the control fluorophore (tdTomato). The predicted signal caused by motion was then subtracted from the denoised signal. Finally, the pre-processed DA signal was z-scored (by subtracting the mean and dividing by the standard deviation; see example data in ***Fig 5.2***) for

each session to allow comparison of signal intensities across sessions and animals. Z-scores were chosen over the ΔF/F method (where the change in fluorescence signal is divided by the baseline signal level) as in dLight photometry baseline signal could include large contributions from autofluorescence.

All pre-processed sessions were visually inspected. Sessions in which there were large artifacts, such as large step change in recorded signals (e.g. due to a malfunctioning or disconnection of the patch cord from the fibre), or where there was a complete loss of signal on one of the channels due to discharged battery during recording, were excluded. Thus, around ~6% of the total session were removed from the analyses, albeit these occurred predominantly in days 1-6.

Data was recorded from a total of 20 mice. Out of these, 12 displayed appropriate dLight modulation, and placement of the fibre was confirmed to be in the NAc core (i.e. 60% success rate). The remaining 8 mice displayed poor dLight modulation, and subsequent histological analysis confirmed that the fibres were misplaced (predominantly into the ventricle). Thus only 12 mice were used for photometry analysis, while behavioural analyses were carried out in all 20 mice.

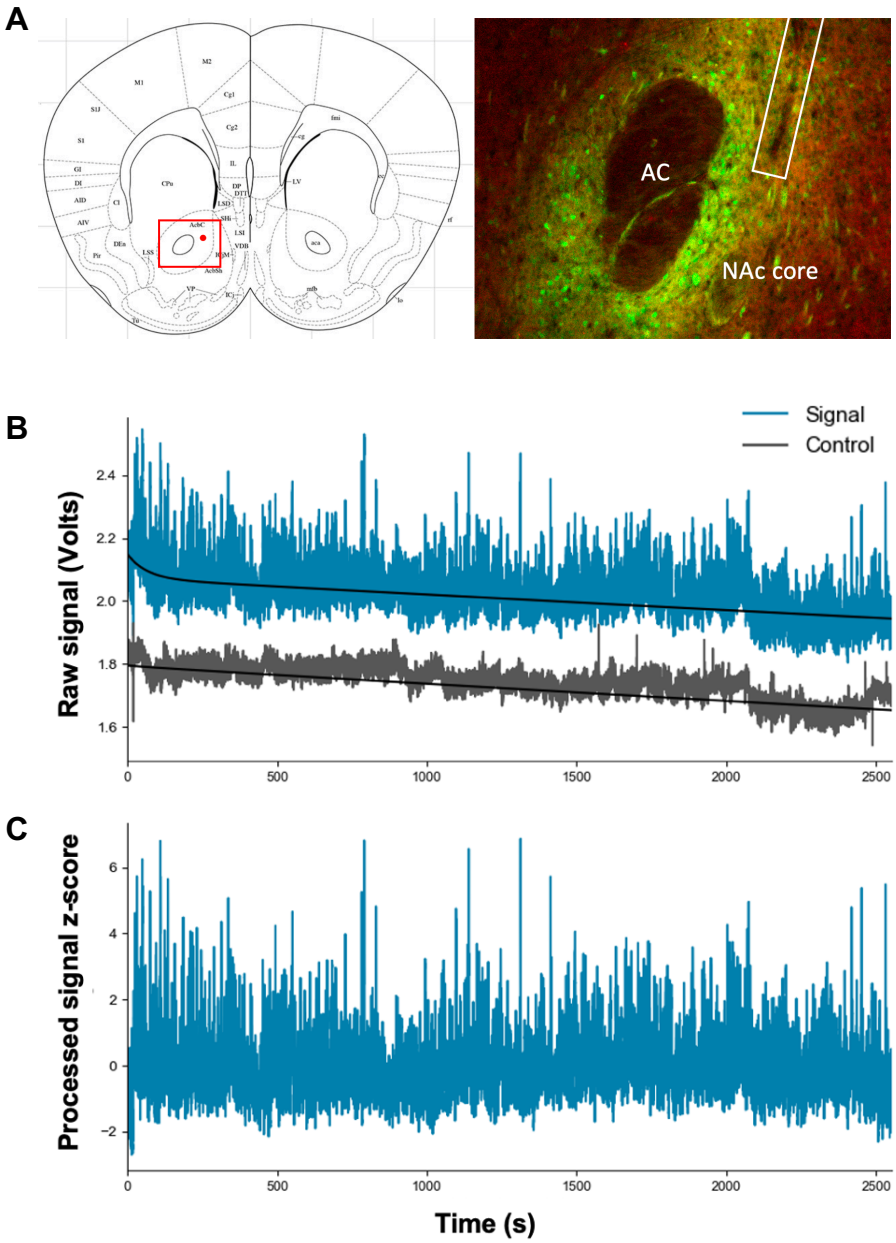

Figure 5.2 | Example of NAc histology and data from a whole recording session at different pre-processing steps. (A) Image of an example section showing viral spread (dLight in green, tdTomato in red) and fibre placement (in white box) in the NAc core according to the stereotaxic atlas (Paxinos & Franklin, 2001). The anterior commissure (AC) was used as a histological marker. **(B)** Example of denoised data from a whole session, prior to photobleaching correction. Signal represents dLight signal and controls represent tdTomato signal. Black line indicates the double exponential fit that will be used for the bleaching correction. **(C)** Example of z-scored data from a whole recording session (z-scoring was achieved subtracting the mean and dividing by the standard deviation).

5.2.6 Analysis of photometry data

Often in photometry experiments using operant setups, time-warping is employed to align each trial based on multiple events of interest (e.g. an initial nose-poke to initiate the task and a second nose-poke to collect the reward). However, in the current experiments mice always nose-poked in the same port from where they would receive a reward 0.5 s later, therefore time-warping was deemed unnecessary. Using a custom-made Python code (Blanco-Pozo et al., 2024; Simpson et al., 2024) pre-processed dLight signals (z-scores) were visually inspected, firstly by aligning with the start of the trial (i.e. when the port would become illuminated; ***Fig 5.3***), and secondly by aligning with the entry into the illuminated port (***Fig 5.3***). The latter trial alignment allowed identification of the two DA peaks of interest, specifically the responses to the sound cue and water reward (or lack of it), and thus was selected to present the data in each condition. Specifically, data were z-scored in a 3.5 s window, starting 1 s prior to entry in the illuminated port and ending 2.5 s after entry. Thus, times from -1 s to 0 represented the last second prior to nose-poke, time from 0 to 0.5 s indicated responses to the auditory cues, and times from 0.5 s to 2.5 s contained response to trial outcome (reward or no reward).

Area under the curve (AUC) analysis was used to compare the DA response to the cue and reward in both VGLUT3 cKO$^{5\text{-HT}}$ mice and controls. To achieve this, aligned trials belonging to each mouse in the time periods of interest (0-0.5 s and 0.5-2.5 s) were averaged, and AUC was calculated for each subject using the trapezoidal rule (*trapz* function NumPy package). Specifically, net AUC analysis was employed,

meaning that when dLight signals were below baseline (i.e. for negative prediction signals) AUC values were negative. This method was chosen based on other recent studies using dLight (Robinson et al., 2019). For statistical analysis, AUCs were compared between genotypes and experimental conditions using t tests or two-way repeated measures ANOVA followed by Šídák's multiple comparisons test, as appropriate. Data are presented as mean ± inter-subject SEM, $p<0.05$ being considered statistically significant. Python (version 3.12.1) was used for plotting of graphs and for analysis described in *Sections 5.2.5* and *5.2.6* except two-way repeated measures ANOVA which were carried out in GraphPad Prism (version 10.2.2) for consistency with the rest of this thesis.

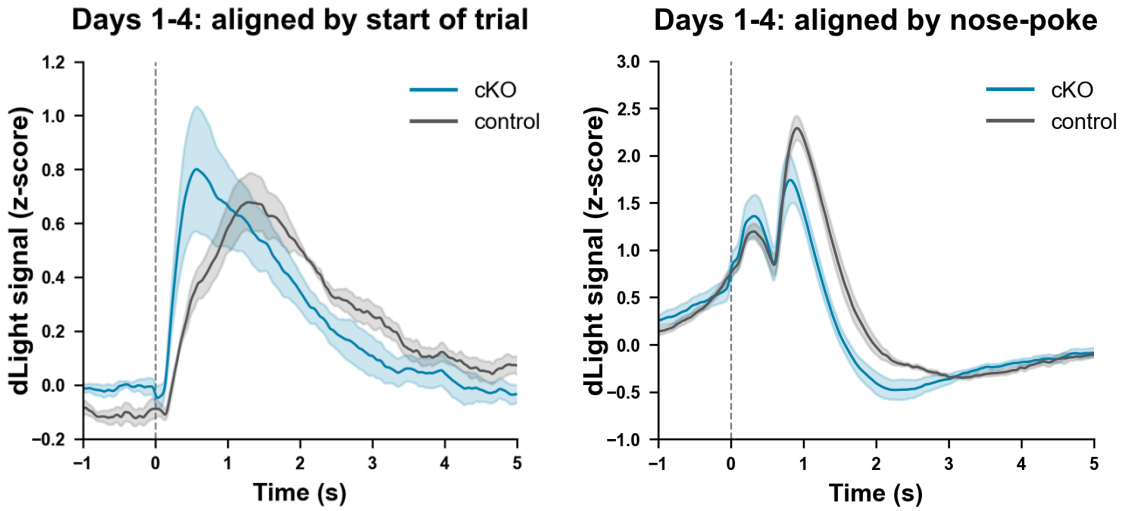

Figure 5.3 | Signal aligned by either the trial start or by nose-poke. Pre-processed trial-aligned signal (z-scored) aligned by the start of the trial (i.e. when the light cue would come on) or by nose-poke into the illuminated port.

5.2.7 Analysis of behavioural data

Behavioural data were analysed by t test, or a one/two-way ANOVA as appropriate, followed by Šídák's multiple comparisons test. For two-way analysis with repeated measures, a two-way ANOVA was used on datasets with no missing values, while a mixed effect model was employed in presence of missing values (e.g. if any session was excluded due to technical issues). Data are presented as mean ± SEM values, $p<0.05$ being considered statistically significant. GraphPad Prism (version 10.2.2) was used for analysis and plotting of graphs.

5.3 Results

5.3.1 *In vivo* DA release in NAc in VGLUT3 cKO$^{5\text{-HT}}$ mice during a reward-based task

The operant task used during the dLight photometry experiment was primarily designed to probe DA release in different stages of a behavioural task (see ***Table 5.1*** for details) in which mice learnt to nose-poke and collect rewards from an illuminated port which was also signalled by auditory cues. Briefly, at the beginning of each trial, the magazine port would become illuminated indicating reward availability, and entry into the illuminated port would trigger an auditory cue followed by water delivery from the same port. The following trial would start after a variable ITI. For all analyses, trials were aligned to the nose poke of the illuminated port (see *Section 5.2.6* for more details), and AUC analysis of dLight signals was carried out in the 0.5 s following the onset of the auditory cue, and in the 2 s

following reward delivery (with the only exception of the first 15 trials of day 1). Behavioural analysis is reported in *Section 5.3.2*, but it is important to note that in this experiment latency to nose-poke the illuminated port was not affected by genotype at any training stage. Similarly, there was no difference between VGLUT3 cKO$^{5\text{-HT}}$ mice and control littermates on the average number of trials per session, which varied from 37.2 ± 2.64 trials on the first day of training up to 124.916 ± 3.40 trials on training day 15.

On day 1, rewards had a fixed size and increased DLight signal was observed following reward delivery in both VGLUT3 cKO$^{5\text{-HT}}$ mice and control littermates. For the first 15 trials, rewards were delivered immediately after the nose-poke concurrent with a sound cue. AUC analysis of the 2.5 s following reward delivery showed no difference between genotypes ($t_{(7)}$=-0.678; p=0.519; Cohen's d=-0.45; ***Fig 5.4***). From the 16th trial onwards, rewards were delivered at the offset of the 0.5 s sound cue. DLight signals from VGLUT3 cKO$^{5\text{-HT}}$ mice again did not differ from control littermates in either the 0.5 s after auditory cue onset ($t_{(7)}$=0.605; p=0.565; Cohen's d=0.406) or in the 2 s after reward delivery ($t_{(7)}$=0.249; p=0.811; Cohen's d=0.167; ***Fig 5.4***). Therefore, both VGLUT3 cKO$^{5\text{-HT}}$ mice and control littermates displayed increased DA release following reward delivery.

On training days 2 and 3, mice received rewards of variable sizes after the 0.5 s sound cue. Interestingly, AUC analysis showed increased dLight signals in response to the auditory cue in VGLUT3 cKO$^{5\text{-HT}}$ mice compared to controls ($F_{(1, 11)}$=7.04, p=0.023; ***Fig 5.5***). In response to the cue there was no effect of reward size

($F_{(2, 22)}$=1.40, p=0.268) nor interaction between reward size and genotype ($F_{(2, 22)}$=0.347, p=0.710). Conversely, the dLight signal in the 2 s following reward delivery was not different between genotypes ($F_{(1, 11)}$=0.742, p=0.408), with a two-way ANOVA again showing an effect of reward size ($F_{(2, 22)}$=65.2, p<0.0001) but no genotype x reward size interaction ($F_{(2, 22)}$=0.043, p=0.958; ***Fig 5.5***). Thus, in days 2 and 3 of training VGLUT3 cKO$^{5\text{-HT}}$ mice had greater DA response to the reward-predictive auditory cue compared to control littermates, but both genotypes displayed similar DA responses to the reward with DA release increasing with bigger reward sizes.

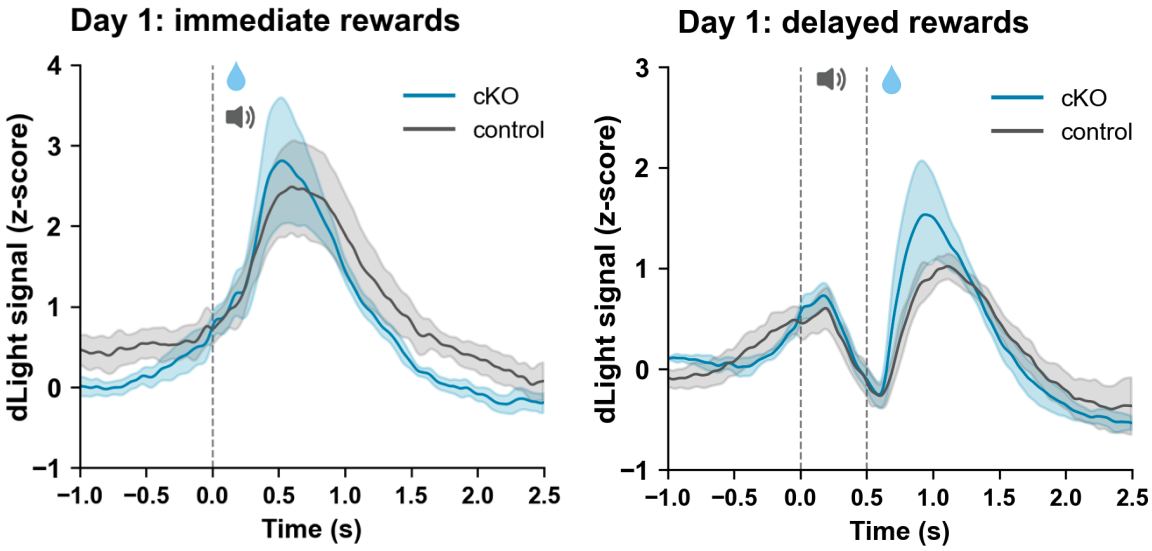

Figure 5.4 | dLight signals in response to cue presentation and immediate or delayed reward delivery on day 1 of training in VGLUT3 cKO$^{5\text{-HT}}$ mice and control littermates. On the first 15 trials of training day 1, sound cue and reward delivery occurred simultaneously (left), while from the 16th trial onward reward delivery occurred 0.5 s after a cue onset and was thus contingent with cue offset (right). Continuous lines represent dLight signals expressed as z-scores, calculated relative to the baseline fluorescence, and aligned to nose-poke of the illuminated port. Shaded areas indicate inter-subject SEM.

Vertical dashed lines represents auditory cue onset and water delivery. Groups were VGLUT3 cKO$^{5\text{-HT}}$ mice (n=5) and controls (n=4).

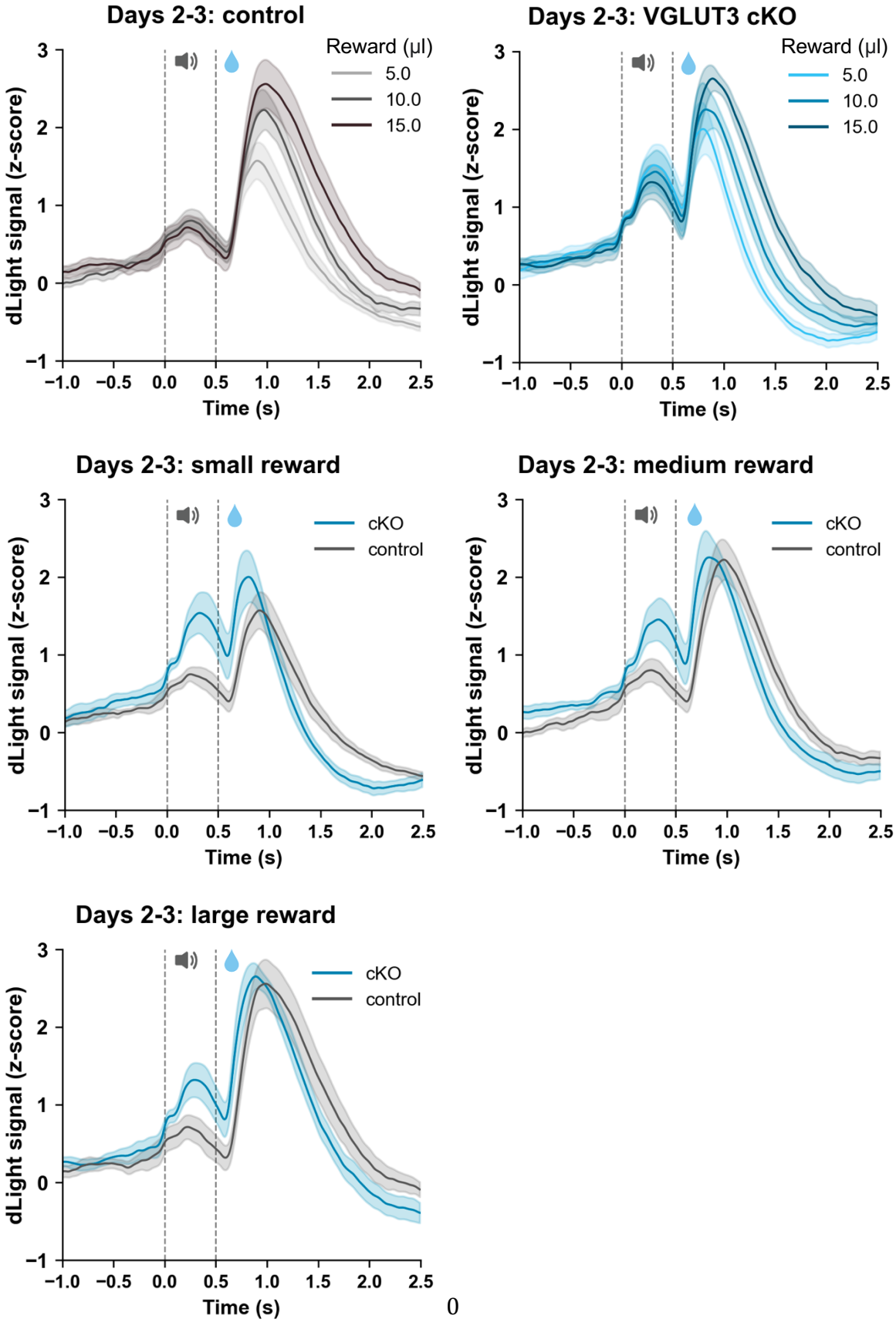

Figure 5.5 | dLight signals in response to auditory cue presentation and 3 different reward sizes on days 2-3 of training, in VGLUT3 cKO$^{5\text{-HT}}$ mice and control littermates. On days 2-3 of training the reward-predictive auditory cue was followed by a water reward of either 5, 10 or 15 ul. All graphs represent the pooled data from day 2 and 3, but separated by genotype (top row) or reward size (middle and bottom row) to aid visualisation. Continuous lines represent dLight signal expressed as z-scores, calculated relative to the baseline fluorescence, and aligned to nose-poke of the illuminated port. Shaded areas indicate inter-subject SEM. Vertical dashed lines represent auditory cue onset and water delivery. Groups were VGLUT3 cKO$^{5\text{-HT}}$ mice (n=6) and controls (n=7).

On day 4 of training, mice were required to wait for ITIs of variable length, prior to being able to collect a fixed reward (10 ul) from the illuminated port, after the 0.5 s auditory cue. ITIs were either long (20-45 s) or short (10-15 s) in alternating blocks, to inspect DA release in presence of infrequent or frequent rewards. Analysis of dLight signals after auditory cue onset revealed no statistically significant difference between genotypes ($F_{(1, 8)}$=0.020, p=0.892; ***Fig 5.6***). There was also no effect of ITI length ($F_{(1, 8)}$=0.441, p=0.526) nor any interaction between ITI length and genotype ($F_{(1, 8)}$=0.417, p=0.537). Conversely, following reward delivery, dLight signals were reduced in VGLUT3 cKO$^{5\text{-HT}}$ mice when compared to controls ($F_{(1, 8)}$=7.240, p=0.028) in a two-way ANOVA. There was also a strong trend effect of ITI length ($F_{(1, 8)}$=4.990, p=0.056) and a trend interaction between genotype and ITI length ($F_{(1, 8)}$=4.150, p=0.076; ***Fig 5.6***). These trends suggest that in blocks with longer ITIs (i.e. less frequent rewards) the DA response decreases in controls, compared to blocks with shorter ITIs. Conversely, in VGLUT3 cKO$^{5\text{-HT}}$ mice DA release was not affected by ITI length, and the overall DA response to rewards was smaller in VGLUT3 cKO$^{5\text{-HT}}$ mice compared to control littermates.

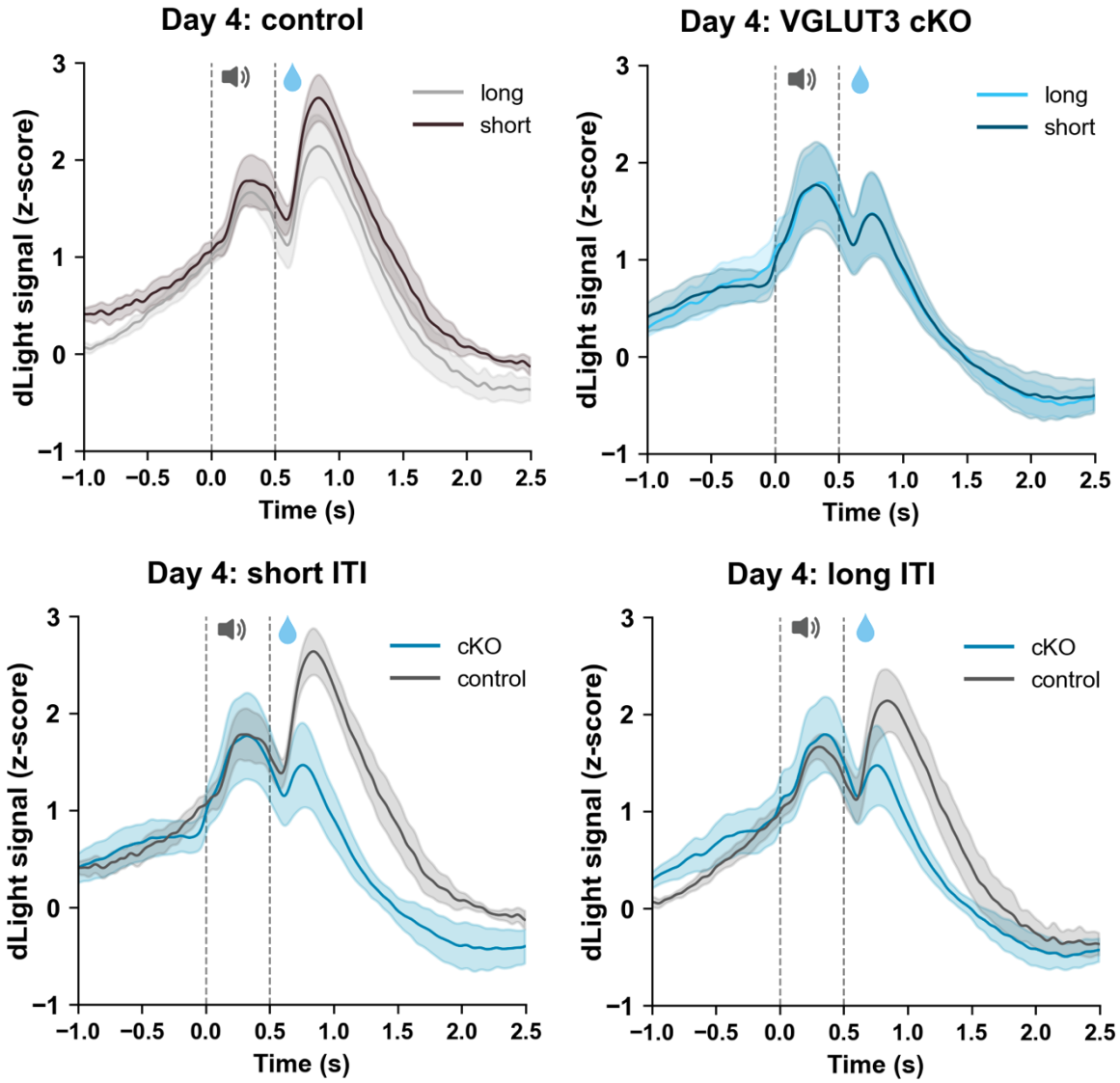

Figure 5.6 | dLight signals in response to auditory cue presentation and reward delivery following varying ITIs, on day 4 of training in VGLUT3 cKO$^{5\text{-HT}}$ mice and controls. On day 4 of training the 0.5 s auditory reward-predictive cue, was always followed by a 10 µl water reward but the ITIs were either long (20-45 s) or short (10-15 s) in alternating blocks. All graphs represent data from the same session but filtered by genotype (top row), or ITI length (bottom row) to aid visualisation. Continuous lines represent dLight signals expressed as z-scores, calculated relative to the baseline fluorescence, and aligned to nose-poke of the illuminated port. Shaded areas indicate inter-subject SEM. Vertical dashed lines represent auditory cue onset and water delivery. Groups were VGLUT3 cKO$^{5\text{-HT}}$ mice (n=6) and controls (n=6).

On training days 5 and 6, the task aimed to investigate DA dynamics during negative prediction errors (i.e. when reward was expected but not received). Hence, mice received a reward only in 70% of nose-pokes into the illuminated port. Rewards were preceded by the usual reward-predicting auditory cue, while a novel white noise cue indicated unrewarded trials. The presence of two different auditory cues allowed the mice to predict trial outcome (i.e. reward or no reward). Therefore, in the 0.5 s following the reward predictive cue mice showed increased DA response compared to the cues predicting lack of reward (effect of trial outcome: $F_{(1, 10)}$=11.3, p=0.007; ***Fig 5.7***). However, this was not affected by genotype ($F_{(1, 10)}$=0.144, p=0.713), and there was no interaction between genotype and trial outcome ($F_{(1, 10)}$=0.848, p=0.379). Conversely, dLight signals trial-aligned times between 0.5 s and 2.5 s showed not only an effect of reward or no reward ($F_{(1, 10)}$=183, p<0.0001; ***Fig 5.7***), but also an effect of genotype ($F_{(1, 10)}$=5.88, p=0.036), and genotype x outcome interaction ($F_{(1, 10)}$=9.17, p=0.013). Specifically, following reward delivery VGLUT3 cKO$^{5\text{-HT}}$ mice displayed a reduction in DA release compared to controls (p=0.003). Conversely in unrewarded trails there was no difference in the negative reward prediction error signal between genotypes (p=0.852).

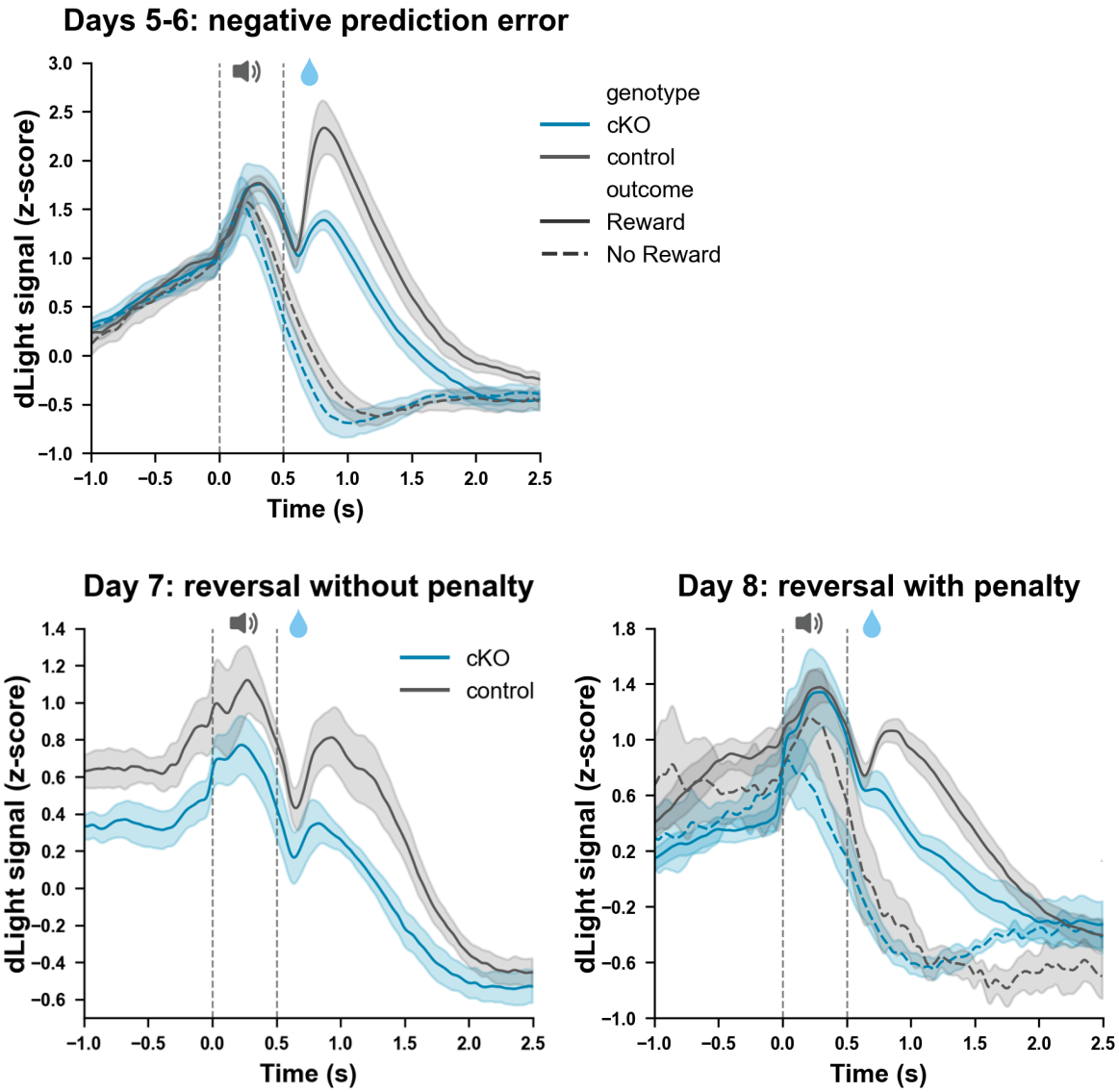

Figure 5.7 | dLight signals in response to a reward-predictive cue followed by reward delivery or a white noise cue followed by no reward, on days 5-8 of training in VGLUT3 cKO$^{5\text{-HT}}$ mice and controls. On days 5-6 of training (top graphs), 70% of entries in the illuminated port (port 1) triggered a 0.5 s reward-predictive cue, which was followed by a water reward. On the remaining trials, entries in the illuminated port triggered a white noise cue followed by no rewards. Days 7 and 8 of training (bottom row) consisted of a reversal learning task as the rewarded port was swapped from port 1 to port 2. On day 7, port 1 was available to nose-poke but did not trigger any sound nor penalty while on day 8 port 1 entries triggered the white noise cue and a 3 s penalty. dLight signals expressed as z-scores (calculated relative to the baseline fluorescence and aligned to nose-poke of the

illuminated port) are represented by continuous lines in rewarded trials, and dashed lines in unrewarded trials. Shaded areas indicate inter-subject SEM. Vertical dashed lines represent auditory cue onset and reward delivery (or lack of it). Groups were VGLUT3 cKO$^{5\text{-HT}}$ mice (n=6) and controls (n=6).

Day 7 was the first day of reversal learning, thus rewards were now delivered from port 2 instead of port 1. Port 2 entries were associated with the usual reward-predicting auditory cue, while port 1 entry was not associated with any sound or penalty. VGLUT3 cKO$^{5\text{-HT}}$ mice did not differ from control littermates in dLight signals after cue onset following a nose-poke at port 2 ($t_{(10)}$=-1.473; p=0.171; Cohen's d=-0.85), but had reduced dLight signals in the 2 s following reward delivery at port 2 ($t_{(10)}$=-2.452; p=0.034; Cohen's d=-1.416; ***Fig 5.7***). Interestingly, VGLUT3 cKO$^{5\text{-HT}}$ mice also displayed reduced dLight signals in the last second prior to the auditory cue ($t_{(10)}$=-2.882; p=0.016; Cohen's d=-1.664; ***Fig 5.7***), which consists of the response to port becoming illuminated prior to nose-poke.

Day 8 was the second day of reversal learning and, similar to day 7, port 2 was always rewarded following the reward-predictive auditory cue. However, port 1 entries now triggered the white noise cue predicting lack of reward, and a 3 s penalty. AUC analysis of dLight signals following the auditory cues revealed no effect of genotype ($F_{(1, 8)}$=1.29, p=0.288) or cue type ($F_{(1, 8)}$=3.02, p=0.120), nor a genotype x cue type interaction ($F_{(1, 8)}$=0.427, p=0.532). Conversely, analysis of dLight signals of trial-aligned times between 0.5 s and 2.5 s found an effect of trial outcome (i.e. reward or no reward; $F_{(1, 8)}$=64.3, p<0.0001), and a trend interaction between genotype and outcome ($F_{(1, 8)}$=4.70, p=0.062), but no effect of genotype ($F_{(1, 8)}$=0.832,

p=0.388). Therefore, there was a positive prediction error signal for rewarded trials (i.e. correct responses in port 2) and a negative prediction error signal for unrewarded trails (i.e. incorrect responses in port 1), with a potential reduction of DA release in VGLUT3 cKO$^{5\text{-HT}}$ mice in rewarded trials.

On days 9-15, mice were trained on a 2-choice task, where either port 1 or port 2 were illuminated, with the same port being repeatedly illuminated in trials belonging to the same block. Entries in the illuminated port (i.e. correct responses) triggered the reward-predictive auditory cue followed by reward delivery, while entries in the non-illuminated port (i.e. incorrect responses) triggered the white noise cue leading to no reward and a 3 s penalty. Trials within the same block were considered non-reversal trails, as the illuminated port was the same as in the previous trial. Conversely, the first trial of each block was considered a reversal trial as the opposite port was illuminated compared to the previous trials. In non-reversal trials, AUC analysis of dLight signals following the auditory cues found an effect of the identity of the auditory cue (i.e. predicting reward or no reward; $F_{(1, 10)}$=39.1, p<0.0001) and a trend effect of genotype ($F_{(1, 10)}$=3.98, p=0.074), but no interaction between genotype and cue type ($F_{(1, 10)}$=0.289, p=0.603). Conversely, analysis of dLight signal of trial-aligned times between 0.5 s and 2.5 s found an effect of trial outcome (i.e. reward or no reward; $F_{(1, 10)}$=110, p<0.0001), but no effect of genotype ($F_{(1, 10)}$=0.366, p=0.559), nor genotype x outcome interaction ($F_{(1, 10)}$=0.033, p=0.861). Specifically, there was a positive prediction error signal for rewarded trials (i.e. correct responses) and a negative prediction error signal for unrewarded trails (i.e. incorrect responses), but it was not affected by genotype.

Analysis of dLight signal in the last second prior to the auditory reward cue also showed no difference between genotypes ($F_{(1, 10)}$=3.23, p=0.102).

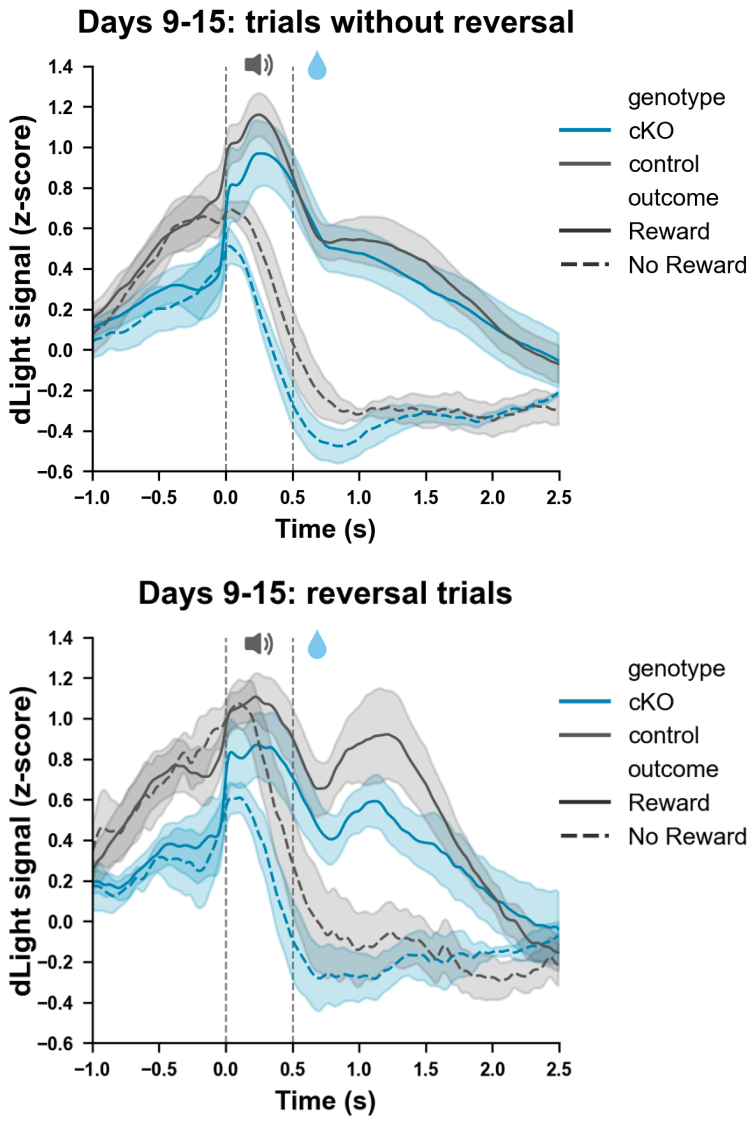

Figure 5.7 | dLight signals in in response to presentation of auditory cues and reward delivery in a 2-choice task, on days 9-15 of training in VGLUT3 cKO$^{5\text{-HT}}$ mice and controls. On days 9-15 mice were trained on a 2-choice task, where either port 1 or port 2 was illuminated, with the same port being illuminated consecutively in blocks or trials. Nose-pokes into an illuminated port (i.e. correct responses) triggered the reward-predictive auditory cue followed by reward delivery, while nose-pokes into the non-illuminated port (i.e. incorrect responses),triggered a white noise cue followed by no reward. Trials were divided into non-reversal trials (top row) and reversal trials (bottom row). dLight signals

expressed as z-scores (calculated relative to the baseline fluorescence and aligned to nose-poke of the illuminated port) are represented by continuous lines in rewarded trials, and dashed lines in unrewarded trials. Shaded areas indicate inter-subject SEM. Vertical dashed lines represent auditory cue onset and reward delivery or lack of it. Groups were VGLUT3 cKO$^{5\text{-HT}}$ mice (n=6) and controls (n=6).

In reversal trials analysis of dLight signal following the auditory cues also found an effect of the identity of the auditory cue ($F_{(1, 10)}$=11.4, p=0.007) and a trend effect of genotype ($F_{(1, 10)}$=3.78, p=0.081) but no outcome x genotype interaction ($F_{(1, 10)}$=0.849, p=0.379). Similarly to non-reversal trials, dLight signals of trial-aligned times between 0.5 s and 2.5 s of reversal trials found an effect of trial outcome ($F_{(1, 10)}$=39.6, p<0.0001) but no effect of genotype ($F_{(1, 10)}$=0.715, p=0.417), nor an outcome x genotype interaction ($F_{(1, 10)}$=0.366, p=0.559). Interestingly, dLight signal in the last second following the auditory cue prior to nose-poke, consisting of the response to port becoming illuminated, was decreased in VGLUT3 cKO$^{5\text{-HT}}$ mice ($F_{(1, 10)}$=9.28, p=0.012), compared to control littermates.

5.3.2 Behavioural analysis of the water-motivated task used during photometry recordings

5.3.2.1 Magazine training in VGLUT3 cKO$^{5\text{-HT}}$ mice and controls

The first 4 days of the water-motivated operant task used during the photometry recordings included different stages of training (see ***Table 5.1*** for details) in which mice learnt to effectively collect rewards from the magazine port. Briefly, on day 1 rewards had a fixed size, on days 2 and 3 rewards randomly alternated between 3 sizes, and on day 4 rewards had a fixed size but the ITI length varied between long

(20-45 s) and short (10-15 s) in blocks of trials. Firstly, data were analysed separately in each of these 3 conditions (fixed reward, varied reward, and varied ITI) and no statistically significant differences between VGLUT3 cKO$^{5\text{-HT}}$ mice and control littermates were found in the number of magazine entries, rewards collected or reward latencies (***Table 5.2***).

Table 5.2 | Behavioural data of the first 6 days of training in the water-based operant paradigm. Days 1-4 involved magazine training and days 5-6 investigated negative prediction errors. Groups were VGLUT3 cKO$^{5\text{-HT}}$ mice (n=11) and controls (n=9). See *Table 5.1* for methods. # p<0.01 indicates trend effects.

Task and parameters	Control (mean ± SEM)	VGLUT3 cKO$^{5\text{-HT}}$ (mean ± SEM)	t test or repeated measures two-way ANOVA
Day 1: Magazine training			
Magazine entries	182.0 ± 32.3	226.5 ± 39.7	$t_{(18)}$=0.843, p=0.410
Rewards	33.6 ± 4.7	40.2 ± 2.8	$t_{(18)}$= 1.268, p=0.221
Rewards latency (s)	20.5 ± 3.4	22.1 ± 3.9	$t_{(14)}$=0.310, p=0.761
Day 2-3: Magazine training with 3 reward sizes			
Magazine entries (day 2)	813.2 ± 159.3	703.8 ± 117.3	Genotype: $F_{(1, 18)}$=0.040, p=0.843; day: $F_{(1, 18)}$=0.692, p=0.416; interaction: $F_{(1, 18)}$=0.819, p=0.377
Magazine entries (day 3)	668.3 ± 106.6	709.9 ± 141.0	
Rewards (day 2)	64.1 ± 9.2	60.9 ±4.6	Genotype: $F_{(1, 18)}$=0.027, p=0.872; day: $F_{(1, 18)}$=4.130, p=0.057; interaction: $F_{(1, 18)}$=2.920, p=0.105
Rewards (day 3)	65.0 ± 8.3	71.2 ± 5.0	
Reward latency (day 2)	7.2 ± 1.2	17.2 ± 6.4	Genotype: $F_{(1, 18)}$=1.19, p=0.291; day: $F_{(1, 18)}$=0.905, p=0.356; interaction: $F_{(1, 18)}$=3.58, p=0.077 #
Reward latency (day 3)	8.9 ± 1.3	11.5 ± 3.6	
Day 4: Magazine training with varying ITI			
Magazine entries *(Fig. 5.9A)*	1052.0 ± 141.9	733.4 ± 90.4	$t_{(18)}$=1.960, p=0.066 #

Number of rewards	91.3 ± 2.7	92.0 ± 3.9	$t_{(18)}$=0.135, p=0.894
Reward latency (s)	9.4 ± 1.0	9.7± 2.3	$t_{(18)}$=0.138, p=0.891
Day 5-6: Negative prediction error			
Magazine entries (day 5)	894.9 ± 147.7	805.3 ± 156.0	Genotype: $F_{(1, 18)}$=0.306, p=0.587; day: $F_{(1, 18)}$=16.900, p=0.001; interaction: $F_{(1, 18)}$=0.012, p=0.911
Magazine entries (day 6) *(Fig. 5.9B)*	515.4 ± 45.0	446.2 ± 80.9	
Rewards (day 5)	65.1 ± 2.1	69.5 ± 2.4	Genotype: $F_{(1, 18)}$=0.016, p=0.902; day: $F_{(1, 18)}$= 0.002, p=0.962; interaction: $F_{(1, 18)}$=3.65, p=0.072 #
Rewards (day 6)	69.0 ± 1.6	65.5 ± 4.2	
Reward latency (day 5)	5.6 ± 1.0	5.6 ± 0.7	Genotype: $F_{(1, 18)}$= 0.516, p=0.482; day: $F_{(1, 18)}$=0.603, p=0.448; interaction: $F_{(1, 18)}$= 0.854, p=0.369
Reward latency (day 6)	5.4 ± 0.7	8.1 ± 2.8	

Interestingly, analysis of magazine entries on day 4 (when the task involved blocks of varying ITI lengths) revealed a trend reduction in total magazine entries in VGLUT3 cKO$^{5\text{-HT}}$ mice compared to controls (see ***Table 5.2***). A two-way ANOVA investigating entries in the two ITI conditions showed that both genotypes performed more entries in the longer ITI ($F_{(1, 18)}$=54.8, p<0.0001), but there was no significant interaction between genotype and ITI length ($F_{(1, 18)}$=2.83, p=0.110; ***Fig. 5.9A***). Although strictly not appropriate due to the lack of a significant interaction, Šídák's post hoc test was carried out to further explore the trend reduction in magazine entries. This revealed that, while both genotypes performed more entries in the long ITI compared to the short ITI, this increase was smaller in VGLUT3 cKO$^{5\text{-HT}}$ mice compared to controls (p=0.035; ***Fig. 5.9A***). Conversely, the two genotypes were not different in number of magazine entries in the short ITI (p=0.035).

On days 5 and 6 mice received a reward only for 70% of entries into the illuminated magazine port, which was otherwise always rewarded. This task was primarily aimed at examining DA dynamics during unrewarded trials which were expected to generate a negative prediction error signal, nonetheless the number of magazine entries and number of rewards were also examined. This analysis revealed no effect of genotype on any of the above parameters, as detailed in ***Table 5.2***. On days 5 and 6 all mice performed a greater number of entries in the ITIs following rewarded trials compared to unrewarded trials (day 5: $F_{(1,\ 18)}$=26.000, p<0.0001; day 6: $F_{(1,\ 18)}$=31.000, p<0.0001, ***Fig. 5.9B***), but there was no effect of genotype (day 5: $F_{(1,\ 18)}$=0.229, p=0.638; day 6: $F_{(1,\ 18)}$=0.527, p=0.477, ***Fig. 5.9B***) nor interaction between trial type and genotype (day 5: $F_{(1,\ 18)}$= 0.424, p=0.523; day 6: $F_{(1,\ 18)}$=0.797, p=0.384, ***Fig. 5.9B***).

Altogether, during training days 1-6 in a two-way repeated measure ANOVA VGLUT3 cKO$^{5\text{-HT}}$ mice did not differ from controls in the number of rewards collected (effect of genotype: $F_{(1,\ 18)}$=0.145, p=0.708; genotype x day interaction: $F_{(5,\ 90)}$=0.845, p=0.522) or magazine entries (effect of genotype: $F_{(1,\ 18)}$=0.619, p=0.442; genotype x day interaction: $F_{(5,\ 90)}$=0.976, p=0.437). Unsurprisingly, both measures were affected by training day given the different protocols adopted on different days (main effect of day on reward: $F_{(5,\ 90)}$=49.5, p<0.0001; main effect of day on magazine entries: $F_{(5,\ 90)}$=15.0, p<0.0001).

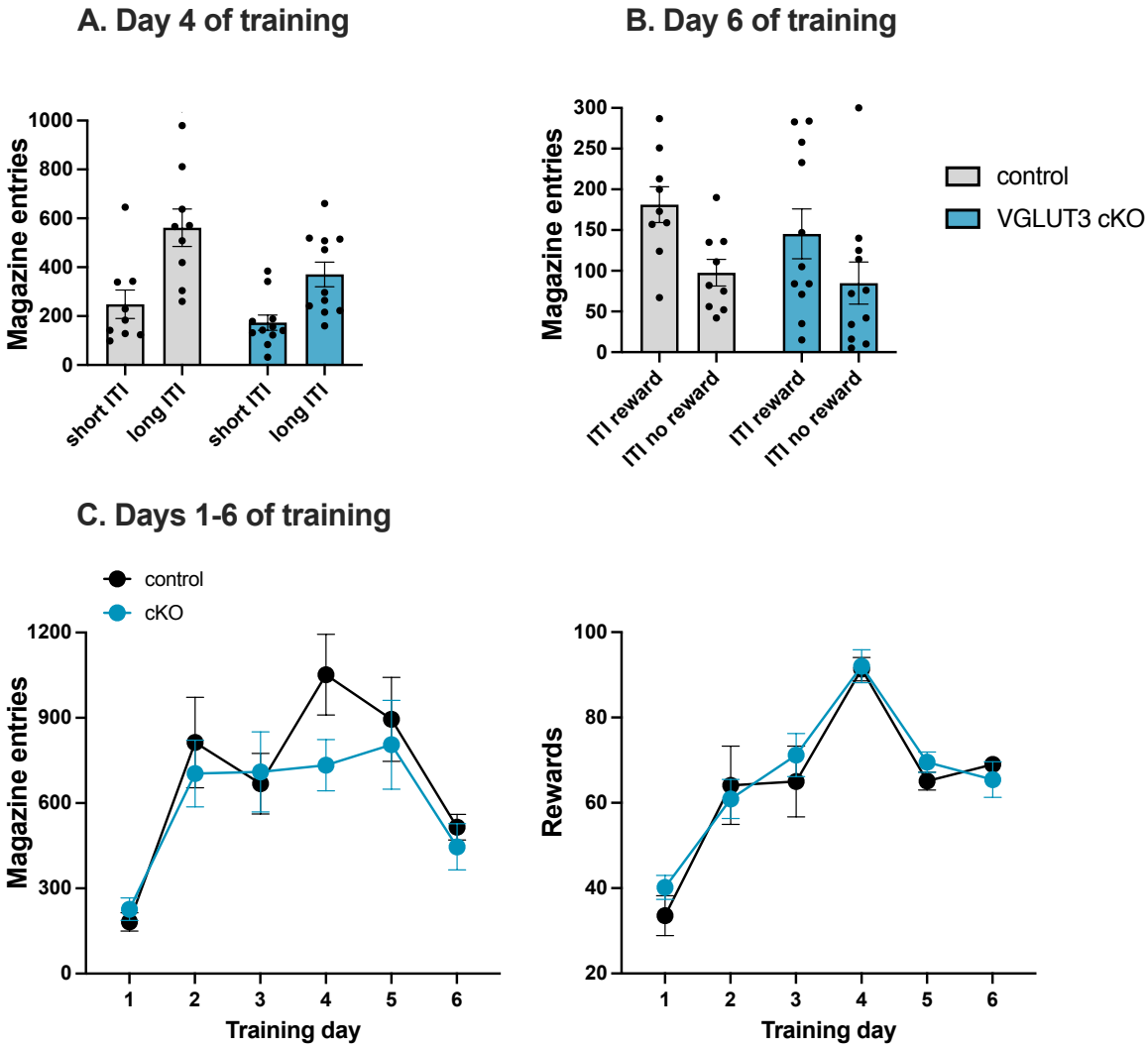

Figure 5.9 | Performance of VGLUT3 cKO$^{5\text{-HT}}$ mice and control littermates in a water-based operant training task. Data from day 4 and 6 of magazine training, involving varying ITI in blocks **(A)** or in the ITI following rewarded and unrewarded trials **(B)**. See table *Table 5.1* for details. Columns represent mean ± SEM values of VGLUT3 cKO$^{5\text{-HT}}$ mice (n=11) and controls (n=9). Individual values are indicated by closed circles Data were analysed by two-way ANOVA, followed by Šídák's multiple comparisons test. *p<0.05. **(C)** Data from days 1-6 of operant training, as described in *Table 5.1.* Closed circles represent mean ± SEM values of VGLUT3 cKO$^{5\text{-HT}}$ mice (n=11) and controls (n=9). Data were analysed by two-way repeated measures ANOVA.

5.3.2.2 Reversal learning operant task

During days 7 to 15 the chamber was equipped with 2 ports, and training involved a reversal learning task. On day 7, port 2 was introduced for the first time. In this first reversal session mice had to learn to obtain a reward from port 2, instead of port 1. Port 1 was available to poke but it did not deliver any reward, nor trigger any sound or penalty. In this paradigm both groups performed a greater number of entries in port 2 compared to port 1 ($F_{(1, 18)}$=39.1, p<0.0001; ***Fig. 5.10A***), but there was no difference between VGLUT3 cKO$^{5\text{-HT}}$ mice and controls in the number of entries in each port ($F_{(1, 18)}$=0.107, p=0.747; ***Fig. 5.10A***) nor any interaction between genotype and port entries ($F_{(1, 18)}$=0.003, p=0.958). Similarly, the number of rewards collected was also not significantly different between groups ($t_{(18)}$=1.463, p=0.161; ***Fig. 5.10A***).

On day 8, the task was similar to day 7, with rewards being delivered at port 2. However, port 1 was now associated with a white noise cue and a time out. Similarly to day 7, on day 8 both groups performed a greater number of overall entries in port 2 compared to port 1 ($F_{(1, 18)}$=37.2, p<0.0001; ***Fig. 5.10B***). There was also no statistically significant difference between VGLUT3 cKO$^{5\text{-HT}}$ mice and controls in the number of entries in each port ($F_{(1, 18)}$=3.10, p=0.095), although VGLUT3 cKO$^{5\text{-HT}}$ mice showed a weak trend for a reduction in entries. Furthermore, there was no interaction between genotype and port entries ($F_{(1, 18)}$=2.33, p=0.1446). Similarly, the number of rewards collected ($t_{(18)}$=1.463, p=0.161; ***Fig. 5.10B***) and incorrect

responses ($t_{(18)}$=1.463, p=0.161) were also not significantly different between groups.

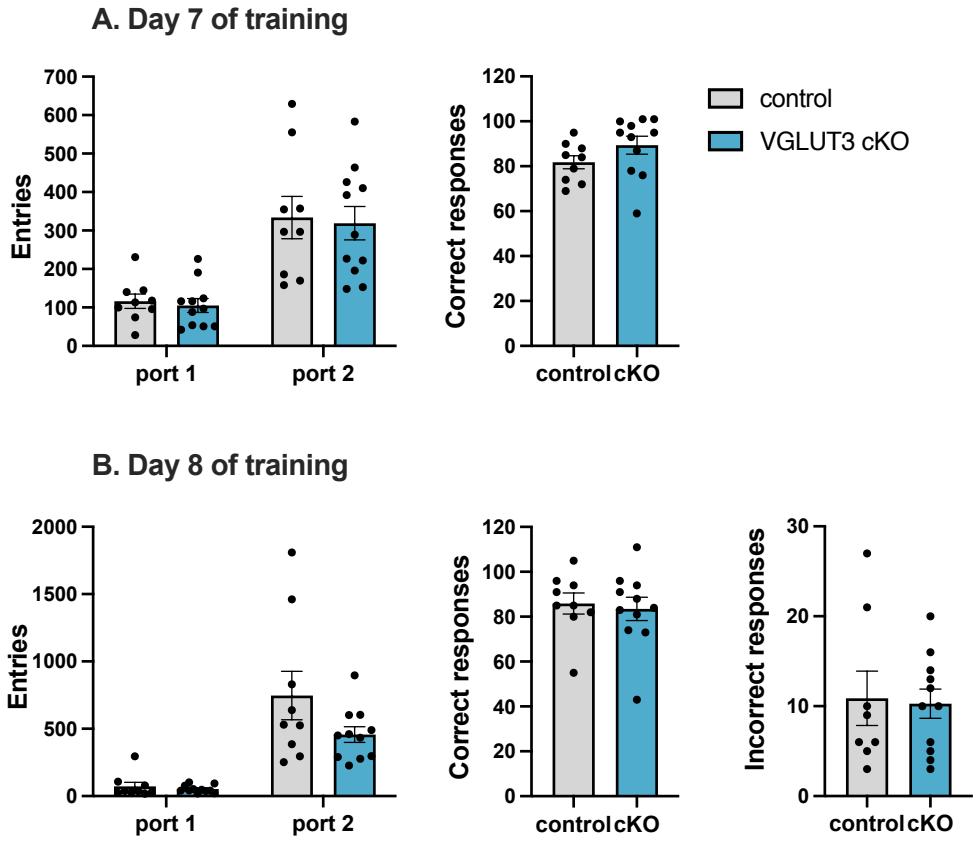

Figure 5.10 | Performance of VGLUT3 cKO$^{5\text{-HT}}$ mice and control littermates in a reversal learning task. Up to day 7 of the operant task mice could collect rewards from port 1, while on days 7 and 8, rewards were delivered from port 2. On day 7 **(A)** no penalty was associated with port 1 entries, while on day 8 **(B)** port 1 entries (when port 2 is illuminated) were recorded as an incorrect response and triggered a time out. See table *Table 5.1* for further details. Columns represent mean ± SEM values of VGLUT3 cKO$^{5\text{-HT}}$ mice (n=11) and controls (n=9). Individual values are indicated by closed circles. Data were analysed by two-way ANOVA or t test.

Lastly, a 2-choice task was run on training days 9 to 15. This involved either port 1 or port 2 being illuminated in successive blocks of trials. Correct entries in the illuminated port triggered a water reward, while incorrect entries in the non-

illuminated port (when the opposite port was illuminated) triggered a time out and no reward (see *Table 5.1* for further details). Since the main focus was on collecting the photometry data, all 20 mice were run till day 9 inclusive (n=11 and n=9) but from day 10 onwards the sample size was reduced to those 12 mice displaying dLight signal (n=6 per genotype). Furthermore, originally the task was planned to run for 12 days, however it was later extended to 15 days to collect further photometry data with two days of break between training day 12 and 13. This caused a decrease in behavioural performance between days 12 and 13. Therefore, it was deemed justified to analyse the behavioural data for days 9-12, instead of till day 15. Interestingly, within this time-frame VGLUT3 cKO$^{5\text{-HT}}$ mice displayed a reduction in the percentage of correct responses (effect of genotype: $F_{(1, 18)}$=4.64, p=0.045; day: $F_{(3, 29)}$=1.68, p=0.192; interaction: $F_{(3, 29)}$=0.201, p=0.895; ***Fig. 5.11***), and an increase in the percentage of incorrect responses (effect of genotype: $F_{(1, 48)}$=5.14, p=0.028; time: $F_{(3, 48)}$=2.04, p=0.120; interaction: $F_{(3, 48)}$=0.181, p=0.909; ***Fig. 5.11***). Conversely, the number of magazine entries was affected by training day ($F_{(3, 30)}$=4.86, p=0.007) but there was no effect of genotype ($F_{(1, 18)}$=0.423. p=0.5234; ***Fig. 5.11***) nor training day x genotype interaction ($F_{(3, 30)}$=0.221, p=0.881). The number of trials was also not affected by genotype ($F_{(1, 18)}$=1.03, p=0.323), nor training day ($F_{(3, 30)}$=1.98, p=0.138; interaction; $F_{(3, 30)}$=0.278, p=0.841: ***Fig. 5.11***).

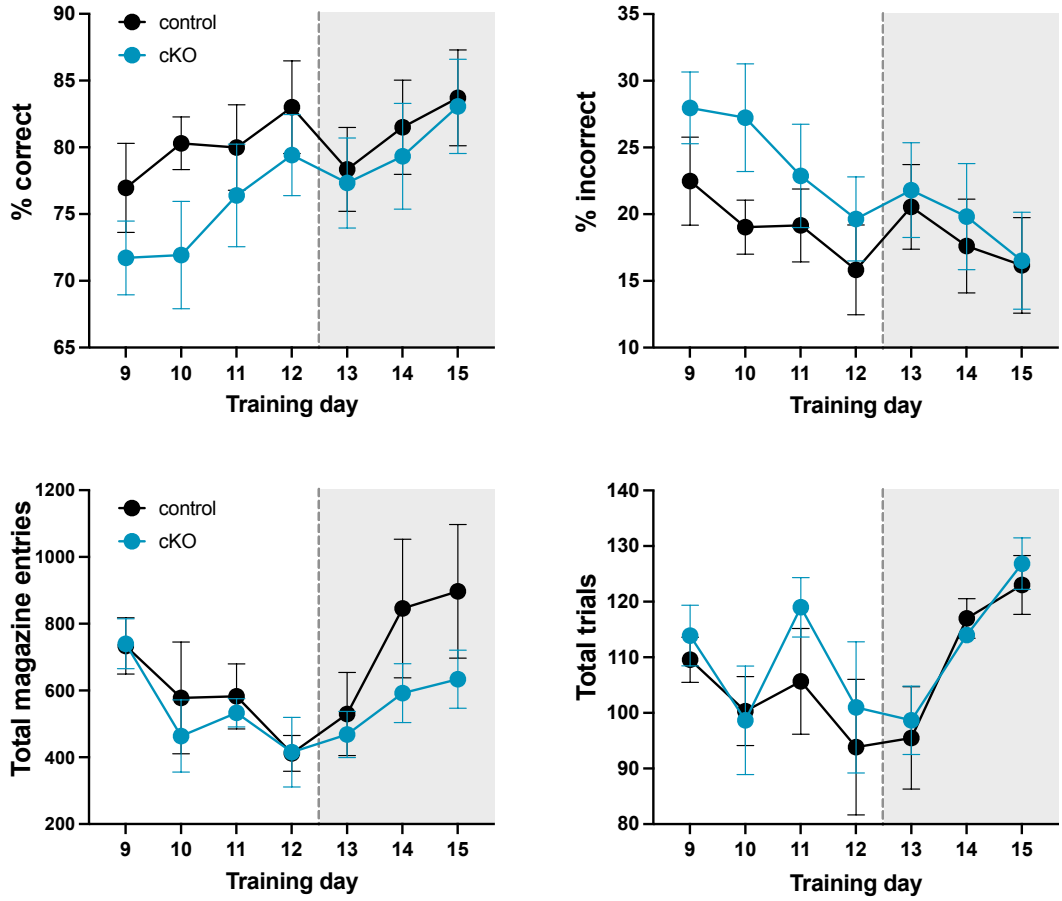

Figure 5.11 | Performance of VGLUT3 cKO$^{5\text{-HT}}$ mice and control littermates in a 2-choice operant task. See table *Table 5.1* for task details. Dotted lines represent 2 days of break in the experimental timeline. Columns represent mean ± SEM values of VGLUT3 cKO$^{5\text{-HT}}$ mice and controls. Group sizes were n=11 for VGLUT3 cKO$^{5\text{-HT}}$ mice and n=9 for controls on day 9, and n=6 for days 10-15, as only mice with dLight signal continued the training. Individual values are indicated by closed circles Data were analyzed by two-way ANOVA.

Conversely, if data were analysed together for days 9-15 then there was no statistically significant difference in the percentage of correct responses (effect of genotype: $F_{(1,\ 18)}$=1.88, day: $F_{(6,\ 59)}$=2.11, p=0.065; p=0.1877; interaction: $F_{(6,\ 59)}$= 0.345, p=0.910) nor in the percentage of incorrect responses (effect of genotype: $F_{(1,\ 18)}$=2.19, p=0.157; day: $F_{(6,\ 60)}$=2.140, p=0.061; interaction: $F_{(6,\ 60)}$=0.343, p=0.912). Similarly, number of magazine entries (effect of genotype: $F_{(1,\ 18)}$=2.34, p=0.144; day:

$F_{(6, 60)}$=3.77, p=0.003; interaction: $F_{(6, 60)}$=0.741, p=0.619) and number of total trials (effect of genotype: $F_{(1, 20)}$=0.800, p=0.382; day: $F_{(6, 58)}$=3.87, p=0.003; interaction: $F_{(6, 58)}$=0.198, p=0.976) were not different between groups.

5.4 Discussion

5.4.1 Summary of key results

In this Chapter, fibre photometry with a DA biosensor was used to investigate DA release in the NAc of VGLUT3 cKO$^{5\text{-HT}}$ mice during an operant task, which involved collecting water rewards by nose-poking an illuminated port. Reward delivery was also signalled by an auditory cue which was triggered by the nose-poke and lasted 0.5 s, with its offset corresponding to reward delivery. On day 1 of training, there was no statistically significant difference in DA response between genotypes. However, on day 2 and 3 VGLUT3 cKO$^{5\text{-HT}}$ mice showed increased DA release in response to the reward-predictive auditory cue, compared to littermate controls. Conversely, on day 4 when ITI length was variable, VGLUT3 cKO$^{5\text{-HT}}$ mice displayed a reduction in DA release in response to the reward. Similarly, on day 5-6, when only on 70% of entries in the illuminated port were rewarded, VGLUT3 cKO$^{5\text{-HT}}$ mice showed a reduction in DA release in response to reward, compared to controls, but there was no difference between genotypes in the negative reward prediction error signals. Altogether, VGLUT3 cKO$^{5\text{-HT}}$ mice displayed an increase in DA response to the reward-predictive cue on days 2 and 3, followed by a decrease in DA response to the reward on days 4-6. Further, on days 1-6 no statistically significant behavioural differences was observed between groups.

On the first day of a reversal learning task (day 7), VGLUT3 cKO$^{5\text{-HT}}$ mice displayed reduced DA release in response to reward delivery. However, the number of entries in the illuminated port did not differ between genotypes. Lastly, during a 2-choice task (days 9-15), VGLUT3 cKO$^{5\text{-HT}}$ mice showed a trend reduction in DA response to the sound cues, but their DA response to reward or no reward was not statistically different from controls. Nonetheless, behavioural analysis of the same task showed that VGLUT3 cKO$^{5\text{-HT}}$ mice performed less correct responses and more incorrect responses on days 9-12 compared to controls. Altogether, during reversal learning VGLUT3 cKO$^{5\text{-HT}}$ mice showed a trend reduction in DA release in response the both the reward and reward-predictive cue, which was accompanied by reduced behavioural performance.

5.4.2 VGLUT3 cKO$^{5\text{-HT}}$ mice show altered dynamics of DA release in the NAc during reward-based learning

The operant paradigm involved several stages of training in which mice learned to nose-poke into an illuminated port to receive a water reward. The reward was preceded by 0.5 s sound cue, except during the first 15 trials of the first training day where reward and cue occurred simultaneously. On this day, there was no genotype difference in DA response to the auditory cue, albeit in both groups this response was relatively small. Furthermore, no statistically significant difference between genotypes was detected on either trials with immediate or delayed reward. However, on this day the sample size was rather small due to technical issues, and

AUC analysis might not be the best-suited method to detect small changes in patterns of DA release. Further AUC analysis could investigate the data using smaller time frames, or response levels across time, additionally analysis of peak signal could also be carried out.

Interestingly, on days 2 and 3, VGLUT3 cKO$^{5\text{-HT}}$ mice showed increased DA release in response to the reward-predictive auditory cue compared to controls (a difference which was not present on day 1). However, VGLUT3 cKO$^{5\text{-HT}}$ mice did not differ from controls in the DA response to the reward. In particular, when mice received rewards of 3 different sizes, NAc DA released progressively increased with larger reward size in both genotypes. Previous evidence from extracellular recordings in awake animals indicates that that NAc DA release is sensitive to the magnitude of the reward, including the specific volume of liquid received (Tobler et al., 2005). This in also in line with the literature theorising that DA encodes a reward prediction error, with greater DA release associated with unexpectedly greater rewards (Glimcher, 2011; Schultz, 2016, 2016; Schultz et al., 1990, 1997). Similarly to day 1, peak analysis of days 2 and 3 (as well as the following training days) could reveal more subtle differences between genotypes. Additionally, further analysis could investigate the data prior to z-scoring (i.e. subtracting the mean and dividing by the standard deviation) to ensure that baseline fluorescence levels were comparable between genotypes.

In the first 3 days of training no behavioural differences between genotypes were detected, which contrasts with the findings of differences in DA release. However,

the behavioural tasks used in this chapter were designed primarily to examine DA dynamics during reward-based learning, thus the training parameters were very low difficulty. Furthermore, in *Chapter 4* no differences between groups were found in a one-session long magazine training in the same operant boxes.

Additionally, on days 2 and 3 the heightened response to the CS cue, might indicate an increased focus on the cue, and a shift towards Pavlovian conditioning, over instrumental learning. However, the current magazine training task was not designed to tease apart the instrumental and Pavlovian learning components, which both involve nose-poke of the illuminated port.

On days 4, 5 and 6, VGLUT3 cKO$^{5\text{-HT}}$ mice did not differ from control littermates in their DA response to the auditory cue, but they did show decreased DA release following reward delivery. As previously discussed (*Section 5.1.1*), during associative learning DA release associated with reward progressively decreases in favour of greater DA release in response to the reward-predictive cue (Ljungberg et al., 1992). The current data suggests that this shift might occur faster in VGLUT3 cKO$^{5\text{-HT}}$ mice compared to control littermates, as this would explain both the initial increase in DA release in response to the auditory cue (days 2-3) and the subsequent decrease in DA release following the reward (days 4, 5 and 6). Furthermore, during reinforcement learning the DA response to the reward is expected to decrease, as over time the predictability of the reward following CS presentation (here the light and auditory cue) increases, leading to a reduction in the reward prediction error signal (Clark et al., 2013). Therefore, the faster decrease in reward prediction error

signal observed in VGLUT3 cKO$^{5\text{-HT}}$ mice, compared to controls, might indicate a faster learning process.

An increased response to the CS, and a more efficient transfer of neuronal activation from the US to the CS, leading to a faster decrease in DA release associated with the US over time, has been previously described in "sign-tracking" rats (Flagel et al., 2011; Gillis & Morrison, 2019). Sign-tracking individuals display a biased focus on the cue, as opposed to the goal of the task ("goal-tracking"), for example by attempting to engage with the cue location directly. A propensity for sign-tracking can cause deficits in operant behaviour such as reduced behavioural flexibility in the attentional set shifting task and reduced behavioural control in a conditional responding task (Enkel et al., 2019; Flagel et al., 2011). Sign-tracking behaviour has been predominantly characterised in rats, thus species-specific differences might occur. However, there are a few examples of sign-tracking and goal-tracking being investigated in mice as well (Darvas et al., 2014; Macpherson & Hikida, 2018; Parker et al., 2010).

Interestingly, behavioural analysis of data from day 4 (with varying ITI lengths) also revealed a trend difference between genotypes, with VGLUT3 cKO$^{5\text{-HT}}$ mice performing a reduced number of port entries which was more evident with longer ITIs. The more efficient transfer of DA release from US to CS might cause VGLUT3 cKO$^{5\text{-HT}}$ mice to be predominantly driven by the Pavlovian CS cue (i.e. the light and auditory cue), leading to a reduction in responses in absence of such cues.

On days 5 and 6, mice received a reward in only 70% of entries in the illuminated port, to investigate negative prediction error signals. As noted above, VGLUT3 cKO$^{5\text{-HT}}$ mice displayed reduced DA response in rewarded trials, compared to controls, but no difference between genotypes was detected on unrewarded trials. Thus, both genotypes displayed a similar negative prediction error with DA levels dropping below baseline.

The magazine training sessions were followed by several task stages probing reversal learning. These were also low difficulty and designed to slowly increase the complexity of the task in steps. On the first day of reversal learning (day 7, reversal task without penalty) compared to controls, DA release in VGLUT3 cKO$^{5\text{-HT}}$ mice was reduced following reward delivery, similarly to what observed in days 4, 5 and 6. Additionally, DA release in VGLUT3 cKO$^{5\text{-HT}}$ mice was also reduced, compared to controls, in the last second prior to the auditory cue. The latter measure comprises the DA response to the light cue, prior to nose-poke in the illuminated port. Further analysis could examine DA release throughout the entire ITI and after the onset of the light cue, to investigate whether this difference in DA release between genotypes arises after cue onset, or persists throughout the trial. As VGLUT3 cKO$^{5\text{-HT}}$ mice display a faster transfer of DA response to the auditory cue, it is likely that they would present a faster transfer of response to the light cue as well.

Again, the observed differences in DA signalling did not affect behaviour on this task, likely due to its low difficulty. Additionally, as previously mentioned, the current task does not allow to easily tease apart the instrumental and Pavlovian components

(both involving nose-poke of the illuminated port), which could mask behavioural differences.

On day 8 (reversal with penalty), no statistically significant difference between genotypes was detected in the analysis of NAc DA release. Data for unrewarded trials appeared noisier than the other trials, suggesting increased inter-subject variability in this condition. There were also no behavioural differences with both genotypes performing the majority of entries in the correct port. In *Chapter 4*, it was hypothesised that VGLUT3 cKO$^{5\text{-HT}}$ mice might have difficulties in reversal learning, as after initial magazine training involving collecting rewards upon entry of the illuminated magazine, they continued to perform increased magazine entries in the subsequent days of training, compared to controls. Nonetheless, similarly to day 7, on day 8 VGLUT3 cKO$^{5\text{-HT}}$ mice did not display any impairments in reversal learning.

The last stage of training involved a choice between 2 ports (days 9-15, 2-choice task) which were illuminated one at a time in successive trials in alternating blocks. This task was chosen due to its similarity to the 5-choice task performed in *Chapter 4*, as both tasks involved selecting one illuminated port out of either 2 or 5 available ports. However, in the current experiment mice would collect the reward directly from the illuminated port, instead of from a separate magazine port located on the same wall, which further highlights the potential low difficulty of the task. In this phase of the task, VGLUT3 cKO$^{5\text{-HT}}$ mice displayed a trend reduction in DA release in response to the sound cue, but this effect did not reach statistical significance. Furthermore, the current AUC analysis did not reveal a statistically significant

difference in the DA response to the reward or lack of it. However, it is possible that the analysis of the data with higher time resolution might reveal differences. Additional analysis, such as regression analysis, could also be implemented for further investigation without an a priori time window.

In the current task VGLUT3 cKO$^{5\text{-HT}}$ mice displayed an increase in incorrect responses and a decrease in correct responses on days 9-12. These behavioural alterations closely match those observed in the water-motivated (5-choice) operant task performed in *Chapter* 4. Furthermore, in accordance with what was observed in *Chapter 2* and *4*, VGLUT3 cKO$^{5\text{-HT}}$ mice were able to learn the task and improve over time, with differences between groups disappearing after day 12. Reduced performance in the current 2-choice task, might be considered evidence of reduced reversal learning, and interestingly sign-tracker rats also display reduced reversal learning and cognitive flexibly in an attentional set shifting task (Enkel et al., 2019). However, sign-tracking individuals also show an apparent faster learning rate in the 5-CSRTT, due to their increased focus on the cue (Maillet et al., 2022), which differs from the increased incorrect responses displayed by VGLUT3 cKO$^{5\text{-HT}}$ mice. Therefore, VGLUT3 cKO$^{5\text{-HT}}$ mice appear to share some behaviour with sign-tracker rats, but there are also some discrepancies.

Altogether, the current DA photometry data suggests a faster acquisition of the CS-US association in VGLUT3 cKO$^{5\text{-HT}}$ mice, compared to control littermates. Moreover, the observed patterns of DA release in VGLUT3 cKO$^{5\text{-HT}}$ mice appears to loosely match those reported in sign-tracking rats (Flagel et al., 2011). VGLUT3 cKO$^{5\text{-HT}}$ mice

also exhibited some behavioural evidence of sign-tracking over goal-tracking in the previous chapters. For example, in the water-motivated operant task described in *Chapter 4*, after a magazine training session involving nose-poking the illuminated magazine to receive a reward, VGLUT3 cKO$^{5\text{-HT}}$ mice continued to displayed increased magazine entries in the following 7 days of training (*Fig. 4.10*), compared to control littermates. In the same task, where nose-poke of one illuminated port out of 5 ports led to reward delivery from a separate magazine, VGLUT3 cKO$^{5\text{-HT}}$ mice also demonstrated increased entries in the 5 ports, compared to controls. Altogether, this increased engagement with cue locations resembles behaviour of sign-tracker rats, which displayed increased contacts with the CS lever to receive a reward and reduced extinction, compared to control (Flagel et al., 2011; Gillis & Morrison, 2019). Conversely, in a separate appetitively-motivated operant paradigm (*Chapter 4, Fig. 4.5*) where milkshake delivery from a magazine was not predicted by any cues, VGLUT3 cKO$^{5\text{-HT}}$ mice showed reduced magazine entries over the 8 days of training. Importantly, on day 1 of this appetitively-motivated paradigm VGLUT3 cKO$^{5\text{-HT}}$ mice already displayed reduced magazine entries following 5 unsignalled administrations of milkshake, without any required action (*Chapter 4, Fig. 4.4*). Conversely, in a separate operant chamber where the magazine was signalled by a light cue, VGLUT3 cKO$^{5\text{-HT}}$ mice did not show any impairments during in magazine training (*Chapter 4, Table 4.3*), and differences in behaviour only occurred in more complex training stages (albeit the smaller size of the chamber might also had an effect on behaviour). Altogether, the data to date suggests that VGLUT3 cKO$^{5\text{-HT}}$ mice have a propensity for sign-tracking behaviour and might be

more efficient at Pavlovian learning, as opposed to goal-tracking and instrumental learning.

Nonetheless, there are some behavioural features of VGLUT3 cKO$^{5\text{-HT}}$ mice which differ from sign-tracker animals. For example, sign-tracking rats show shorter response latencies, reduced impulse control, with increased premature and perseverative responses, but also increased in correct responses in 5-CSRTT (Colaizzi et al., 2020; Enkel et al., 2019; Flagel et al., 2011; Maillet et al., 2022). Conversely, VGLUT3 cKO$^{5\text{-HT}}$ mice displayed an increase in incorrect responses, without any difference in premature or perseverative responses (*Chapter 5* and *Chapter 4*). Therefore, sign-tracking can only partially explain the observed behavioural phenotype. Altogether, the current data indicates an apparent dissociation with VGLUT3 cKO$^{5\text{-HT}}$ mice demonstrating more dynamic NAc DA signalling compared to controls, suggesting more effective acquisition of associative learning. Albeit, this was accompanied by reduced behavioural performance, characterised by decreased correct responses and increased incorrect responses.

5.4.3 Possible mechanisms underlying altered DA dynamics

Previous *in vitro* electrophysiological evidence indicated that 5-HT-glutamate co-releasing neurons excite VTA DA neurons projecting the NAc, in an AMPA- and 5-HT$_3$ receptor-dependent manner (Wang et al., 2019). Furthermore, optogenetic activation of 5-HT-glutamate co-releasing neurons promoted conditioned place preference and self-stimulation (Liu et al., 2020). Conversely, 5-HT inputs to VTA

have been suggested to be primarily inhibitory, and 5-HT has been shown to inhibit the reinforcing effects of self-stimulation (Abler et al., 2012; Amit et al., 1991; Di Matteo et al., 2001, 2008). Additionally, evidence indicates that both 5-HT and dual 5-HT-glutamate neurons are activated during reward-based learning (Liu et al., 2014; Wang et al., 2019). As VGLUT3 cKO$^{5\text{-HT}}$ mice are predicted to lack glutamate co-release from 5-HT neurons, it was hypothesised that this would lead to reduced excitation of VTA DA neurons. As VTA DA neurons project to the NAc, this reduced excitation would cause a decrease in NAc DA release during reward-based learning. Whilst this hypothesis could be consistent with the decrease in NAc DA release found in the later stages of learning, it contrasts with findings of increased DA release in response to the reward-predictive auditory cue. Furthermore, as previously discussed (*Section 5.4.2*), the current photometry data suggests that VGLUT3 cKO$^{5\text{-HT}}$ mice might have a faster transfer of DA signalling from the reward to the reward-predictive cues, compared to control littermates. Therefore, it is possible that in control mice glutamate co-released from 5-HT neurons might contribute to modulating the magnitude of the reward prediction error (e.g. by reducing the response to the reward-predictive cue), thus lack of this regulation might lead to increased DA response to the cue. Conversely, the reduction in DA release to the reward later in the training, might indicate that VGLUT3 cKO$^{5\text{-HT}}$ mice are learning faster to predict reward occurrence.

The mechanism leading to this increase in the DA response to the auditory CS cue is unclear and might suggest an initial increased excitation of DA neurons, which is hard to reconcile with reduced excitatory influences from glutamatergic neurons

projecting to the VTA. It is possible that glutamate might exert inhibitory effects on VTA neurons, via metabotropic glutamate receptors (mGLURs). Indeed, DA release has previously been suggested to be inhibited via VGLUT3-dependent glutamate, through mGLURs located on DA terminals (Karasawa et al., 2006; Sakae et al., 2015). Interestingly, mGLUR antagonism had no effect in mice with global VGLUT3 deletion, while blocking mGLUR in wildtype mice àhad a similar effect on DA release to deleting VGLUT3 (Sakae et al., 2015). Future experiments could investigate the effects of mGLUR antagonists on NAc DA release in VGLUT3 cKO$^{5\text{-HT}}$ mice.

Additionally, the presumed lack of co-released glutamate might affect NAc DA function via other pathways. For example, 5-HT projections to the prefrontal cortex have been shown to be activated by reward, and have been suggested to mediate waiting for rewards and appraisal of reward value (Miyazaki et al., 2024; Seymour et al., 2012). Additionally, DRN 5-HT neurons also project directly to the NAc, and may influence reward mechanisms (Brown & Molliver, 2000; Chang et al., 2011; Dölen et al., 2013; Li et al., 1989; Yoshimoto et al., 1992).

Furthermore, the lack of VGLUT3 in 5-HT neurons might lead to long-term compensatory changes that could affect DA function. For example, it was shown in *Chapter 2* that VGLUT3 cKO$^{5\text{-HT}}$ mice display increased gene expression of DA D_1 receptors and 5-HT_{1B} receptors. D_1 receptors have been associated with signalling phasic DA release (Dreyer et al., 2010), with administration of D_1 antagonists attenuating the acquisition of sign-tracking behaviour (Clark et al., 2013). Specifically, recent evidence showed that acquisition of sign-tracking in mice

was inhibited by blocking neurotransmission of NAc D_1 receptors in medium spiny neurons, confirming a specific role for D_1 receptors in sign-tracking (Macpherson & Hikida, 2018). Therefore, the apparent increase in sign-tracking behaviour observed in VGLUT3 cKO$^{5\text{-HT}}$ mice could be at least be partly mediated to the increased expression in NAc DA D_1 receptors.

Lastly it is possible that modulation of 5-HT function caused by the lack of glutamate might also play a role. For example, if VGLUT3 synergised with VMAT2, thus promoting vesicular accumulation of 5-HT (Amilhon et al., 2010; El Mestikawy et al., 2011), lack of VGLUT3 might lead to reduced 5-HT release onto VTA DA neurons in the presence of rewarding stimuli. This could cause a reduction in 5-HT-dependent inhibition, which could be consistent with an initial increase in DA release in the NAc. Future experiments could investigate these hypotheses further, for example by examining 5-HT function in *in vivo* in VGLUT3 cKO$^{5\text{-HT}}$ mice.

Chapter 6
General discussion

6.1 Summary of main findings

5-HT is a key neurotransmitter for emotional processing which is involved in a wide range of functions, including stress coping, anxiety, and depressive behaviour, but also cognition and reward processing. Recently it has been shown that the majority of 5-HT neurons in the DRN release not only 5-HT but also glutamate (Johnson, 1994; Schäfer et al., 2002; Sengupta et al., 2017). Glutamate co-release from 5-HT neurons is mediated by VGLUT3 (Fremeau et al., 2002; Gras et al., 2002), and 5-HT-glutamate co-release has been observed in several projections including to the hippocampus, amygdala, and striatum (Kapoor et al., 2016; Liu et al., 2014; Sengupta et al., 2017; Varga et al., 2009). Transgenic mice with global VGLUT3 deletion have been used to investigate the role of co-released glutamate across multiple different systems (Amilhon et al., 2010; Balázsfi et al., 2018; De Almeida et al., 2023; Sakae et al., 2015), but the function of glutamate co-released specifically from 5-HT neurons had not previously been investigated.

The experiments described in this thesis aimed to fill this gap by probing the behavioural role of glutamate co-released from 5-HT neurons using a transgenic mouse model with conditional VGLUT3 KO in 5-HT neurons. Upon validation of this model, VGLUT3 cKO$^{5\text{-HT}}$ mice were used to investigate the role of glutamate co-released from 5-HT neurons in anxiety, stress coping and reward processing,

based on previous evidence that co-released glutamate might be involved in these behaviours (Amilhon et al., 2010; Liu et al., 2020; Ren et al., 2018).

6.1.1 Validation of VGLUT3 cKO$^{5\text{-HT}}$ mice, gene expression and neurochemistry

Firstly, in *Chapter 2* a combination of qPCR and immunohistochemistry confirmed a reduction of VGLUT3 expression in DRN 5-HT neurons of VGLUT3 cKO$^{5\text{-HT}}$ mice. QPCR analyses also found evidence that adaptation to this loss of glutamate led to an increase of 5-HT$_{1A}$ receptor expression in the prefrontal cortex, and an increase of 5-HT$_{1B}$ and DA D$_1$ receptor expression in the NAc. Additionally, analyses of 5-HT neurochemistry revealed evidence of a reduction in 5-HT turnover in the DRN.

6.1.2 5-HT-glutamate co-release in anxiety and anhedonia

Behavioural analysis of VGLUT3 cKO$^{5\text{-HT}}$ mice compared to control littermates carried out in *Chapter 2* found no gross behavioural alteration, and no difference in natural behaviours or food/water consumption. Furthermore, no behavioural differences between genotypes were found in the open field, EPM and light/dark box, suggesting that glutamate co-released from 5-HT neurons is not involved in anxiety-like behaviour. However, VGLUT3 cKO$^{5\text{-HT}}$ mice displayed a reduction in sucrose preference, suggesting a putative anhedonic state (*Chapter 2*). As anhedonia can be linked to both stress sensitivity and decreased sensitivity to reward for a (review see Pizzagalli, 2014; Stanton et al., 2019), both of these behaviours were investigated in subsequent studies.

6.1.3 5-HT-glutamate co-release in stress coping

In *Chapter* 3, triple-label immunohistochemistry demonstrated that acute, uncontrollable swim stress increased c-Fos in VGLUT3 expressing 5-HT neurons in the ventral DRN of wildtype mice. Interestingly, when VGLUT3 cKO$^{5\text{-HT}}$ mice were exposed to swim stress they showed an increase in climbing behaviour, a measure of active coping. Additionally, wildtype mice also showed increased climbing following acute fluoxetine administration, revealing an interesting parallel between the behavioural effects of genetic loss of VGLUT3 in 5-HT neurons and 5-HT reuptake inhibition. Therefore, it was hypothesised that both fluoxetine and the predicted lack of co-released glutamate might increase active coping by shifting the 5-HT-glutamate balance at their receptors in favour of 5-HT.

6.1.4 5-HT-glutamate co-release in reward processing

In *Chapter 4*, VGLUT3 cKO$^{5\text{-HT}}$ mice demonstrated reduced performance in 3 reward-based learning tasks, involving different set-ups (a spatial Y maze and 2 kinds of operant chambers), different kinds of rewards (sweet solutions and water), and different behavioural paradigms. In all these tasks VGLUT3 cKO$^{5\text{-HT}}$ mice were able to learn over time, but they demonstrated reduced choice accuracy. These deficits were particularly evident in more challenging associative learning tasks (e.g. involving choices between multiple nose-poke ports, and reward collection from a separate magazine), while deficits were not present in simpler magazine training tasks involving a single illuminated port. Conversely, performance of VGLUT3

cKO$^{5\text{-HT}}$ mice did not differ from controls in short-term memory tests including a spatial novelty preference test and the novel object recognition test. Additionally, our collaborators showed that VGLUT3 cKO$^{5\text{-HT}}$ mice do not differ from controls during fear conditioning, suggesting unimpaired associative learning in the aversive domain. Therefore, it was concluded that VGLUT3 cKO$^{5\text{-HT}}$ mice showed impairments specific to reward-based learning, but the exact nature of this deficit needs to be clarified in future work.

6.1.5 NAc DA dynamics in VGLUT3 cKO$^{5\text{-HT}}$ mice

In *Chapter 5*, experiments involving *in vivo* fibre photometry with a DA biosensor investigated DA release in the NAc of behaving VGLUT3 cKO$^{5\text{-HT}}$ mice, to probe whether the observed impairments in reward-based learning were associated with altered mesolimbic DA function. Interestingly, on training days 2 and 3 VGLUT3 cKO$^{5\text{-HT}}$ mice demonstrated increased DA release in response to the reward-predictive CS cues, but as learning progressed, they displayed reduced DA response to the reward, compared to controls. This was interpreted as evidence of a faster transfer of DA neuronal activation from the reward (CS) to the reward-predictive cue (US)(Clark et al., 2013). These patterns of neuronal activation potentially resemble those of sign-tracking rats, which display increased focus on the reward-predictive cue (Flagel et al., 2011). Sign-tracking behaviour could also be consistent with some of the behavioural deficits of VGLUT3 cKO$^{5\text{-HT}}$ mice and therefore warrants further investigation.

6.2 Interactions between 5-HT-glutamate co-release and DA

6.2.1 5-HT-glutamate co-release and DA in reward and addiction

The faster US-to-CS transfer of DA activity in VGLUT3 cKO$^{5\text{-HT}}$ mice (*Chapter 5*) was, at first glance, surprising in the light of the reduced behavioural performance of these mice in several reward-based tasks. However, an increase in potassium-evoked DA release in the NAc was previously reported in voltammetry experiments in mice with global VGLUT3 KO (Sakae et al., 2015). Interestingly, global VGLUT3 KO mice showed increased DA D_1 receptor density in the NAc (Sakae et al., 2015), and in *Chapter 2* it was shown that VGLUT3 cKO$^{5\text{-HT}}$ mice also demonstrated increased NAc D_1 receptor gene expression.

Mice with global VGLUT3 KO also demonstrated altered reward processing through increased sensitivity to cocaine as measured by cocaine-induced locomotor activity, conditioned place preference and operant self-administration (Sakae et al., 2015). This effect was attributed to the lack of VGLUT3 in tonically active cholinergic interneurons in the NAc, but the current data suggest that glutamate co-released from 5-HT neurons might also be involved. Interestingly, this link between VGLUT3 and reward processing observed in mice might also translate to humans. In fact, an increased frequency of rare functional variants of the VGLUT3 gene (Slc17a8), was observed in individuals with cocaine and/or opiate addiction (Sakae et al., 2015). The current data suggest that VGLUT3-dependent glutamate release from 5-HT

neurons might contribute to modulating the magnitude of the reward prediction error (e.g. by reducing responses to the reward-predictive cue).

The current hypothesis that VGLUT3 cKO$^{5\text{-HT}}$ mice might have a propensity for sign-tracking over goal-tracking might also indicate a role for 5-HT-glutamate co-release in addiction (Colaizzi et al., 2020; Tomie et al., 2008). It has previously been suggested that the sign-tracking conditioned response is poorly controlled, with long-term retention and spontaneous recovery that resemble addiction relapse (Kuhn et al., 2018; Uslaner et al., 2006; Valyear et al., 2017). Additionally, the activation of DA pathways observed in sign-tracking behaviour provides similarities with the DA enhancing neurobiological effects of abused drugs (see Tomie et al., 2008 for a review). Previous studies also showed that sign-tracking behaviour predicts vulnerability to alcohol self-administration (Krank, 2003; Uslaner et al., 2006; Valyear et al., 2017). Therefore, further experiments could investigate addictive behaviours in VGLUT3 cKO$^{5\text{-HT}}$ mice, for example by examining long-term retention and relapse-like behaviour and probing the vulnerability of these mice to drug self-administration.

6.2.2 5-HT-glutamate co-release and DA in stress coping

The interaction between the 5-HT and DA systems was discussed in *Chapter 5* with a focus on reward processing. However, both 5-HT and DA are also involved in stress, in particular coping with acute and chronic stressors. For example, within the VTA, diverse populations of DA neurons are responsive not only to reward and

reward-predictive cues, but also to aversive stimuli and a variety of alerting signals such as sensory events, novelty, and salience (Brischoux et al., 2009; Bromberg-Martin et al., 2010; Horvitz, 2000; Matsumoto & Hikosaka, 2009). This impact of stress on DA neurons is thought to mediate adaptive behaviours and coping strategies in response to changes in the environment (Baik, 2020). Specifically, it has been suggested that mild to moderate stressors that are novel, short-lasting, or controllable increase the activity of NAc DA neurons, while intense, chronic and unpredictable stressors have inhibitory effects on DA neurons (Cabib & Puglisi-Allegra, 2012; Holly & Miczek, 2016; Horvitz, 2000; Marinelli, 2007). Therefore, NAc DA release has been shown to increase during the initial response to acute swim stress and thought to mediate active coping strategies (e.g. swimming and climbing). Conversely, over time the swim stress is progressively perceived as inescapable, thus DA release is inhibited and falls below pre-stress levels, concurrent with a switch towards passive coping strategies, such as immobility (Cabib & Puglisi-Allegra, 2012). This increased DA release concurrent with active coping, and decreased DA release in association to passive coping is perhaps unsurprising due to the role of DA in movement initiation (Syed et al., 2015; Walton et al., 2011).

Whilst both 5-HT and DA play a role in stress coping, their interaction is not straightforward. It has been hypothesised that during stress coping 5-HT might regulate NAc DA via DRN projections to the cortex and the amygdala, thus modulating active or passive coping outcomes (Puglisi-Allegra & Andolina, 2015). This hypothesis could be consistent with optogenetic evidence that ventral DRN 5-HT-glutamate neurons projecting to the prefrontal cortex modulate coping

behaviours (Ren et al., 2018). Nonetheless, more recently VTA-projecting 5-HT-glutamate co-releasing neurons have been shown to regulate stress susceptibility following chronic social defeat. Specifically, activation of 5-HT-glutamate neurons promoted resilience in susceptible mice (Zou et al., 2020), likely via their projections to VTA DA neurons (Chaudhury et al., 2013).

In *Chapter 3*, it was hypothesised that increased active coping in VGLUT3 cKO$^{5\text{-HT}}$ mice, could be caused by a shift in the 5-HT-glutamate balance at their receptors in favour of 5-HT. Thus, is possible that this shift towards 5-HT might mediate stress coping by impacting the activity of VTA DA neurons, either directly via DRN projections to the VTA or indirectly through 5-HT projections to the cortex and amygdala (***Fig. 6.1***). As these DA VTA neurons project to the NAc, future experiments could investigate this further by measuring *in vivo* NAc DA release during acute stress in VGLUT3 cKO$^{5\text{-HT}}$ mice, such as in an operant paradigm involving unpredictable foot shock.

6.2.3 Potential impact of 5-HT-glutamate co-release on other projections

In this thesis, it was hypothesised that 5-HT-glutamate DRN projections to the VTA, would impact NAc DA release. This was based on *in vitro* electrophysiological evidence that 5-HT-glutamate co-releasing neurons excite DA VTA neurons, leading to DA release in the NAc (Wang et al., 2019). Indeed, the VTA is a key site for future experiments to test the impact of changes to glutamate transmission on DA neuronal excitability, both by AMPA or mGLUR (as discussed in *Chapter 5*, *Section 5.4.3*).

However, changes in DA release might be caused by the putative lack of glutamate co-release in other projections, which in turn interact with the VTA and/or NAc.

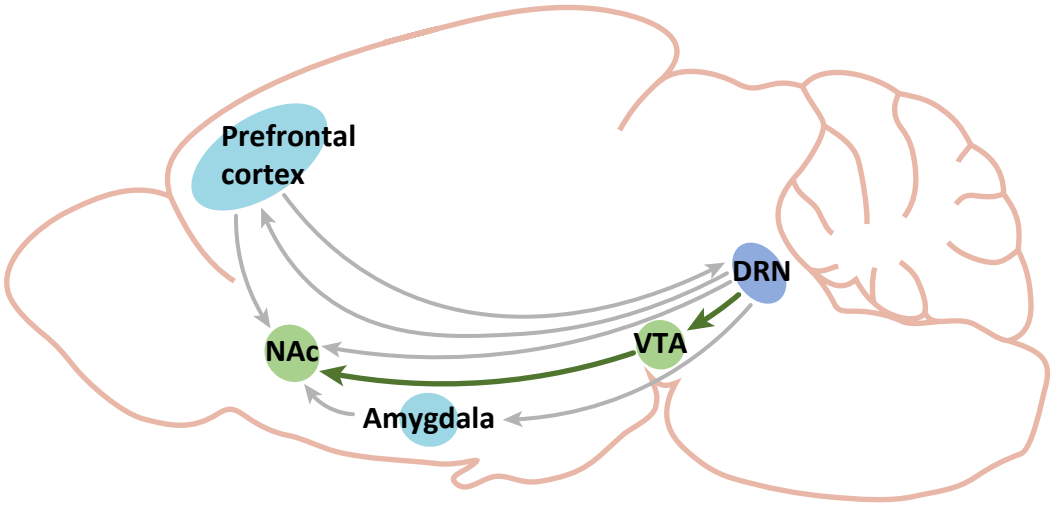

Figure 6.1 | Schematic of DRN projections.

For example, as mentioned above 5-HT-glutamate projections to the prefrontal cortex and the amygdala have been implicated in coping with acute stress (Puglisi-Allegra & Andolina, 2015; Ren et al., 2018). Furthermore, 5-HT projections to the prefrontal cortex have been shown to be activated by reward (Ren et al., 2018), and have been suggested to mediate both appraisal of reward value (Seymour et al., 2012) and waiting for future rewards (Miyazaki et al., 2020). Lastly, DRN 5-HT neurons also project directly to the NAc, and may influence reward mechanisms. For example, evidence suggests that NAc 5-HT release has been implicated in the rewarding properties of both addictive substances and social reward (Brown & Molliver, 2000; Chang et al., 2011; Dölen et al., 2013; Li et al., 1989; Yoshimoto et al., 1992). Altogether, altered 5-HT-glutamate co-release in the cortex, amygdala and

NAc might contribute to the observed behavioural phenotype of VGLUT3 cKO$^{5\text{-HT}}$ mice.

6.3 5-HT-glutamate co-release and phenotype switch

Understanding the consequences of an altered balance between 5-HT and glutamate is important as levels of VGLUT3 have been reported to be plastic and vary throughout the lifetime of the individual. For examples, levels of VGLUT3 expression have been shown to change during neurodevelopment and early post-natal life (Boulland et al., 2004; Gras et al., 2005), and point mutations in the gene encoding VGLUT3 (Slc17a8) may result in life-long alterations in VGLUT3 expression (Ramet et al., 2017; Sakae et al., 2015). Furthermore, it has recently been shown that 5-HT neurons are capable of changing their neurotransmitter identity or co-release profile in response to physiological and environmental stimuli, in a process known as "phenotype switching" (Dulcis et al., 2013; Li et al., 2020; Spitzer, 2015). For example, a decrease in VGLUT3 expression in the ventral DRN was observed in rats exposed to repeated social defeat (Prakash et al., 2020). Interestingly, in susceptible rats (i.e. rats demonstrating chronic stress-induced anhedonia) this decrease in VGLUT3 was concurrent with an increase in TPH2 in the ventral DRN. This suggests that in susceptible animals chronic social defeat triggers a phenotype switch from dual 5-HT-glutamate neurons towards purely 5-HT neurons (Prakash et al., 2020). Another study (Li et al., 2020), reported a co-transmitter switch from glutamate to GABA in 5-HT neurons in the lateral wings of the DRN following exposure to acute

stress. This co-transmitter switch was shown to underlie the acquisition of generalised fear and overriding it prevented fear generalisation (Li et al., 2020).

The above studies are examples of stress-induced changes in the neuronal phenotype of 5-HT neurons. Neurotransmitter or co-transmitter switches may occur in different brain regions, and in response to a wider variety of triggers, including in response to injury, disease (see Vaaga et al., 2014 for a review), and drugs administration (Lai et al., 2023; Marta et al., 2022). For example, as 5-HT-glutamate co-releasing neurons have previously been implicated in the action of SSRIs, further research could investigate whether a phenotype switch may occur in these neurons following chronic SSRI treatment (Fischer et al., 2015).

The possibility of phenotype switching highlights the relevance of the VGLUT3 cKO$^{5\text{-HT}}$ model, as this could be regarded as a model of phenotype switch where all 5-HT-glutamate co-releasing neurons have switched their phenotype towards 5-HT only neurons. Altogether, the current findings suggest that if changes in VGLUT3 expression were to occur in 5-HT neurons, they could impact coping strategies and reward processing, potentially involving changes in modulation of NAc DA.

6.4 Additional future directions

6.4.1 Vesicular synergy between VGLUT3 and VMAT2

Mechanisms of 5-HT-glutamate co-release, and particularly whether release occurs form the same or separate vesicles, are still uncertain. Nonetheless, it is important

to understand how changes in VGLUT3 expression might impact on both glutamate and 5-HT release (Amilhon et al., 2010; El Mestikawy et al., 2011; Trudeau & El Mestikawy, 2018). As previously discussed (e.g. *Chapter 1, Section 1.3.3.3*), there is evidence of vesicular synergy between VGLUT3 and VMAT2 (Trudeau & El Mestikawy, 2018) as amino acid uptake assays indicate that hippocampal and cortical vesicles accumulate more 5-HT in the presence of glutamate (Amilhon et al., 2010). If vesicular synergy was to occur, loss of VGLUT3 might lead to a decrease in both 5-HT and glutamate release. In *Chapter 2*, reduced 5-HT turnover was found in the DRN of VGLUT3 cKO$^{5\text{-HT}}$ mice which is potentially consistent with synergism of VGLUT3 with VMAT2.

Conversely, optogenetic evidence has demonstrated that low frequency (≤1 Hz) stimulation of 5-HT terminals in the amygdala preferentially release glutamate, whilst 5-HT release was observed in response to higher stimulation frequencies (10–20 Hz; Sengupta et al., 2017). Similarly, optogenetic activation of 5-HT neurons by a single-pulse light stimulation elicited glutamate-mediated excitation in the VTA, while prolonged stimulation of the same neurons (20 Hz for 30 s), produced 5-HT mediated currents (Zou et al., 2020). This frequency-dependent release might support the concept that 5-HT and glutamate are released from separate vesicles (Trudeau & El Mestikawy, 2018). In this case loss of VGLUT3 would cause a preferential loss of glutamate versus 5-HT release at the synapse.

Future experiments in VGLUT3 cKO$^{5\text{-HT}}$ mice could use *in vivo* fibre photometry with a 5-HT biosensor (e.g. GRAB$_{5\text{-HT}}$; Wan et al., 2021) in the VTA, to directly investigate

if 5-HT release is reduced in these mice, compared to controls. Furthermore, use of both glutamate and 5-HT biosensors would help to clarify whether the phenotype of these VGLUT3 cKO$^{5\text{-HT}}$ mice is linked a concurrent reduction of both glutamate and 5-HT release from dual 5-HT-glutamate co-releasing neurons.

6.4.2 Potential adaptations to the loss of glutamate

The current VGLUT3 cKO$^{5\text{-HT}}$ mouse model allowed a novel approach to investigate the function of 5-HT-glutamate co-release. However, the genetic lack of VGLUT3 from birth could lead to a variety of compensatory responses. Understanding these compensatory changes might provide valuable insights into adaptation to reduction of VGLUT3 in humans, which could occur following genetic mutations or phenotype switch, as discussed in *Section 6.3*. However, these compensations may also mask VGLUT3 function by causing secondary phenotypes. Future studies could confirm the current findings using a conditional KO construct whereby VGLUT3 is depleted in a temporarily controlled manner. This could be achieved either using a Cre-dependent viral vector delivering a small interfering RNA targeting VGLUT3 in SERT-Cre mice, or a transgene driven by a drug-sensitive promotor.

6.4 Conclusion

In this thesis, a novel VGLUT3 cKO$^{5\text{-HT}}$ mouse model with putative lack of glutamate co-release from 5-HT neurons displayed anhedonia in the sucrose preference test and impairments in several reward-based learning tasks. Furthermore, the VGLUT3 cKO$^{5\text{-HT}}$ mice also showed evidence of increased active coping behaviour when

exposed to acute uncontrollable stress. These behavioural changes were concurrent with increased NAc DA release in response to reward-predictive cues, and evidence of a faster US-CS transfer of DA neuronal activity. Therefore, it is possible that the observed behavioural changes might be linked to altered mesolimbic DA function. Nonetheless, the predicted lack of co-released glutamate from other DRN 5-HT projections, or other compensatory changes might also play a role.

Altogether, the current thesis provides new insights into a role of 5-HT-glutamate co-release in stress coping and reward processing. Future research is needed to clarify how the interactions between the 5-HT and DA systems lead to these observed behavioural effects.

Bibliography

Abela, A. R., Browne, C. J., Sargin, D., Prevot, T. D., Ji, X. D., Li, Z., Lambe, E. K., & Fletcher, P. J. (2020). Median raphe serotonin neurons promote anxiety-like behavior via inputs to the dorsal hippocampus. Neuropharmacology, 168, 107985.

Abler, B., Grön, G., Hartmann, A., Metzger, C., & Walter, M. (2012). Modulation of Frontostriatal Interaction Aligns with Reduced Primary Reward Processing under Serotonergic Drugs. The Journal of Neuroscience, 32(4), 1329.

Adrover, M. F., Shin, J. H., & Alvarez, V. A. (2014). Glutamate and dopamine transmission from midbrain dopamine neurons share similar release properties but are differentially affected by cocaine. Journal of Neuroscience, 34(9), 3183–3192.

Akam, T., Lustig, A., Rowland, J. M., Kapanaiah, S. K. T., Esteve-Agraz, J., Panniello, M., Márquez, C., Kohl, M. M., Kätzel, D., & Costa, R. M. (2022). Open-source, Python-based, hardware and software for controlling behavioural neuroscience experiments. Elife, 11, e67846.

Akam, T., & Walton, M. E. (2019). pyPhotometry: Open source Python based hardware and software for fiber photometry data acquisition. Scientific Reports, 9(1).

Akerboom, J., Chen, T.-W., Wardill, T. J., Tian, L., Marvin, J. S., Mutlu, S., Calderón, N. C., Esposti, F., Borghuis, B. G., & Sun, X. R. (2012). Optimization of a GCaMP calcium indicator for neural activity imaging. Journal of Neuroscience, 32(40), 13819–13840.

Allers, K. A., & Sharp, T. (2003). Neurochemical and anatomical identification of fast- and slow-firing neurones in the rat dorsal raphe nucleus using juxtacellular labelling methods in vivo. Neuroscience, 122(1), 193–204.

Amat, J., Baratta, M. V., Paul, E., Bland, S. T., Watkins, L. R., & Maier, S. F. (2005). Medial prefrontal cortex determines how stressor controllability affects behavior and dorsal raphe nucleus. Nature Neuroscience, 8(3), 365–371.

Amat, J., Matus-Amat, P., Watkins, L. R., & Maier, S. F. (1998). Escapable and inescapable stress differentially and selectively alter extracellular levels of 5-HT in the ventral hippocampus and dorsal periaqueductal gray of the rat. Brain Research, 797, 12–22.

Amilhon, B., Lepicard, È., Renoir, T., Mongeau, R., Popa, D., Poirel, O., Miot, S., Gras, C., Gardier, A. M., Gallego, J., Hamon, M., Lanfumey, L., Gasnier, B., Giros, B., & El Mestikawy, S. (2010). VGLUT3 (vesicular glutamate transporter type 3) contribution to the regulation of serotonergic transmission and anxiety. Journal of Neuroscience, 30(6), 2198–2210.

Amit, Z., Smith, B. R., & Gill, K. (1991). Serotonin uptake inhibitors: effects on motivated consummatory behaviors. The Journal of Clinical Psychiatry, 52 Suppl, 55–60.

Amo, R., Fredes, F., Kinoshita, M., Aoki, R., Aizawa, H., Agetsuma, M., Aoki, T., Shiraki, T., Kakinuma, H., & Matsuda, M. (2014). The habenulo-raphe serotonergic circuit encodes an aversive expectation value essential for adaptive active avoidance of danger. Neuron, 84(5), 1034–1048.

Arias-Carrión, O., Stamelou, M., Murillo-Rodríguez, E., Menéndez-González, M., & Pöppel, E. (2010). Dopaminergic reward system: a short integrative review. International Archives of Medicine, 3(1), 24.

Asinof, S. K., & Paine, T. A. (2014). The 5-choice serial reaction time task: a task of attention and impulse control for rodents. JoVE (Journal of Visualized Experiments), 90, e51574.

Baik, J. H. (2020). Stress and the dopaminergic reward system. Experimental and Molecular Medicine, 52(12), 1879–1890.

Baker, K. G., Halliday, G. M., Hornung, J.-P., Geffen, L. B., Cotton, R. G. H., & To¨rk, I. (1991). Distribution, morphology and number of monoamine-synthesizing and substance P-containing neurons in the human dorsal raphe nucleus. Neuroscience, 42(3), 757–775.

Balázsfi, D., Fodor, A., Török, B., Ferenczi, S., Kovács, K. J., Haller, J., & Zelena, D. (2018). Enhanced innate fear and altered stress axis regulation in VGluT3 knockout mice. Stress, 21(2), 151–161.

Bannerman, D. M., Deacon, R. M. J., Offen, S., Friswell, J., Grubb, M., & Rawlins, J. N. P. (2002). Double dissociation of function within the hippocampus: spatial memory and hyponeophagia. Behavioral Neuroscience, 116(5), 884.

Bari, A., Dalley, J. W., & Robbins, T. W. (2008). The application of the 5-choice serial reaction time task for the assessment of visual attentional processes and impulse control in rats. Nature Protocols, 3(5), 759–767.

Barkus, C., Dawson, L. A., Sharp, T., & Bannerman, D. M. (2012). GluN1 hypomorph mice exhibit wide-ranging behavioral alterations. Genes, Brain, and Behavior, 11(3), 342–351.

Barnes, N. M., & Sharp, T. (1999). A review of central 5-HT receptors and their function. Neuropharmacology, 38(8), 1083–1152.

Beekman, M., Flachskamm, C., & Linthorst, A. C. E. (2005). Effects of exposure to a predator on behaviour and serotonergic neurotransmission in different brain regions of C57bl/6N mice. European Journal of Neuroscience, 21(10), 2825–2836.

Beier, K. T., Steinberg, E. E., DeLoach, K. E., Xie, S., Miyamichi, K., Schwarz, L., Gao, X. J., Kremer, E. J., Malenka, R. C., & Luo, L. (2015). Circuit architecture of VTA dopamine neurons revealed by systematic input-output mapping. Cell, 162(3), 622–634.

Belin, M. F., Nanopoulos, D., Didier, M., Aguera, M., Steinbusch, H., Verhofstad, A., Maitre, M., & Pujol, J. F. (1983). Immunohistochemical evidence for the presence of γ-aminobutyric acid and serotonin in one nerve cell. A study on the raphe nuclei of the rat using antibodies to glutamate decarboxylase and serotonin. Brain Research, 275(2), 329–339.

Bengel, D., Jöhren, O., Andrews, A. M., Heils, A., Mößner, R., Sanvitto, G. L., Saavedra, J. M., Lesch, K.-P., & Murphy, D. L. (1997). Cellular localization and expression of the serotonin transporter in mouse brain. Brain Research, 778(2), 338–345.

Berridge, K. C., & Robinson, T. E. (1998). What is the role of dopamine in reward: hedonic impact, reward learning, or incentive salience? Brain Research Reviews, 28(3), 309–369.

Beyer, C. E., & Cremers, T. I. F. H. (2008). Do selective serotonin reuptake inhibitors acutely increase frontal cortex levels of serotonin? European Journal of Pharmacology, 580(3), 350–354.

Björklund, A., & Dunnett, S. B. (2007). Dopamine neuron systems in the brain: an update. Trends in Neurosciences, 30(5), 194–202.

Blakely, R. D., De Felice, L. J., & Hartzell, H. C. (1994). Molecular physiology of norepinephrine and serotonin transporters. Journal of Experimental Biology, 196(1), 263–281.

Blakely, R. D., Ramamoorthy, S., Schroeter, S., Qian, Y., Apparsundaram, S., Galli, A., & DeFelice, L. J. (1998). Regulated phosphorylation and trafficking of antidepressant-sensitive serotonin transporter proteins. Biological Psychiatry, 44(3), 169–178.

Blanco-Pozo, M., Akam, T., & Walton, M. E. (2024). Dopamine-independent effect of rewards on choices through hidden-state inference. Nature Neuroscience, 27(2), 286–297.

Blier, P., & de Montigny, C. (1994). Current advances and trends in the treatment of depression. Trends in Pharmacological Sciences, 15(7), 220–226.

Blitz, D. M., & Nusbaum, M. P. (1999). Distinct functions for cotransmitters mediating motor pattern selection. Journal of Neuroscience, 19(16), 6774–6783.

Bogdanova, O. V, Kanekar, S., D'Anci, K. E., & Renshaw, P. F. (2013). Factors influencing behavior in the forced swim test. Physiology & Behavior, 118, 227–239.

Bonapersona, V., Schuler, H., Damsteegt, R., Adolfs, Y., Pasterkamp, R. J., van den Heuvel, M. P., Joëls, M., & Sarabdjitsingh, R. A. (2022). The mouse brain after foot shock in four dimensions: temporal dynamics at a single-cell resolution. Proceedings of the National Academy of Sciences, 119(8), e2114002119.

Borisovska, M., Bensen, A. L., Chong, G., & Westbrook, G. L. (2013). Distinct modes of dopamine and GABA release in a dual transmitter neuron. Journal of Neuroscience, 33(5), 1790–1796.

Bortolato, M., Chen, K., & Shih, J. C. (2010). Chapter 2.4 - The Degradation of Serotonin: Role of MAO. In C. P. Müller & B. L. Jacobs (Eds.), Handbook of Behavioral Neuroscience (Vol. 21, pp. 203–218). Elsevier.

Boulland, J. L., Qureshi, T., Seal, R. P., Rafiki, A., Gundersen, V., Bergersen, L. H., Fremeau, R. T., Edwards, R. H., Storm-Mathisen, J., & Chaudhry, F. A. (2004). Expression of the vesicular glutamate transporters during development indicates the widespread corelease of multiple neurotransmitters. Journal of Comparative Neurology, 480(3), 264–280.

Boureau, Y.-L., & Dayan, P. (2011). Opponency revisited: competition and cooperation between dopamine and serotonin. Neuropsychopharmacology, 36(1), 74–97.

Bourin, M., & Hascoët, M. (2003). The mouse light/dark box test. European Journal of Pharmacology, 463(1–3), 55–65.

Brezina, V. (2010). Beyond the wiring diagram: signalling through complex neuromodulator networks. Philosophical Transactions of the Royal Society B: Biological Sciences, 365(1551), 2363–2374.

Brischoux, F., Chakraborty, S., Brierley, D. I., & Ungless, M. A. (2009). Phasic excitation of dopamine neurons in ventral VTA by noxious stimuli. Proceedings of the National Academy of Sciences, 106(12), 4894–4899.

Bromberg-Martin, E. S., Matsumoto, M., & Hikosaka, O. (2010). Dopamine in Motivational Control: Rewarding, Aversive, and Alerting. Neuron, 68(5), 815–834.

Brown, P., & Molliver, M. E. (2000). Dual serotonin (5-HT) projections to the nucleus accumbens core and shell: relation of the 5-HT transporter to amphetamine-induced neurotoxicity. Journal of Neuroscience, 20(5), 1952–1963.

Burnstock, G. (1980). Do some nerve cells release more than one transmitter? Commentaries in the Neurosciences, 151–160.

Cabib, S., & Puglisi-Allegra, S. (2012). The mesoaccumbens dopamine in coping with stress. In Neuroscience and Biobehavioral Reviews (Vol. 36, Issue 1, pp. 79–89).

Carlisle, H. J. (1970). Intermittent heat as a reinforcer for rats in the cold. Physiology & Behavior, 5(8), 861–866.

Carratalá-Ros, C., López-Cruz, L., Martínez-Verdú, A., Olivares-García, R., Salamone, J. D., & Correa, M. (2021). Impact of Fluoxetine on Behavioral Invigoration of Appetitive and Aversively Motivated Responses: Interaction With Dopamine Depletion. Frontiers in Behavioral Neuroscience, 15.

Chang, B., Daniele, C. A., Gallagher, K., Madonia, M., Mitchum, R. D., Barrett, L., Vezina, P., & McGehee, D. S. (2011). Nicotinic excitation of serotonergic projections from dorsal raphe to the nucleus accumbens. Journal of Neurophysiology, 106(2), 801–808.

Chaouloff, F., Berton, O., & Mormède, P. (1999). Serotonin and Stress. Neuropsychopharmacology, 21(1), 28–32.

Chaudhury, D., Walsh, J. J., Friedman, A. K., Juarez, B., Ku, S. M., Koo, J. W., Ferguson, D., Tsai, H.-C., Pomeranz, L., & Christoffel, D. J. (2013). Rapid regulation of depression-related behaviours by control of midbrain dopamine neurons. Nature, 493(7433), 532–536.

Chen, T.-W., Wardill, T. J., Sun, Y., Pulver, S. R., Renninger, S. L., Baohan, A., Schreiter, E. R., Kerr, R. A., Orger, M. B., & Jayaraman, V. (2013). Ultrasensitive fluorescent proteins for imaging neuronal activity. Nature, 499(7458), 295–300.

Chohan, M. O., Esses, S., Haft, J., Ahmari, S. E., & Veenstra-VanderWeele, J. (2020). Altered baseline and amphetamine-mediated behavioral profiles in dopamine transporter Cre (DAT-Ires-Cre) mice compared to tyrosine hydroxylase Cre (TH-Cre) mice. Psychopharmacology, 237(12), 3553–3568.

Clark, J. J., Collins, A. L., Sanford, C. A., & Phillips, P. E. M. (2013). Dopamine encoding of pavlovian incentive stimuli diminishes with extended training. Journal of Neuroscience, 33(8), 3526–3532.

Cohen, J. Y., Amoroso, M. W., & Uchida, N. (2015). Serotonergic neurons signal reward and punishment on multiple timescales. ELife, 4, e06346.

Cohen, J. Y., Haesler, S., Vong, L., Lowell, B. B., & Uchida, N. (2012). Neuron-type-specific signals for reward and punishment in the ventral tegmental area. Nature, 482(7383), 85–88.

Colaizzi, J. M., Flagel, S. B., Joyner, M. A., Gearhardt, A. N., Stewart, J. L., & Paulus, M. P. (2020). Mapping sign-tracking and goal-tracking onto human behaviors. Neuroscience & Biobehavioral Reviews, 111, 84–94.

Commons, K. G., Cholanians, A. B., Babb, J. A., & Ehlinger, D. G. (2017). The Rodent Forced Swim Test Measures Stress-Coping Strategy, Not Depression-like Behavior. ACS Chemical Neuroscience, 8(5), 955–960.

Cools, R., Nakamura, K., & Daw, N. D. (2011). Serotonin and dopamine: unifying affective, activational, and decision functions. Neuropsychopharmacology, 36(1), 98–113.

Cools, R., Roberts, A. C., & Robbins, T. W. (2008). Serotoninergic regulation of emotional and behavioural control processes. Trends in Cognitive Sciences, 12(1), 31–40.

Costa, A. P. R., Vieira, C., Bohner, L. O. L., Silva, C. F., Santos, E. C. da S., De Lima, T. C. M., & Lino-de-Oliveira, C. (2013). A proposal for refining the forced swim test in Swiss mice. Progress in Neuro-Psychopharmacology and Biological Psychiatry, 45, 150–155.

Costa, K. M., Schenkel, D., & Roeper, J. (2021). Sex-dependent alterations in behavior, drug responses and dopamine transporter expression in heterozygous DAT-Cre mice. Scientific Reports, 11(1),3334

Couch, Y., Xie, Q., Lundberg, L., Sharp, T., & Anthony, D. C. (2015). A model of post-infection fatigue is associated with increased TNF and 5-HT2A receptor expression in mice. PLoS ONE, 10(7),e0130643

Cowen, P. J., & Browning, M. (2015). What has serotonin to do with depression? World Psychiatry, 14(2), 158–160.

Crawley, J., & Goodwin, F. K. (1980). Preliminary report of a simple animal behavior model for the anxiolytic effects of benzodiazepines. Pharmacology Biochemistry and Behavior, 13(2), 167–170.

Cuello, A. C. (1982). Co-transmission: proceedings of a symposium held at Oxford during the 50th anniversary meeting of the British Pharmacological Society. Springer.

Cunha, C., Smiley, J. F., Chuhma, N., Shah, R., Bleiwas, C., Menezes, E. C., Seal, R. P., Edwards, R. H., Rayport, S., Ansorge, M. S., Castellanos, F. X., & Teixeira, C. M. (2020). Perinatal interference with the serotonergic system affects VTA function in the adult via glutamate co-transmission. Molecular Psychiatry, 26(9), 4795–4812

Dahlström, A., & Fuxe, K. (1964). Localization of monoamines in the lower brain stem. Experientia, 20(7), 398–399.

Darvas, M., Wunsch, A. M., Gibbs, J. T., & Palmiter, R. D. (2014). Dopamine dependency for acquisition and performance of Pavlovian conditioned response. Proceedings of the National Academy of Sciences, 111(7), 2764–2769.

David, D. J. P., Renard, C. E., Jolliet, P., Hascoët, M., & Bourin, M. (2003). Antidepressant-like effects in various mice strains in the forced swimming test. Psychopharmacology, 166(4), 373–382.

Daw, N. D., Kakade, S., & Dayan, P. (2002). Opponent interactions between serotonin and dopamine. Neural Networks, 15(4–6), 603–616.

Day, J. J., & Carelli, R. M. (2007). The Nucleus Accumbens and Pavlovian Reward Learning. The Neuroscientist, 13(2), 148–159.

De Almeida, C., Chabbah, N., Eyraud, C., Fasano, C., Bernard, V., Pietrancosta, N., Fabre, V., El Mestikawy, S., & Daumas, S. (2023). Absence of VGLUT3 Expression Leads to Impaired Fear Memory in Mice. ENeuro, 10(2), ENEURO.0304-22.2023

De Brouwer, G., Fick, A., Harvey, B. H., & Wolmarans, D. W. (2019). A critical inquiry into marble-burying as a preclinical screening paradigm of relevance for anxiety and obsessive–compulsive disorder: Mapping the way forward. Cognitive, Affective, & Behavioral Neuroscience, 19, 1–39.

De Kloet, E. R., & Molendijk, M. L. (2016). Coping with the Forced Swim Stressor: Towards Understanding an Adaptive Mechanism. Neural Plasticity, 2016(1), 6503162

Deacon, R. M. J. (2006). Assessing nest building in mice. Nature Protocols, 1(3), 1117–1119.

Deacon, R. M. J. (2009). Digging in mice: Marble burying, burrowing, and direct observation reveal changes in mouse behavior. Neuromethods, 42, 37–45.

Deakin, J. F. W., & Graeff, F. G. (1991). 5-HT and mechanisms of defence. Journal of Psychopharmacology, 5(4), 305–315.

Deguchi, T., & Barchas, J. (1972). Regional distribution and developmental change of tryptophan hydroxylase activity in rat brain1. Journal of Neurochemistry, 19(3), 927–929.

Devoto, P., Flore, G., Pani, L., & Gessa, G. L. (2001). Evidence for co-release of noradrenaline and dopamine from noradrenergic neurons in the cerebral cortex. Molecular Psychiatry, 6(6), 657–664.

Devoto, P., Flore, G., Saba, P., Fà, M., & Gessa, G. L. (2005). Co-release of noradrenaline and dopamine in the cerebral cortex elicited by single train and repeated train stimulation of the locus coeruleus. BMC Neuroscience, 6, 1–11.

Di Giovanni, G., Di Matteo, V., Pierucci, M., & Esposito, E. (2008). Serotonin–dopamine interaction: electrophysiological evidence. In G. Di Giovann, V. Di Matteo, & E. Esposito (Eds.), Progress in Brain Research, 172, 45–71

Di Matteo, V., De Blasi, A., Di Giulio, C., & Esposito, E. (2001). Role of 5-HT2C receptors in the control of central dopamine function. Trends in Pharmacological Sciences, 22(5), 229–232.

Di Matteo, V., Di Giovanni, G., Pierucci, M., & Esposito, E. (2008). Serotonin control of central dopaminergic function: focus on in vivo microdialysis studies. Progress in Brain Research, 172, 7–44.

Diaz, V., & Lin, D. (2020). Neural circuits for coping with social defeat. Current Opinion in Neurobiology, 60, 99–107.

Diederen, K. M. J., & Fletcher, P. C. (2020). Dopamine, Prediction Error and Beyond. The Neuroscientist, 27(1), 30–46.

Doherty, M. D., & Pickel, V. M. (2000). Ultrastructural localization of the serotonin 2A receptor in dopaminergic neurons in the ventral tegmental area. Brain Research, 864(2), 176–185.

Dölen, G., Darvishzadeh, A., Huang, K. W., & Malenka, R. C. (2013). Social reward requires coordinated activity of nucleus accumbens oxytocin and serotonin. Nature, 501(7466), 179–184.

Domjan, M. (2018). The essentials of conditioning and learning. American Psychological Association.

Douma, E. H., & de Kloet, E. R. (2020). Stress-induced plasticity and functioning of ventral tegmental dopamine neurons. Neuroscience & Biobehavioral Reviews, 108, 48–77.

Dragunow, M., & Faull, R. (1989). The use of c-fos as a metabolic marker in neuronal pathway tracing. Journal of Neuroscience Methods, 29(3), 261–265.

Dreyer, J. K., Herrik, K. F., Berg, R. W., & Hounsgaard, J. D. (2010). Influence of phasic and tonic dopamine release on receptor activation. Journal of Neuroscience, 30(42), 14273–14283.

Dulawa, S. C., & Hen, R. (2005). Recent advances in animal models of chronic antidepressant effects: The novelty-induced hypophagia test. Neuroscience & Biobehavioral Reviews, 29(4), 771–783.

Dulcis, D., Jamshidi, P., Leutgeb, S., & Spitzer, N. C. (2013). Neurotransmitter Switching in the Adult Brain Regulates Behavior. Science, 340(6131), 449–453.

Eccles, J. C., Fatt, P., & Koketsu, K. (1954). Cholinergic and inhibitory synapses in a pathway from motor-axon collaterals to motoneurones. The Journal of Physiology, 126(3), 524–562.

Eccles, J. C., Jones, R. V., & Paton, W. D. M. (1997). From electrical to chemical transmission in the central nervous system: The closing address of the Sir Henry Dale Centennial Symposium Cambridge, 19 September 1975. Notes and Records of the Royal Society of London, 30(2), 219–230.

El Mansari, M., Sánchez, C., Chouvet, G., Renaud, B., & Haddjeri, N. (2005). Effects of acute and long-term administration of escitalopram and citalopram on serotonin neurotransmission: An in vivo electrophysiological study in rat brain. Neuropsychopharmacology, 30(7), 1269–1277.

El Mestikawy, S., Wallén-Mackenzie, Å., Fortin, G. M., Descarries, L., & Trudeau, L.-E. (2011). From glutamate co-release to vesicular synergy: vesicular glutamate transporters. Nature Reviews Neuroscience, 12(4), 204–216.

Enkel, T., Bartsch, D., & Bähner, F. (2019). Sign- and goal-tracking rats show differences in various executive functions. Behavioural Brain Research, 371, 111979.

Erspamer, V., & Asero, B. (1952). Identification of Enteramine, the Specific Hormone of the Enterochromaffin Cell System, as 5-Hydroxytryptamine. Nature, 169(4306), 800–801.

Ettenberg, A. (2009). The runway model of drug self-administration. Pharmacology Biochemistry and Behavior, 91(3), 271–277.

Eurofins Genomics. (2024). Oligo Analysis Tool. https://eurofinsgenomics.eu/en/ecom/tools/oligo-analysis/

Fasano, C., Rocchetti, J., Pietrajtis, K., Zander, J. F., Manseau, F., Sakae, D. Y., Marcus-Sells, M., Ramet, L., Morel, L. J., Carrel, D., Dumas, S., Bolte, S., Bernard, V., Vigneault, E., Goutagny, R., Ahnert-Hilger, G., Giros, B., Daumas, S., Williams, S., & El Mestikawy, S. (2017). Regulation of the hippocampal network by VGLUT3-Positive CCK-GABAergic basket cells. Frontiers in Cellular Neuroscience, 11.

Favier, M., Pietrancosta, N., El Mestikawy, S., & Gangarossa, G. (2021). Leveraging VGLUT3 Functions to Untangle Brain Dysfunctions. Trends in Pharmacological Sciences, 42(6), 475–490.

Fazekas, C. L., Balázsfi, D., Horváth, H. R., Balogh, Z., Aliczki, M., Puhova, A., Balagova, L., Chmelova, M., Jezova, D., Haller, J., & Zelena, D. (2019). Consequences of VGluT3 deficiency on learning and memory in mice. Physiology and Behavior, 212.

Fischer, A. G., Jocham, G., & Ullsperger, M. (2015). Dual serotonergic signals: A key to understanding paradoxical effects? Trends in Cognitive Sciences, 19(1), 21–26.

Fitzpatrick, P. F. (1999). Tetrahydropterin-Dependent Amino Acid Hydroxylases. Annual Review of Biochemistry, 68(Volume 68, 1999), 355–381.

Flagel, S. B., Clark, J. J., Robinson, T. E., Mayo, L., Czuj, A., Willuhn, I., Akers, C. A., Clinton, S. M., Phillips, P. E. M., & Akil, H. (2011). A selective role for dopamine in stimulus-reward learning. Nature, 469(7328), 53–59.

Fonseca, M. S., Murakami, M., & Mainen, Z. F. (2015). Activation of dorsal raphe serotonergic neurons promotes waiting but is not reinforcing. Current Biology, 25(3), 306–315.

Fremeau, R. T., Burman, J., Qureshi, T., Tran, C. H., Proctor, J., Johnson, J., Zhang, H., Sulzer, D., Copenhagen, D. R., Storm-Mathisen, J., Reimer, R. J., Chaudhry, F. A., & Edwards, R. H. (2002). The identification of vesicular glutamate transporter 3 suggests novel modes of signaling by glutamate. Proceedings of the National Academy of Sciences, 99(22), 14488–14493.

Fujita, M., Shimada, S., Maeno, H., Nishimura, T., & Tohyama, M. (1993). Cellular localization of serotonin transporter mRNA in the rat brain. Neuroscience Letters, 162(1), 59–62.

Gardner, K. L., Thrivikraman, K. V., Lightman, S. L., Plotsky, P. M., & Lowry, C. A. (2005). Early life experience alters behavior during social defeat: Focus on serotonergic systems. Neuroscience, 136(1), 181–191.

Gartside, S. E., Umbers, V., Hajós, M., & Sharp, T. (1995). Interaction between a selective 5-HT1A receptor antagonist and an SSRI in vivo: effects on 5-HT cell firing and extracellular 5-HT. British Journal of Pharmacology, 115(6), 1064–1070.

Gaspar, P., & Lillesaar, C. (2012). Probing the diversity of serotonin neurons. Philosophical Transactions of the Royal Society B: Biological Sciences, 367(1601), 2382–2394.

Geddes, J. R., Freemantle, N., Mason, J., Eccles, M., Boynton, J., & Group, C. C. M. D. (1996). Selective serotonin reuptake inhibitors (SSRIs) versus other antidepressants for depression. Cochrane Database of Systematic Reviews, 2006(2).

Gianni, G., & Pasqualetti, M. (2023). Wiring and Volume Transmission: An Overview of the Dual Modality for Serotonin Neurotransmission. ACS Chemical Neuroscience, 14(23), 4093–4104.

Gillis, Z. S., & Morrison, S. E. (2019). Sign Tracking and Goal Tracking Are Characterized by Distinct Patterns of Nucleus Accumbens Activity. Eneuro, 6(2), ENEURO.0414-18.2019.

Glimcher, P. W. (2011). Understanding dopamine and reinforcement learning: The dopamine reward prediction error hypothesis. Proceedings of the National Academy of Sciences, 108, 15647–15654.

Golden, S. A., Covington, H. E., Berton, O., & Russo, S. J. (2011). A standardized protocol for repeated social defeat stress in mice. Nature Protocols, 6(8), 1183–1191.

Gorlova, A., Ortega, G., Waider, J., Bazhenova, N., Veniaminova, E., Proshin, A., Kalueff, A. V., Anthony, D. C., Lesch, K. P., & Strekalova, T. (2020). Stress-induced aggression in heterozygous TPH2 mutant mice is associated with alterations in serotonin turnover and expression of 5-HT6 and AMPA subunit 2A receptors. Journal of Affective Disorders, 272, 440–451.

Gouveia, K., & Hurst, J. L. (2019). Improving the practicality of using non-aversive handling methods to reduce background stress and anxiety in laboratory mice. Scientific Reports, 9(1), 20305.

Graeff, G., Guimarães, F. S., De Andrades, T. G., Deakins, J. F. (1996). Role of 5-HT in Stress, Anxiety, and Depression. Pharmacology Biochemistry and Behavior, 54(I), 129–141.

Grahn, R. E., Will, M. J., Hammack, S. E., Maswood, S., Mcqueen, M. B., Watkins, L. R., & Maier, S. F. (1999). Activation of serotonin-immunoreactive cells in the dorsal raphe nucleus in rats exposed to an uncontrollable stressor. Brain Research, 826, 35–43.

Granger, A. J., Mulder, N., Saunders, A., & Sabatini, B. L. (2016). Cotransmission of acetylcholine and GABA. Neuropharmacology, 100, 40–46.

Gras, C., Amilhon, B., Lepicard, È. M., Poirel, O., Vinatier, J., Herbin, M., Dumas, S., Tzavara, E. T., Wade, M. R., Nomikos, G. G., Hanoun, N., Saurini, F., Kemel, M.-L., Gasnier, B., Giros, B., & Mestikawy, S. El. (2008). The vesicular glutamate transporter VGLUT3 synergizes striatal acetylcholine tone. Nature Neuroscience, 11(3), 292–300.

Gras, C., Herzog, E., Bellenchi, G. C., Ronique Bernard, V., Ravassard, P., Pohl, M., Gasnier, B., Giros, B., & Mestikawy, S. El. (2002). A Third Vesicular Glutamate Transporter Expressed by Cholinergic and Serotoninergic Neurons.

Gras, C., Vinatier, J., Amilhon, B., Guerci, A., Christov, C., Ravassard, P., Giros, B., & El Mestikawy, S. (2005). Developmentally regulated expression of VGLUT3 during early post-natal life. Neuropharmacology, 49(6), 901–911.

Guilloux, J. P., David, D. J. P., Xia, L., Nguyen, H. T., Rainer, Q., Guiard, B. P., Repérant, C., Deltheil, T., Toth, M., Hen, R., & Gardier, A. M. (2011). Characterization of 5-HT1A/1B-/- mice: An animal model sensitive to anxiolytic treatments. Neuropharmacology, 61(3), 478–488.

Gullino, L. S., Fuller, C., Dunn, P., Collins, H. M., El Mestikawy, S., & Sharp, T. (2024). Evidence for a role of 5-HT-glutamate co-releasing neurons in acute stress mechanisms. ACS Chemical Neuroscience, 15(6), 1185–1196.

Gunaydin, L. A., Grosenick, L., Finkelstein, J. C., Kauvar, I. V, Fenno, L. E., Adhikari, A., Lammel, S., Mirzabekov, J. J., Airan, R. D., & Zalocusky, K. A. (2014). Natural neural projection dynamics underlying social behavior. Cell, 157(7), 1535–1551.

Haas, H. L., Sergeeva, O. A., & Selbach, O. (2008). Histamine in the nervous system. Physiological Reviews.

Hajós, M., & Sharp, T. (1996). Burst-firing activity of presumed 5-HT neurones of the rat dorsal raphe nucleus: electrophysiological analysis by antidromic stimulation. Brain Research, 740(1), 162–168.

Hale, M. W., Hay-Schmidt, A., Mikkelsen, J. D., Poulsen, B., Bouwknecht, J. A., Evans, A. K., Stamper, C. E., Shekhar, A., & Lowry, C. A. (2008). Exposure to an open-field arena increases c-Fos expression in a subpopulation of neurons in the dorsal raphe nucleus, including neurons projecting to the basolateral amygdaloid complex. Neuroscience, 157(4), 733–748.

Hale, M. W., Shekhar, A., & Lowry, C. A. (2012). Stress-related serotonergic systems: Implications for symptomatology of anxiety and affective disorders. Cellular and Molecular Neurobiology, 32(5), 695–708.

Harmer, C. J., Duman, R. S., & Cowen, P. J. (2017). How do antidepressants work? New perspectives for refining future treatment approaches. The Lancet Psychiatry, 4(5), 409–418.

Harris-Warrick, R. M., & Johnson, B. R. (2010). Checks and balances in neuromodulation. Frontiers in Behavioral Neuroscience, 4, 47.

He, J., Hommen, F., Lauer, N., Balmert, S., & Scholz, H. (2020). Serotonin transporter dependent modulation of food-seeking behavior. PLOS ONE, 15(1), e0227554-.

Hedlund, P. B., Kelly, L., Mazur, C., Lovenberg, T., Sutcliffe, J. G., & Bonaventure, P. (2004). 8-OH-DPAT acts on both 5-HT1A and 5-HT7 receptors to induce hypothermia in rodents. European Journal of Pharmacology, 487(1), 125–132.

Hendricks, T. J., Fyodorov, D. V, Wegman, L. J., Lelutiu, N. B., Pehek, E. A., Yamamoto, B., Silver, J., Weeber, E. J., David Sweatt, J., & Deneris, E. S. (2003). Pet-1 ETS Gene Plays a Critical Role in 5-HT Neuron Development and Is Required for Normal Anxiety-like and Aggressive Behavior. School of Medicine Lucki, 37, 233–247.

Herdegen, T., & Leah, J. D. (1998). Inducible and constitutive transcription factors in the mammalian nervous system: control of gene expression by Jun, Fos and Krox, and CREB/ATF proteins. Brain Research Reviews, 28(3), 370–490.

Hillarp, N.-Å., Fuxe, K., & Dahlström, A. (1966). C. Demonstration and mapping of central neurons containing dopamine, noradrenaline, and 5-hydroxytryptamine and their reactions to psychopharmaca. Pharmacological Reviews, 18(1), 727.

Himanshu, Dharmila, Sarkar, D., & Nutan. (2020). A review of behavioral tests to evaluate different types of anxiety and anti-anxiety effects. Clinical Psychopharmacology and Neuroscience, 18(3), 341–351.

Hioki, H., Nakamura, H., Ma, Y. F., Konno, M., Hayakawa, T., Nakamura, K. C., Fujiyama, F., & Kaneko, T. (2010). Vesicular glutamate transporter 3-expressing nonserotonergic projection neurons constitute a subregion in the rat midbrain raphe nuclei. Journal of Comparative Neurology, 518(5), 668–686.

Hnasko, T. S., Chuhma, N., Zhang, H., Goh, G. Y., Sulzer, D., Palmiter, R. D., Rayport, S., & Edwards, R. H. (2010). Vesicular glutamate transport promotes dopamine storage and glutamate corelease in vivo. Neuron, 65(5), 643–656.

Hökfelt, T., Arvidsson, U., Cullheim, S., Millhorn, D., Nicholas, A. P., Pieribone, V., Seroogy, K., & Ulfhake, B. (2000). Multiple messengers in descending serotonin neurons: localization and functional implications. Journal of Chemical Neuroanatomy, 18(1–2), 75–86.

Hökfelt, T., Bartfai, T., & Bloom, F. (2003). Neuropeptides: opportunities for drug discovery. The Lancet Neurology, 2(8), 463–472.

Hollis, F., & Kabbaj, M. (2014). Social defeat as an animal model for depression. ILAR Journal, 55(2), 221–232.

Holly, E. N., & Miczek, K. A. (2016). Ventral tegmental area dopamine revisited: Effects of acute and repeated stress. Psychopharmacology, 233(2), 163–186.

Hornung, J.-P. (2010). The Neuronatomy of the Serotonergic System. In C. P. Müller & B. L. Jacobs (Eds.), Handbook of Behavioral Neuroscience, 21, 51–64.

Horvitz, J. C. (2000). Mesolimbocortical and nigrostriatal dopamine responses to salient non-reward events. Neuroscience, 96(4), 651–656.

Hoyer, D., Hannon, J. P., & Martin, G. R. (2002). Molecular, pharmacological and functional diversity of 5-HT receptors. Pharmacology Biochemistry and Behavior, 71(4), 533–554.

Hu, E., Mueller, E., Oliviero, S., Papaioannou, V. E., Johnson, R., & Spiegelman, B. M. (1994). Targeted disruption of the c-fos gene demonstrates c-fos-dependent and -independent pathways for gene expression stimulated by growth factors or oncogenes. The EMBO Journal, 13(13), 3094-3103–3103.

Huang, K. W., Ochandarena, N. E., Philson, A. C., Hyun, M., Birnbaum, J. E., Cicconet, M., & Sabatini, B. L. (2019). Molecular and anatomical organization of the dorsal raphe nucleus. ELife, 8, e46464.

Hurst, J. L., & West, R. S. (2010). Taming anxiety in laboratory mice. Nature Methods, 7(10), 825–826.

Hwang, D. Y., Hong, S., Jeong, J. W., Choi, S., Kim, H., Kim, J., & Kim, K. S. (2009). Vesicular monoamine transporter 2 and dopamine transporter are molecular targets of Pitx3 in the ventral midbrain dopamine neurons. Journal of Neurochemistry, 111(5), 1202–1212.

Hyttel, J. (1994). Pharmacological characterization of selective serotonin reuptake inhibitors (SSRIs). International Clinical Psychopharmacology, 9, 19–26.

Ikemoto, S. (2010). Brain reward circuitry beyond the mesolimbic dopamine system: a neurobiological theory. Neuroscience & Biobehavioral Reviews, 35(2), 129–150.

Jacobs, B. L., & Azmitia, E. C. (1981). Distribution of serotonin-immunoreactivity in the central nervous system of the rat—Cell bodies and terminals. Neuroscience, 6(4), 557–618.

Jacobs, B. L., & Fornal, C. A. (1991). Activity of brain serotonergic neurons in the behaving animal. Pharmacological Reviews, 43(4), 563.

Jin, Z. L., Chen, X. F., Ran, Y. H., Li, X. R., Xiong, J., Zheng, Y. Y., Gao, N. N., & Li, Y. F. (2017). Mouse strain differences in SSRI sensitivity correlate with serotonin transporter binding and function. Scientific Reports, 7(1).

Jirkof, P. (2014). Burrowing and nest building behavior as indicators of well-being in mice. Journal of Neuroscience Methods, 234, 139–146.

Johansson, O., Hökfelt, T., Jeffcoate, S. L., White, N., & Sternberger, L. A. (1980). Ultrastructural localization of TRH-like immunoreactivity. Experimental Brain Research, 38, 1–10.

Johnson, M. D. (1994). Synaptic glutamate release by postnatal rat serotonergic neurons in microculture. Neuron, 12(2), 433–442.

Jonas, P., Bischofberger, J., & Sandkühler, J. (1998). Corelease of two fast neurotransmitters at a central synapse. Science, 281(5375), 419–424.

Kapanaiah, S. K. T., van der Veen, B., Strahnen, D., Akam, T., & Kätzel, D. (2021). A low-cost open-source 5-choice operant box system optimized for electrophysiology and optophysiology in mice. Scientific Reports, 11(1).

Kapoor, V., Provost, A. C., Agarwal, P., & Murthy, V. N. (2016). Activation of raphe nuclei triggers rapid and distinct effects on parallel olfactory bulb output channels. Nature Neuroscience, 19(2), 271–282.

Karasawa, J. I., Yoshimizu, T., & Chaki, S. (2006). A metabotropic glutamate 2/3 receptor antagonist, MGS0039, increases extracellular dopamine levels in the nucleus accumbens shell. Neuroscience letters, 393(2-3), 127-130.

Kelly, K. J., Donner, N. C., Hale, M. W., & Lowry, C. A. (2011). Swim stress activates serotonergic and nonserotonergic neurons in specific subdivisions of the rat dorsal raphe nucleus in a temperature-dependent manner. Neuroscience, 197, 251–268.

Kim, H., Kim, M., Im, S. K., & Fang, S. (2018). Mouse Cre-LoxP system: general principles to determine tissue-specific roles of target genes. Laboratory Animal Research, 34(4), 147–159.

Klapdop, K., & Van Der Staay. (1996). The Morris Water-Escape Task in Mice: Strain Differences and Effects of Intra-Maze Contrast and Brightness. Physiology & Behavior, 60(5), 1247–1254.

Komada, M., Takao, K., & Miyakawa, T. (2008). Elevated plus maze for mice. JoVE (Journal of Visualized Experiments), 22, e1088.

Koubi, D., Bezin, L., Cottet-Emard, J.-M., Gharib, A., Bobillier, P., & Sarda, N. (2001). Regulation of expression and enzymatic activities of tyrosine and tryptophan hydroxylases in rat brain after acute electroconvulsive shock. Brain Research, 905(1), 161–170.

Kovács, K. J. (1998). Invited review c-Fos as a transcription factor: a stressful (re)view from a functional map. Neurochemistry International, 33(4), 287–297.

Kramer, P. F., Christensen, C. H., Hazelwood, L. A., Dobi, A., Bock, R., Sibley, D. R., Mateo, Y., & Alvarez, V. A. (2011). Dopamine D2 Receptor Overexpression Alters Behavior and Physiology in Drd2-EGFP mice. The Journal of Neuroscience, 31(1), 126.

Krank, M. D. (2003). Pavlovian conditioning with ethanol: sign-tracking (autoshaping), conditioned incentive, and ethanol self-administration. Alcoholism: Clinical and Experimental Research, 27(10), 1592–1598.

Kuhn, B. N., Campus, P., Flagel, S. B., Tomie, A., & Morrow, J. (2018). The neurobiological mechanisms underlying sign-tracking behavior. Sign-Tracking and Drug Addiction.

Kupfermann, I. (1991). Functional studies of cotransmission. Physiological Reviews, 71(3), 683–732.

Labouesse, M. A., Cola, R. B., & Patriarchi, T. (2020). GPCR-based dopamine sensors—a detailed guide to inform sensor choice for in vivo imaging. International Journal of Molecular Sciences, 21(21), 8048.

Lai, J. Ic., Porcu, A., Romoli, B., Keisler, M., Manfredsson, F. P., Powell, S. B., & Dulcis, D. (2023). Nicotine-mediated recruitment of GABAergic neurons to a dopaminergic phenotype attenuates motor deficits in an alpha-Synuclein Parkinson's model. International Journal of Molecular Sciences, 24(4), 4204.

Lang, B., Kahnau, P., Hohlbaum, K., Mieske, P., Andresen, N. P., Boon, M. N., Thöne-Reineke, C., Lewejohann, L., & Diederich, K. (2023). Challenges and advanced concepts for the assessment of learning and memory function in mice. In Frontiers in Behavioral Neuroscience, 17

Lee, S., Kim, K., & Zhou, Z. J. (2010). Role of ACh-GABA cotransmission in detecting image motion and motion direction. Neuron, 68(6), 1159–1172.

Leger, M., Quiedeville, A., Bouet, V., Haelewyn, B., Boulouard, M., Schumann-Bard, P., & Freret, T. (2013). Object recognition test in mice. Nature Protocols, 8(12), 2531–2537.

Lesch, K.-P. (1998). Review : Serotonin Transporter and Psychiatric Disorders: Listening to the Gene. The Neuroscientist, 4(1), 25–34.

Li, H., Jiang, W., Ling, L., Pratelli, M., Chen, C., Gupta, V., Godavarthi, S. K., & Spitzer, N. C. (2024). Generalized fear after acute stress is caused by change in neuronal cotransmitter identity. Science, 383(6688), 1252–1259.

Li, H.-Q., Pratelli, M., Godavarthi, S., Zambetti, S., & Spitzer, N. C. (2020). Decoding Neurotransmitter Switching: The Road Forward. The Journal of Neuroscience, 40(21), 4078–4089.

Li, Y. Q., Rao, Z. R., & Shi, J. W. (1989). Serotoninergic projections from the midbrain periaqueductal gray to the nucleus accumbens in the rat. Neuroscience Letters, 98(3), 276–279.

Li, Y., Zhong, W., Wang, D., Feng, Q., Liu, Z., Zhou, J., Jia, C., Hu, F., Zeng, J., Guo, Q., Fu, L., & Luo, M. (2016). Serotonin neurons in the dorsal raphe nucleus encode reward signals. Nature Communications, 7(1), 10503.

Liguz-Lecznar, M., & Skangiel-Kramska, J. (2007). Vesicular glutamate transporters (VGLUTs): the three musketeers of glutamatergic system. Acta Neurobiologiae Experimentalis, 67(3), 207.

Lino-de-Oliveira, C., de Oliveira, R. M. W., Pádua Carobrez, A., de Lima, T. C. M., Bel, E. A. Del, & Guimarães, F. S. (2006). Antidepressant treatment reduces Fos-like immunoreactivity induced by swim stress in different columns of the periaqueductal gray matter. Brain Research Bulletin, 70(4–6), 414–421.

Linthorst, A. C. E., & Reul, J. M. H. M. (2010). Chapter 4.1 - The Impact of Stress on Serotonergic Neurotransmission. Handbook of Behavioral Neuroscience, 21, 475–491

Lister, R. G. (1987). The use of a plus-maze to measure anxiety in the mouse. Psychopharmacology, 92(2), 180–185.

Liu, C., Maejima, T., Wyler, S. C., Casadesus, G., Herlitze, S., & Deneris, E. S. (2010). Pet-1 is required across different stages of life to regulate serotonergic function. Nature Neuroscience, 13(10), 1190–1198.

Liu, S., Plachez, C., Shao, Z., Puche, A., & Shipley, M. T. (2013). Olfactory bulb short axon cell release of GABA and dopamine produces a temporally biphasic inhibition–excitation response in external tufted cells. Journal of Neuroscience, 33(7), 2916–2926.

Liu, Z., Lin, R., & Luo, M. (2020). Reward Contributions to Serotonergic Functions. Annual Review of Neuroscience, 43(Volume 43, 2020), 141–162.

Liu, Z., Zhou, J., Li, Y., Hu, F., Lu, Y., Ma, M., Feng, Q., Zhang, J. en, Wang, D., Zeng, J., Bao, J., Kim, J. Y., Chen, Z. F., El Mestikawy, S., & Luo, M. (2014). Dorsal raphe neurons signal reward through 5-HT and glutamate. Neuron, 81(6), 1360–1374.

Ljungberg, T., Apicella, P., & Schultz, W. (1992). Responses of monkey dopamine neurons during learning of behavioral reactions. Journal of Neurophysiology, 67(1), 145–163.

Lkhagvasuren, B., Oka, T., Nakamura, Y., Hayashi, H., Sudo, N., & Nakamura, K. (2014). Distribution of Fos-immunoreactive cells in rat forebrain and midbrain following social defeat stress and diazepam treatment. Neuroscience, 272, 34–57.

Lowry, C. A. (2002). Functional Subsets of Serotonergic Neurones: Implications for Control of the Hypothalamic-Pituitary-Adrenal Axis. Journal of Neuroendocrinology, 14(11), 911–923.

Lucki, I. (1997). The forced swimming test as a model for core and component behavioral effects of antidepressant drugs. Behavioural Pharmacology, 8(6), 523–532.

Lucki, I., Dalvi, A., & Mayorga, A. J. (2001). Sensitivity to the effects of pharmacologically selective antidepressants in different strains of mice. Psychopharmacology, 155(3), 315–322.

Luo, M., Zhou, J., & Liu, Z. (2015). Reward processing by the dorsal raphe nucleus: 5-HT and beyond. Learning and Memory, 22(9), 452–460.

Mackintosh, N. J. (1974). The psychology of animal learning. Academic Press.

Macpherson, T., & Hikida, T. (2018). Nucleus accumbens dopamine D1-receptor-expressing neurons control the acquisition of sign-tracking to conditioned cues in mice. Frontiers in Neuroscience, 12, 418.

Maillet, D., Mandin, V., & Huppé-Gourgues, F. (2022). Speed of task acquisition in sign-tracker and goal-tracker rats using 5-CSRTT. Psychology & Neuroscience, 15(3), 281.

Malagié, I., Trillat, A.-C., Jacquot, C., & Gardier, A. M. (1995). Effects of acute fluoxetine on extracellular serotonin levels in the raphe: an in vivo microdialysis study. European Journal of Pharmacology, 286(2), 213–217.

Mansouri-Guilani, N., Bernard, V., Vigneault, E., Vialou, V., Daumas, S., El Mestikawy, S., & Gangarossa, G. (2019). VGLUT3 gates psychomotor effects induced by amphetamine. Journal of Neurochemistry, 148(6), 779–795.

Marinelli, M. (2007). Dopaminergic reward pathways and effects of stress. Stress and Addiction, 41–83.

Marta, P., Hakimi, A. M., Thaker, A., Li, H., Godavarthi, S. K., & Spitzer, N. C. (2022). Drug-induced change in transmitter identity is a shared mechanism generating cognitive deficits. BioRxiv, 2022–2026.

Martinez, M., Calvo-Torrent, A., & Herbert, J. (2002). Mapping brain response to social stress in rodents with c-fos expression: A review. Stress, 5(1), 3–13.

Matias, S., Lottem, E., Dugué, G. P., & Mainen, Z. F. (2017). Activity patterns of serotonin neurons underlying cognitive flexibility. Elife, 6, e20552.

Matsuda, S., Peng, H., Yoshimura, H., Wen, -Chun, Fukuda, T., & Sakanaka, M. (1996). Persistent c-fos expression in the brains of mice with chronic social stress. Neuroscience Research, 26(2), 157–170.

Matsumoto, M., & Hikosaka, O. (2009). Two types of dopamine neuron distinctly convey positive and negative motivational signals. Nature, 459(7248), 837–841.

Matthews, G. A., Nieh, E. H., Vander Weele, C. M., Halbert, S. A., Pradhan, R. V, Yosafat, A. S., Glober, G. F., Izadmehr, E. M., Thomas, R. E., & Lacy, G. D. (2016). Dorsal raphe dopamine neurons represent the experience of social isolation. Cell, 164(4), 617–631.

McDevitt, R. A., Tiran-Cappello, A., Shen, H., Balderas, I., Britt, J. P., Marino, R. A. M., Chung, S. L., Richie, C. T., Harvey, B. K., & Bonci, A. (2014). Serotonergic versus nonserotonergic dorsal raphe projection neurons: Differential participation in reward circuitry. Cell Reports, 8(6), 1857–1869.

Merighi, A., Salio, C., Ferrini, F., & Lossi, L. (2011). Neuromodulatory function of neuropeptides in the normal CNS. Journal of Chemical Neuroanatomy, 42(4), 276–287.

Miyazaki, K., Miyazaki, K. W., & Doya, K. (2011). Activation of dorsal raphe serotonin neurons underlies waiting for delayed rewards. Journal of Neuroscience, 31(2), 469–479.

Miyazaki, K., Miyazaki, K. W., & Doya, K. (2012). The role of serotonin in the regulation of patience and impulsivity. Molecular Neurobiology, 45(2), 213–224.

Miyazaki, K., Miyazaki, K. W., Sivori, G., Yamanaka, A., Tanaka, K. F., & Doya, K. (2020). Serotonergic projections to the orbitofrontal and medial prefrontal cortices differentially modulate waiting for future rewards. Science Advances, 6(48), eabc7246.

Miyazaki, K. W., Miyazaki, K., Tanaka, K. F., Yamanaka, A., Takahashi, A., Tabuchi, S., & Doya, K. (2014). Optogenetic Activation of Dorsal Raphe Serotonin Neurons Enhances Patience for Future Rewards. Current Biology, 24(17), 2033–2040.

Molendijk, M. L., & de Kloet, E. R. (2019). Coping with the forced swim stressor: Current state-of-the-art. Behavioural Brain Research, 364, 1–10.

Morales, M., & Pickel, V. M. (2012). Insights to drug addiction derived from ultrastructural views of the mesocorticolimbic system. Annals of the New York Academy of Sciences, 1248(1), 71–88.

Morgan, J. I., Cohen, D. R., Hempstead, J. L., & Curran, T. (1987). Mapping Patterns of c-fos Expression in the Central Nervous System After Seizure. Science, 237(4811), 192–197.

Morgan, J. I., & Curran, T. (1986). Role of ion flux in the control of c-fos expression. Nature, 322(6079), 552–555.

Muzerelle, A., Scotto-Lomassese, S., Bernard, J. F., Soiza-Reilly, M., & Gaspar, P. (2016). Conditional anterograde tracing reveals distinct targeting of individual serotonin cell groups (B5–B9) to the forebrain and brainstem. Brain Structure and Function, 221(1), 535–561.

Nakamura, K., & Hasegawa, H. (2009). Production and Peripheral Roles of 5-HTP, a Precursor of Serotonin. International Journal of Tryptophan Research, 2, 37–43

Nakamura, K., Sugawara, Y., Sawabe, K., Ohashi, A., Tsurui, H., Xiu, Y., Ohtsuji, M., Lin, Q. S., Nishimura, H., Hasegawa, H., & Hirose, S. (2006). Late Developmental Stage-Specific Role of Tryptophan Hydroxylase 1 in Brain Serotonin Levels. The Journal of Neuroscience, 26(2), 530.

Nemeroff, C. B., & Owens, M. J. (2002). Treatment of mood disorders. Nature Neuroscience, 5(11), 1068–1070.

Nestler, E. J., Hyman, S. E., Holtzman, D. M., & Malenka, R. C. (2015). Widely projecting systems: Monoamines, acetylcholine, and orexin. Molecular Neuropharmacology: A Foundation for Clinical Neuroscience, 158–194.

Nickell, J. R., Siripurapu, K. B., Vartak, A., Crooks, P. A., & Dwoskin, L. P. (2014). Chapter Two - The Vesicular Monoamine Transporter-2: An Important Pharmacological Target for the Discovery of Novel Therapeutics to Treat Methamphetamine Abuse. In L. P. Dwoskin (Ed.), Advances in Pharmacology (Vol. 69, pp. 71–106). Academic Press.

Nicola, S. M. (2010). The flexible approach hypothesis: unification of effort and cue-responding hypotheses for the role of nucleus accumbens dopamine in the activation of reward-seeking behavior. Journal of Neuroscience, 30(49), 16585–16600.

Nollet, M., Hicks, H., McCarthy, A. P., Wu, H., Möller-Levet, C. S., Laing, E. E., Malki, K., Lawless, N., Wafford, K. A., Dijk, D. J., & Winsky-Sommerer, R. (2019). REM sleep's unique associations with corticosterone regulation, apoptotic pathways, and behavior in chronic stress in mice. Proceedings of the National Academy of Sciences of the United States of America, 116(7), 2733–2742.

Numa, C., Nagai, H., Taniguchi, M., Nagai, M., Shinohara, R., & Furuyashiki, T. (2019). Social defeat stress-specific increase in c-Fos expression in the extended amygdala in mice: Involvement of dopamine D1 receptor in the medial prefrontal cortex. Scientific Reports, 9(1).

Nusbaum, M. P., Blitz, D. M., Swensen, A. M., Wood, D., & Marder, E. (2001). The roles of co-transmission in neural network modulation. Trends in Neurosciences, 24(3), 146–154.

Ogawa, S. K., Cohen, J. Y., Hwang, D., Uchida, N., & Watabe-Uchida, M. (2014). Organization of monosynaptic inputs to the serotonin and dopamine neuromodulatory systems. Cell Reports, 8(4), 1105–1118.

Ogawa, S. K., & Watabe-Uchida, M. (2018). Organization of dopamine and serotonin system: Anatomical and functional mapping of monosynaptic inputs using rabies virus. Pharmacology Biochemistry and Behavior, 174, 9–22.

Ohmura, Y., Tsutsui-Kimura, I., Sasamori, H., Nebuka, M., Nishitani, N., Tanaka, K. F., Yamanaka, A., & Yoshioka, M. (2020). Different roles of distinct serotonergic pathways in anxiety-like behavior, antidepressant-like, and anti-impulsive effects. Neuropharmacology, 167, 107703

Okaty, B. W., Commons, K. G., & Dymecki, S. M. (2019). Embracing diversity in the 5-HT neuronal system. Nature Reviews Neuroscience, 20(7), 397–424.

Okaty, B. W., Freret, M. E., Rood, B. D., Brust, R. D., Hennessy, M. L., deBairos, D., Kim, J. C., Cook, M. N., & Dymecki, S. M. (2015). Multi-scale molecular deconstruction of the serotonin neuron system. Neuron, 88(4), 774–791.

Okaty, B. W., Sturrock, N., Lozoya, Y. E., Chang, Y., Senft, R. A., Lyon, K. A., Alekseyenko, O. V., & Dymecki, S. M. (2020). A single-cell transcriptomic and anatomic atlas of mouse dorsal raphe Pet1 neurons. ELife, 9, 1–44.

Osborne, N. N. (2013). Dale's Principle and Communication Between Neurones: Based on a Colloquium of the Neurochemical Group of the Biochemical Society, Held at Oxford University, July 1982. Elsevier.

Pan, W.-X., & Hyland, B. I. (2005). Pedunculopontine tegmental nucleus controls conditioned responses of midbrain dopamine neurons in behaving rats. Journal of Neuroscience, 25(19), 4725–4732.

Pan, W.-X., Schmidt, R., Wickens, J. R., & Hyland, B. I. (2005). Dopamine cells respond to predicted events during classical conditioning: evidence for eligibility traces in the reward-learning network. Journal of Neuroscience, 25(26), 6235–6242.

Parker, J. G., Zweifel, L. S., Clark, J. J., Evans, S. B., Phillips, P. E. M., & Palmiter, R. D. (2010). Absence of NMDA receptors in dopamine neurons attenuates dopamine release but not conditioned approach during Pavlovian conditioning. Proceedings of the National Academy of Sciences, 107(30), 13491–13496.

Patriarchi, T., Cho, J. R., Merten, K., Howe, M. W., Marley, A., Xiong, W.-H., Folk, R. W., Broussard, G. J., Liang, R., Jang, M. J., Zhong, H., Dombeck, D., von Zastrow, M., Nimmerjahn, A., Gradinaru, V., Williams, J. T., & Tian, L. (2018). Ultrafast neuronal imaging of dopamine dynamics with designed genetically encoded sensors. Science, 360(6396), eaat4422.

Paul, E. D., Johnson, P. L., Shekhar, A., & Lowry, C. A. (2014). The Deakin/Graeff hypothesis: Focus on serotonergic inhibition of panic. In Neuroscience and Biobehavioral Reviews (Vol. 46, Issue P3, pp. 379–396). Elsevier Ltd.

Paulus, E. V, & Mintz, E. M. (2016). Circadian rhythms of clock gene expression in the cerebellum of serotonin-deficient Pet-1 knockout mice. Brain Research, 1630, 10–17.

Paxinos, G., & Franklin, K. B. J. (2001). The mouse brain in stereotaxic coordinates. Academic Press. San Diego, 296.

Pelletier, G., Leclerc, R., & Dupont, A. (1977). Electron microscope immunohistochemical localization of substance P in the central nervous system of the rat. Journal of Histochemistry & Cytochemistry, 25(12), 1373–1375.

Pelletier, G., Steinbusch, H. W. M., & Verhofstad, A. A. J. (1981). Immunoreactive substance P and serotonin present in the same dense-core vesicles. Nature, 293(5827), 71–72.

Pellow, S., Chopin, P., File, S. E., & Briley, M. (1985). Validation of open: closed arm entries in an elevated plus-maze as a measure of anxiety in the rat. Journal of Neuroscience Methods, 14(3), 149–167.

Perona, M. T. G., Waters, S., Hall, F. S., Sora, I., Lesch, K. P., Murphy, D. L., Caron, M., & Uhl, G. R. (2008). Animal models of depression in dopamine, serotonin, and norepinephrine transporter knockout mice: Prominent effects of dopamine transporter deletions. Behavioural Pharmacology, 19(5–6), 566–574.

Petit-Demouliere, B., Chenu, F., & Bourin, M. (2005). Forced swimming test in mice: A review of antidepressant activity. Psychopharmacology, 177(3), 245–255.

Peyron, C., Petit, J.-M., Rampon, C., Jouvet, M., & Luppi, P.-H. (1997). Forebrain afferents to the rat dorsal raphe nucleus demonstrated by retrograde and anterograde tracing methods. Neuroscience, 82(2), 443–468.

Phillips, P. E. M., Stuber, G. D., Heien, M. L. A. V, Wightman, R. M., & Carelli, R. M. (2003). Subsecond dopamine release promotes cocaine seeking. Nature, 422(6932), 614–618.

Pistell, P. J., & Ingram, D. K. (2010). Development of a water-escape motivated version of the Stone T-maze for mice. Neuroscience, 166(1), 61–72.

Pizzagalli, D. A. (2014). Depression, stress, and anhedonia: Toward a synthesis and integrated model. Annual Review of Clinical Psychology, 10, 393–423.

Planchez, B., Surget, A., & Belzung, C. (2019). Animal models of major depression: drawbacks and challenges. Journal of Neural Transmission, 126(11), 1383–1408.

Porsolt, R. D., Le Pichon, M., & Jalfre, M. (1977). Depression: a new animal model sensitive to antidepressant treatments. Nature, 266(5604), 730–732.

Potter, D. D., Furshpan, E. J., & Landis, S. C. (1981). Multiple-transmitter status and "Dale's Principle." Neurosci Comment, 1(1).

Pourhamzeh, M., Moravej, F. G., Arabi, M., Shahriari, E., Mehrabi, S., Ward, R., Ahadi, R., & Joghataei, M. T. (2022). The Roles of Serotonin in Neuropsychiatric Disorders. In Cellular and Molecular Neurobiology (Vol. 42, Issue 6, pp. 1671–1692). Springer.

Prakash, N., Stark, C. J., Keisler, M. N., Luo, L., Der-Avakian, A., & Dulcis, D. (2020). Serotonergic Plasticity in the Dorsal Raphe Nucleus Characterizes Susceptibility and Resilience to Anhedonia. The Journal of Neuroscience : The Official Journal of the Society for Neuroscience, 40(3), 569–584.

Puglisi-Allegra, S., & Andolina, D. (2015). Serotonin and stress coping. Behavioural Brain Research, 277, 58–67.

Qi, J., Zhang, S., Wang, H. L., Wang, H., De Jesus Aceves Buendia, J., Hoffman, A. F., Lupica, C. R., Seal, R. P., & Morales, M. (2014). A glutamatergic reward input from the dorsal raphe to ventral tegmental area dopamine neurons. Nature Communications, 5.

Radford-Smith, D. E., Probert, F., Burnet, P. W. J., & Anthony, D. C. (2022). Modifying the maternal microbiota alters the gut–brain metabolome and prevents emotional dysfunction in the adult offspring of obese dams. Proceedings of the National Academy of Sciences, 119(9), e2108581119.

Ramet, L., Zimmermann, J., Bersot, T., Poirel, O., De Gois, S., Silm, K., Sakae, D. Y., Mansouri-Guilani, N., Bourque, M. J., Trudeau, L. E., Pietrancosta, N., Daumas, S., Bernard, V., Rosenmund, C., & El Mestikawy, S. (2017). Characterization of a human point mutation of VGLUT3 (p.A211V) in the rodent brain suggests a nonuniform distribution of the transporter in synaptic vesicles. Journal of Neuroscience, 37(15), 4181–4199.

Rasmussen, K., McCreary, A. C., & Shanks, E. A. (2004). Attenuation of the effects of fluoxetine on serotonergic neuronal activity by pindolol in rats. Neuroscience Letters, 355(1–2), 1–4.

Rein, B., Ma, K., & Yan, Z. (2020). A standardized social preference protocol for measuring social deficits in mouse models of autism. Nature Protocols, 15(10), 3464–3477.

Ren, J., Friedmann, D., Xiong, J., Liu, C. D., Ferguson, B. R., Weerakkody, T., DeLoach, K. E., Ran, C., Pun, A., Sun, Y., Weissbourd, B., Neve, R. L., Huguenard, J., Horowitz, M. A., & Luo, L. (2018). Anatomically Defined and Functionally Distinct Dorsal Raphe Serotonin Sub-systems. Cell, 175(2), 472-487.e20.

Ren, J., Qin, C., Hu, F., Tan, J., Qiu, L., Zhao, S., Feng, G., & Luo, M. (2011). Habenula "Cholinergic" Neurons Corelease Glutamate and Acetylcholine and Activate Postsynaptic Neurons via Distinct Transmission Modes. Neuron, 69(3), 445–452.

Rescorla, R. A. (1988). Behavioral studies of Pavlovian conditioning. Annual Review of Neuroscience, 11(1), 329–352.

Rio, D. C., Ares, M., Hannon, G. J., & Nilsen, T. W. (2010). Purification of RNA using TRIzol (TRI reagent). Cold Spring Harbor Protocols, 2010(6), pdb-prot5439.

Robinson, J. E., Coughlin, G. M., Hori, A. M., Cho, J. R., Mackey, E. D., Turan, Z., Patriarchi, T., Tian, L., & Gradinaru, V. (2019). Optical dopamine monitoring with dLight1 reveals mesolimbic phenotypes in a mouse model of neurofibromatosis type 1. eLife, 8, e48983.

Roche, M., Commons, K. G., Peoples, A., & Valentino, R. J. (2003). Circuitry Underlying Regulation of the Serotonergic System by Swim Stress. The Journal of Neuroscience, 23(3), 970–977.

Roitman, M. F., Stuber, G. D., Phillips, P. E. M., Wightman, R. M., & Carelli, R. M. (2004). Dopamine operates as a subsecond modulator of food seeking. Journal of Neuroscience, 24(6), 1265–1271.

Root, D. H., Mejias-Aponte, C. A., Zhang, S., Wang, H.-L., Hoffman, A. F., Lupica, C. R., & Morales, M. (2014). Single rodent mesohabenular axons release glutamate and GABA. Nature Neuroscience, 17(11), 1543–1551.

Rosas-Sánchez, G. U., German-Ponciano, L. J., & Rodríguez-Landa, J. F. (2022). Considerations of Pool Dimensions in the Forced Swim Test in Predicting the Potential Antidepressant Activity of Drugs. Frontiers in Behavioral Neuroscience, 15.

Rueter, L. E., & Jacobs, B. L. (1996). A microdialysis examination of serotonin release in the rat forebrain induced by behavioral/environmental manipulations. Brain Research, 739(1–2), 57–69.

Sakae, D. Y., Marti, F., Lecca, S., Vorspan, F., Martín-García, E., Morel, L. J., Henrion, A., Gutiérrez-Cuesta, J., Besnard, A., Heck, N., Herzog, E., Bolte, S., Prado, V. F., Prado, M. A. M., Bellivier, F., Eap, C. B., Crettol, S., Vanhoutte, P., Caboche, J., … El Mestikawy, S. (2015). The absence of VGLUT3 predisposes to cocaine abuse by increasing dopamine and glutamate signaling in the nucleus accumbens. Molecular Psychiatry, 20(11), 1448–1459.

Salamone, J. D., & Correa, M. (2012). The mysterious motivational functions of mesolimbic dopamine. Neuron, 76(3), 470–485.

Salamone, J. D., Correa, M., Farrar, A. M., Nunes, E. J., & Pardo, M. (2009). Dopamine, behavioral economics, and effort. Frontiers in Behavioral Neuroscience, 3, 764.

Salamone, J. D., Pardo, M., Yohn, S. E., López-Cruz, L., SanMiguel, N., & Correa, M. (2016). Mesolimbic dopamine and the regulation of motivated behavior. Behavioral Neuroscience of Motivation, 27, 231–257.

Salinas, A. G., Lee, J. O., Augustin, S. M., Zhang, S., Patriarchi, T., Tian, L., Morales, M., Mateo, Y., & Lovinger, D. M. (2023). Distinct sub-second dopamine signaling in dorsolateral striatum measured by a genetically-encoded fluorescent sensor. Nature Communications, 14(1), 5915.

Salio, C., Lossi, L., Ferrini, F., & Merighi, A. (2006). Neuropeptides as synaptic transmitters. Cell and Tissue Research, 326(2), 583–598.

Sanderson, D. J., Gray, A., Simon, A., Taylor, A. M., Deacon, R. M. J., Seeburg, P. H., Sprengel, R., Good, M. A., Rawlins, J. N. P., & Bannerman, D. M. (2007). Deletion of glutamate receptor-A (GluR-A) AMPA receptor subunits impairs one-trial spatial memory. Behavioral Neuroscience, 121(3), 559—569.

Santarelli, L., Saxe, M., Gross, C., Surget, A., Battaglia, F., Dulawa, S., Weisstaub, N., Lee, J., Duman, R., Arancio, O., Belzung, C., & Hen, R. (2003). Requirement of hippocampal neurogenesis for the behavioral effects of antidepressants. Science, 301(5634), 805–809.

Saunders, A., Granger, A. J., & Sabatini, B. L. (2015). Corelease of acetylcholine and GABA from cholinergic forebrain neurons. Elife, 4, e06412.

Saunders, A., Oldenburg, I. A., Berezovskii, V. K., Johnson, C. A., Kingery, N. D., Elliott, H. L., Xie, T., Gerfen, C. R., & Sabatini, B. L. (2015). A direct GABAergic output from the basal ganglia to frontal cortex. Nature, 521(7550), 85–89.

Schäfer, M. K. H., Varoqui, H., Defamie, N., Weihe, E., & Erickson, J. D. (2002). Molecular cloning and functional identification of mouse vesicular glutamate transporter 3 and its expression in subsets of novel excitatory neurons. Journal of Biological Chemistry, 277(52), 50734–50748.

Scheggi, S., De Montis, M. G., & Gambarana, C. (2018). Making sense of rodent models of anhedonia. International Journal of Neuropsychopharmacology, 21(11), 1049–1065. h

Schindler, C. W., & Goldberg, S. R. (2013). Chapter 29 - Animal Models of Reward Behavior. In P. M. Conn (Ed.), Animal Models for the Study of Human Disease (pp. 709–726). Academic Press.

Schultz, W. (2002). Getting formal with dopamine and reward. Neuron, 36(2), 241–263.

Schultz, W. (2016). Dopamine reward prediction error coding. Dialogues in Clinical Neuroscience, 18(1), 23–32.

Schultz, W., Apicella, P., & Ljungberg, T. (1993). Responses of monkey dopamine neurons to reward and conditioned stimuli during successive steps of learning a delayed response task. The Journal of Neuroscience, 13(3), 900.

Schultz, W., Dayan, P., & Montague, P. R. (1997). A neural substrate of prediction and reward. Science, 275(5306), 1593–1599.

Schultz, W., Dayan, P., & Read Montague, P. (1990). A Neural Substrate of Prediction and Reward. Science, 275(5306), 1593–1599.

Schweimer, J. V., & Ungless, M. A. (2010). Phasic responses in dorsal raphe serotonin neurons to noxious stimuli. Neuroscience, 171(4), 1209–1215.

Sclafani, A., Bahrani, M., Zukerman, S., & Ackroff, K. (2010). Stevia and saccharin preferences in rats and mice. Chemical Senses, 35(5), 433–443.

Scott, M. M., Wylie, C. J., Lerch, J. K., Murphy, R., Lobur, K., Herlitze, S., Jiang, W., Conlon, R. A., Strowbridge, B. W., & Deneris, E. S. (2005). A genetic approach to access serotonin neurons for in vivo and in vitro studies. 102(45), 16472–16477.

Seibenhener, M. L., & Wooten, M. C. (2015). Use of the open field maze to measure locomotor and anxiety-like behavior in mice. Journal of Visualized Experiments, 96, 52434.

Senba, E., Matsunaga, K., Tohyama, M., & Noguchi, K. (1993). Stress-induced c-fos expression in the rat brain: activation mechanism of sympathetic pathway. Brain Research Bulletin, 31(3), 329–344.

Sengupta, A., Bocchio, M., Bannerman, D. M., Sharp, T., & Capogna, M. (2017). Control of Amygdala Circuits by 5-HT Neurons via 5-HT and Glutamate Cotransmission. The Journal of Neuroscience, 37(7), 1785.

Sengupta, A., & Holmes, A. (2019). A Discrete Dorsal Raphe to Basal Amygdala 5-HT Circuit Calibrates Aversive Memory. Neuron, 103(3), 489-505.e7.

Serchov, T., van Calker, D., & Biber, K. (2016). Sucrose Preference Test to Measure Anhedonic Behaviour in Mice. Bio-protocol, 6(19), e1958.

Seymour, B., Daw, N. D., Roiser, J. P., Dayan, P., & Dolan, R. (2012). Serotonin Selectively Modulates Reward Value in Human Decision-Making. The Journal of Neuroscience, 32(17), 5833.

Shabel, S. J., Proulx, C. D., Piriz, J., & Malinow, R. (2014). GABA/glutamate co-release controls habenula output and is modified by antidepressant treatment. Science, 345(6203), 1494–1498.

Sharp, T., & Barnes, N. M. (2020). Central 5-HT receptors and their function; present and future. Neuropharmacology, 177, 108155.

Sharp, T., & Cowen, P. J. (2011). 5-HT and depression: is the glass half-full? Current Opinion in Pharmacology, 11(1), 45–51.

Sheng, M., & Greenberg, M. E. (1990). The regulation and function of c-fos and other immediate early genes in the nervous system. Neuron, 4(4), 477–485.

Shikanai, H., Yoshida, T., Konno, K., Yamasaki, M., Izumi, T., Ohmura, Y., Watanabe, M., & Yoshioka, M. (2012). Distinct Neurochemical and Functional Properties of GAD67-Containing 5-HT Neurons in the Rat Dorsal Raphe Nucleus. The Journal of Neuroscience, 32(41), 14415.

Sigma-Aldrich. (2014). OligoEvaluator.

Simpson, E. H., Akam, T., Patriarchi, T., Blanco-Pozo, M., Burgeno, L. M., Mohebi, A., Cragg, S. J., & Walton, M. E. (2024). Lights, fiber, action! A primer on in vivo fiber photometry. Neuron, 112(5), 718–739.

Skinner, B. F. (1988). Preface to the behavior of organisms. Journal of the Experimental Analysis of Behavior, 50(2), 355.

Soiza-Reilly, M., & Commons, K. G. (2011). Glutamatergic drive of the dorsal raphe nucleus. Journal of Chemical Neuroanatomy, 41(4), 247–255.

Song, F., Freemantle, N., Sheldon, T. A., House, A., Watson, P., Long, A., & Mason, J. (1993). Selective serotonin reuptake inhibitors: meta-analysis of efficacy and acceptability. British Medical Journal, 306(6879), 683–687.

Sossin, W. S., Sweet-Cordero, A., & Scheller, R. H. (1990). Dale's hypothesis revisited: different neuropeptides derived from a common prohormone are targeted to different processes. Proceedings of the National Academy of Sciences, 87(12), 4845–4848.

Spaethling, J. M., Piel, D., Dueck, H., Buckley, P. T., Morris, J. F., Fisher, S. A., Lee, J., Sul, J.-Y., Kim, J., Bartfai, T., Beck, S. G., & Eberwine, J. H. (2014). Serotonergic neuron regulation informed by in vivo single-cell transcriptomics. The FASEB Journal, 28(2), 771–780.

Spector, A. C., & Smith, J. C. (1984). A detailed analysis of sucrose drinking in the rat. Physiology & Behavior, 33(1), 127–136.

Spitzer, N. C. (2015). Neurotransmitter Switching? No Surprise. Neuron, 86(5), 1131–1144.

Staddon, J. E. R., & Cerutti, D. T. (2003). Operant conditioning. Annual Review of Psychology, 54(1), 115–144.

Stahl, S. M. (1998). Mechanism of action of serotonin selective reuptake inhibitors Serotonin receptors and pathways mediate therapeutic effects and side effects. Journal of Affective Disorders, 51(3), 215–235.

Stanton, C. H., Holmes, A. J., Chang, S. W. C., & Joormann, J. (2019). From Stress to Anhedonia: Molecular Processes through Functional Circuits. Trends in Neurosciences, 42(1), 23–42.

Steinbusch, H. W., Nieuwenhuys, R., Verhofstad, A. A., & Van der Kooy, D. (1981). The nucleus raphe dorsalis of the rat and its projection upon the caudatoputamen. A combined cytoarchitectonic, immunohistochemical and retrograde transport study. Journal de Physiologie, 77(2–3), 157–174.

Stevens, C. F., & Williams, J. H. (2000). "Kiss and run" exocytosis at hippocampal synapses. Proceedings of the National Academy of Sciences, 97(23), 12828–12833.

Strekalova, T., Gorenkova, N., Schunk, E., Dolgov, O., & Bartsch, D. (2006). Selective effects of citalopram in a mouse model of stress-induced anhedonia with a control for chronic stress. Behavioural Pharmacology, 17, 271–287.

Strekalova, T., & Steinbusch, H. (2010). Measuring behavior in mice with chronic stress depression paradigm. Progress in Neuro-Psychopharmacology and Biological Psychiatry, 34(2), 348–361.

Südhof, T. C. (2012). Calcium control of neurotransmitter release. Cold Spring Harbor Perspectives in Biology, 4(1), a011353.

Sulzer, D., Joyce, M. P., Lin, L., Geldwert, D., Haber, S. N., Hattori, T., & Rayport, S. (1998). Dopamine neurons make glutamatergic synapses in vitro. Journal of Neuroscience, 18(12), 4588–4602.

Sulzer, D., & Rayport, S. (2000). Dale's principle and glutamate corelease from ventral midbrain dopamine neurons. Amino Acids, 19, 45–52.

Sunal, R., Gümüşel, B., & Kayaalp, S. O. (1994). Effect of changes in swimming area on results of "behavioral despair test." Pharmacology Biochemistry and Behavior, 49(4), 891–896.

Svensson, E., Apergis-Schoute, J., Burnstock, G., Nusbaum, M. P., Parker, D., & Schiöth, H. B. (2019). General principles of neuronal co-transmission: Insights from multiple model systems. Frontiers in Neural Circuits, 12.

Syed, E. C. J., Grima, L. L., Magill, P. J., Bogacz, R., Brown, P., & Walton, M. E. (2015). Action initiation shapes mesolimbic dopamine encoding of future rewards. Nature Neuroscience, 19(1), 34–36.

Takamori, S., Malherbe, P., Broger, C., & Jahn, R. (2002). Molecular cloning and functional characterization of human vesicular glutamate transporter 3. EMBO Reports, 3(8), 798–803.

Takase, L. F., Nogueira, M. I., Baratta, M., Bland, S. T., Watkins, L. R., Maier, S. F., Fornal, C. A., & Jacobs, B. L. (2004). Inescapable shock activates serotonergic neurons in all raphe nuclei of rat. Behavioural Brain Research, 153(1), 233–239.

Tang, M., He, T., Meng, Q. Y., Broussard, J. I., Yao, L., Diao, Y., Sang, X. B., Liu, Q. P., Liao, Y. J., Li, Y., & Zhao, S. (2014). Immobility responses between mouse strains correlate with distinct hippocampal serotonin transporter protein expression and function. International Journal of Neuropsychopharmacology, 17(11), 1737–1750.

Taylor, N. E., Pei, J., Zhang, J., Vlasov, K. Y., Davis, T., Taylor, E., Weng, F.-J., Van Dort, C. J., Solt, K., & Brown, E. N. (2019). The role of glutamatergic and dopaminergic neurons in the periaqueductal gray/dorsal raphe: separating analgesia and anxiety. Eneuro, 6(1), ENEURO.0018–18.2019.

Tobler, P. N., Fiorillo, C. D., & Schultz, W. (2005). Adaptive coding of reward value by dopamine neurons. Science, 307(5715), 1642–1645.

Tomie, A., Grimes, K. L., & Pohorecky, L. A. (2008). Behavioral characteristics and neurobiological substrates shared by Pavlovian sign-tracking and drug abuse. Brain Research Reviews, 58(1), 121–135.

Tordoff, M. G., Alarcon, L. K., & Lawler, M. P. (2008). Preferences of 14 rat strains for 17 taste compounds. Physiology and Behavior, 95(3), 308–332.

Tritsch, N. X., Ding, J. B., & Sabatini, B. L. (2012). Dopaminergic neurons inhibit striatal output through non-canonical release of GABA. Nature, 490(7419), 262–266.

Tritsch, N. X., Oh, W.-J., Gu, C., & Sabatini, B. L. (2014). Midbrain dopamine neurons sustain inhibitory transmission using plasma membrane uptake of GABA, not synthesis. Elife, 3, e01936.

Trudeau, L. E., & El Mestikawy, S. (2018). Glutamate cotransmission in cholinergic, GABAergic and monoamine systems: Contrasts and commonalities. Frontiers in Neural Circuits, 12.

Twarog, B. M., & Page, I. H. (1953). Serotonin Content of Some Mammalian Tissues and Urine and a Method for Its Determination. American Journal of Physiology-Legacy Content, 175(1), 157–161.

Uslaner, J. M., Acerbo, M. J., Jones, S. A., & Robinson, T. E. (2006). The attribution of incentive salience to a stimulus that signals an intravenous injection of cocaine. Behavioural Brain Research, 169(2), 320–324.

Vaaga, C. E., Borisovska, M., & Westbrook, G. L. (2014). Dual-transmitter neurons: functional implications of co-release and co-transmission. Current Opinion in Neurobiology, 29, 25–32.

Valyear, M. D., Villaruel, F. R., & Chaudhri, N. (2017). Alcohol-seeking and relapse: A focus on incentive salience and contextual conditioning. Behavioural Processes, 141, 26–32.

Van Bockstaele, E. J., & Chan, J. (1997). Electron microscopic evidence for coexistence of leucine5-enkephalin and γ-aminobutyric acid in a subpopulation of axon terminals in the rat locus coeruleus region. Brain Research, 746(1–2), 171–182.

Vandermaelen, C. P., & Aghajanian, G. K. (1983). Electrophysiological and pharmacological characterization of serotonergic dorsal raphe neurons recorded extracellularly and intracellularly in rat brain slices. Brain Research, 289(1–2), 109–119.

Varga, V., Losonczy, A., Zemelman, B. V, Borhegyi, Z., Nyiri, G., Domonkos, A., Hangya, B., Holderith, N., Magee, J. C., & Freund, T. F. (2009). Fast Synaptic Subcortical Control of Hippocampal Circuits. Science, 326(5951), 449–453.

Veniaminova, E., Cespuglio, R., Chernukha, I., Schmitt-Boehrer, A. G., Morozov, S., Kalueff, A. V., Kuznetsova, O., Anthony, D. C., Lesch, K. P., & Strekalova, T. (2020). Metabolic, Molecular, and Behavioral Effects of Western Diet in Serotonin Transporter-Deficient Mice: Rescue by Heterozygosity? Frontiers in Neuroscience, 14.

Vertes, R. P. (1991). A PHA-L analysis of ascending projections of the dorsal raphe nucleus in the rat. Journal of Comparative Neurology, 313(4), 643–668.

Vertes, R. P., & Linley, S. B. (2008). Efferent and afferent connections of the dorsal and median raphe nuclei in the rat. In Serotonin and sleep: molecular, functional and clinical aspects. Birkäuser Basel.

Vigneault, É., Poirel, O., Riad, M., Prud'homme, J., Dumas, S., Turecki, G., Fasano, C., Mechawar, N., & El Mestikawy, S. (2015). Distribution of vesicular glutamate transporters in the human brain. Frontiers in Neuroanatomy, 9.

Vilim, F. S., Cropper, E. C., Price, D. A., Kupfermann, I., & Weiss, K. R. (2000). Peptide Cotransmitter Release from Motorneuron B16 inAplysia californica: Costorage, Corelease, and Functional Implications. Journal of Neuroscience, 20(5), 2036–2042.

Vogelgesang, S., Niebert, S., Renner, U., Möbius, W., Hülsmann, S., Manzke, T., & Niebert, M. (2017). Analysis of the serotonergic system in a mouse model of Rett syndrome reveals unusual upregulation of serotonin receptor 5b. Frontiers in Molecular Neuroscience, 10.

Voisin, A. N., Mnie-Filali, O., Giguère, N., Fortin, G. M., Vigneault, E., El Mestikawy, S., Descarries, L., & Trudeau, L. É. (2016). Axonal segregation and role of the vesicular glutamate transporter VGLUT3 in serotonin neurons. Frontiers in Neuroanatomy, 10.

Walther, D. J., Peter, J.-U., Bashammakh, S., Hörtnagl, H., Voits, M., Fink, H., & Bader, M. (2003). Synthesis of Serotonin by a Second Tryptophan Hydroxylase Isoform. Science, 299(5603), 76.

Walton, M. E., & Bouret, S. (2019). What is the relationship between dopamine and effort? Trends in Neurosciences, 42(2), 79–91.

Walton, M. E., Gan, J. O., & Phillips, P. E. M. (2011). The influence of dopamine in generating action from motivation.

Wan, J., Peng, W., Li, X., Qian, T., Song, K., Zeng, J., Deng, F., Hao, S., Feng, J., Zhang, P., Zhang, Y., Zou, J., Pan, S., Shin, M., Venton, B. J., Zhu, J. J., Jing, M., Xu, M., & Li, Y. (2021). A genetically encoded sensor for measuring serotonin dynamics. Nature Neuroscience, 24(5), 746–752.

Wang, H. L., Zhang, S., Qi, J., Wang, H., Cachope, R., Mejias-Aponte, C. A., Gomez, J. A., Mateo-Semidey, G. E., Beaudoin, G. M. J., Paladini, C. A., Cheer, J. F., & Morales, M. (2019). Dorsal Raphe Dual Serotonin-Glutamate Neurons Drive Reward by Establishing Excitatory Synapses on VTA Mesoaccumbens Dopamine Neurons. Cell Reports, 26(5), 1128-1142.e7.

Winkler, H., Apps, D. K., & Fischer-Colbrie, R. (1986). The molecular function of adrenal chromaffin granules: established facts and unresolved topics. Neuroscience, 18(2), 261–290.

Wise, R. A., & Rompre, P.-P. (1989). Brain dopamine and reward. Annual Review of Psychology, 40, 191–225.

Wojcik, S. M., Katsurabayashi, S., Guillemin, I., Friauf, E., Rosenmund, C., Brose, N., & Rhee, J.-S. (2006). A shared vesicular carrier allows synaptic corelease of GABA and glycine. Neuron, 50(4), 575–587.

Xia, X., Lessmann, V., & Martin, T. F. J. (2009). Imaging of evoked dense-core-vesicle exocytosis in hippocampal neurons reveals long latencies and kiss-and-run fusion events. Journal of Cell Science, 122(1), 75–82.

Yoshimoto, K., McBride, W. J., Lumeng, L., & Li, T.-K. (1992). Alcohol stimulates the release of dopamine and serotonin in the nucleus accumbens. Alcohol, 9(1), 17–22.

Yu, T., Guo, M., Garza, J., Rendon, S., Sun, X.-L., Zhang, W., & Lu, X.-Y. (2011). Cognitive and neural correlates of depression-like behaviour in socially defeated mice: an animal model of depression with cognitive dysfunction. International Journal of Neuropsychopharmacology, 14(3), 303–317.

Yu, X., Ye, Z., Houston, C. M., Zecharia, A. Y., Ma, Y., Zhang, Z., Uygun, D. S., Parker, S., Vyssotski, A. L., & Yustos, R. (2015). Wakefulness is governed by GABA and histamine cotransmission. Neuron, 87(1), 164–178.

Yu, Z., Lin, D., Zhong, Y., Luo, B., Liu, S., Fei, E., Lai, X., Zou, S., & Wang, S. (2019). Transmembrane protein 108 involves in adult neurogenesis in the hippocampal dentate gyrus. Cell and Bioscience, 9(1).

Zhang, Z., Wu, Y., Wang, Z., Dunning, F. M., Rehfuss, J., Ramanan, D., Chapman, E. R., & Jackson, M. B. (2011). Release mode of large and small dense-core vesicles specified by different synaptotagmin isoforms in PC12 cells. Molecular Biology of the Cell, 22(13), 2324–2336.

Zhong, W., Li, Y., Feng, Q., & Luo, M. (2017). Learning and stress shape the reward response patterns of serotonin neurons. Journal of Neuroscience, 37(37), 8863–8875.

Zou, W. J., Song, Y. L., Wu, M. Y., Chen, X. T., You, Q. L., Yang, Q., Luo, Z. Y., Huang, L., Kong, Y., Feng, J., Fang, D. X., Li, X. W., Yang, J. M., Mei, L., & Gao, T. M. (2020). A discrete serotonergic circuit regulates vulnerability to social stress. Nature Communications, 11(1), 4218.